Refinery Integration of By-Products from Coal-Derived Jet Fuels

SEMI-ANNUAL PROGRESS REPORT

September 18, 2006 – March 17, 2007

Caroline E. Burgess Clifford, André Boehman, Chunshan Song,
Bruce Miller, Gareth Mitchell

Date Issued: May 14, 2007

Grant DE-FC26-03NT41828

The Pennsylvania State University
The Energy Institute
C205 Coal Utilization Laboratory
University Park, PA 16802

Disclaimer

Abstract

This report summarizes the accomplishments toward project goals during the no cost extension period of the third year of the project to assess the properties and performance of coal based products. These products are in the gasoline, diesel and fuel oil range and result from coal based jet fuel production from an Air Force funded program. Specific areas of progress include generation of coal based material that has been fractionated into the desired refinery cuts for a third round of testing, the use of a research gasoline engine to test coal-based gasoline, and modification of diesel engines for use in evaluating diesel produced in the project. At the pilot scale, the hydrotreating process was modified to separate the heavy components from the LCO and RCO fractions before hydrotreating in order to improve the performance of the catalysts in further processing. Hydrotreating and hydrogenation of the product has been completed, and due to removal of material before processing, yield of the jet fuel fraction has decreased relative to an increase in the gasoline fraction. Characterization of the gasoline fuel indicates a dominance of single ring alkylcycloalkanes that have a low octane rating; however, blends containing these compounds do not have a negative effect upon gasoline when blended in refinery gasoline streams. Characterization of the diesel fuel indicates a dominance of 3-ring aromatics that have a low cetane value; however, these compounds do not have a negative effect upon diesel when blended in refinery diesel streams. Both gasoline and diesel continue to be tested for combustion performance. The desulfurization of sulfur containing components of coal and petroleum is being studied so that effective conversion of blended coal and petroleum streams can be efficiently converted to useful refinery products. Activated carbons have proven useful to remove the heavy sulfur components, and unsupported Ni/Mo and Ni/Co catalysts have been very effective for hydrodesulfurization. Equipment is now in place to begin fuel oil evaluations

to assess the quality of coal based fuel oil. Combustion and characterization of the latest fuel oil (the high temperature fraction of RCO from the latest modification) indicates that the fraction is heavier than a No. 6 fuel oil. Combustion efficiency on our research boiler is ~63% for the heavy RCO fraction, lower than the combustion performance for previous co-coking fuel oils and No. 6 fuel oil. Emission testing indicates that the coal derived material has more trace metals related to coal than petroleum, as seen in previous runs. An additional coal has been procured and is being processed for the next series of delayed co-coking runs. The co-coking of the runs with the new coal have begun, with the coke yield similar to previous runs, but the gas yield is lower and the liquid yield is higher. Characterization of the products continues. Work continues on characterization of liquids and solids from co-coking of hydrotreated decant oils; liquid yields include more saturated and hydro- aromatics, while the coke quality varies depending on the conditions used. Pitch material is being generated from the heavy fraction of co-coking.

TABLE OF CONTENTS

List of Tables

List of Figures

Refinery Integration of By-Products from Coal-Derived Jet Fuels

Introduction

This program is investigating the fate of each major product from a refinery complex, except jet fuel, resulting from the refinery integration of coal-derived jet fuel production via a combined RCO/LCO strategy by studying the physical and chemical nature of all products that are perturbed by introduction of coal components into the refinery.

The impact of the proposed research is to provide the scientific and fundamental engineering basis to integrate the production of coal-based jet fuel into existing refinery operations in a time frame consistent with availability and economic forecasts related to petroleum-derived as opposed to coal-based feedstocks. The results of these studies lead to the integration of all non-jet-fuel streams into current refinery operations in concert with desired production of coal-based jet fuel engine testing toward the end of the first decade of the new century. For successful utilization of coal-based jet fuels all non-jet-fuel components must fit existing and future product stream specifications.

Executive Summary

Penn State has been working for more than a decade on the development of an advanced, thermally stable, coal-based jet fuel, JP-900. Two process routes to JP-900 have been identified, one involving the hydrotreating of blends of refined chemical oil (RCO, a by-product of the coal tar industry) with light cycle oil (LCO), and the other involving the addition of coal to delayed cokers. However, no refinery is operated for the primary purpose of making jet fuel. The conversion of the jet fuel section of a refinery to production of coal-based JP-900 would necessarily impact the quantity and quality of the other refinery products, such as gasoline, diesel fuel, fuel oil, and coke. The overall objective of this project is to examine the characteristics and quality of the streams *other than the jet fuel*, and to determine the effect those materials would have on other unit operations in the refinery.

The present report documents the activities of the no cost extension of year three of what is envisioned to be a four-year program. Our collateral work on jet fuel, funded by the Air Force Office of Scientific Research, is focused exclusively on that product. Thus as we branch out into the study of the other refinery streams, under this present contract, much of the effort in the last year has been devoted to the evaluation of product streams to streamline operations.

The overall project involves pilot-scale production of materials at Intertek PARC Technical Services (Harmarville, PA). The coal-based gasoline and diesel fuel is being evaluated in appropriate internal combustion engines. Desulfurization, denitrogenation, and saturation of aromatics are being tested. There is also a component to examine the production of high-value aromatic compounds. The initial products of coal-based fuel oil were tested in a research boiler, although not enough fuel was available to do complete characterization. The pitch and coke co-coking from initial runs has been characterized. These interrelated activities are designed to evaluate the full range of products from coal-based thermally stable jet fuel production and to lead toward process integration in existing refineries.

The third run for hydrotreatment of blends of refined chemical oil and light cycle oil, followed by fractionation of the total product, was performed at Intertek PARC. The various distillation cuts have been provided to the researchers at Penn State for analytical characterization and for use in the appropriate evaluation tests. In addition, decant oil was hydrotreated at several levels of severity for use in the co-coking work. In this report period, Intertek PARC has distilled samples of RCO (75% yield) and LCO (63% yield) separately before hydrotreatment, and is in the process of finishing hydrotreatment to provide new fuels for Year 4 evaluation. The hydrotreatment and hydrogenation has been completed, and the yield of jet fuel has decreased and the yield of gasoline has increased. The fuel oil fraction has been separated and provided to those in Task 4 for evaluation.

Characterization of the gasoline fuel indicates a dominance of single ring alkylcycloalkanes that have a low octane rating (Research Octane Number is 61.0 for EI-174); however, blends containing these compounds do not have a negative effect upon gasoline when blended in refinery gasoline streams.

Characterization of the diesel fuel indicates a dominance of 3-ring aromatics that have a low cetane value; however, these compounds do not have a negative effect upon diesel when blended in refinery diesel streams. The two compounds that have been chosen to represent the coal-based diesel are fluorene and phenanthrene. These compounds were blended with a low sulfur diesel fuel from BP (BP-15). This reporting period, ethylhexyl nitrate (EHN) slightly improved the combustion performance of the blend of BP-15 and 5% phenanthrene, but did not appear quite as effective with fluorene.

The desulfurization of sulfur containing components of coal and petroleum is being studied so that effective conversion of blended coal and petroleum streams can be efficiently converted to useful refinery products. The development of unsupported finely dispersed Ni/Mo and Co/Mo catalyst prepared in house shows increased sulfur removal compared to commercial Ni/Mo catalyst. Adsorptive desulfurization of LCO using activated carbon worked well, by removing the heavy sulfur and nitrogen compounds before hydrogenation. For the saturation of two-ring aromatics component of Task 3, zeolite catalyst supports exhibit higher sulfur tolerance.

Equipment is now in place to begin fuel oil evaluations to assess the quality of coal based fuel oil. It was reported in the last report that combustion and characterization of a the initial co-processed fuel oils indicates that the fuel oil is somewhere in between a No. 4 and a No. 6 fuel oil. Emission testing indicates the fuel burns similarly to these two fuels, but trace metals for the coal-based material are different than petroleum-based fuel oils. The boiler efficiency of the most recent fuel oil, the bottom fraction of RCO (62.3%), is lower than the efficiency than No. 6 fuel oil (70%). Trace metal evaluation of this fuel oil indicates a dominance of trace metals from coal rather than from petroleum, even though the coal only constitutes 20% of the feed.

Much less work was accomplished in Task 5 during this reporting period because funds were not available to continue building analytical procedures, acquiring background information and pursuing parallel lines of research to accomplish our principle goal to evaluate of co-coking using coal and refinery solvents. Although work was suspended on coker liquids evaluation, coal extraction and the manufacture and testing of carbon artifacts, our efforts were focused on completing the preparation of the new clean Marfork coal product and to begin co-coking runs that would generate liquid and solid products for characterization. Co-coking has begun and the first two runs of twelve were completed during this performance period. Work was continued on the evaluation of cokes generated in tubing bombs from hydrotreated decant oil using X-ray diffraction and the measurement of the coefficient of thermal expansion (CTE) using a Thermal Mechanical Analysis technique. This preliminary study revealed that X-ray diffraction parameters (full width and half maximum of the 002 peak and Lc) may be sufficiently sensitive to mark the beginning of mesophase development in the green cokes that contain significant amounts of isotropic carbon as determined by optical microscopy. Evaluation of green cokes using X-ray diffraction suggested that the most hydrotreated decant oils produced the best coke. However, measurement of *cte* suggested that the most aromatic (or least hydrotreated) decant oils produced better coke. We will continue to study the meaning of this apparent controversy. Work continued on the development of pitch products from the liquids of co-coking that would be equal to that used in anode production for the aluminum industry. Several pitch products were prepared by heat soaking and thermal oxidation and preliminary evaluation showed that while the altered pitches contained moieties of greater mass than the original material, masses in the range of 350-450 daltons were missing and it appeared that they were mainly derived from the original petroleum products instead of the coal. As suggested in our last report, increasing the amount of coal above 20% caused processing problems and decreased the quality of the carbon product. To increase the potential of capturing more coal-derived liquids, co-coking of the cleaned Pittsburgh FCE (EI-186) at 30 wt. % was completed. These results were compared with earlier runs using a Canterberry Product (Lower Kittanning) coal that had been co-coked with decant oil at 30 wt. %. Our preliminary results showed that there was a significant decrease in the amount of liquid material produced and the coke artifact was composed largely of shot coke. Once the Marfork co-coking tests at 20 wt. % are completed, a more controlled study using the two clean coal products will be tested at higher coal loading.

Experimental

The respective experimental details for each of the tasks of this project are described within the individual Tasks I – V detailed later in this report.

Results and Discussion

The results of each task of this project are documented and discussed within the appropriate Task I – V detailed later in this report.

Conclusions

Each of the individual tasks of this project has progressed as proposed; however, the work during the no cost extension for Year 3 has been limited to tasks that need to be completed for Year 3 or to tasks by students being supported on the project. This report describes the procurement of equipment into the appropriate laboratories, the establishment of experimental procedures and the generation of results that indicate the relevance and feasibility of the proposed work.

Progress has been made to produce hydrotreated products, differing from conventional refinery products but also compatible with conventional materials. Specific areas of progress include generation of coal based material that has been fractionated before hydrotreatment followed by hydrotreatment of the lighter material, research on a gasoline engine, and research on diesel engines for use in evaluating diesel produced in the project, testing of the fuel oil fraction in the research boiler, and cleaning of new coal along with the first test runs of that coal. In this year's work, distillation was done at the beginning of the process to remove components potentially detrimental to hydrotreatment catalysts. When fractionating, ~63% of LCO and ~75% of RCO was distilled for further hydrotreatment; hydrotreatment has been completed, in which gasoline, jet fuel, and diesel will be tested at a future date. Currently, the only fuel tested from the process change is fuel oil, as hydrotreatment continues on the light fractions.

Characterization of the gasoline fuel indicates a dominance of single ring alkylcycloalkanes that have a low octane rating (Research Octane Number is 61.0 for EI-174); however, blends containing these compounds do not have a negative effect upon gasoline when blended in refinery gasoline streams. The method for condensing products from low temperature oxidation has been upgraded using a dry ice/acetone bath. Characterization of the diesel fuel indicates a dominance of 3-ring aromatics that have a low cetane value; however, these compounds do not have a negative effect upon diesel when blended in refinery diesel streams. The two compounds that have been chosen to represent the coal-based diesel are fluorene and phenanthrene. These compounds were blended with a low sulfur diesel fuel from BP (BP-15). This reporting period, ethylhexyl nitrate (EHN) slightly improved the combustion performance of the blend of BP-15 and 5% phenanthrene, but did not appear quite as effective with fluorene. For both the gasoline and diesel fuels, the performance of engines will continue to be evaluated.

The desulfurization of sulfur containing components of coal and petroleum is being studied so that effective conversion of blended coal and petroleum streams can be efficiently converted to useful refinery products. The development of a finely unsupported dispersed Ni/Mo and Co/Mo catalyst prepared in house shows increased sulfur removal compared to commercial Ni/Mo catalyst. Adsorptive desulfurization of LCO using activated carbon worked well, by removing the heavy sulfur and nitrogen compounds before hydrogenation. For the saturation of two-ring aromatics component of Task 3, zeolite catalyst supports exhibit higher sulfur tolerance, and research continued on methods to improve sulfur tolerance. Metal aluminophosphate catalysts have been synthesized for use in making value-added chemicals from two-ring aromatics. Currently, aluminophosphate catalysts have been modified by adding iron, and characterization of the catalysts continues.

Equipment is now in place to begin fuel oil evaluations to assess the quality of coal based fuel oil. It was reported in the last report that combustion and characterization of the first co-processed fuel oil indicates that the fuel is somewhere in between a No. 4 and a No. 6 fuel oil. Emission testing indicates the fuel burns similarly to these two fuels, but trace metals for the coal-based material are different than petroleum-based fuel oils. The boiler efficiency of the most recent fuel oil, the bottom fraction of RCO (62.3%), is lower than the efficiency than No. 6 fuel oil (70%). The trace metal emission evaluation has been completed, and the emissions reflect emissions that would mainly be from coal.

Previous co-coking studies using cleaned coal are highly reproducible in the pilot-scale delayed coker. Evaluation of the coke indicated that while the coke produced is of very good quality, the metals content of the carbon is still high in iron and silica. The most recent work has focused on obtaining a coal with a lower mineral matter content, from the Marfolk mine in West Virginia. Coal has been cleaned to ~1% ash, and the first two delayed coking experiments have been completed; the yield information indicates an increase in liquid yield and a decrease in gas yield compared to runs with Pittsburgh coal, while the coke yield remained about the same.

The best conditions for co-coking of hydrotreated decant oil with coal in tubing reactors are under atmospheric conditions at 18 h. Hydrotreatment reduced levels of heteroatoms and increased coke quality under atmospheric conditions; however, using autogeneous conditions, the original decant oil produced the best quality products. When co-coking with hydrotreated decant oil in the lab scale coker, increased hydrotreatment improved the quality of the liquids produced, by increasing the saturated cyclic compounds. Introduction of coal into the co-coking process increased the aromatic content of the liquids.

Methods to improve the quality of pitch produced from the liquids from co-coking have been helpful (soaking and oxidation); the methods of distillation and extraction will also be evaluated.

Technical Discussion

Background

Penn State has been involved in a multi-phase fifteen-year program to develop an advanced thermally stable jet fuel for the Air Force **[1-1 -1-4]**. This fuel would resist breaking down at high temperatures (900°F), so it could be used for cooling sensitive parts on high-performance aircraft, as well as providing the propulsion. It is provisionally called JP-900.

At its inception, the JP-900 program presumed that this new fuel would be made entirely or substantially from coal. There are three reasons for this.

Scientific validity. Penn State's researchers have shown clearly that the kinds of chemicals in the fuel that make it stable at 900°F (hydroaromatics and naphthenes) can be derived in abundant amounts from coal. This has been demonstrated in numerous peer-reviewed publications **[1-5 – 1-10].**

Long-term security. Unlike petroleum, coal is a secure, domestic energy resource, for which centuries' worth of reserves remain in the U.S.

Stable procurement. Both petroleum and natural gas are vulnerable to significant price spikes. In contrast, coal companies are willing to write twenty-year delivery contracts at a guaranteed stable price. In turn, this would help stabilize the price of military fuel for decades to come.

To ultimately produce an advanced thermally stable coal-based jet fuel a practical and economically viable process, compatible with current refinery practice, is necessary. The evaluation of this scenario is the subject of this proposal. No refinery is operated for the specific purpose of making jet fuel. Furthermore, refineries are highly integrated, in that many of the individual operations are dependent on, or use streams from, other operations. Therefore, in order to insure that the production of coal-based JP-900 in the jet fuel section of a refinery is acceptable to refinery operators, it is crucial to have data showing the effect of the by-products from coal-based JP-900 production (i.e., the $<180^{o}$C and the $>270^{o}$C fractions) on the quantity and quality of the other refinery products: gasoline, diesel, fuel oil, pitch, and coke.

Options for integrating coal, or a coal liquid product that is currently available commercially (a by-product coal tar distillate from the metallurgical coke industry) into existing refineries are illustrated in **Figure 1-1**. With respect to the first two options, coal can either be added to the coker directly or be co-processed with the resid. Of these, addition of the coal to coker has been selected – in consultation with our refinery partner – as the better option to produce sufficient quantities of coal-based fuel for thermal stability and combustion testing. Each of these approaches has a unique set of technical challenges in terms of specifying the proper feedstocks (for both petroleum- and coal-based components), process conditions (temperature and pressure) and processing approaches.

Previous work at Penn State has resulted in significant progress in identifying the remaining critical barriers to realization of coal-based fuels **[1-11 – 1-20].**

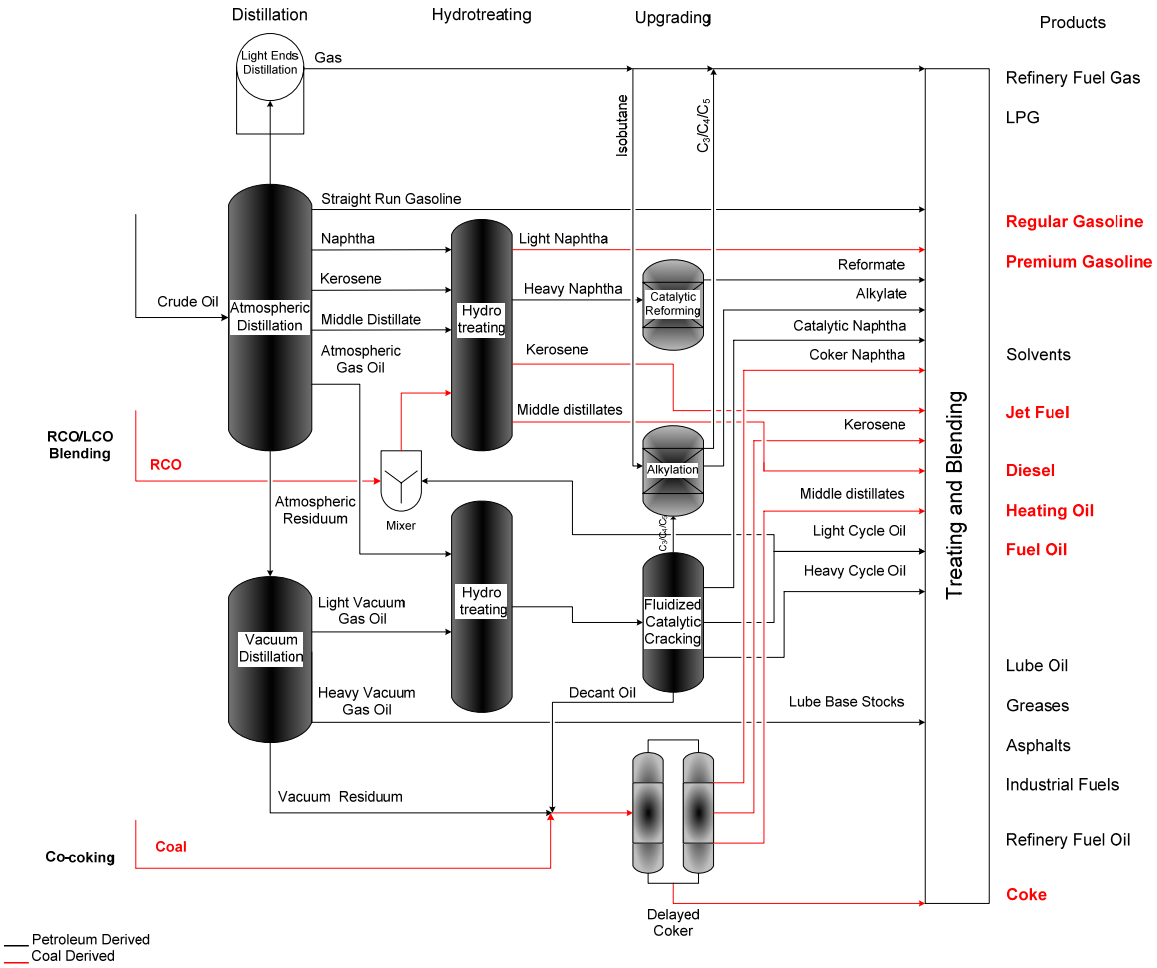

Figure 1-1. Schematic of Integration of Coal into Existing Refineries.

Objectives

A number of potential JP-900-type jet fuels have been produced by Pennsylvania Applied Research Corporation (PARC) from the hydrotreatment of a coal-derived refined chemical oil (RCO) and its mixture with a petroleum-derived light cycle oil (LCO).

The overall objective of this project is to examine the characteristics and quality of the streams other than the jet fuel, and what effect those materials would have on the other unit operations in the refinery, the quality and value of the other products. Broadly, these additional

by-products are the liquids lighter and heavier than jet fuel itself, i.e., the <180°C and the >270°C fractions produced after hydrotreating the RCO/LCO blend and fractionating to recover the jet fuel and other refinery streams.

Prior to the beginning of this project, virtually all work was focused on the jet fuel. However, as we have noted above, no refinery is run for the specific purpose of making jet fuel. Therefore, to make these processes acceptable for adoption in refineries, it is vital to assess their impact on the other major operations and products in a refinery. The acquisition of that knowledge is the basis of this project.

These studies will impact all of the major product streams in a conventional petroleum-based refinery. Therefore, replacing petroleum feedstock with domestic coal, gasoline, diesel, fuel oil and pitch components will favorably impact reducing dependence on, and security of supply of, foreign petroleum resources.

The objectives of the project are to:

- Investigate and develop an understanding of the most promising refinery integration of all process streams resulting from the production of coal-based jet fuel.
- Demonstrate the quality of each of the process streams in terms of refinery requirements to maintain a stable, profitable refinery operation.
- Demonstrate the performance of key process streams in practical testing used for application of these streams.

This fundamental research was proposed as a four-year program. In this document we report activities and accomplishments for the first half of the second contract year. The approach chosen draws on previous work that has now successfully produced a coal-based JP-900 fuel at pilot-plant scale for initial investigations in the fuel stabilization and combustion studies **[1-21 –**

1-23]. In that work, it has been shown that hydrotreated blends of light cycle oil and refined chemical oil (a coal-derived liquid) resulted in the most thermally stable product to date.

This program is investigating the fate of each major product from a refinery complex, except jet fuel, resulting from the refinery integration of coal-derived jet fuel production via a combined RCO/LCO strategy by studying the physical and chemical nature of all products that are perturbed by introduction of coal components into the refinery.

The impact of the proposed research is to provide the scientific and fundamental engineering basis to integrate the production of coal-based jet fuel into existing refinery operations in a time frame consistent with availability and economic forecasts related to petroleum-derived as opposed to coal-based feedstocks. The results of these studies lead to the integration of all non-jet-fuel streams into current refinery operations in concert with desired production of coal-based jet fuel engine testing toward the end of the first decade of the new century. For successful utilization of coal-based jet fuels all non-jet-fuel components must fit existing and future product stream specifications.

Coal tar fractions have been successfully demonstrated to be suitable feedstocks for the production of jet fuels for high-speed aircraft **[1-22, 1-23]**. The jet fuel, as prepared and evaluated in our Air Force project, is a 180-270^{o}C product, cut from a mixture of RCO/LCO total liquid product. Of this product the <180^{o}C cut represents ~4% of the total product and the >270^{o}C fraction represents just over 40% of the total liquid product **[1-24]**. These streams must either be blended as is, chemically converted and then blended, converted to chemicals, or used as feed to the coker.

Scope of Work for Year 3

The technical approach consists of five carefully planned goals whose successful completion will lead to the achievement of the project objectives. These goals include:

- pilot-scale fuel production at PARC,
- evaluation of coal-based gasoline and diesel products in internal combustion engines,
- desulfurization and denitrogenation of coal-based fuels, the saturation of aromatics to improve stability, and the development of chemicals from coal,
- evaluation of coal-based fuel oil, and
- evaluation of pitch and coke materials from coal-based fuel production.

These interrelated goals are designed to evaluate the full utilization of products from coal-based thermally stable jet fuel production and lead toward process integration into existing refineries.

Tasks to be Performed

We are critically analyzing the performance and value of the streams produced from combination of coal-derived components and normal refinery process streams.

The critical analyses include:

- evaluation of gasoline range material in spark-ignited gasoline engines
- evaluation of diesel-range product for use in compression-ignited diesel engines
- evaluation of heavier range materials as heating oils and boiler fuels
- evaluation of products from co-coking strategies as precursors to higher value cokes and carbons.

The following summarizes the technical achievements for the first six months of the third project year.

Task 1. Pilot-Scale Fuel Production at PARC

C. Burgess Clifford (PSU), J. Banes (PARC)

Subtask 1.1 LCO and RCO Procurement

Intertek PARC prepared to do a new run of blended light cycle oil (LCO) and refined chemical oil (RCO); the LCO was procured from United Refining Company in Warren, PA. The RCO was procured from Koppers, Inc., Harmarville, PA. The process was modified at this point in the program to reduce the impact of the coal-derived material on typical refinery catalysts. It was discovered in the previous runs that the 570˚F+ material in the 1:1 LCO/RCO feed was reducing the efficiency of the catalyst. The feed was distilled in order to remove the 570˚F+ fraction. Each of the feed components were distilled separately and then blended together to obtain the final feed for processing. A schematic of the previous runs and the current modifications is shown in **Figure 1-2 (a)-(c).**

The RCO (PR-1660) was distilled in the 150-gallon batch still to remove the 570°F+ material. Three distillations were needed to distill the nine drums of RCO. The first two distillations were done by taking an atmospheric cut at 435°F to take out the light ends and the naphthalene. Once that cut was completed the still was then cooled and vacuum was added to make three additional cuts at 560, 570 and 580°F. The 10°F cuts were taken to best match the desired cut point. The third distillation was done atmospherically.

The first distillation (X-1318) went smoothly during the atmospheric cut to 445°F. Then the still was cooled and 120 mm Hg of vacuum was pulled down. The vacuum lines to the pump plugged with naphthalene crystals and the still was shut down to clean the system. The still was

restarted with a vacuum of 150 mm Hg. It ran and finished the three cuts with no further interruptions.

The second distillation (X-1332) ran very similarly to the first distillation. The atmospheric cut came off at 437°F. Again the still was cooled and the vacuum was pulled down to 150 mm Hg. The vacuum came down to 115 mm Hg before the unit had to be shut down to clean out the vacuum system and change the vacuum oil. Once cleaned, the still was restarted with 100 mm Hg of vacuum and ran at this condition throughout the three cuts with no other problems.

The third and final distillation (X-1333) did not run as the other two had. It started the same with an atmospheric cut first, however it was only taken to 426°F. The still was then shutdown during the weekend and started back up with 150 mm Hg of vacuum. This caused a considerable amount of naphthalene to plug the vacuum system. Due to time constraints the distillation was finished at atmospheric conditions to make a final cut of 560°F. The vacuum lines were later cleaned out and the naphthalene added back into the first cut. This distillation yielded a total loss of only 2.2 wt%. The still data sheets and the simulated distillations, ASTM method D-2887, are in Appendix A. The yield of RCO that will be used for further processing was ~75%.

After the distillations were finished a simulated distillation (SIMDIS GC) was taken on each cut from each distillation. With this information and the yield data, a calculated SIMDIS GC was done to determine the amount of each cut to blend to achieve the proper end point. The calculation as well as the still data sheets and the SIMDIS GC, ASTM method D-2887, are in Appendix A.

The LCO distillation was done at the United Refining Plant in Warren, PA. They cut nine drums of LCO which had a 95 wt% point of 684°F to 594°F. Both the full range and the distilled LCO simulated distillations, ASTM method D-2887, are in Appendix B. The yield of LCO that will be used for further processing is ~63%.

The final blend of RCO and LCO was done at a 1:1 ratio by weight. The LCO was added to the blend tank first at a weight of 2,676 lbs. This was done to keep the 570°F- RCO liquid in the blend to ensure the complete mixture of the two components. If the components were not blended in this way, the naphthalene in the RCO may have set up on the walls of the tank and would not mix completely. The RCO was added next to the blend tank at a weight of 2,676 lbs also. The blend was mixed in the tank for three hours and then drummed off into 55-gallon drums for processing in P67.

In previous work, a simulated distillation (D2887) of LCO and RCO samples was done, and is shown in **Table 1-1**. **[1-25]** Intertek PARC sent LCO and RCO samples of the current run for analysis, and will be compared to the previous analyses. The RCO bottoms was also collected in 55-gal drums (2 drums) and sent to Penn State for testing as a fuel oil for combustion. Discussion on this aspect will be included in Task 4.

(a)

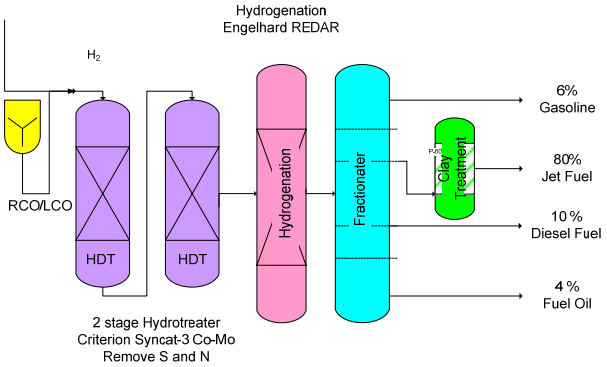

(b)

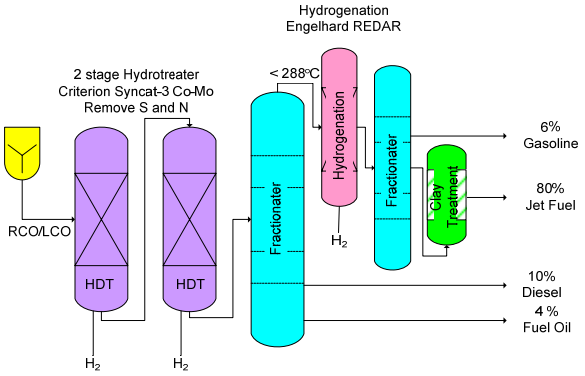

(c)

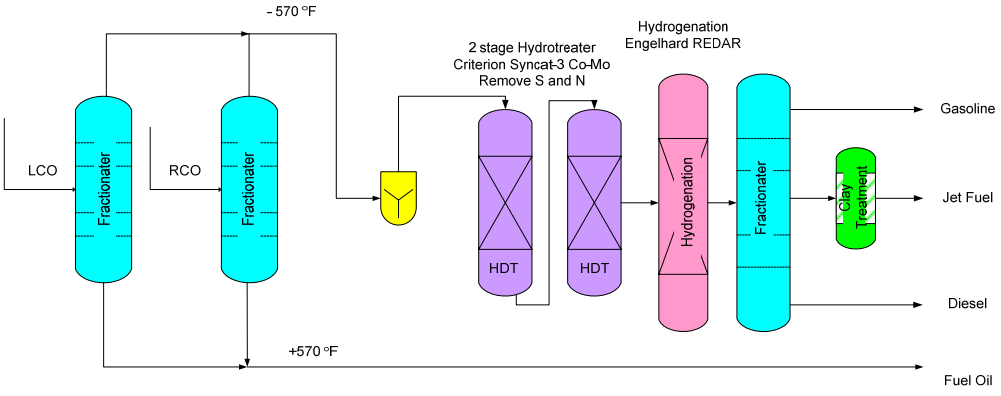

Figure 1-2: (a) Schematic of Fuel Hydrotreating and Hydrogenation, first runs, **(b)** Schematic of Fuel Hydrotreating and Hydrogenation, second runs, **(c)** Modification of Schematic of Fuel Hydrotreating and Hydrogenation currently being run at Intertek PARC, Harmaville, PA.

Table 1-1 United LCO and Koppers RCO
Simulated Distilllations – Previous Run

SAMPLE	LCO PR 1244	RCO PR 1238	1:1 RCO:LCO PR 1251
Instrument	5880	5880	5880
IBP	350	335	341
5%	451	390	396
10%	485	429	431
20%	516	433	436
30%	533	435	440
40%	553	437	486
50%	570	438	534
60%	593	451	551
70%	618	500	577
80%	651	545	625
90%	684	598	667
95%	705	650	704
FBP	771	894	813
% at 356ºF (180ºC)	0.15	1.91	1.36
% at 518ºF (270ºC)	31.2	74.0	45.5
% at 572ºF (300ºC)	50.9	85.1	68.1

Subtask 1.2 Catalyst Preparation

Catalyst, necessary for the deep hydrotreating of total liquid product (TLP), was obtained in this task. In recent work **[1-1, 1-24]**, PARC has used two catalysts for processing. For hydrotreating to remove sulfur and nitrogen, Grace AT-505 catalyst, PC-948, was used. For a deeply hydrogenation of the LCO/RCO blend, USED Engelhard REDAR precious metals hydrogenation catalyst was used. It is expected that these catalysts will be as effective in converting the coal-based blend to a deeply hydrotreated total liquid product. This product has been found to be rich in hydroaromatic components and as a result the jet fuel is thermally very stable. These catalysts must be activated by presulfiding after drying in a flow of hydrogen.

1.2.1 Hydrotreating catalyst - sulfiding

PARC's adiabatic unit P67 was charged with Grace AT-505 catalyst, PC-948, in the amounts shown below. Reactor 1 was loaded with inerts in the quench zones as shown in **Figure 1-3**.

Reactor 1	2190 cc	1964 gm
Reactor 2	2655 cc	2382 gm
Total	4845 cc	4346 gm

The catalyst was sulfided before feed was put into the unit. The catalyst was dried at 300°F under a 15.2 scf/hr nitrogen flow at atmospheric pressure for 30 minutes. The unit was

then set to 450 psig under hydrogen at a gas rate of 30.4 scf/hr. The H_2S scrubber was not used during sulfiding to ensure that the catalyst was always in a sulfur rich environment. Sulfiding feed consisting of hydrotreated diesel with 1.5 wt% sulfur as dimethyldisulfide was started into the unit at a rate of 3924 g/hr. The temperatures were then raised on both reactors to 450˚F at a rate of 75˚F/hr. This temperature was held until there was H_2S breakthrough and then taken up to 550˚F at a rate of 50˚F/hr. Once this temperature was reached it was held for one hour and then reduced to 300˚F and the unit was then ready for run feed.

The operating conditions summary is contained in **Table 1-2**, while the GC analyses of products is in **Table 1-3**.

Figure 2

P63-67 #1 Reactor Layout

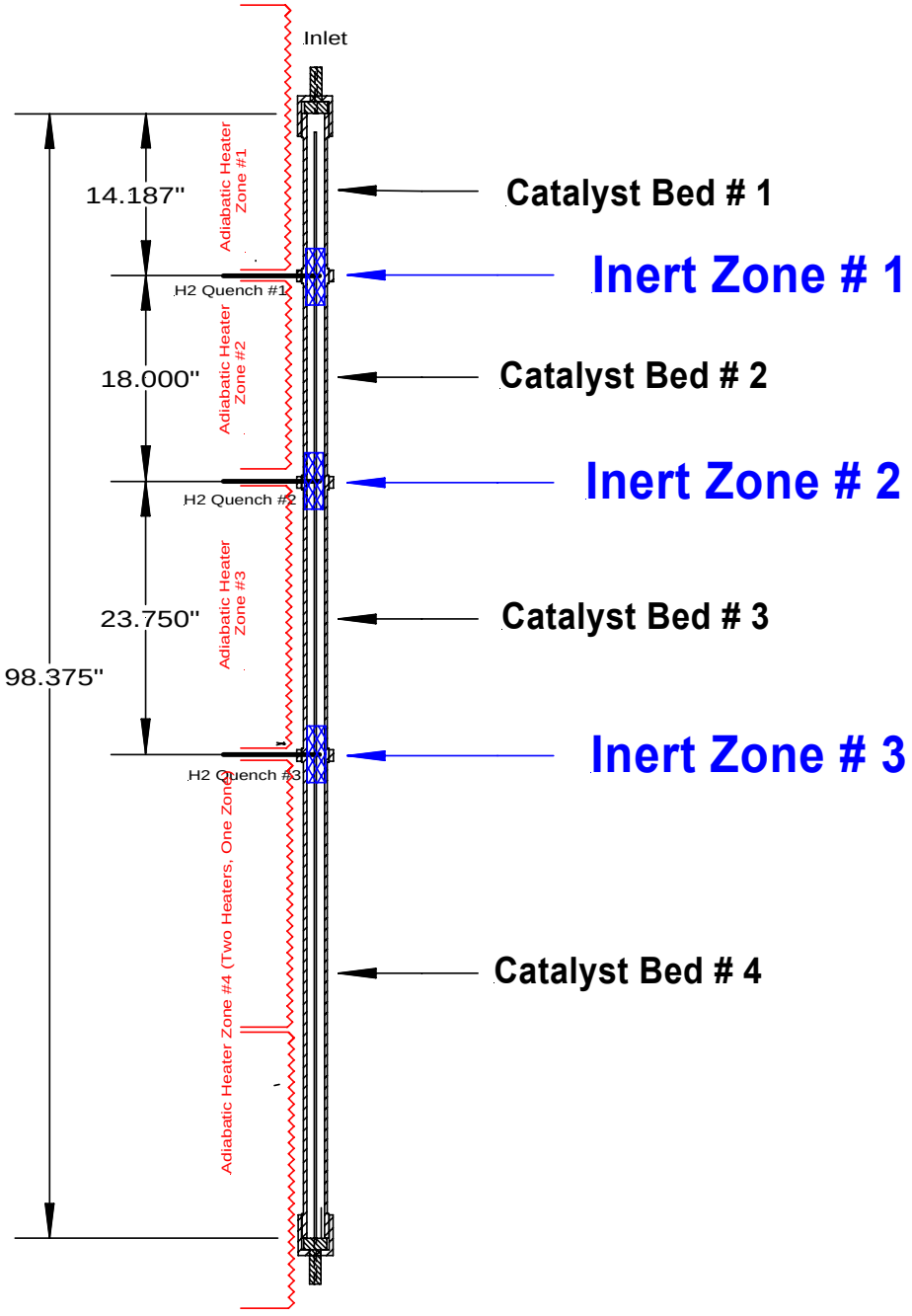

Figure 1-3: Reactor P67 layout.

Table 1-2: Hydrotreating of 1:1 LCO/RCO Feed Cut to 570°F.

CATALYST CHARGE		ml	gm
	Rx1	2190	1964
	Rx2	2655	2382
	Total	4845	4346

Run No. P-67	Time	Date 2006	Feed gms/hr	Reactor 1 Temps In	Out	WABT	Reactor 2 Temps In	Bed 4/Out	WABT	Comb. WABT	Press. psig	LHSV	Inlet gas scf/bbl	Quench scf/bbl	Makeup scf/bbl	% H2 Inlet	H_2 Cons. scf/bbl	Wt. Bal %	TLP Analyses Sp. Gr.	API	Sulfur ppm	Nitrogen ppm	Tetralin Wt %	356°F- wt%
			4 HOUR AVERAGE																					
108-SU	***0000***	***7/16***	***Start of catalyst drying @ 300°F***																					
108-SU	***1600***	***7/18***	***Start of catalyst sulfiding***																					
108-SU	***0200***	***7/20***	***Finished Catalyst sulfiding and switched to run feed***																***1.0107***	***9.0***	***14100***	***2300***	***-***	***2.1***
108-1	0400	7/20	2785	485	598	539	509	509	548	543	577	0.61	2856	0	1295	91.9	649	79.3	0.9735	13.9				
108-1	***2000***	***7/20***	***Shutdown due to compressor failure***																					
108-1	***1200***	***7/25***	***Started up with new compressor***																					
108-1	0400	7/26	2459	527	614	578	485	406	478	528	597	0.50	3036	3676	1650	99.2	1327	98.7	0.9390	19.2	4.8	NA	32.6	
108-1	0400	7/27	2498	549	707	605	552	566	598	602	595	0.51	3032	3118	2337	98.9	1959	99.3	0.9340	20.0	4.3	NA	28.9	
108-1	0400	7/28	2466	549	594	572	550	616	622	597	599	0.50	3017	3615	2149	99.1	1764	98.1	0.9433	18.5	5.3	5.4	28.8	5.9
108-1	***0600***	***7/28***	***Switched to Feed drum # 2***																					
108-1	**1200**	**7/28**	**Finished Product Drum # 1**																		**143.8**	**66.2**	**29.2**	**5.4**
108-1	***1200***	***7/28***	***Shutdown due to metals in the compressor check***																					
108-2	***2000***	***7/28***	***Started unit up again***																					
108-2	0400	7/29	2404	536	452	488	522	475	532	510	600	0.49	3216	4020	1126	99.3	-	101.8	0.9427	18.6	No analysis, lining out the unit			
108-2	0400	7/30	2504	550	605	574	550	575	606	590	601	0.51	2934	2947	2104	99.3	1769	98.6	0.9427	18.6	8.6	3.2	29.8	5.3
108-2	0400	7/31	2455	548	601	572	551	611	621	596	599	0.50	3028	2762	2112	99.0	1775	98.6	0.9433	18.5	4.9	4.8	29.5	5.4
108-2	0400	8/1	2459	550	592	572	549	611	618	595	605	0.50	2943	3122	2061	98.9	1720	98.8	0.9456	18.1	7.7	19.0	30.6	6.3
108-2	***1700***	***8/1***	***Switched to Feed drum # 3***																					
108-2	**2000**	**8/1**	**Finished Product Drum # 2**																		**6.4**	**8.1**	**26.7**	**5.6**
108-2	0400	8/2	2482	549	588	571	549	612	614	593	596	0.51	2951	3165	2005	99.0	1673	98.9	0.9469	17.9	11.0	40.5	30.2	6.3
108-3	***1400***	***8/2***	***Increased the outlet temperature of each bed to 650°F***																					
108-3	0400	8/3	2419	595	642	614	601	600	629	622	599	0.49	3103	7222	2228	98.8	1863	91.7	0.9387	19.2	3.8	1.6	27.8	6.4
108-3	0400	8/4	2468	601	639	605	609	650	642	624	600	0.50	2602	6601	2435	98.6	2014	96.5	0.9343	20.0	3.2	<1	28.5	7.2
108-3	**0400**	**8/4**	**Finished Product Drum # 3**																		**2.8**	**9.7**	**28.8**	**6.2**
108-3	***2000***	***8/4***	***Switched to Feed Drum # 4***																					
108-3	0400	8/5	2467	596	533	574	589	693	652	613	595	0.50	3045	9081	2414	97.9	1947	97.7	0.9393	19.2	<1	<1	26.7	6.4
108-3	0400	8/6	2435	598	242	567	603	677	646	606	596	0.50	3068	9036	2568	98.9	2097	97.7	0.9387	19.2	<1	<1	28.0	6.3
108-3	0400	8/7	2500	598	661	608	600	653	632	620	596	0.51	2984	7904	2470	98.9	1997	97.5	0.9384	19.3	1.5	<1	28.0	6.8
108-3	***2000***	***8/7***	***Switched to Feed Drum # 5***																					
108-3	0400	8/8	2524	595	703	624	629	676	661	643	596	0.52	2955	5148	2669	98.5	2218	97.8	0.9353	19.8	<1	<1	30.4	6.6
108-3	**1200**	**8/8**	**Finished Product Drum # 4**																		**4.2**	**2.3**	**28.9**	**6.3**
108-3	0400	8/9	2460	597	628	605	600	652	634	619	600	0.50	3022	7671	2807	99.1	2322	97.8	0.9387	19.2	<1	<1	32.0	6.4
108-3	0400	8/10	2436	598	625	612	598	645	628	620	600	0.50	3012	7726	2774	98.9	2312	97.7	0.9381	19.3	<1	<1	31.2	6.3
108-3	0400	8/11	2460	598	670	619	606	656	636	628	598	0.50	3009	7184	2906	98.8	2427	98.1	0.9377	19.4	<1	<1	29.1	6.5
108/3	***0800***	***8/11***	***Switched to Feed Drum # 6 (Partial Drum)***																					
108-3	**2000**	**8/11**	**Finished Product Drum # 5**																		**1.1**	**<1**	**29.5**	**5.6**
108-3	0400	8/12	2495	599	668	624	609	653	641	633	600	0.51	2994	5996	2508	98.3	2051	97.6	0.9378	19.4	<1	<1	28.8	6.3
108-3	0400	8/13	2390	599	677	618	604	655	638	628	595	0.49	3114	6155	2591	99.0	1914	100.7	0.9381	19.3	<1	<1	28.4	6.3
108-3	***0600***	***8/13***	***Switched to Feed Drum # 7***																					
108-3	0400	8/14	2589	601	601	606	598	662	639	622	598	0.53	2945	7538	2396	99.1	1951	96.4	0.9409	18.9	3.6	<1	28.9	6.3
108-3	0400	8/15	2448	602	609	605	625	640	647	626	600	0.50	3078	8083	2268	98.3	1956	97.3	0.9390	19.2	2.7	<1	26.6	6.3
108-3	**0400**	**8/15**	**Finished Product Drum # 6**																		**<1**	**<1**	**27.1**	**5.7**
108-3	***1600***	***8/15***	***Unit shutdown due to compressor discharge check plugged***																					
110-1	***2000***	***10/11***	***Unit started up to finish hydrotreating***																					
110-1	0400	10/12	1469	216	203	215	265	233	255	235	600	0.30	52978	0	47407	98.0	17902	164.9	1.0107	8.5	-	-	-	-
110-1	0400	10/13	2496	522	545	567	523	474	518	543	608	0.51	3158	377	2562	98.4	1232	100.9	1.0107	8.5	-	-	-	-
110-1	0400	10/14	2390	598	598	610	591	650	624	617	603	0.49	922	2784	2598	59.8	2130	102.7	0.9409	18.9	11.1	-	29.7	-
110-1	***2400***	***10/14***	***Shutdown unit due to plug in bleed off and reactivator lines***																					
110-2	***2200***	***10/16***	***Started up unit with hydrogen flow only until reactors are at 300°F***																					
110-2	0400	10/17	8	254	90	131	389	155	249	190	605	0.00	564685	#DIV/0!	489350	92.4	-	225.1	0.9421	18.7	-	-	-	-
110-2	0400	10/18	2405	555	638	598	464	376	451	524	597	0.49	4272	0	2763	49.8	2088	110.0	0.9421	18.7	-	-	-	-
110-2	0400	10/19	2417	614	662	630	595	622	621	625	608	0.50	3374	2898	2691	93.9	2131	100.0	0.9340	20.0	4.4	-	28.9	6.2
110-2	0400	10/20	2378	617	643	629	607	647	637	633	604	0.49	2900	2842	2398	98.6	2202	99.4	0.9322	20.3	5.4	-	27.3	-
110-2	0400	10/21	2481	618	644	629	597	633	625	627	601	0.51	2935	2784	2469	98.3	2063	100.4	0.9355	19.8	4.6	-	29.6	7.0
110-2	**2000**	**10/21**	**Finished Product Drum # 1**																**0.9390**	**19.2**	**6.7**	**<1**	**28.4**	**5.4**
110-2	0400	10/22	2452	621	662	637	616	652	642	640	601	0.50	2898	2463	2493	98.7	2099	97.7	0.9325	20.3	3.3	-	27.6	7.2
110-2	0400	10/23	2446	619	651	636	612	650	641	639	597	0.50	3066	2588	2448	98.6	2049	98.4	0.9334	20.1	1.2	-	28.0	7.0
110-2	0400	10/24	2492	620	634	634	606	635	630	632	600	0.51	2900	2842	2398	98.6	2013	98.7	0.9337	20.0	3.0	-	27.8	7.0
110-2	**2400**	**10/24**	**Finished Product Drum # 2**																**0.9340**	**20.0**	**4.5**	**<1**	**27.5**	**6.4**
110-2	0400	10/25	2456	619	637	632	617	659	648	640	602	0.50	3008	2684	2390	56.6	2057	97.5	0.9313	20.4	4.1	-	27.5	7.2
110-2	0400	10/26	2464	620	665	639	610	655	647	643	598	0.50	2985	2055	2557	99.0	2180	98.2	0.9334	20.1	8.3	-	28.5	6.4
110-2	0400	10/27	2519	620	657	637	622	650	644	640	601	0.51	2905	2146	2518	98.9	2158	97.4	0.9280	21.0	2.0	-	**26.1**	6.3
110-2	0400	10/28	2487	621	652	635	615	653	644	640	602	0.51	3059	2314	2419	98.8	2059	98.3	0.9377	19.4	107.4	-	29.3	6.2
110-2	**0800**	**10/28**	**Finished Product Drum # 3**																**0.9326**	**20.2**	**3.4**	**<1**	**28.5**	**6.2**
110-2	0400	10/29	2456	622	645	634	617	650	645	639	600	0.50	2979	2414	2345	98.4	1983	97.9	0.9374	19.4	310.4	-	29.6	6.3
110-2	0400	10/30	2456	623	648	637	617	653	644	640	600	0.50	2976	2300	2319	98.8	1959	97.9	0.9377	19.4	25.9	-	26.0	6.2
110-2	0400	10/31	2473	623	659	634	630	651	649	641	600	0.50	2969	2216	2321	98.7	1971	98.1	0.9387	19.2	3.4	-	28.4	6.1
110-2	**1200**	**10/31**	**Finished Product Drum # 4**																		**5.0**	**<1**	**29.6**	**6.2**
110-2	0400	11/1	2438	622	646	635	625	654	645	640	602	0.50	3016	2275	2307	98.4	1955	97.8	0.9307	20.5	2.2	-	28.6	6.2
110-2	0400	11/2	2436	623	645	636	627	653	647	642	600	0.50	3015	2304	2313	98.4	1953	98.5	0.9368	19.5	5.3	-	29.4	6.1
110-2	0400	11/3	2420	625	646	628	628	651	648	638	600	0.50	2980	1951	2095	98.1	1741	99.3	0.9387	19.2	2.9	-	28.2	6.2
110-2	***0600***	***11/3***	***Finished SR-0269 and started repassing off-stream product***																					
110/2	**0800**	**11/3**	**Finished Product Drum # 5 (This is the last First Pass TLP)**																**0.9354**	**19.8**	**2.5**	**<1**	**28.6**	**6.2**
110-2	0400	11/4	2289	650	662	645	640	658	654	650	599	0.50	3003	829	1153	98.8	791	98.7	0.9107	23.9	<1	-	19.2	5.3
110-2	0400	11/5	2287	653	646	646	638	648	647	647	600	0.50	3053	301	1034	98.9	678	97.2	0.9212	22.1	<1	-	21.6	5.3
110-2	0400	11/6	2255	654	648	647	640	649	648	647	599	0.49	3001	0	1016	98.9	662	98.5	0.9230	21.8	<1	-	21.4	5.3
110-2	***1800***	***11/6***	***Second reactor plugged. Heats turned off and 2nd reactor is by-passed***																					
110-2	**2000**	**11/6**	**Finished Product Drum # 6 (First second pass TLP)**																**0.9183**	**22.6**	**2.2**	**<1**	**20.8**	**5.7**
110-2	0400	11/7	2260	635	641	638	603	549	539	588	597	0.50	3114	1600	1135	98.9	776	97.9	0.9297	20.7	<1	-	28.0	6.2
110-2	0400	11/8	2330	636	649	642	315	278	285	464	602	0.51	2949	1489	1053	98.9	712	98.5	0.9352	19.8	1.8	-	27.7	6.1
110-2	0400	11/9	2265	637	649	643	180	173	172	408	596	0.49	3067	1476	1062	98.8	714	98.2	0.9352	19.8	<1	-	27.8	6.1
110-2	**2000**	**11/9**	**Finished Product Drum # 7**																**0.9334**	**20.1**				

Table 1-3: Daily GC Analyses of Hydrotreated TLP Products.

Column: 150 meter x 0.25mm, Supelco DH150 Petrocal FID Film Thickness 1 micron **United Refining LCO - RCO Hydrotreating**

GC No.	SAMPLE	Benz	Cyclo Hexane	Et B	Xyl's	Indan (1)	t-Dec	c-Dec	Tetralin	N	MNS		EtN's	DMN'S								TOTAL DMN's	TOTAL MNS	Tri- Me Subst MN's	Tetra	5+6	Other
											2MN	1MN		2,6	2,7	1,7	1,6	2,3	1,5	1,2	1,8						
3592	SR-0269	-	0.90	-	0.34	0.32	-	0.04	-	36.24	5.81	3.05	2.09	2.15	1.88	3.86	1.94	1.22	0.44	0.74	0.36	12.59	8.86	5.32	2.93	0.57	33.49
3594	P67-108 TLP 7/26/06	0.02	0.66	-	0.88	1.39	2.32	0.70	32.61	0.48	2.13	0.05	2.58	0.11	0.22	0.14	0.61	0.83	1.57	0.14	0.54	4.16	2.18	2.03	0.88	-	90.27
3596	P67-108 TLP 7/27/06	0.05	1.10	-	0.91	1.25	3.81	1.31	28.94	1.08	1.91	0.16	2.47	0.31	0.32	0.16	0.67	0.80	1.33	0.11	0.42	4.12	2.07	2.00	2.19	-	88.54
3598	P67-108 TLP 7/28/06	0.02	0.87	-	0.89	1.33	2.35	0.79	28.76	2.85	1.83	0.45	2.42	0.49	0.53	0.87	0.88	0.79	1.18	0.18	0.45	5.37	2.28	2.71	2.96	-	83.83
3606	**DRUM # 1 TLP**	**-**	**0.35**	**-**	**0.82**	**1.32**	**2.51**	**0.85**	**29.24**	**3.59**	**1.87**	**0.43**	**2.52**	**0.45**	**0.48**	**0.79**	**0.84**	**0.86**	**1.27**	**0.18**	**0.49**	**5.36**	**2.30**	**2.07**	**-**	**-**	86.68
3600	P67-108 TLP 7/30/06	0.02	0.86	-	0.84	1.34	2.96	0.85	29.83	1.02	1.92	0.14	2.47	0.26	0.29	0.11	0.69	0.81	1.31	0.10	0.52	4.09	2.06	2.11	2.33	-	88.39
3601	P67-108 TLP 7/31/06	0.02	0.96	-	0.90	1.39	2.50	0.82	29.48	2.67	1.85	0.43	2.45	0.47	0.51	0.82	0.87	0.80	1.23	0.17	0.47	5.34	2.28	2.19	1.03	0.30	86.19
3605	P67-108 TLP 8/1/06	-	0.49	-	0.90	1.40	2.05	0.68	30.61	2.78	1.96	0.32	2.56	0.47	0.52	0.83	0.90	0.83	1.24	0.17	0.51	5.47	2.28	2.26	-	-	87.21
3609	**DRUM # 2 TLP**	**-**	**0.38**	**-**	**0.78**	**1.23**	**3.30**	**0.95**	**26.72**	**2.07**	**1.71**	**0.30**	**2.26**	**0.38**	**0.42**	**0.56**	**0.76**	**0.74**	**1.13**	**0.15**	**0.44**	**4.58**	**2.01**	**1.78**	**8.85**	**-**	**80.71**
3608	P67-108 TLP 8/2/06	-	0.49	-	0.90	1.46	1.68	0.55	30.23	3.18	1.88	0.47	2.35	1.67	0.79	0.48	0.53	0.80	1.15	0.18	0.50	6.10	2.35	2.25	2.54	-	83.58
3612	P67-108 TLP 8/3/06	0.03	0.90	-	0.83	1.27	4.29	1.30	27.81	1.82	1.78	0.29	2.41	0.39	0.42	0.52	0.77	0.80	1.33	0.15	0.41	4.79	2.07	2.00	1.58	0.25	87.49
3614	P67-108 TLP 8/4/06	0.03	0.99	-	0.88	1.29	3.85	1.19	28.49	1.63	1.83	0.25	2.45	0.37	0.40	0.47	0.76	0.79	1.35	0.14	0.43	4.71	2.08	1.93	1.25	-	88.40
3620	**DRUM # 3 TLP**	**0.02**	**0.78**	**-**	**0.85**	**1.32**	**3.36**	**1.05**	**28.79**	**2.15**	**1.84**	**0.31**	**2.43**	**0.41**	**0.44**	**0.58**	**0.80**	**0.79**	**1.26**	**0.15**	**0.44**	**4.87**	**2.15**	**2.01**	**1.67**	**-**	**87.15**
3616	P67-108 TLP 8/5/06	0.04	0.97	-	0.87	1.32	3.59	1.15	26.71	3.93	1.64	0.59	2.28	0.61	0.63	0.98	0.93	0.77	0.11	0.21	0.36	4.60	2.23	2.17	2.32	-	84.75
3617	P67-108 TLP 8/6/06	0.03	0.94	-	0.84	1.31	3.41	1.08	28.04	2.64	1.77	0.43	2.38	0.48	0.50	0.71	0.84	0.78	1.23	0.17	0.41	5.12	2.20	1.98	1.85	-	86.21
3621	P67-108 TLP 8/7/06	0.03	0.91	-	0.87	1.29	3.74	1.21	28.01	2.04	1.78	0.32	2.39	0.43	0.45	0.59	0.80	0.78	1.27	0.16	0.41	4.89	2.10	1.88	1.74	-	87.35
3624	P67-108 TLP 8/8/06	0.05	1.44	-	1.04	1.44	5.42	1.75	30.40	2.68	1.99	0.44	2.87	0.63	0.64	0.83	1.04	0.27	0.95	1.42	-	5.78	2.43	-	1.18		87.93
3623	**DRUM # 4 TLP**	**0.03**	**0.83**	**-**	**0.85**	**1.32**	**3.37**	**1.08**	**28.86**	**1.93**	**1.83**	**0.29**	**2.42**	**0.4**	**0.43**	**0.55**	**0.78**	**0.79**	**1.3**	**0.15**	**0.43**	**4.83**	**2.12**	**1.85**	**1.81**	**0.04**	**87.42**
3626	P67-108 TLP 8/9/06	0.03	1.28	-	0.95	1.56	3.37	1.07	31.98	1.82	1.96	0.29	2.57	0.4	0.43	0.52	0.81	0.85	1.4	0.16	0.48	5.05	2.25	0.11	-	-	90.77
3628	P67-108 TLP 8/10/06	0.03	1.35	-	0.90	1.45	3.29	1.03	31.15	1.67	1.90	0.26	2.48	0.36	0.4	0.48	0.77	0.89	1.42	0.14	0.46	4.92	2.16	2.44	0.40	-	88.41
3630	P67-108 TLP 8/11/06	0.03	1.03	-	0.90	1.38	3.71	1.18	29.06	1.83	1.80	0.28	2.39	0.39	0.41	0.52	0.76	0.77	1.29	0.14	0.42	4.70	2.08	1.91	1.49	-	87.99
3632	**DRUM # 5 TLP**	**0.01**	**0.63**	**-**	**0.77**	**1.35**	**3.21**	**1.03**	**29.50**	**1.69**	**1.83**	**0.26**	**2.43**	**0.37**	**0.4**	**0.49**	**0.76**	**0.78**	**1.33**	**0.14**	**0.44**	**4.71**	**2.09**	**2.28**	**1.81**	**-**	**87.42**
3633	P67-108 TLP 8/12/06	0.02	0.93	-	0.81	1.26	3.23	1.04	28.79	1.73	1.85	0.27	2.46	0.38	0.42	0.52	0.78	0.8	1.35	0.15	0.45	4.85	2.12	2.51	1.69	-	87.10
3634	P67-108 TLP 8/13/06	0.02	0.93	-	0.82	1.26	3.02	0.98	28.41	1.80	1.85	0.29	2.48	0.4	0.43	0.55	0.8	0.8	1.35	0.15	0.45	4.93	2.14	2.56	1.84	0.35	86.38
3635	P67-108 TLP 8/14/06	0.03	0.84	-	0.83	1.32	2.74	0.89	28.93	2.75	1.82	0.44	2.46	0.49	0.53	0.75	0.88	0.8	1.27	0.18	0.44	5.34	2.26	2.78	0.92	0.30	85.65
3637	P67-108 TLP 8/15/06	0.04	0.64	-	0.77	1.14	2.60	0.83	26.64	1.21	1.76	0.2	2.33	0.32	0.35	0.38	0.69	0.76	1.29	0.13	0.44	4.36	1.96	2.60	3.69	3.61	82.57
3638	**DRUM # 6 TLP**	**0.02**	**0.63**	**-**	**0.75**	**1.21**	**2.87**	**0.93**	**27.11**	**1.77**	**1.74**	**0.28**	**2.32**	**0.37**	**0.41**	**0.52**	**0.74**	**0.75**	**1.25**	**0.14**	**0.42**	**4.60**	**2.02**	**2.23**	**4.17**	**4.01**	**81.20**
3645	P67-110 TLP 10/14/06	0.02	0.82	-	0.80	1.33	3.23	1.16	29.67	2.24	1.94	0.38	2.59	0.42	0.49	0.76	0.86	0.8	1.29	0.14	0.45	5.21	2.32	2.47	0.38	0.30	87.08
3647	P67-110 TLP 10/19/06	0.03	1.09	-	0.87	1.27	4.09	1.38	28.94	0.95	1.85	0.14	2.47	0.28	0.29	0.26	0.66	0.79	1.42	0.1	0.44	4.24	1.99	1.97	2.16	-	88.69
3649	P67-110 TLP 10/20/06	0.03	1.09	-	0.89	1.24	5.00	1.7	27.27	1.39	1.76	0.20	2.37	0.34	0.34	0.38	0.69	0.77	1.3	0.12	0.39	4.33	1.96	2.15	2.34	-	87.83
3651	P67-110 TLP 10/21/06	0.03	1.06	-	0.88	1.32	3.14	1.08	29.57	1.07	1.91	0.16	2.50	0.3	0.32	0.32	0.69	0.8	1.4	0.11	0.48	4.42	2.07	2.01	2.48	-	87.95
3654	**P67-110 DRUM # 1**	**0.01**	**0.63**	**-**	**0.77**	**1.29**	**3.45**	**1.20**	**28.39**	**1.30**	**1.94**	**0.21**	**1.87**	**0.34**	**0.37**	**0.40**	**0.75**	**0.82**	**1.38**	**0.12**	**0.48**	**4.66**	**2.15**	**2.21**	**2.22**	**-**	**87.46**
3652	P67-110 TLP 10/22/06	0.04	1.18	-	0.90	1.29	4.60	1.57	27.59	1.48	1.81	0.22	1.95	0.36	0.37	0.42	0.72	0.78	1.3	0.13	0.41	4.49	2.03	2.14	1.59	-	88.27
3653	P67-110 TLP 10/23/06	0.04	1.18	-	0.88	1.27	4.17	1.42	28.00	1.43	1.86	0.22	2.01	0.36	0.37	0.42	0.73	0.8	1.36	0.13	0.43	4.60	2.08	1.81	0.27	0.38	89.43
3656	P67-110 TLP 10/24/06	0.03	0.97	-	0.84	1.24	3.10	1.06	27.80	1.03	1.81	0.16	2.40	0.3	0.32	0.31	0.67	0.79	1.36	0.12	0.46	4.33	1.97	2.20	3.81	-	86.66
3661	**P67-110 DRUM # 2**	**0.03**	**0.83**	**-**	**0.87**	**1.26**	**4.19**	**1.43**	**27.46**	**1.46**	**1.81**	**0.23**	**2.42**	**0.36**	**0.37**	**0.42**	**0.72**	**0.78**	**1.31**	**0.13**	**0.42**	**4.51**	**2.04**	**2.13**	**2.28**	**-**	**87.58**
3658	P67-110 TLP 10/25/06	0.04	1.36	-	0.90	1.29	3.76	1.27	27.46	1.57	1.80	0.24	2.44	0.37	0.39	0.47	0.74	0.78	1.33	0.13	0.42	4.63	2.04	2.12	3.50	-	86.14
3660	P67-110 TLP 10/26/06	0.03	0.95	-	0.87	1.28	3.77	1.32	28.50	1.89	1.88	0.29	2.52	0.42	0.44	0.56	0.80	0.81	1.34	0.15	0.44	4.96	2.17	2.29	0.10	0.39	88.20
3672	P67-110 TLP 10/27/06	0.02	0.88	0.15	0.78	1.14	3.28	1.12	26.08	1.38	1.72	0.21	2.29	0.33	0.35	0.41	0.68	0.73	1.25	0.12	0.22	4.09	1.93	1.96	5.66	5.00	79.98
3664	P67-110 TLP 10/28/06	0.02	0.78	-	0.85	1.32	3.49	1.20	29.32	1.58	1.92	0.24	2.55	0.37	0.39	0.46	0.76	0.81	1.39	0.13	0.46	4.77	2.16	2.21	0.25	0.28	88.75
3663	**P67-110 DRUM # 3**	**0.03**	**0.93**	**-**	**0.87**	**1.28**	**3.84**	**1.31**	**28.46**	**1.61**	**1.86**	**0.24**	**2.48**	**0.37**	**0.40**	**0.47**	**0.75**	**0.79**	**1.34**	**0.13**	**0.44**	**4.69**	**2.10**	**2.15**	**1.33**	**0.44**	**87.68**
3665	P67-110 TLP 10/29/06	0.02	0.76	-	0.91	1.35	3.40	1.16	29.56	1.48	1.93	0.22	2.54	0.35	0.38	0.43	0.75	0.80	1.39	0.13	0.47	4.70	2.15	2.00	0.27	0.28	89.12
3666	P67-110 TLP 10/30/06	0.02	0.78	-	0.77	1.16	2.97	1.01	26.01	1.37	1.72	0.21	2.28	0.32	0.35	0.41	0.68	0.72	1.25	0.11	0.22	4.06	1.93	2.00	4.37	7.40	78.87
3668	P67-110 TLP 10/31/06	0.02	0.95	-	0.86	1.24	3.26	1.12	28.40	1.49	1.93	0.24	2.59	0.37	0.40	0.46	0.77	0.83	1.42	0.13	0.25	4.63	2.17	2.26	1.15	0.58	87.72
3671	**P67-110 DRUM # 4**	**0.02**	**0.75**	**0.16**	**0.87**	**1.32**	**3.23**	**1.11**	**29.58**	**1.44**	**1.96**	**0.22**	**2.58**	**0.35**	**0.39**	**0.43**	**0.75**	**0.82**	**1.41**	**0.13**	**0.25**	**4.53**	**2.18**	**2.18**	**0.03**	**0.32**	**89.32**
3670	P67-110 TLP 11/1/06	0.02	0.73	0.16	0.91	1.30	3.46	1.18	28.64	1.50	1.87	0.23	2.46	0.35	0.38	0.44	0.73	0.78	1.37	0.13	0.23	4.41	2.10	2.10	3.19	-	86.70
3674	P67-110 TLP 11/2/06	0.02	0.77	0.16	0.87	1.31	3.33	1.13	29.35	1.54	1.94	0.24	2.57	0.36	0.39	0.46	0.77	0.81	1.43	0.13	0.24	4.59	2.18	1.76	0.18	0.39	89.36
3676	P67-110 TLP 11/3/06	0.02	0.79	0.15	0.86	1.20	2.91	1.00	28.17	1.45	1.94	0.29	2.59	0.36	0.40	0.46	0.77	0.82	1.44	0.13	0.25	4.63	2.23	1.78	2.34	-	87.57
3677	**P67-110 DRUM # 5**	**0.02**	**0.76**	**0.15**	**0.86**	**1.27**	**3.25**	**1.10**	**28.63**	**1.73**	**1.89**	**0.28**	**2.53**	**0.38**	**0.41**	**0.50**	**0.77**	**0.81**	**1.39**	**0.13**	**0.24**	**4.63**	**2.17**	**1.79**	**1.44**	**0.37**	**87.87**
3679	P67-110 TLP 11/4/06	0.04	1.13	0.11	0.57	0.82	10.70	3.02	19.23	1.41	1.49	0.62	2.28	0.38	0.69	0.45	0.71	0.80	1.04	0.13	0.24	4.44	2.11	2.33	1.98	0.67	87.06
3680	P67-110 TLP 11/5/06	0.04	1.02	0.11	0.59	0.92	9.60	2.75	21.56	1.32	1.58	0.60	2.26	0.36	0.70	0.39	0.68	0.76	1.02	0.12	0.26	4.29	2.18	2.05	2.13	0.61	87.42
3682	P67-110 TLP 11/6/06	0.03	0.73	-	0.55	0.90	9.49	2.62	21.39	1.38	1.58	0.58	2.26	0.37	0.70	0.42	0.68	0.76	1.03	0.12	0.27	4.35	2.16	2.15	3.29	-	86.67
3685	**P67-110 DRUM # 6**	**0.03**	**0.82**	**0.12**	**0.62**	**0.91**	**10.50**	**2.88**	**20.81**	**1.36**	**1.54**	**0.64**	**2.23**	**0.36**	**0.70**	**0.40**	**0.67**	**0.76**	**1.01**	**0.12**	**0.27**	**4.29**	**2.18**	**2.12**	**0.88**	**0.41**	**88.76**
3684	P67-110 TLP 11/7/06	0.03	0.76	0.21	0.76	1.23	4.43	1.35	28.02	1.45	1.81	0.33	2.43	0.37	0.75	0.42	0.72	0.77	1.30	0.12	0.42	4.87	2.14	2.06	2.99	-	86.49
3686	P67-110 TLP 11/8/06	0.03	0.86	0.19	0.73	1.21	4.28	1.32	27.71	1.64	1.78	0.25	2.41	0.40	0.74	0.48	0.75	0.77	1.29	0.13	0.41	4.97	2.03	2.40	3.84	-	85.12
3689	P67-110 TLP 11/9/06	0.03	0.83	0.19	0.72	1.20	4.17	1.29	27.83	1.62	1.79	0.24	2.41	0.40	0.75	0.47	0.75	0.77	1.30	0.13	0.42	4.99	2.03	2.39	3.82	-	85.15
3691	**P67-110 DRUM # 7**																										

1.2.2 Hydrogenation catalyst reduction

PARC's adiabatic unit P67 was charged with USED Engelhard REDAR precious metals hydrogenation catalyst, PC-765, in amounts shown below. The No 1 reactor was loaded with inert material in the quench zones as indicated in **Figure 1-3**.

Rx 1	2539 ml	1869 gm
Rx 2	2660 ml	1957 gm
Total	5199 ml	3826 gm

The catalyst was reduced prior to introducing run feed. Hydrogen was introduced at a flow rate of about 47 scf/hr at 600 psig. Reactor temperatures were then brought up to 212˚F temperature slowly over a period of 9 hrs and then held for about 1 hr before continuing to raise the temperature to about 392˚F (200˚C) over a period of 8 hrs. The unit was held at 392˚F for about 2 hrs and then the heats turned down and the unit was cooled to 300°F.

Subtask 1.3 Hydrotreatment of Blended Product

Production of deeply hydrotreated total liquid product (TLP) to provide material for other tasks in this project by large-scale production of TLP is necessary. The following describes the pilot plant and the results of hydrotreatment and hydrogenation of the fractionated LCO/RCO blend.

1.3.1 Pilot Plant Description

PARC's two adiabatic units, P63 and P67 were used in this project. These units use an adiabatic system to control heat loss in the first reactor while the second reactor is used as a pseudo adiabatic system via isothermal controls keeping a temperature gradient across the reactor. A simplified flow diagram is shown in **Figure 1-4**.

The units were run on gas recycle with a specification of 98% H_2 for P67 and 95% H_2 for P63 in the inlet gas stream. The recycle gas stream was passed through an amine scrubber to remove H_2S. The inlet gas stream is made of make-up hydrogen and the recycle gas stream. This mixed gas stream is sampled by the on-line gas chromatograph. The inlet gas was premixed with the feed before entering the preheater of the first reactor.

The product was then sent to the fractionation tower where it was stripped of H_2S and ammonia and left the unit as TLP. The tower system was run at atmospheric pressure.

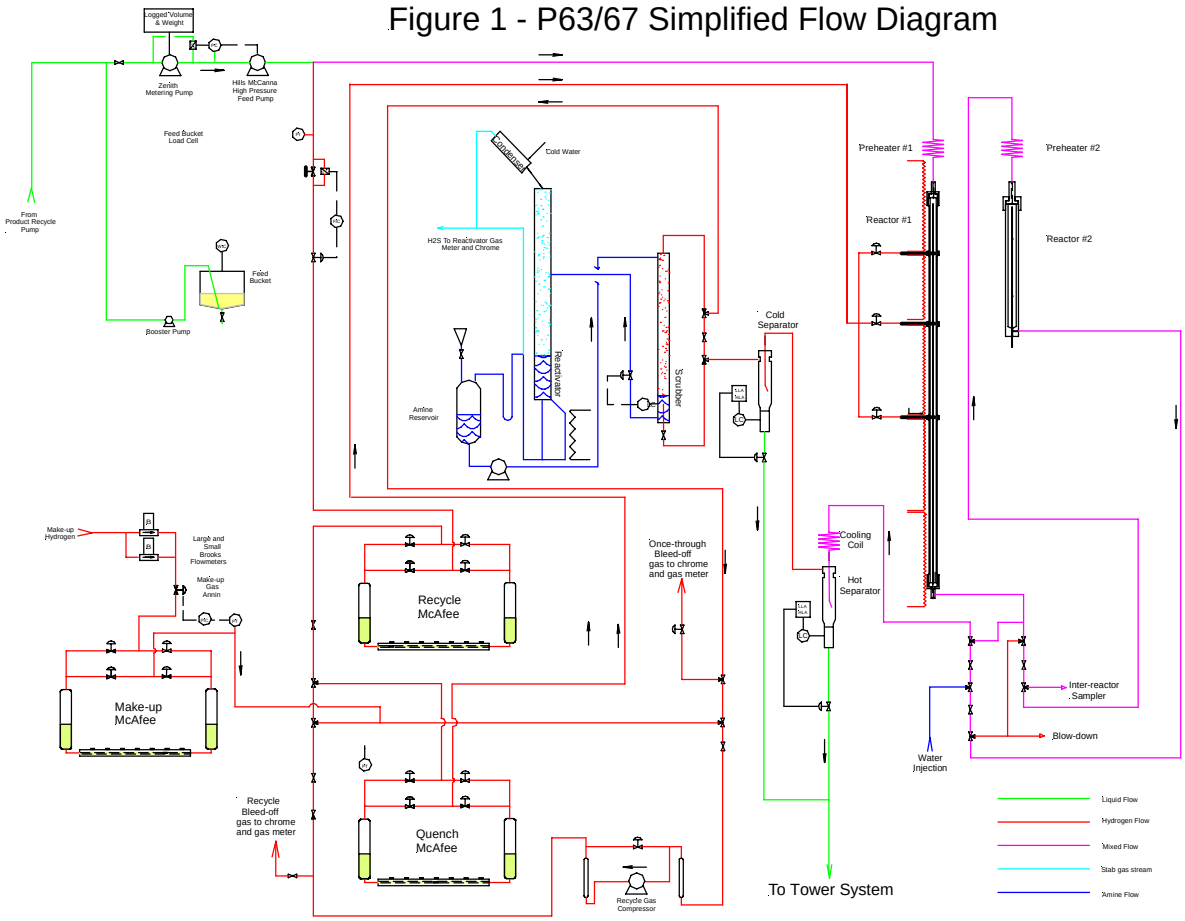

Figure 1-4: P63/67 Simplified Flow Diagram

1.3.2. Hydrotreating (HDT) Operation and Results

1.3.2.1. Hydrotreating of 1:1 LCO/RCO Blend (570°F-)

After the sulfiding was finished and the reactor was cooled to 300˚F, the 570°F- distilled feed was added to the unit and heated up to an outlet run temperature of 650°F in each reactor. The pressure was increased from 450 to 600 psig and the gas inlet rate was set to 3000 scf/bbl. The sulfur and nitrogen content of this feed was 1.41 wt% and 2300 ppm respectively.

Feed to the hydrotreating unit was a 1:1 blend of LCO and RCO distilled to 570°F-. **Figure 1-1(c)** shows how this feed was prepared. The feed was introduced at an inlet

temperature of 550˚F and a unit pressure of 600 psig. This entire run was run at a LHSV of 0.5. The run feed had a sulfur level of 14,100 ppm and a nitrogen level of 2,300 ppm. At this stage the H_2S scrubber and reactivator were cut into the unit. These components were not cut in during the sulfiding procedure in order to build up a H_2S level in the unit. The catalyst remained at the same activity with a hydrogen consumption rate of ~2000 scf/bbl. The first drum was an off-stream drum (sulfur of 144 ppm and nitrogen of 66 ppm) that was repassed at the end of the run to lower the sulfur and nitrogen to 2.2 ppm and <1 ppm respectively. The remaining 11 drums all had sulfur and nitrogen levels below 7 ppm and 10 ppm respectively. The summary of operations and analysis are shown in **Tables 1-2** and **1-3**.

1.3.2.2. Hydrogenation of HDT 1:1 LCO/RCO 570ºF (1st Pass)

Feed to the hydrogenation reactor was 1:1 RCO:LCO which had been hydrotreated through P67 as described above. The operations and analysis can be seen in **Tables 1-4** and **1-5**. After run feed was introduced reactor 1 established a ΔT of about 100˚F and Rx 2 about 50˚F. The hydrotreated feed had <7 ppm sulfur and <10 ppm nitrogen and a specific gravity of between 0.934 and 0.942. The naphthalene and tetralin content was 1.5 wt% and 29.0 wt%. The hydrogenated total liquid product had a 356°F- cut point at 14.0 wt% initially. The smoke point was 14.0 mm and there was still 8 wt% tetralin left in the product. Multiple adjustments were made to try and achieve the desired smoke point by decreasing the tetralin concentration. **Table 1-6** summarizes the conditions used and the corresponding product compositions achieved. Condition changes had the objective of achieving a smoke point of at least 19 mm. This was achieved at Condition 6 (LHSV=0.3, WABT=690°F, Pressure=1200 psig).

The operating conditions are summarized in **Table 1-4** while the daily GC analyses of the TLP are given in **Table 1-5**.

Table 1-4: Hydrogenation of hydrotreated 1:1 LCO/RCO feed cut to 570°F.

CATALYST CHARGE		REDAR CATALYST ml	gm
	Rx1	2190	1964
	Rx2	2655	2382
	Total	4845	4346

Run No. P-67	Time	Date 2006/ 2007	Feed gms/hr	Reactor 1 Temps In	Out	WABT	Reactor 2 Temps In	Out	WABT	Comb. WABT	Press. psig	LHSV	Inlet gas scf/bbl	Quench scf/bbl	Makeup scf/bbl	% H2 Inlet	H_2 Cons. scf/bbl	Wt. Bal %	TLP Analyses Sp. Gr.	API	Sulfur ppm	Nitrogen ppm	Tetralin Wt %	Decalin Wt %	T+D Wt%	Smk Pt mm (19mm spec)	FIA Arom. vol %	356°F- wt%
												4 HOUR AVERAGE																
114-SU	***0000***	***12/9***	***Start of catalyst reduction @ 392°F***																									
114-1	***1300***	***12/10***	***Started feed in with P67-110 TLP drum # 1***																									
114-1	0400	12/11	2276	510	484	570	460	343	421	496	598	0.49	3019	0	1710	98.5	1284	103.7	0.9221	22.0	5.2	<1	14.7	20.8	35.5	-	53.0	6.3
114-1	1500	12/11	Grab sample taken for 6890																				3.9	28.8	32.7			
114-1	0400	12/12	2275	566	669	631	596	649	607	619	599	0.50	3626	2178	2126	89.4	1735	100.5	0.8814	29.0	-	<1	3.4	27.9	31.3	15.0	26.0	9.2
114-2	***1500***	***12/12***	***Increased the first reactor WABT to 650°F with a max temperature of 680°F***																									
114-2	0400	12/13	2291	598	680	649	602	651	613	631	606	0.50	1994	6136	1994	98.9	1578	98.3	0.8789	29.5	<1	<1	4.3	26.7	31.059765	15.0	29.0	11.5
114-3	***1500***	***12/13***	***Increased the first reactor WABT to 670°F with a max temperature of 690°F; increased the second reactor temperature to 660 outlet.***																									
114-3	**2000**	**12/13**	**Product Drum 1 properties**																		**17.0**	**<1**	**8.8**	**22.9**	**31.7**	**14.0**	**37.9**	**9.2**
114-3	***2000***	***12/13***	***Feed switch to P67-110 TLP drum # 2***																									
114-3	0400	12/14	2322	644	690	661	614	662	621	644	699	0.50	2900	5621	1706	98.8	1296	98.5	0.8838	28.6	<1	<1	8.8	22.9	31.69	14.0	37.9	13.0
114-3	***1500***	***12/14***	***Reduced LHSV to 0.3***																									
114-3	0400	12/15	1370	646	697	669	586	664	602	635	608	0.30	2985	6563	2122	99.2	1448	99.1	0.8783	29.6	<1	<1	6.8	22.3	29.07	14.0	32.0	14.0
114-4	***1500***	***12/15***	***Increased the first reactor temperature to 690 F and the second reactor to 650 F***																									
114-4	0400	12/16	1377	691	713	690	634	702	647	668	601	0.30	2971	5937	1914	98.3	1264	98.6	0.8816	29.0	<1	<1	6.94	17.95	24.89	14.0	40.7	17.0
114-4	0400	12/17	1401	699	712	690	632	709	650	670	596	0.30	2944	5353	1742	98.5	1087	94.5	0.8855	28.3	<1	<1	8.34	17.48	25.82	14.0	44.8	17.0
114-5	***1300***	***12/17***	***Increased pressure to 900 psig***																									
114-5	0400	12/18	1390	661	717	690	639	699	650	670	902	0.30	3019	8043	2724	98.8	1945	96.8	0.8628	32.5	<1	<1	2.08	22.78	24.86	16.5	19.3	20.0
114-6	***1000***	***12/18***	***Increased pressure to 1200 psig***																									
114-6	***1600***	***12/18***	***Feed switch to P67-110 TLP drum # 3***																									
114-6	**2000**	**12/18**	**Product Drum 2 properties**																**0.8784**	**29.6**	**1.8**	**<1**	**5.6**	**20.9**	**26.5**	**14.0**	**35.2**	**14.8**
114-6	0400	12/19	1401	615	719	693	644	696	651	672	1199	0.30	2755	???	3672	99.0	2396	96.5	0.8468	35.6	1.9	<1	0.77	20.39	21.16	22.0	6.2	27.0
114-7	***1400***	***12/19***	***Increased LHSV to 0.5***																									
114-7	0400	12/20	2375	631	711	690	646	672	650	670	1203	0.50	3018	8678	3018	98.8	2302	97.3			<1	<1	0.66	23.48	24.14	21.0	8.0	22.0
114-7	0400	12/21	2311	628	714	689	647	673	651	670	1204	0.50	2985	9352	3056	98.6	2434	98.1	0.8483	35.3	<1	<1	0.75	24.1	24.85	21.0	6.4	25.0
114-7	0400	12/22	2311	628	714	689	647	673	651	670	1204	0.50	2985	9352	3056	98.6	2434	98.1	0.8483	35.3	<1	<1	0.73	21.5	22.23	20.1	6.4	27.5
114-7	***1000***	***12/22***	***Feed switch to P67-110 TLP drum # 4***																									
114-7	**1200**	**12/22**	**Product Drum 3 properties**																**0.8478**	**35.4**	**<1**	**<1**	**0.83**	**23.7**	**24.53**	**20.0**	**7.6**	**23.0**
114-7	0400	12/23	2306	628	725	692	646	676	651	671	1203	0.50	3008	9264	3102	98.6	2492	97.1	0.8453	35.9	<1	<1	0.8	19.7	20.5	20.0	6.6	29.7
114-7	0400	12/24	2300	631	717	688	646	674	652	670	1199	0.50	2990	8943	3189	98.6	2576	96.6	0.8458	35.8	<1	<1	0.73	21.3	22.03	20.5	6.3	28.0
114-7	0400	12/25	2337	639	713	691	646	657	650	671	1197	0.51	2918	9264	3077	98.6	2457	95.9	0.8471	35.5	<1	<1	0.72	21.2	21.92	20.4	6.5	28.0
114-7	**2000**	**12/25**	**Product Drum 4 properties**																**0.8471**	**35.5**	**<1**	**<1**	**0.87**	**20.1**	**20.97**	**20.2**	**6.5**	**26.0**
114-7	***2200***	***12/25***	***Feed switch to P67-110 TLP drum # 5***																									
114-7	0400	12/26	2310	641	721	690	646	674	651	671	1205	0.50	3044	9762	3133	98.7	2527	97.7	0.8451	35.9	<1	<1	0.69	22.1	22.79	19.8	6.3	28.0
114-7	0400	12/27	2321	641	722	691	646	674	651	671	1200	0.50	2991	10018	3151	98.5	2542	98.1	0.8448	36.0	<1	<1	0.8	20.2	20.97	21.0	6.4	29.0
114-7	0400	12/28	2316	636	722	690	646	675	651	671	1202	0.50	3007	9923	3162	98.6	2557	97.0	0.8433	36.3	<1	<1	0.8	17.2	17.97	21.5	6.1	35.0
114-7	0400	12/29	2315	634	721	688	645	674	651	669	1199	0.50	2981	9573	2781	98.7	2460	95.8	0.8413	36.7	<1	<1	0.72	18.9	19.62	21.5	5.0	34.0
114-7	***0600***	***12/29***	***Feed switch to P67-110 TLP drum # 6***																									
114-7	**1200**	**12/29**	**Product Drum 5 properties**																**0.8436**	**36.2**	**<1**	**<1**	**0.73**	**19.8**	**20.53**	**20.2**	**6.4**	**29.5**
114-7	0400	12/30	2262	646	714	691	645	658	650	670	1198	0.50	2989	7834	2305	98.4	2014	96.2	0.8343	38.1	<1	<1	0.59	19.0	19.59	20.5	3.6	32.5
114-7	0400	12/31	2271	646	723	690	643	675	649	670	1204	0.50	2988	7889	2316	98.5	2023	96.7	0.8317	38.6	<1	<1	0.53	18.7	19.23	21.5	3.8	37.0
114-7	0400	1/1	2279	649	721	690	645	677	651	671	1203	0.50	2937	8003	2312	98.5	2019	97.3	0.8336	38.3	<1	<1	0.63	17.9	18.53	20.5	3.4	35.0
114-7	***1600***	***1/1***	***Feed switch to P67-110 TLP drum # 7***																									
114-7	**2000**	**1/1**	**Product Drum 6 properties**																**0.8332**	**38.3**	**<1**	**<1**	**0.62**	**20.6**	**21.22**	**22.0**	**4.0**	**32.0**
114-7	0400	1/2	2330	643	733	688	644	676	650	669	1198	0.51	2993	9684	2811	98.3	2506	97.5	0.8358	37.8	<1	<1	0.82	17.5	18.32	21.2	5.6	36.0
114-7	0400	1/3	2315	644	718	687	644	673	650	668	1197	0.50	3038	9979	2951	98.5	2637	96.2	0.8356	37.8	<1	<1	0.69	18.4	19.09	22.0	4.4	33.0
114-7	0400	1/4	2315	646	730	691	645	677	651	671	1196	0.50	3020	9649	2929	98.6	2616	96.8	0.8346	38.0	<1	<1	0.77	17.8	18.57	22.0	5.0	36.5
114-7	***1000***	***1/4***	***Feed switch to P67-108 TLP drum # 2***																									
114-7	**2000**	**1/4**	**Product Drum 7 properties**																**0.8341**	**38.1**	**<1**	**<1**	**0.71**	**18.9**	**19.61**	**22.0**	**5.3**	**32.5**
114-7	0400	1/5	2312	645	724	690	645	673	651	670	1208	0.50	3030	10195	2893	98.3	2584	97.5	0.8361	37.7	<1	<1	0.62	22.5	23.12	22.0	4.7	32.0
114-7	0400	1/6	2324	646	724	690	644	673	650	670	1199	0.51	2959	9927	2856	98.6	2547	97.3	0.8393	37.1	<1	<1	0.72	23.9	24.62	22.0	5.5	30.0
114-7	0400	1/7	2322	648	725	691	637	674	650	671	1201	0.50	3002	10047	2885	98.5	2569	97.1	0.8428	36.4	<1	<1	0.81	21.9	22.71	22.0	5.5	29.8
114-7	***1400***	***1/7***	***Feed switch to P67-108 TLP drum # 3***																									
114-7	**0000**	**1/8**	**Product Drum 8 properties**																**0.8394**	**37.1**	**<1**	**<1**	**0.79**	**22.1**	**22.89**	**21.5**	**5.7**	**29.3**
114-7	0400	1/8	2307	652	725	691	645	674	651	671	1208	0.50	3045	10220	2852	98.6	2534	97.7	0.8421	36.5	<1	<1	0.82	21.7	22.52	21.5	5.2	29.8
114-7	0400	1/9	2323	651	730	690	643	673	650	670	1197	0.51	2978	10251	3102	98.5	2778	96.4	0.8411	36.7	<1	<1	0.88	23.0	23.88	21.5	5.6	30.7
114-8	***1200***	***1/9***	***Decreased the unit pressure to 900 psig***																									
114-8	0400	1/10	2311	677	726	690	639	675	649	670	898	0.50	3075	9070	2522	98.2	2237	95.7	0.8522	34.6	<1	<1	3.1	21.0	24.1	15.5	18.3	25.5
114-8	0400	1/11	2324	683	726	691	640	679	651	671	896	0.50	3035	8817	2687	98.5	2395	94.3	0.8597	33.1	<1	<1	3.4	20.3	23.7	16.0	17.8	26.5
114-8	**0400**	**1/11**	**Product Drum 9 properties**																**0.8487**	**35.2**	**<1**	**<1**	**2.2**	**24.2**	**26.4**	**17.5**	**13.2**	**26.0**
114-8	***0800***	***1/11***	***Feed switch to P67-108 TLP drum 4***																									
114-9	***1200***	***1/11***	***Increased the LHSV to 1.0 and decreased the unit pressure to 600 psig***																									
114-9	0400	1/12	4605	698	705	690	634	672	648	669	605	1.00	3033	1814	507	98.4	417	99.3	0.9159	23.0	1.4	<1	20.7	8.7	29.4	8.0	73.2	11.0
114-9	**2200**	**1/12**	**Product Drum # 10 properties**																**0.9159**	**23.0**								
114-9	***2300***	***1/12***	***Feed switch to P67-114 TLP drum 10***																									
114-10	0400	1/13	4460	706	695	688	640	666	648	668	600	1.00	3051	1597	352	98.1	264	99.6	0.9200	22.3	<1	<1	16.0	12.0	28	10.0	60.3	13.5
114-10	***1600***	***1/13***	***Decreased the LHSV to 0.5, increased the unit pressure to 1200 psig and set temperatures to 670°F***																									
114-10	0400	1/14	2237	661	691	666	669	703	674	670	1196	0.50	3061	6130	1595	99.2	1317	97.6	0.8708	31.0	<1	<1	2.7	24.3	27	15.0	20.4	17.6
114-10	0400	1/15	2237	660	690	672	667	699	671	672	1202	0.50	3095	6207	1685	99.3	1404	97.4	0.8655	32.0	<1	<1	2.0	24.1	26.1	15.5	16.3	20.5
114-11	***1400***	***1/15***	***Increased WABT to 680°F on both reactors***																									
114-11	0400	1/16	2233	661	704	679	677	709	681	680	1200	0.50	3166	6133	1683	99.2	1403	97.5	0.8605	32.9	<1	<1	1.7	22.0	23.7	16.0	17.7	21.5
114-12	***1400***	***1/16***	***Increased WABT to 690°F on both reactors***																									
114-12	**2000**	**1/16**	**Product Drum # 11 properties**																**0.8792**	**29.6**	**<1**	**<1**	**2.4**	**23.6**	**26**	**15.5**	**21.6**	**17.5**
114-12	***2100***	***1/16***	***Feed switch to P67-114 Tlp drum 11***																									
114-12	0400	1/17	2143	673	705	690	688	717	690	690	1197	0.50	2994	2800	1030	98.8	743	95.9	0.8507	34.8	<1	<1	0.8	20.8	21.62	18.5	8.3	28.0
114-12	0400	1/18	2151	679	705	690	688	722	690	690	1199	0.51	2947	2913	772	98.8	483	96.0	0.8416	36.6	<1	<1	0.7	19.9	20.6	20.5	6.0	31.0
114-12	0400	1/19	2135	682	706	690	688	720	690	690	1201	0.50	3021	3197	781	98.6	498	97.1	0.8416	36.6	<1	<1	0.7	18.5	19.2	20.5	5.8	31.0
114-12	0400	1/20	2226	674	712	697	680	721	685	686	1201	0.50	2944	6024	1417	99.1	1092	96.4	0.8391	37.1	<1	<1	0.8	19.2	20	20.5	5.8	24.7
114-12	***0400***	***1/20***	***Feed switch to P67-108 TLP drum 5***																									
114-12	**0800**	**1/20**	**Product Drum # 12 properties (triple pass product from drums 10 and 11)**																**0.8432**	**36.3**	**<1**	**<1**	**1.1**	**20.2**	**21.3**	**20.0**	**8.7**	**28.5**
114-12	0400	1/21	2314	666	712	688	685	715	691	689	1199	0.50	3015	7955	2579	98.8	2254	95.2	0.8587	33.3	<1	<1	2.5	23.1	25.6	16.5	16.8	23.6
114-12	0400	1/22	2323	665	723	689	684	714	690	689	1204	0.51	3006	8445	2353	98.7	2012	95.8	0.8555	33.9	<1	<1	2.7	22.0	24.7	16.0	18.5	33.0
114-12	0400	1/23	2312	667	716	690	684	713	690	690	1199	0.50	2983	8342	2390	98.5	2014	96.3	0.8587	33.3	<1	<1	2.6	21.9	24.5	16.0	18.2	25.0
114-12	**1200**	**1/23**	**Product Drum # 13 properties**																**0.8576**	**33.5**	**<1**	**<1**	**2.6**	**20.2**	**22.8**	**16.0**	**19.4**	**23.8**
114-12	***1600***	***1/23***	***Feed switch to P67-108 TLP drum 6***																									
114-13	***1600***	***1/23***	***Increased WABT to 700°F on both reactors***																									
114-13	0400	1/24	2308	676	737	702	693	727	701	702	1203	0.50	2985	8241	2485	98.4	2138	95.7	0.8519	34.6	<1	<1	2.6	18.3	20.9	17.0	18.4	30.0
114-13	0400	1/25	2315	676	724	698	692	726	700	699	1201	0.51	3491	9000	2463	86.8	2113	96.1	0.8514	34.7	<1	<1	2.6	18.8	21.4	15.5	18.6	28.0
114-13	0400	1/26	2318	676	732	700	692	709	700	700	1200	0.50	2983	8101	2487	98.1	2156	95.3	0.8517	34.6	<1	<1	2.6	19.0	21.6	16.5	18.5	30.3
114-13	**2000**	**1/26**	**Product Drum # 14 properties**																**0.8517**	**34.6**	**<1**	**<1**	**3.0**	**18.9**	**21.9**	**16.0**	**21.0**	**27.6**
114-13	***2200***	***1/26***	***Feed switch to P67-114 TLP drum 1***																									
114-13	0400	1/27	2167	686	719	698	694	726	699	698	1202	0.50	3029	5041	1531	98.4	1209	96.2	0.8416	36.6	<1	<1	1.2	19.2	20.4	19.5	9.8	32.0
114-13	0400	1/28	2160	686	722	700	696	731	701	700	1203	0.49	3049	4529	1425	98.5	1062	95.6	0.8368	37.6	<1	<1	0.9	19.7	20.6	20.0	7.8	33.0
114-13	0400	1/29	2173	686	719	700	695	729	700	700	1201	0.50	3011	4417	1453	98.3	1079	94.7	0.8346	38.0	<1	<1	0.8	19.8	20.6	20.0	7.2	33.3
114-13	0400	1/30	2181	686	722	701	695	735	701	701	1202	0.50	3006	4419	1446	98.4	1077	95.0	0.8316	38.7	<1	<1	0.8	20.5	21.3	20.5	8.9	35.0
114-13	**1200**	**1/30**	**Product Drum # 15 properties**																**0.8361**	**37.7**	**<1**	**<1**	**1.0**	**19.9**	**20.9**	**20.0**	**9.1**	**32.3**
114-13	***1200***	***1/30***	***Feed switch to P67-114 TLP drum 2***																									
114-13	0400	1/31	2170	690	718	699	696	734	700	700	1201	0.50	3030	4143	1367	98.5	996	94.7	0.8307	38.8	<1	<1	0.7	18.6	19.3	21.0	6.4	38.5
114-13	0400	2/1	2166	691	719	700	696	734	701	700	1203	0.50	3033	4159	1367	98.2	998	94.9	0.8302	39.0	<1	<1	0.7	15.6	16.3	20.5	6.7	38.5
114-13	0400	2/2	2157	692	720	700	696	731	701	700	1205	0.50	3003	4298	1370	98.5	995	95.3	0.8307	38.8	<1	<1	0.8	16.8	17.6		7.0	38.0
114-13		**2/2**	**Product Drum # 16 properties**																				**<1**	**<1**	**0.9**	**16.6**	**17.5**	**20.0**	**7.8**	**37.0**
114-13	0400	2/3	2115	697	713	698	695	729	699	699	1197	0.49	3079	3720	1119	98.3	733	94.9	0.8273	39.5	<1	<1	0.6	15.2	15.8		4.1	43.5
114-13	0400	2/4	2157	696	710	700	697	730	701	700	1199	0.51	2978	3650	1095	98.4	717	94.1	0.8196	41.2	<1	<1	0.6	15.3	15.9		3.4	47.0
114-13	0400	2/5	2159	694	713	701	697	731	701	701	1199	0.51	2935	3470	1271	98.2	890	93.5	0.8179	41.5	<1	<1	0.6	13.9	14.5		3.5	48.5
114-13	0400	2/6	2043	693	716	701	698	732	701	701	1199	0.49	3120	3683	1171	98.4	790	95.5	0.8172	41.7	<1	<1	0.6	12.8	13.4	22.5	3.6	49.0
114-13	**1200**	**2/6**	**Product Drum # 17 properties**																**0.8205**	**41.0**	**<1**	**<1**	**0.5**	**14.6**	**15.1**	**23.5**	**4.4**	**46.5**
114-13	0400	2/7	2105	691	715	701	697	730	700	701	1201	0.50	2983	3707	1263	98.4	875	93.4	0.8137	42.4	<1	<1	0.5	11.6	12.1		3.3	52.0
114-13	0400	2/8	2115	685	715	701	697	730	700	701	1197	0.51	2995	3296	1206	98.4	724	94.3	0.8107	43.1	<1	<1	0.5	11.5	12.0		3.7	52.5
114-13	0400	2/9	2106	685	715	700	698	711	701	700	1201	0.50	3010	3379	1391	98.5	749	91.5	0.8114	42.9	<1	<1	0.5	12.1	12.6	25.0	3.5	53.0
114-13		**2/9**	**Product Drum # 18 properties**																**0.8119**	**42.8**	**<1**	**<1**	**0.5**	**11.7**	**12.2**			**53.0**

Table 1-5: Daily GC analyses of hydrogenated TLP products.

Column: 150 meter x 0.25mm, Supelco DH150 Petrocal   FID   Film Thickness 1 micron   **United Refining LCO - RCO Hydrotreating**

GC No.	SAMPLE	Benz	Cyclo	Et B	Xyl's	Indan	t-Dec	c-Dec	Tetralin	N	MNS		EtN's	DMN'S								TOTAL	TOTAL	Tri-	Tetra	5+6	Other	N+T+D
			Hexane			(1)					2MN	1MN		2,6	2,7	1,7	1,6	2,3	1,5	1,2	1,8	DMN's	MNS	Me Subst MN's				
3691	P67-114 0400 12/11/06	0.01	1.42	0.10	0.58	0.70	15.36	5.41	14.68	0.63	1.25	0.86	1.98	0.17	0.63	0.24	0.49	0.63	1.15	0.07	0.21	3.59	2.11	1.36	2.21	-	90.10	36.08
3692	P67-114 1500 12/11/06	0.16	1.89	0.38	0.68	0.24	21.70	7.06	3.88	0.99	0.57	0.87	1.32	0.20	0.44	0.18	0.40	0.38	0.40	0.13	0.08	2.21	1.44	0.73	0.24	-	94.39	33.63
3694	P67-114 0400 12/12/06	0.11	1.51	0.34	0.62	0.23	21.07	6.84	3.40	1.09	0.23	0.78	1.25	0.23	0.43	0.26	0.43	0.38	0.39	0.08	0.12	2.32	1.01	0.94	2.16		92.48	32.40
3696	P67-114 0400 12/13/06	0.33	2.54	0.50	0.67	0.29	20.62	6.10	4.34	1.06	0.16	0.49	1.29	0.21	0.40	0.21	0.38	0.31	0.28	0.08	0.08	1.95	0.65	0.92	1.32		94.10	32.12
3697	P67-114 TLP Drum # 1	0.15	1.45	0.01	0.60	0.46	17.76	5.13	8.78	1.04	0.40	0.08	1.55	0.25	0.52	0.29	0.45	0.44	0.56	0.08	0.15	2.74	0.48	1.15			94.59	32.71
3699	P67-114 0400 12/14/06	0.43	2.32	0.62	0.96	0.41	17.20	5.07	6.78	1.06	0.79	0.36	1.49	0.29	0.47	0.30	0.46	0.48	0.33	0.08	0.06	2.47	1.15	1.21	2.48	0.65	90.98	30.11
	P67-114 0400 12/15/06																											
3703	P67-114 0400 12/16/06	0.64	1.57	0.74	1.28	0.53	14.77	3.18	6.94	1.46	0.71	0.26	1.28	0.31	0.37	0.39	0.38	0.35	0.21	0.08	0.10	2.19	0.97	0.88	2.91	0.73	90.86	26.35
3704	P67-114 0400 12/17/06	0.64	1.56	0.84	1.13	0.62	14.33	3.15	8.34	1.82	0.86	0.05	1.37	0.36	0.37	0.49	0.43	0.06	0.22	0.09	0.11	2.13	0.91	1.24	3.20	0.72	89.98	27.64
3705	P67-114 0400 12/18/06	0.61	1.47	0.29	0.36	0.21	18.75	4.03	2.08	0.93	0.26	0.34	0.83	0.16	0.27	0.14	0.25	0.15	0.18	0.06	0.05	1.26	0.60	0.19	3.27	0.58	93.17	25.79
3708	P67-114 TLP Drum # 2	0.31	0.91	0.46	0.77	0.27	16.92	3.98	5.61	1.23	0.57	0.34	1.27	0.29	0.41	0.32	0.23	0.26	0.08	0.08	0.10	1.77	0.91	0.90	1.66	0.40	93.13	27.74
3707	P67-114 0400 12/19/06	0.90	1.32	0.07	0.32	0.60	17.68	2.71	0.77	0.88	0.14	0.19	0.38	0.09	0.17	0.07	0.13	0.06	0.10	0.05	0.04	0.71	0.33	0.17	2.07	0.36	95.48	22.04
3710	P67-114 0400 12/20/06	0.87	1.51	0.10	0.32	0.40	19.61	3.87	0.66	0.78	0.47	0.35	0.39	0.06	0.14	0.04	0.12	0.06	0.10	0.05	0.06	0.63	0.82	0.26	7.45	8.47	81.59	24.92
3714	P67-114 0400 12/21/06	1.10	1.83	0.10	0.38	0.52	20.38	3.71	0.75	0.92	0.11	0.07	0.14	0.15	0.17	0.04	0.14	0.08	0.05	0.08	0.05	0.76	0.18	0.21	2.82	0.63	94.48	25.76
3721	P67-114 0400 12/22/06	1.23	1.92	0.12	0.41	0.58	18.25	3.26	0.73	0.87	0.10	0.06	0.11	0.14	0.23	0.03	0.11	0.22	0.06	0.08	0.18	1.05	0.16	0.28	3.76	0.62	93.26	23.11
3724	P67-114 TLP Drum # 3	0.64	1.51	0.09	0.39	0.54	19.77	3.87	0.83	0.93	0.11	0.07	0.27	0.15	0.17	0.05	0.13	0.21	0.08	0.20	0.09	1.08	0.18	0.22	3.82	0.62	93.15	25.40
3720	P67-114 0400 12/23/06	1.24	1.76	0.13	0.46	0.60	16.84	2.89	0.80	0.84	0.10	0.08	0.12	0.13	0.14	0.07	0.11	0.19	0.08	0.07	0.16	0.95	0.18	0.19	2.90	0.63	94.31	21.37
3719	P67-114 0400 12/24/06	1.23	1.85	0.12	0.44	0.58	18.14	3.25	0.73	0.87	0.10	0.07	0.11	0.13	0.15	0.03	0.11	0.22	0.10	0.07	0.17	0.98	0.17	0.28	3.40	0.59	93.71	22.99
3718	P67-114 0400 12/25/06	1.29	1.86	0.13	0.44	0.57	17.92	3.29	0.72	0.86	0.10	0.07	0.11	0.14	0.21	0.03	0.1	0.18	0.06	0.07	0.18	0.97	0.17	0.28	3.41	0.66	93.65	22.79
3725	P67-114 TLP Drum # 4	0.60	1.24	0.1	0.42	0.57	16.93	3.16	0.77	0.87	0.12	0.10	0.26	0.14	0.08	0.06	0.12	0.09	0.07	0.08	0.06	0.70	0.22	0.19	2.99	0.52	94.51	21.73
3717	P67-114 0400 12/26/06	1.26	2.00	0.13	0.48	0.59	18.77	3.35	0.69	0.80	0.09	0.06	0.62	0.14	0.21	0.07	0.11	0.22	0.1	0.07	0.18	1.10	0.15	0.23	3.89	0.76	93.07	23.61
3716	P67-114 0400 12/27/06	1.28	1.84	0.13	0.47	0.60	17.14	3.06	0.77	0.86	0.09	0.06	0.56	0.13	0.18	0.07	0.1	0.2	0.09	0.07	0.17	1.01	0.15	0.22	3.14	0.66	93.96	21.83
3723	P67-114 0400 12/28/06	1.90	2.07	0.18	0.42	0.66	14.84	2.42	0.77	0.76	0.08	0.06	0.15	0.12	0.14	0.06	0.1	0.16	0.05	0.05	0.12	0.80	0.14	0.14	3.45	0.57	94.14	18.79
3727	P67-114 0400 12/29/06	2.45	2.47	0.14	0.45	0.59	16.05	2.78	0.72	0.82	0.09	0.06	0.16	0.11	0.16	0.06	0.09	0.18	0.05	0.05	0.14	0.84	0.15	0.15	3.63	0.63	93.78	20.37
3728	P67-114 TLP Drum # 5	1.20	1.71	0.13	0.38	0.60	16.82	3.01	0.73	0.83	0.11	0.08	0.19	0.13	0.21	0.06	0.10	0.20	0.08	0.07	0.16	1.01	0.19	0.23	3.12	0.57	94.05	21.39
3731	P67-114 0400 12/30/06	1.93	1.81	0.15	0.49	0.63	16.62	2.38	0.59	0.83	0.10	0.08	0.16	0.14	0.21	0.09	0.16	0.17	0.06	0.15	0.04	1.02	0.18	0.23	2.15	0.45	95.14	20.42
3732	P67-114 0400 12/31/06	2.58	1.94	0.21	0.60	0.72	16.46	2.21	0.53	0.70	0.07	0.05	0.22	0.19	0.03	0.09	0.15	0.14	0.07	0.14	0.05	0.86	0.12	0.20	1.90	0.32	95.90	19.90
3733	P67-114 0400 1/1/07	0.22	1.91	0.17	0.53	0.67	15.68	2.21	0.63	0.80	0.09	0.07	0.12	0.09	0.13	0.05	0.1	0.15	0.05	0.13	0.06	0.76	0.16	0.17	2.49	0.46	95.16	19.32
3730	P67-114 TLP Drum # 6	1.80	1.71	0.15	0.5	0.66	18.02	2.57	0.62	0.86	0.10	0.07	0.14	0.10	0.17	0.05	0.07	0.16	0.08	0.15	0.04	0.82	0.17	0.23	0.72	-	97.20	22.07
3734	P67-114 0400 1/2/07	2.42	1.71	0.17	0.54	0.64	15.12	2.41	0.82	0.74	0.10	0.09	0.22	0.12	0.06	0.05	0.04	0.04	0.08	0.04	0.06	0.49	0.19	0.15	1.85	0.35	96.23	19.09
3736	P67-114 0400 1/3/07	2.02	1.78	0.14	0.44	0.60	15.73	2.67	0.69	0.84	0.12	0.10	0.23	0.05	0.14	0.19	0.1	0.07	0.11	0.16	0.05	0.87	0.22	0.23	0.72	-	97.12	19.93
3739	P67-114 0400 1/4/07	2.41	1.78	0.17	0.52	0.65	15.54	2.30	0.77	0.77	0.10	0.09	0.21	0.18	0.21	0.21	0.1	0.06	0.09	0.13	0.05	1.03	0.19	0.12	0.84	-	97.05	19.38
3742	P67-114 TLP Drum # 7	1.88	1.71	0.15	0.48	0.63	16.18	2.67	0.71	0.82	0.11	0.09	0.22	0.04	0.12	0.17	0.10	0.06	0.10	0.15	0.06	0.80	0.20	0.23	0.58	-	97.37	20.38
3741	P67-114 0400 1/5/07	2.18	2.26	0.16	0.49	0.62	19.54	3.02	0.62	0.76	0.09	0.06	0.19	0.18	0.08	0.02	0.08	0.17	0.09	0.16	0.07	0.85	0.15	0.25	3.14	-	94.85	23.94
3744	P67-114 0400 1/6/07	2.04	2.24	0.14	0.49	0.61	20.63	3.28	0.72	0.81	0.10	0.07	0.34	0.12	0.06	0.05	0.14	0.05	0.08	0.04	0.07	0.61	0.17	0.19	-	-	98.22	25.44
3745	P67-114 0400 1/7/07	1.90	1.94	0.12	0.46	0.55	18.80	3.07	0.81	0.86	0.13	0.09	0.38	0.13	0.07	0.06	0.12	0.05	0.10	0.04	0.04	0.61	0.22	0.19	0.52	-	97.60	23.54
3747	P67-114 TLP Drum # 8	1.71	1.92	0.13	0.47	0.56	18.93	3.15	0.79	0.87	0.13	0.09	0.37	0.13	0.07	0.06	0.12	0.05	0.09	0.05	0.04	0.61	0.22	0.17	-	-	98.13	23.74
3746	P67-114 0400 1/8/07	1.82	1.96	0.13	0.44	0.57	18.71	3.01	0.82	0.86	0.13	0.09	0.37	0.13	0.07	0.05	0.11	0.05	0.08	0.04	0.04	0.57	0.22	0.16	0.58	-	97.61	23.40
3749	P67-114 0400 1/9/07	1.97	2.26	0.14	0.41	0.10	19.85	3.15	0.88	0.83	0.11	0.06	0.09	0.15	0.32	0.03	0.12	0.18	0.08	0.08	0.20	1.16	0.17	0.10	-	-	97.74	24.71
3752	P67-114 0400 1/10/07	1.52	1.91	0.08	0.87	0.41	17.55	3.45	3.07	0.86	0.33	0.08	0.79	0.10	0.14	0.11	0.11	0.13	0.15	0.06	0.05	0.85	0.41	0.33	0.27	-	97.28	24.93
3754	P67-114 0400 1/11/07	1.78	2.16	0.08	0.69	0.38	16.94	3.40	3.36	0.37	0.34	0.08	0.81	0.11	0.14	0.12	0.11	0.13	0.15	0.05	0.05	0.86	0.42	0.32	0.18	-	97.85	24.07
3755	P67-114 TLP Drum # 9	1.62	2.13	0.10	0.64	0.50	20.54	3.74	2.16	0.43	0.10	0.06	0.51	0.16	0.13	0.04	0.06	0.08	0.10	0.04	0.04	0.65	0.16	0.34	-	-	98.42	26.87
3759	P67-114 0400 1/12/07	0.46	1.21	0.02	1.25	1.06	6.58	2.09	20.72	2.37	1.43	0.40	2.21	0.42	0.52	0.71	0.63	0.64	0.54	0.12	0.18	3.76	1.83	1.58	1.08	0.30	89.08	31.76
3761	P67-114 0400 1/13/07	0.43	1.25	0.02	1.29	0.88	9.54	2.53	16.02	1.83	1.25	0.04	1.92	0.34	0.43	0.56	0.52	0.52	0.39	0.10	0.16	3.02	1.29	1.32	1.69	-	90.85	29.92
3762	P67-114 0400 1/14/07	1.02	1.73	0.03	0.68	0.19	18.63	5.73	2.66	0.87	0.52	0.46	1.12	0.21	0.09	0.16	0.33	0.24	0.23	0.11	0.10	1.47	0.98	0.64	1.33	0.32	94.39	27.89
3763	P67-114 0400 1/15/07	1.21	1.83	0.05	0.69	0.18	19.25	4.92	1.98	0.86	0.46	0.36	0.93	0.17	0.15	0.12	0.25	0.16	0.20	0.07	0.06	1.18	0.82	0.49	0.61	-	96.04	27.01
3765	P67-114 0400 1/16/07	1.00	1.52	0.05	0.68	0.18	17.66	4.28	1.70	0.82	0.41	0.31	0.78	0.16	0.07	0.12	0.22	0.13	0.16	0.06	0.04	0.96	0.72	0.41	1.86	5.24	89.99	24.46
3768	P67-114 TLP Drum # 11	0.63	1.28	0.04	0.67	0.28	18.44	5.23	2.41	0.86	0.11	0.10	1.04	0.09	0.09	0.14	0.12	0.21	0.21	0.11	0.09	1.06	0.21	0.55	1.58	1.20	94.54	26.94
3767	P67-114 0400 1/17/07	1.27	1.49	0.10	0.44	0.52	17.96	2.84	0.82	0.86	0.10	0.28	0.45	0.10	0.18	0.09	0.15	0.07	0.10	0.05	0.08	0.82	0.38	0.25	-	-	97.69	22.48
3772	P67-114 0400 1/18/07	1.39	1.39	0.12	0.38	0.58	17.46	2.39	0.72	0.85	0.09	0.10	0.37	0.08	0.16	0.07	0.12	0.11	0.09	0.04	0.06	0.73	0.19	0.23	-	-	98.00	21.42
3774	P67-114 0400 1/19/07	1.32	1.44	0.12	0.37	0.59	16.20	2.33	0.73	0.85	0.09	0.10	0.37	0.10	0.15	0.07	0.12	0.11	0.20	0.16	0.06	0.97	0.19	0.22	-	0.38	97.39	20.11
3778	P67-114 0400 1/20/07	1.58	1.47	0.14	0.41	0.61	17.05	2.15	0.75	0.82	0.08	0.10	0.35	0.09	0.13	0.06	0.10	0.09	0.18	0.16	0.06	0.87	0.18	0.23	-	0.33	97.57	20.77
3779	P67-114 TLP Drum # 12	1.03	1.19	0.11	0.43	0.55	17.58	2.57	1.13	0.88	0.09	0.26	0.43	0.14	0.17	0.08	0.13	0.07	0.14	0.04	0.07	0.84	0.35	0.21	1.54	0.29	95.89	22.16
3777	P67-114 0400 1/21/07	1.69	1.79	0.06	0.91	0.33	18.56	4.57	2.48	0.87	..35	0.31	0.83	0.14	0.25	0.12	0.22	0.13	0.16	0.06	0.06	1.14	0.31	0.46	1.11	-	96.11	26.48
3776	P67-114 0400 1/22/07	1.75	1.86	0.07	0.99	0.35	17.86	4.12	2.70	0.86	0.35	0.28	0.83	0.16	0.26	0.13	0.23	0.14	0.16	0.06	0.05	1.19	0.63	0.37	-	-	96.95	25.54
3781	P67-114 0400 1/23/07	1.74	1.80	0.07	0.97	0.34	17.68	4.25	2.58	0.85	0.35	0.29	0.82	0.16	0.25	0.13	0.23	0.13	0.16	0.06	0.05	1.17	0.64	0.37	0.59	-	96.38	25.36
3782	P67-114 TLP Drum # 13	1.57	1.62	0.06	0.95	0.33	17.58	4.37	2.65	0.84	0.36	0.33	0.90	0.18	0.30	0.16	0.27	0.17	0.21	0.09	0.07	1.45	0.69	1.42	-	-	95.60	25.44
3784	P67-114 0400 1/24/07	0.17	1.89	0.10	1.21	0.40	15.64	2.95	2.57	0.82	0.34	0.21	0.70	0.15	0.22	0.13	0.21	0.16	0.13	0.06	0.05	1.11	0.55	0.31	0.50	-	96.71	21.98
3786	P67-114 0400 1/25/07	0.17	1.78	0.08	1.15	0.37	15.61	3.20	2.62	0.84	0.35	0.24	0.76	0.17	0.25	0.15	0.24	0.20	0.17	0.08	0.07	1.33	0.59	0.39	1.07	0.26	95.52	22.27
3788	P67-114 0400 1/26/07	0.18	1.86	0.09	1.23	0.39	15.90	3.10	2.63	0.84	0.34	0.22	0.72	0.15	0.23	0.14	0.21	0.17	0.14	0.06	0.05	1.15	0.56	0.44	-	-	97.01	22.47
3793	P67-114 TLP Drum # 14	0.16	1.83	0.09	1.22	0.38	15.83	3.11	3.02	0.85	0.35	0.23	0.77	0.17	0.25	0.15	0.24	0.20	0.18	0.08	0.05	1.32	0.58	0.41	-	-	96.84	22.81
3790	P67-114 0400 1/27/07	0.07	1.65	0.14	0.88	0.49	17.07	2.16	1.15	0.82	0.31	0.11	0.44	0.13	0.16	0.09	0.14	0.07	0.08	0.04	0.07	0.78	0.42	0.17	-	-	97.81	21.20
3791	P67-114 0400 1/28/07	0.06	1.63	0.15	0.92	0.51	17.89	1.84	0.90	0.82	0.29	0.08	0.36	0.12	0.14	0.07	0.11	0.12	0.11	0.04	0.06	0.77	0.37	0.19	0.25	-	97.60	21.45
3792	P67-114 0400 1/29/07	0.05	1.64	0.16	0.69	0.51	17.98	1.84	0.84	0.82	0.29	0.07	0.35	0.12	0.14	0.07	0.11	0.09	0.17	0.04	0.06	0.80	0.36	0.13	-	-	97.89	21.48
3795	P67-114 0400 1/30/07	0.06	1.66	0.02	0.79	0.53	18.74	1.78	0.77	0.74	0.25	0.05	0.31	0.10	0.11	0.06	0.09	0.07	0.06	0.03	0.06	0.58	0.30	0.23	1.11	0.27	96.77	22.03
3796	P67-114 TLP Drum # 15	0.05	1.49	0.01	0.76	0.51	17.96	1.92	1.01	0.84	0.08	0.08	0.39	0.12	0.15	0.08	0.12	0.10	0.08	0.04	0.07	0.76	0.16	0.22	-	-	98.02	21.73
3798	P67-114 0400 1/31/07	0.04	1.07	0.20	0.75	0.67	17.02	1.53	0.66	0.64	0.24	0.05	0.26	0.04	0.09	0.04	0.06	0.13	0.11	0.11	0.06	0.64	0.29	0.12	2.12	-	96.19	19.85
3800	P67-114 0400 2/1/07	0.03	1.39	0.17	0.71	0.65	14.06	1.43	0.74	0.72	0.28	0.08	0.31	0.11	0.12	0.06	0.09	0.07	0.15	0.04	0.06	0.70	0.36	0.18	-	-	98.04	16.95
3802	P67-114 0400 2/2/07	0.03	1.23	0.01	0.68	0.65	15.28	1.47	0.76	0.72	0.28	0.08	0.32	0.11	0.12	0.06	0.09	0.07	0.06	0.03	0.05	0.59	0.36	0.16	-	-	98.17	18.23
3807	P67-114 TLP Drum # 16	0.03	1.37	0.25	0.59	0.66	15.11	1.55	0.86	0.73	0.14	0.19	0.33	0.06	0.12	0.06	0.04	0.07	0.16	0.12	0.05	0.68	0.33	0.15	-	-	98.11	18.25
3804	P67-114 0400 2/3/07	0.02	1.85	0.16	0.53	0.69	13.94	1.34	0.63	0.34	0.11	0.18	0.25	0.05	0.10	0.05	0.11	0.10	0.12	0.03	0.05	0.61	0.29	0.15	0.15	-	98.46	16.25
3805	P67-114 0400 2/4/07	0.02	2.18	0.16	0.57	0.73	13.99	1.25	0.58	0.31	0.08	0.12	0.18	0.15	0.05	0.06	0.07	0.07	0.07	0.07	-	0.54	0.20	0.06	0.40	-	98.49	16.13
3808	P67-114 0400 2/5/07	0.02	1.82	0.15	0.55	0.71	12.83	1.12	0.57	0.57	0.09	0.14	0.18	0.15	0.06	0.02	0.04	0.07	0.08	0.02	0.03	0.47	0.23	0.10	0.76	0.15	97.72	15.09
3810	P67-114 0400 2/6/07	0.02	2.17	0.16	0.56	0.73	11.67	1.10	0.60	0.56	0.07	0.10	0.07	0.11	0.13	0.04	0.05	0.05	0.03	0.06	0.06	0.53	0.17	0.11	-	0.26	98.37	13.93
3814	P67-114 TLP Drum # 17	0.02	2.18	0.17	0.61	0.74	13.37	1.21	0.53	0.52	0.07	0.10	0.18	0.15	0.05	0.06	0.07	0.07	0.02	0.07	0.07	0.56	0.17	0.06	-	0.29	98.40	15.63
3816	P67-114 0400 2/7/07	0.02	1.78	0.14	0.74	0.73	10.59	1.01	0.53	0.51	0.06	0.10	0.15	0.11	0.04	0.07	-	0.05	0.03	0.05	-	0.35	0.16	0.11	-	-	98.87	12.64
3820	P67-114 0400 2/8/07	0.02	1.80	0.14	0.74	0.73	10.48	0.99	0.53	0.51	0.06	0.09	0.14	0.11	0.04	0.06	-	0.04	0.03	0.05	-	0.33	0.15	0.11	0.08	-	98.82	12.51
3822	P67-114 0400 2/9/07	0.02	1.95	0.15	0.79	0.75	11.10	0.99	0.48	0.42	0.05	0.07	0.13	0.10	-	-	-	0.05	0.03	0.05	-	0.23	0.12	0.11	-	0.35	98.77	12.99
3824	P67-114 TLP Drum # 18	0.02	1.73	0.14	0.77	0.74	10.74	1.01	0.53	0.51	0.06	0.09	0.14	0.11	0.04	0.06	-	0.05	0.03	0.05	-	0.34	0.15	0.11	-	0.21	98.68	12.79
																											100.00	
GC ANALYSES OF HYDROGENATED TLP PRODUCT DRUMS																											100.00	
3697	P67-114 TLP Drum # 1	0.15	1.45	0.01	0.60	0.46	17.76	5.13	8.78	1.04	0.40	0.08	1.55	0.25	0.52	0.29	0.45	0.44	0.56	0.08	0.15	2.74	0.48	1.15			94.59	32.71
3708	P67-114 TLP Drum # 2	0.31	0.91	0.46	0.77	0.27	16.92	3.98	5.61	1.23	0.57	0.34	1.27	0.29	0.41	0.32	0.23	0.26	0.08	0.08	0.10	1.77	0.91	0.90	1.66	0.40	93.13	27.74
3724	P67-114 TLP Drum # 3	0.64	1.51	0.09	0.39	0.54	19.77	3.87	0.83	0.93	0.11	0.07	0.27	0.15	0.17	0.05	0.13	0.21	0.08	0.20	0.09	1.08	0.18	0.22	3.82	0.62	93.15	25.40
3725	P67-114 TLP Drum # 4	0.60	1.24	0.1	0.42	0.57	16.93	3.16	0.77	0.87	0.12	0.10	0.26	0.14	0.08	0.06	0.12	0.09	0.07	0.08	0.06	0.70	0.22	0.19	2.99	0.52	94.51	21.73
3728	P67-114 TLP Drum # 5	1.20	1.71	0.13	0.38	0.60	16.82	3.01	0.73	0.83	0.11	0.08	0.19	0.13	0.21	0.06	0.10	0.20	0.08	0.07	0.16	1.01	0.19	0.23	3.12	0.57	94.05	21.39
3730	P67-114 TLP Drum # 6	1.80	1.71	0.15	0.5	0.66	18.02	2.57	0.62	0.86	0.10	0.07	0.14	0.10	0.17	0.05	0.07	0.16	0.08	0.15	0.04	0.82	0.17	0.23	0.72	-	97.20	22.07
3742	P67-114 TLP Drum # 7	1.88	1.71	0.15	0.48	0.63	16.18	2.67	0.71	0.82	0.11	0.09	0.22	0.04	0.12	0.17	0.10	0.06	0.10	0.15	0.06	0.80	0.20	0.23	0.58	-	97.37	20.38
3747	P67-114 TLP Drum # 8	1.71	1.92	0.13	0.47	0.56	18.93	3.15	0.79	0.87	0.13	0.09	0.37	0.13	0.07	0.06	0.12	0.05	0.09	0.05	0.04	0.61	0.22	0.17	-	-	98.13	23.74
3755	P67-114 TLP Drum # 9	1.62	2.13	0.10	0.64	0.50	20.54	3.74	2.16	0.43	0.10	0.06	0.51	0.16	0.13	0.04	0.06	0.08	0.10	0.04	0.04	0.65	0.16	0.34	-	-	98.42	26.87
3768	P67-114 TLP Drum # 11	0.63	1.28	0.04	0.67	0.28	18.44	5.23	2.41	0.86	0.11	0.10	1.04	0.09	0.09	0.14	0.12	0.21	0.21	0.11	0.09	1.06	0.21	0.55	1.58	1.20	94.54	26.94
3779	P67-114 TLP Drum # 12	1.03	1.19	0.11	0.43	0.55	17.58	2.57	1.13	0.88	0.09	0.26	0.43	0.14	0.17	0.08	0.13	0.07	0.14	0.04	0.07	0.84	0.35	0.21	1.54	0.29	95.89	22.16
3782	P67-114 TLP Drum # 13	1.57	1.62	0.06	0.95	0.33	17.58	4.37	2.65	0.84	0.36	0.33	0.90	0.18	0.30	0.16	0.27	0.17	0.21	0.09	0.07	1.45	0.69	1.42	-	-	95.60	25.44
3793	P67-114 TLP Drum # 14	0.16	1.83	0.09	1.22	0.38	15.83	3.11	3.02	0.85	0.35	0.23	0.77	0.17	0.25	0.15	0.24	0.20	0.18	0.08	0.05	1.32	0.58	0.41	-	-	96.84	22.81
3796	P67-114 TLP Drum # 15	0.05	1.49	0.01	0.76	0.51	17.96	1.92	1.01	0.84	0.08	0.08	0.39	0.12	0.15	0.08	0.12	0.10	0.08	0.04	0.07	0.76	0.16	0.22	-	-	98.02	21.73
3807	P67-114 TLP Drum # 16	0.03	1.37	0.25	0.59	0.66	15.11	1.55	0.86	0.73	0.14	0.19	0.33	0.06	0.12	0.06	0.04	0.07	0.16	0.12	0.05	0.68	0.33	0.15	-	-	98.11	18.25
3814	P67-114 TLP Drum # 17	0.02	2.18	0.17	0.61	0.74	13.37	1.21	0.53	0.52	0.07	0.10	0.18	0.15	0.05	0.06	0.07	0.07	0.02	0.07	0.07	0.56	0.17	0.06	-	0.29	98.40	15.63
3824	P67-114 TLP Drum # 18	0.02	1.73	0.14	0.77	0.74	10.74	1.01	0.53	0.51	0.06	0.09	0.14	0.11	0.04	0.06	-	0.05	0.03	0.05	-	0.34	0.15	0.11	-	0.21	98.68	12.79

Table 1-6: Average yield data for conditions 1 through 13.

	AVERAGE OVER EACH CONDITION								
	LHSV	RX 1	RX 2	Pressure	Smoke Pt.	Tetralin	Decalin	FIA Arom.	356°F-
	cc/cc-hr	WABT, °F	WABT, °F	psig	mm	wt%	wt%	vol%	wt%
Condition 1	0.5	630	600	600	15	3.4	27.9	26	9.2
Condition 2	0.5	650	600	600	15	4.3	26.7	29	11.5
Condition 3	0.5	670	600	600	14	8.8	22.9	37.9	13
Condition 4	0.3	690	650	600	14	8.3	17.5	44.8	17
Condition 5	0.3	690	650	900	16.5	2.1	22.8	19.3	20
Condition 6	0.3	690	650	1200	22	0.8	20.4	6.2	27
Condition 7	0.5	690	650	1200	20.9	0.7	20.6	5.6	30.4
Condition 8	0.5	690	650	900	16	2.8	21.8	16.6	26
Condition 9	1.0	690	650	600	9	18	10.5	68	12.3
Condition 10	0.5	670	670	1200	15	2.5	24.2	18	19.3
Condition 11	0.5	680	680	1200	16	1.7	22	17.7	21.5
Condition 12	0.5	690	690	1200	18.5	1.7	21.5	15	27
Condition 13	0.5	700	700	1200	16.5	2.6	18.5	19.5	29

1.3.2.3. Hydrogenation of HDT 1:1 LCO/RCO 570F (2nd Pass) Condition 14

Since this condition achieved a smoke point of 22 the feed rate was increased to an LHSV of 0.5 (Condition 7) which achieved a smoke point of 21 mm. However, it was observed that as the operating conditions were adjusted to achieve the target smoke point and corresponding low aromatics level and maximum decalin content, the fraction of the liquid product boiling below 356ºF (356ºF-) was progressively increasing. Reference to **Table 1-4** indicates that at the start of the hydrogenation operation, with incomplete conversation of the tetralin to decalin the 356ºF- was in the range of 6 to 12 wt% (Days 1- 4). As the conversion level of tetralin was raised the 356ºF- level increased to 20 on Day 10 (Drum 2), to 25 wt% by Day 14 (Drum 3) and to 34 wt% after 21 days (Drum 5).

Since the previous program had employed a lower operating pressure the pressure was reduced from 1200 psig to 900 and then to 600 psig Conditions 8 and 9 to determine if the higher operating pressure was responsible for the high 356ºF- production. However, the decrease in pressure, while the reactor temperature was maintained resulted in an increase in tetralin level and a corresponding decrease in smoke point. Consequently the pressure was adjusted back to 1200 psig while the temperature was reduced to determine if operating temperature was responsible for the high 356ºF- production (Conditions 10 and 11). This resulted in a reduced amount of 356ºF- and tetralin but the smoke point achieved was below the target of 19 mm. Condition 9 employed a higher space velocity as an attempt to be able to decrease the amount of time required to produce on spec product. This approach was not successful. The LHSV feed rate was therefore returned to 0.5 where it was held for the remainder of the production . Increases in reactor temperatures were subsequently made until the target smoke point was achieved. The amount of 356ºF- returned to about the 30wt% level.

Once all of the hydrotreated TLP had been passed once through the hydrogenation operation (January 26, 2007) the first 4 drums of single pass hydrogenated TLP were passed a second time at 700F, 1200 psig and 0.5LSV. This operation yield even higher levels of 356ºF- (37 to 53%) and smoke points in the range of 20 to 25.

Subtask 1.4: Fractionation into Refinery Product Slate

1.4.1. Batch Fractionation of Total Liquid Product (TLP)

The TLP was batch fractioned in PARC's 150 gallon still to remove the 356ºF- component. The still charges were individual drums from the hydrogenation step, i.e. the total hydrogenated product was not pre-blended. The individual batch yields are contained in **Table 1-7**.

Table 1-7: Individual batch yields for fractionation of TLP.

	356ºF-	356-560ºF	550-650ºF	650ºF+	560ºF+
Program					
Current (14)	6.8%	55.8%			37.4%
13 (2004)	5.9%	79.5%	9.4%	5.2%	14.7%

1.4.2. Overall Product Yields

In order to compare product yields from Program 13, which employed full boiling range RCO and LCO, yields were calculated on an overall basis which takes into account the 560ºF material that had been removed from the hydrotreater feed. In the case of the RCO the feed was batched distilled to remove the 560ºF+ boiling material while in the case of the LCO, United Refining provided LCO which had been similarly treated on the continuous fractionation unit in the refinery.

The calculated fraction yields are shown below in comparison to those obtained in Program 13 in late 2004. To arrive at the full range basis the approach was as follows:

1. The amount of 560ºF + in the LCO was taken from the SIMDIS GC data in **Table 1-8** and Appendix B.
2. The amount of 560ºF+ material in the RCO was taken from the average of the three batch distillations done at PARC.
3. The combined weighted average for 50/50 by weight mixture of RCO and LCO was calculated from the individual percentages of the 560ºF+ and the weighting factors of 0.5 each. This gave a value of 37.45wt%
4. The relative yields of 356ºF- (180ºC-) and 356-560ºF from the 1st hydrogenated product batch distillation were then adjusted to a basis that would have included the 560ºF+ in the feed material by multiplying the batch distillation yield by 100-37.45.

As can be seen from the data given above, the current program gave much higher yield of 560ºF+ (37.4 vs 14.7) and a correspondingly lower yield of 356 to 560ºF jet fuel (55.8 vs 79.5). This leads us to speculate that a higher amount of the 560ºF+, when left in the feed, would have been converted into 560ºF- product. Since the full range LCO had 50% of its components in the 560ºF+ range it might be reasonable to assume that this might contribute more to this effect.

1.4.3. Comparisons with Previous Programs

(a) Product properties

Table 1-9 compares the properties of the 10 drums of JP-900 (SR-0225 and SR0227CT) produced in late 2004 and tested at Wright Patterson with the 356ºF+ jet fraction from the first batch distillation (X-1390). The boiling range, specific gravity, flash point and total decalin of X-1390 were somewhat lower than those of SR-0225.

Aromatics content measured by the silica gel column separation ASTM method D 1319 (Fluorescent Indicator Analysis or FIA) was somewhat higher for the current product X-1390 though the smoke points, which are directly related to aromatic content were close to the same. Nevertheless the aromatics content is well below the JP-5 and JP-8 spec level of 25% maximum and the smoke point meets the spec of 19 minimum.

Table 1-8: Feed simulated distillation analyses (ASTM D2887).

	100%	570°F+	PR-	590°F-	1:1	1:1 570°F-	RCO Components			
Description	RCO	RCO	LCO	LCO	RCO/LCO	RCO/LCO	Solv.	Naphth.	MNF	NSR
°F										
IBP		452	233	284		325	182	393	408	423
5		519	405	436		408	288	409	425	449
10		545	447	448		409	324	409	441	455
15		572	481	454		409	328	410	450	488
20		589	488	479		409	338	410	450	509
25		590	498	485		410	355	410	450	510
30		591	516	487		410	357	410	451	520
35		591	524	491		410	358	410	454	534
40		595	536	492		447	358	410	455	540
45		620	546	500		450	358	411	476	551
50		625	561	513		475	358	411	486	586
55		651	574	519		486	359	411	497	591
60		659	587	525		491	359	411	509	592
65		660	601	531		500	360	411	510	592
70		670	616	539		510	366	411	511	595
75		677	625	545		520	395	411	520	616
80		720	640	554		530	409	411	534	659
85		787	652	569		541	410	411	540	671
90		869	665	577		554	410	412	572	704
95		963	684	594		577	411	412	591	821
FBP		1082		645		616	436	413	671	1005

Table 1-9: Jet fuel property comparison

	<-US Mil Spec->		Commercial Specs			114013	114014		
PARC Sample Code			**PR1630**	**PR1631**		**SR-0225**	**X-1390**		
						(1)	**(2)**		
PSU Sample Code						**EI-171**			
Sim Dist wt%(5890)	***JP-5***	***JP-8***	***JP-5***	***JP-5***	***JP-8***				
IBP, °F			268	274	234	296	271		
5, °F			309	320	301	343	322		
10, °F	**365 max**	**367 max**	326	339	320	359	339		
50, °F			398	413	397	401	386		
95, °F			488	490	503	520	508		
EP, °F	**608 max**	**626 max**	528	518	547	574	611		
Specific Gravity, g/cc	**.788-.845**	**.775-.840**	0.8031	0.809		0.8713	0.8508		
Sulfur, ppm	**4000 max**	**3000 max**	1300	1100		0.71	1.07		
Nitrogen, ppm			0.494	9.58		0.70	0.30		
Aromatics vol% (D1319)	**25 max**	**25 max**				1.3	7.6		
Olefins vol% (D1319)	**5 max**	**5 max**				0.5	2.0		
Saturates vol% (D1319)						98.2	90.4		
Smoke Pt-PARC, mm (D1322)						25.5			
Smoke Pt-PSU, mm (D1322)	**19 min**	**19 min**	24.57	23.95					
Carbon Deposit mg/cm3						36.93			
Flash Point CC, °F (D93)	**140 min**	**100 min**	109.5	122.2		141.0	131.0		
Flash Point OC, °F (D92)									
Composition wt%									
Cyclohexane			0.39	0.4		0.50	0.04		
Xylenes			0.23	0.51		0.07	0.23		
Indan			0.18	0.16		0.24	0.65		
Indene			0.52	0.41		0.48	0.40		
t-decalin			0.45	0.46		29.33	22.35		
c-decalin			0.15	0.16		5.97	3.94		
Tetralin			0.95	0.86		0.41	0.93		
Naphthalene			0.51	0.71		1.21	1.03		
2-Methylnaphthalene			0.58	0.79		0.36	0.15		
1-Methylnaphthalene			0.37	0.42		1.05	0.23		
Ethylnaphthalenes			0.63	0.68		0.59	0.23		
Dimethylnaphthalenes			1.69	1.74		0.83	0.50		
Trimethylnaphthalenes			0.04	-		0.79	0.07		
T,P&Hmethyl-n's			0.4	1.89		0.64	0.34		
Other, 100 - All Naphthalenes			95.8	93.8		94.5	97.5		

(1) SR-0225 is the hydrogenated product from the blend of 150 still runs X-1103, 1104 & 1106 distilled to give 356°F to 518°F product
(2) X-1390 is the 340°F+ product from the distillation of the first three drums from P67-114 on the 150-still

(b) Operating Conditions

Table 1-10 summarizes some of the operating conditions and some of the product properties for five previous programs (1, 5, 9, 10 and 13) and compares them to the current program (14). This comparison is not straight forward since the Jet fraction was arrived at by different routes and in some cases also employed different catalysts and different batches of Koppers RCO and different sources of LCO. Each of these factors may have an influence on product properties. Nevertheless, it was made with a view to it yielding what factors might be most important in influencing product property trends.

Program 1 used LCO supplied by BP and employed a pressure of 2100 psig in the hydrogenation step based on the catalyst suppliers recommendations and previous work conducted by BP. Total decalin yield was 34%. All later programs utilized lower pressure in the hydrogenation step.

Programs 9 and 13 all employed pre-fractioned feeds in the hydrogenation step. Decalin yield was 26 to 44% respectively. The latter value was anomalously high compared to most other programs.

Program 8, in which hydrotreated feed, pre-fractionated to 218-572F, yielded a high amount of 356F – of **20 to 28%.** Program 9 had 20% 356F- in the hydrogenated TLP produced at 700 psig. In comparison to these earlier programs the 356F- yield in the current program 14 is consistently higher at **26 to 33%** and when subjected to a second hydrogenation pass at 1200 psig, became even higher at **32 to 53%.** We currently do not have an explanation for this observation. However, the data suggests that operating at a pressure of 1200 psig rather than 700 psig (Program 9) does increase the 356F- yield. We had suspected, based on some information from the catalyst supplier, that operating with

very low sulfur feed might be responsible. However, the data in Table 8 does not appear to support this.

Table 1-10: Feed and jet fuel product composition summary.

Prog	YEAR	MATERIAL	FEED	LHSV	Press psig	Feed S ppm	TLP---------->				JET FRACTION---------->						
HYDROTREATING							N	T	D's	N+T+D	% 356F- in TLP	Dist X No	N	T	D's	N+T+D	% 356F- from Dist
114001	2000	FEED	**Full Range**			**7,700**	32.3			32.3							
		HDT Pass 1		1	710		6.47	24.54	2.43	33.4							
		HDT Pass 2	X-127	0.5	710	**30 est**	4.25	23.33	6.42	34.0	12	X-205	4.56	24.89	5.17	34.62	9.3
114005	2003	FEED	**Full Range**			**10,900**	33			33.0							
		HDT Pass 1		0.8	600		1-12	22-30	0.1-0.2	31-34							
		HDT Pass 2		0.4	600	**700 est**	1.40	20.57	11.55	33.5	5	X-868	2.41	34.68	20.09	57.18	4.6
114008	2004	FEED	**218-572F (X-942)**			**117**	39.03	0.05		39.1							
		HDT Pass 1		0.25	600		6	21	10	37	20	X-954 4-bt	6	22.6	11.8	40.4	10.3
		HDT Pass 1		0.25	1000		2	15	21	38	28	X-969 4-bt	2.5	18.5	20.5	41.5	10.7
114010	2004	FEED	**Full Range**			**12700**	30.96		0.07	31.03							
		HDT Pass 1		1	600		16.9	13.7	0.2	30.8	7						
		HDT Pass 2		0.45	600	**1,200**	7	21	4	32	8						
114014	2006	FEED	**570F-**			**14,100**	36.2		0.04	36.2							
		HDT DR 3	Dr3	0.5	600		2.15	28.79	4.41	35.4	5 - 7						
HYDROGENATION																	
114001		HYD Pass 1		1.1	2100	**<3**	0.91	2.43	30.39	33.7							
	180-330C	HYD Pass 2	X-205	1.1	2100	**<1**	0.93	0.45	32.91	34.3	5	X-205	1.07	0.38	34.07	35.52	7.9
		HYD Pass 2		1.1	2100	**<1**	0.94	0.21	34.23	35.4							
114009	2004	FEED	**HDT 570F-**			**2**	8.62	25.37	2.47	36.5							
	P80	HYD Pass 2	X-992	1	700, 1200 & 2100		1	0.7	37	38.7			1.05	0.7	35.5	37.25	12
		FEED	Full Range HDT			**22**	7.54	21.94	2.12	31.6							
		HYD Pass 2		1	700		0.75	2.38	22.65	25.8	12	X-1014	0.92	2.83	26.47	30.22	20
			6/18/2004	1	700		0.82	1.15	26.73	28.7							
114010	2004	FEED	Full Range HDT	1		**10-22**	8	19	4	31.0							
		HYD Pass 1		0.5	600		6	20.1	4.8	30.9	10-36	X-1058	1.7	7.5	28.1	37.3	
		HYD Pass 2		0.5	600	**16**	1	5	25	31.0	10						
114013	2004	FEED	**HDT+HDY 1st Pass 550F-**			**1 - 4.6**				32 - 37.6							
		HYD Pass 2	1LHSV, 1200psig	1	1200		1.21	0.41	35.3	36.9	14 - 27						
		FEED SR224	**HDT JET FRACT**				10.8	32.24	3.36	46.4	5.8						
		HYD Pass 1					0.6	22	23	45.6	6-9						
		HYD Pass 2	Dr 7	0.5	1200	**17**	1.19	0.19	44.64	46.0	7 - 16						
114014	2007	FEED	**570F-**			**2 to 7**											
	Jan/Feb	HDY DR 2		0.3	900		1.23	5.61	20.9	27.7		X-1390	1.0	0.9	26.29	28.2	19.2
		HDY DR 3-8		0.5	1200												
		HDY DR 7		0.5	1200		0.82	0.71	18.85	20.4	32.5						
		HDY DR 8		0.5	1200		0.87	0.79	22.08	23.7	29.3						
		HDY DR 9		0.5	900		0.43	2.16	24.28	26.9	26.0						
		HDY 2nd PASS	HDY 570F- 1st Pass	0.5	1200	**<1**	0.52	0.53	**14.48**	**15.5**	32-53						

(c) Yield Loss

The fact that a second pass of hydrogenated TLP in Program 14 resulted in a substantial increase in 356ºF- material in the TLP and a substantial loss of decalin from about 23 to 15 % suggests the decalin was undergoing ring opening, presumably by hydrocracking. It is possible that deliberate addition of organic nitrogen compounds might suppress this reaction. This is an accepted practice in hydrocracking operations employing zeolites where it is required to minimize production of products boiling at lower temperature than the desired gasoline, jet or diesel fuel.

A recent publication by UOP (National Petroleum Refiners Association, Annual Meeting, Paper No AM-07-40) maybe verification that this speculation is correct. This article announced UOP's new process UOP-LCO-X™. This process converts LCO to Benzene, Toluene and Xylenes (BTX) in a three step process as follows:

1. Hydrotreating to remove sulfur and nitrogen (required to provided sulfur and nitrogen free BTX)
2. Conversion step to converted 2 and 3 member aromatic rings to single ring aromatics
3. Aromatics maximization. This step appears to involve transalkylation of substituted benzenes to reduced the degree of substitution and possibly dehydrogenation of substituted cyclohexanes resulting from ring opening of decalins produced by saturation in Step 2

The details of the type of catalyst employed in Steps 2 and 3 are not revealed.

Task 2. Evaluation of Coal-based Gasoline and Diesel Products in IC Engines and Related Studies

By introducing coal-derived streams into the refinery, several perturbations to the quality and quantity of refinery streams may result and directly impact vehicular fuels production. The coal contribution to the refinery streams will affect the quality, composition and performance of the resulting vehicular fuels. The fraction of the hydrotreated streams that boils below 180°C will be directed to the gasoline pool. Having components from coal is expected to boost octane number and aromatic content, and therefore, boost value. The >270°C cut of the hydrotreated stream would be low in sulfur due to the severe hydrotreatment. The effect on flash point will need to be determined if this stream is sent to the fuel oil pool and/or diesel pool. If this stream is combined with diesel fuel, it will add cycloparaffins, which will increase energy density and boost value. However, the impact on cetane number and sooting tendency is unclear. The following task structure will permit assessment of the impact of refinery integration of JP-900 production on gasoline and diesel fuel.

Subtask 2.1. Impact on Gasoline Quality and Performance

Under this subtask, our efforts have consisted of optimizing the signal quality from the fiber optic sensors for measuring in-cylinder flame propagation in the SI engine and ignition studies of methyl cyclohexane to understand the impact of the coal-derived compounds on knocking and flame propagation.

Subtask 2.1.1 Preparation of Laboratory and Instrumentation

Combustion and emission properties of the coal-based gasoline in SI engine application are being studied in a single-cylinder Ricardo Hydra research engine and a single-cylinder Waukesha CFR octane rating engine. Under this subtask, we developed instrumentation for combustion analysis that involves the use of photodiodes attached to eight fiber-optic eyes mounted on an instrumented spark plug [See Figures 2-1 and 2-2]. This novel circuit design has been a major part of the work by doctoral student Yi Yang during Year 4 of the project, with assistance by an undergraduate electrical engineer, Emil Laftchiev, who is working toward his senior thesis. To date, our examination of the decomposition chemistry of methyl cyclohexane (a model for coal-derived gasoline) has resulted in an ACS preprint **[2-1]** and another recently submitted ACS preprint to be presented at the ACS National Meeting in Boston in 2007. **[2-2]**

Figure 2-1 Optic-fiber Spark Plug for the CFR Octane Rating Engine

Figure 2-2 Close-up of the Electrodes and Eight Optical Openings

Subtask 2.1.2 Impact on Chemical and Physical Properties

Due to disruption of the funding to the project, no work was done on this task for the last six months.

Subtask 2.2 Impact on Diesel Fuel Quality and Performance

Under this subtask, we returned to a significant focus on facility development activities, involving refinement and enhancement of two existing engine test stands, one housing a Navistar V-8 7.3L turbodiesel engine and the other housing a DDC 4-cylinder 2.5L turbodiesel engine.

2.2.1 Acquisition, Installation and Instrumentation of Ignition Test Equipment

This work has been completed, with some updated information on configuration and procedures given in Section 2.1.1. The equipment was applied to ignition studies of diesel and other fuels and has resulted in a paper appearing in *Combustion & Flame.* **[2-3]**.

2.2.2. Development of Analytical Methods and Test Procedures

The modification of the CFR Octane Rating engine to serve as a rapid compression machine for ignition studies represents a unique adaptation of a standard instrument and is providing a means of comparing experimental data with kinetic models of the ignition process.

2.2.3. Evaluation of Capabilities and Needs for Supplemental Measurements and Analyses

Due to disruption of the funding to the project, we postponed a plan for upgrading an existing gas chromatograph for hydrocarbon speciation from engine exhausts. We intended to perform the upgrade of the GC (from packed to capillary columns) and use a method that is the same as in the Shimadzu GC-MS. When it is able to be completed, this upgrade will allow the GC results to be interpreted through the species identification capabilities of the GC-MS.

2.2.4. Impact on Chemical and Physical Properties

We continued work on examination of the relationship between sooting tendency, combustion phasing and NOx emissions, extending the work we reported in the Year 3 Annual Report on doping of fuel with phenanthrene to probe the relationship between radiation heat transfer and NOx emissions. **[2-4]** Master's student Yu Zhang is working on a thesis on the subject of NOx emissions in which this interplay between sooting formation and NOx emissions was a central issue. **[2-5]**

2.2.5 Impact on CI Engine Emissions and Performance

In-Cylinder Imaging of Coal-Derived Diesel Combustion

For the purpose of better understanding the impact of the coal-derived compounds on the injection, ignition and combustion of diesel fuels in a practical engine, we have developed an installation of an existing AVL 513D Engine Videoscope (purchased under

an NSF Research Equipment Grant, # CTS-0079073) in our Navistar V-8 7.3L turbodiesel engine. This required design and machining access for an endoscope probe and a light guide to visualize the fuel spray and the spray flame. The modified cylinder head is ready for use and will be implemented after some other development work on the engine test stand. To improve control over the preparation of the cylinder charge, doctoral student Elana Chapman has been working on development of a novel intake air preheating system based on an extruded high temperature ceramic heat exchanger. This upgrade to the engine test stand will permit more precise control of start of combustion and thereby the phasing of the combustion process.

Task 3. Desulfurization, Denitrogenation, Saturation of Aromatics, Chemicals from Coal

Chunshan Song, Jae Hyung Kim, Hyun Jae Kim, Vasudha Dhar, Boonyawan Yoosuk and Xiaoliang Ma

Subtask 3.1: Desulfurization and Denitrogenation

Since environmental regulations on sulfur content of fuel is stringent, ultra-deep hydrodesulfurization (HDS) of fuels has become an important research area **[**3-1**]**. It was effective on June, 2006 that the sulfur level must be lower than 15 ppm S in diesel fuels, as dictated by the US EPA. In order to improve efficiency of HDS, therefore, many studies on deep hydrodesulfurization of model and real diesel fuels are being conducted with various methods and different catalysts by many research groups **[**3-1-3-7**]**. Hydrodesulfurization is currently a major process in petroleum refineries to reduce the sulfur in the liquid hydrocarbon fuels. However, it was found by many researchers that the nitrogen compounds coexisting in middle–distillate oil inhibit the deep hydrodesulfurization and the removal of such nitrogen compounds from the middle–distillate oil can improve significantly the deep hydrodesulfurization performance **[3-2, 3-3, 3-8]**. Recently, PSU-SARS, explored in our laboratory, is to remove sulfur in the fuels by selective adsorption on adsorbents. The major advantages of this process are that the process can run at ambient temperature and pressure without using hydrogen gas and the spent adsorbents can be regenerated either by solvent washing or by oxidation using air. The idea in PSU-SARS process can be also applied to pre-denitrogenation of the middle–distillate oil to improve the deep hydrodesulfurization performance.

In the adsorption part of this study, the adsorptive denitrogenation of basic or very reactive nitrogen compounds such as quinoline or indole was focused on, and these compounds influence hydrodesulfurization. It is expected that these nitrogen compounds may be removed easily by adsorption as compared with sulfur compounds because they are much more reactive than sulfur compounds in the hydrotreating process. Therefore, the performance of HDS may be improved, even though basic or reactive nitrogen compounds are removed from middle-distillate oil. Also, the unsupported sulfide catalysts, which are newly developed in our laboratory, have been further investigated with direct measurement of active sites by the adsorption of sulfur compounds which were used as reactant for HDS.

3.1.1 Experimental

3.1.1.1 Unsupported Mo sulfide catalysts

The unsupported Mo based sulfide catalysts were synthesized by using hydrothermal method. Ammonium tetrathiomolybdate (ATTM, $(NH_4)_2MoS_4$), nickel nitrate hexahydrate ($Ni(NO_3)_2{\cdot}6H_2O$) and cobalt nitrate hexahydrate ($Co(NO_3)_2{\cdot}6H_2O$) were purchased from Aldrich Chemical Company and were used without further purification. The catalyst synthesis was carried out in a batch reactor of 25 ml. ATTM was dissolved in 10 g of deionized water, in which 1 g of organic solvent (decalin) was added as well. Ni or Co precursor, $Co(NO_3)_2{\cdot}6H_2O$ or $Ni(NO_3)_2{\cdot}6H_2O$, was dissolved in the minimum amount of water and then loaded to the batch reactor with the mixture solution of Mo solution and organic solvent. The atomic ratio of Me/(Me+Mo) was 0.43 (Me = Ni or Co). The reactor was purged and then pressurized with hydrogen to 2.8 MPa

and placed in a preheated fluidized sand bath at 350°C. After 2 h, the reactor was removed from the sand bath and immediately quenched in water bath. The unsupported catalysts synthesized were collected and submerged in an organic solvent in order to avoid oxidation.

The adsorption properties of organic sulfur compounds on the unsupported Mo sulfides were examined in a fixed bed flow system. The adsorption experiment was carried out at ambient temperature and pressure without using H_2 gas. The unsupported catalyst was packed in a stainless steel column having a bed dimension of 4.6 mm i.d. and 37.5 mm length. The model fuel contained 0.045 mole% of DBT and 0.045 mole% of 4,6-DMDBT in decalin, and was sent into the column by HPLC pump, with a liquid hourly space velocity (LHSV) of 1.04 h^{-1}. The effluent from the top of the column was collected periodically for quantitative analysis. Catalytic performance was tested by a simultaneous HDS of DBT and 4,6-DMDBT, which was carried out in a horizontal micro-reactor (25 ml). The reactor was charged with the synthesized catalyst (0.023 g) and 4 g of reactant mixture (0.4 mole% of 4,6-DMDBT and 0.4 mole% of DBT in decalin). The sealed reactor was purged with hydrogen and then pressurized up to 2.1 MPa and placed in a fluidized sand bath which was preheated up to 300°C. The reactor was agitated vertically at a rate of 200 strokes/min. The temperature inside the reactor was monitored by a thermocouple. After the reaction, the reactor was removed from the sand bath and immediately quenched in a cold-water bath. Finally, liquid products and the catalysts were collected. The liquid products were analyzed qualitatively by a Shimadzu GC/MS (GC12A/QP-500) and quantitatively by a Hewlett Packard GC-FID

(HP5890) with a XTI-5 column (Restek). Both GC/MS and GC-FID were programmed from 55^{o}C to 240 ^{o}C at heating rate of 5 ^{o}C/min.

3.1.1.2 Modification of activated carbon for adsorptive denitrogenation and desulfurization

In the previous report, activated carbon showed high adsorption capacity for sulfur as well as nitrogen in a model fuel and light cycle oil (LCO). The activated carbon was further modified by several metals in order to be improved for adsorption properties. Metals (Cu, Ce, Ni, Fe and Ag) were impregnated on a commercial activated carbon, Nuchar SA20, provided by Westvaco and had surface area of 1843 m^2/g and average pore size of 28.6Å. After impregnation, the activated carbon samples were dried at 110°C. Before adsorptive desulfurization and denitrogenation, the carbon samples were pretreated in a flow of N_2 at 400°C for 2 h in order to reduce the metals, and then cooled down to room temperature to perform adsorption of the model fuel at 25°C. Analysis of tested model fuel was performed by using a SRI GC equipped with a capillary column (XTI-5, Restek) and a flame ionized detector (FID).

In order to compare the adsorptive selectivity for aromatic, sulfur and nitrogen compounds in diesel, a model diesel fuel, which contained the equal molar concentration of naphthalene (Nap), 1-methylnaphthalene (1-MNap), dibenzothiophene (DBT), 4,6-dimethyl-dibenzothiophene (4,6-DMDBT), indole and quinoline in a mixture, was prepared. The molar concentration of each compound in the model fuel was 10.7 mmol/g. The corresponding total sulfur concentration and nitrogen concentration in the fuel was 687 and 303 ppmw, respectively. The model fuel also contained about 10 wt.% of

butybenzene to mimic the monoaromatics in real diesel. All these compounds were purchased from Aldrich Chemical Co. and used as such without further purification.

3.1.2 Results and discussion

3.1.2.1 Unsupported Mo sulfide catalysts

Figure 3-1 shows the breakthrough curves of 4,6-DMDBT and DBT adsorption on the unsupported Mo sulfide. The first breakthrough compound was DBT at 4.2 g-F/g-C (gram of fuel to gram of catalyst) of breakthrough amount. After breakthrough, the C/C_o value (a ratio of the outlet concentration to the initial concentration in the model fuel) for the DBT increased to over 1.0. After the saturation point, the C/C_o value increased gradually to 1.12 and returned to 1.0 at the treated fuel amount of 25.2 g-F/g-C. After the model fuel was treated by adsorption at 5.9 g-F/g-C, 4,6-DMDBT was detected in the treated fuel. Then, the C/C_o value of 4,6-DMDBT increased slowly and reached saturation point at 55.2 g-F/g-C. According to the breakthrough order, it is interesting that the adsorption capacity of 4,6-DMDBT was higher than that of DBT over the unsupported Mo sulfide catalyst.

Figure 3-2 shows the breakthrough curves of 4,6-DMDBT and DBT over the unsupported NiMo sulfide. Unlike the unsupported Mo sulfide, 4,6-DMDBT and DBT broke through at the same time and the breakthrough amount of the treated fuel was 32.7 g-F/g-C. After breakthrough, the C/C_o value of 4,6-DMDBT increased and reached to the maximum at 1.07 and then, returned to 1.0 while, after breakthrough, the C/C_o value of DBT increased gradually and reached 1.0 at 47.8 g-F/g-C.

Figure 3-3 shows the breakthrough curves of 4,6-DMDBT and DBT over the unsupported CoMo sulfide, which had similar breakthrough amount of the treated fuel with the unsupported NiMo sulfide. DBT and 4,6-DMDBT broke through simultaneously at 6.1 g-F/g-C of the breakthrough amount. After breakthrough, the C/C_o value of both 4,6-DMDBT and DBT increased gradually and synchronously reached 1.0 around 52.3 g-F/g-C. However, the amount of DBT adsorbed was higher than that of 4,6-DMDBT over the unsupported CoMo sulfide.

Generally, adsorption performance depends on both the surface chemical property (active sites and their density) and physical property (surface area, pore size, distribution of active sites). The unsupported Mo, NiMo and CoMo sulfides showed different adsorptive selectivity for 4,6-DMDBT and DBT adsorption and the displacement phenomena was also observed as reported in our previous report and publication [**3-11**]. After saturation ($C/C_o = 1$) of one of the sulfur compounds, the outlet concentration of the one increases continuously above its initial concentration in the model fuel and reaches the maximum value and then, decreases gradually to the initial value when the other sulfur compound becomes saturated. This phenomenon results from a partially reversible adsorption of the weaker adsorbate and another reason may be that the compound has relatively lower adsorptive affinity than the other compound adsorbing strongly on catalyst. It results in at least a partial displacement of the weaker adsorbate by the stronger adsorbate. Interestingly, different sulfur compounds were displaced by the other sulfur compounds on different unsupported sulfide catalysts in this study.

The adsorption of sulfur compounds on the unsupported Mo sulfide showed that 4,6-DMDBT adsorbed 2.1 times more than DBT as shown in Table 3-1. A part of the

adsorbed DBT was displaced by 4,6-DMDBT. The results indicate that the interaction of 4,6-DMDBT on the adsorption site is stronger than that of DBT. It is interesting that the methyl groups on the aromatic rings of 4,6-DMDBT show significant and positive effects on the adsorption selectivity of Mo sulfide indicating that the methyl groups enhance the adsorption affinity or interaction through the aromatic rings since the methyl group may lead the increase of electron density on the aromatic rings. The adsorptive selectivity coincides very well with the HDS reactivity of 4,6-DMDBT and DBT on the unsupported Mo sulfide catalyst (Table 3-1). Higher adsorption capacity and stronger interaction of 4,6-DMDBT on the active sites probably cause the higher conversion of 4,6-DMDBT than that of DBT on HDS over the unsupported Mo sulfide. On the unsupported NiMo sulfide, however, the adsorption selectivity of DBT was higher than that of 4,6-DMDBT and the displacement phenomenon was also observed in this sulfide. The amount of DBT adsorbed was higher than that of 4,6-DMDBT which was also displaced by DBT. Unlike the Mo sulfide, the selective order indicates that methyl groups on the 4- and 6-position of DBT strongly inhibit the adsorption of 4,6-DMDBT on the NiMo sulfide. These results indicate that a direct interaction between the sulfur atom and the adsorption site on the NiMo sulfide might play an important role in the selective adsorption of DBT and 4,6-DMDBT and the two methyl groups inhibit the approach of the sulfur atom to the adsorption site. On the CoMo sulfide, interestingly, both DBT and 4,6-DMDBT broke through and saturated at same time although the adsorption capacity of DBT was slightly higher than that of 4,6-DMDBT as shown in Table 3-1and Figure 3-3. Therefore, the displacement phenomenon was not observed and this indicates that the methyl groups on the aromatic ring do not affect on adsorption of the DBT type sulfur compounds to

adsorb on the CoMo sulfide while they inhibit strongly on the adsorption over NiMo sulfide. It results in that the HDS reactivity of DBT and 4,6-DMDBT was very similar as shown in Table 3-1.

The total adsorption capacities for sulfur compounds on the basis of the catalyst weight increase in the order of CoMo > NiMo > Mo sulfide. The unsupported Mo sulfide showed the highest adsorption capacity for 4,6-DMDBT, but the capacity decreased after the addition of the promoters (Ni and Co) to the sulfide catalyst. On the other hand, the adsorption capacity for DBT increased when Ni and Co was added. Table 3-1 shows the turn over frequency (TOF) on three unsupported sulfide catalysts for DBT and 4,6-DMDBT HDS on the basis of adsorption site which was measured from the adsorption capacity in adsorption experiment. The unsupported Mo sulfide catalyst showed the lowest TOF values for both DBT and 4,6-DMDBT HDS. The TOF values increased 4 times on the promoted sulfide catalysts although the number of active sites (adsorption capacity) was similar to that on the unsupported Mo sulfide. It indicates that the active sites of the promoted Mo sulfide catalyst are intrinsically much more active than those of the unpromoted Mo sulfide. Based on the results of adsorption capacities and TOF values, therefore, the promoters (Ni and Co) affect not only on the number of active sites but also on the activity of active sites of the unsupported Mo sulfide catalyst.

3.1.2.2 Modification of activated carbon for adsorptive denitrogenation and desulfurization

Quinoline and indole were used as model nitrogen compounds and they are very reactive under HDS reaction conditions (high H_2 pressure and temperature). Consequently, they affect on HDS of sulfur compounds significantly. Therefore, the

removal of these nitrogen compounds will improve HDS efficiency considerably. In our previous study, the activated carbon showed higher adsorptive capacity and selectivity for both sulfur and nitrogen compounds, especially for the sulfur compounds with methyl groups, such as 4,6-DMDBT. The adsorptive selectivity for the model compounds over the activated carbon increased in the order of Nap < 1-MNap < 4,6-DMDBT < DBT < quinoline < indole.

In order to increase adsorption capacities and selectivity for the sulfur and nitrogen compounds, in this study, the activated carbon was modified with some metals. Figure 3-4 shows the breakthrough of DBT and 4,6-DMDBT on the activated carbon-based adsorbents. The activated carbon and other adsorbents were pretreated at 400°C for 2 h with N_2 flow to reduce loaded metals.

On the activated carbon, the adsorption capacity for 4,6-DMDBT was higher than that for DBT as reported in our previous study. Loaded metals increased the adsorption capacity for DBT, while they did not affect on the adsorption capacity for 4,6-DMDBT. On the basis of breakthrough capacity as shown in Table 3-2, specifically, Ag and Ce improved significantly the DBT capacity to 0.215 mmol/g-A from 0.173 mmol/g-A while other metals improved little the capacity. On the breakthrough capacity of 4,6-DMDBT, the effect of Cu, Ni and Fe was negative, but only that of Ag was slight positive.

The displacement phenomenon was also observed on the adsorption of Nap, 1-MN, DBT and 4,6-DMDBT. The C/C_0 ratio of DBT increased rapidly around 1.6 and then decreased to 1.2 when the adsorption of 4,6-DMDBT broke through and finally was stabilized at 1.0 when a nitrogen compound broke through. Therefore, DBT was mainly

displaced by 4,6-DMDBT at first stage and then was by quinoline. Figure 3-5 shows the breakthrough of both sulfur compounds on the activated carbon and its modified ones.

Figure 3-6 shows the breakthrough of quinoline and indole on the activated carbon-based adsorbents. Most loaded metals increased the breakthrough capacity of quinoline except Ag which slightly decreased the capacity. However, these metals did not help the breakthrough capacity of 4,6-DMDBT, but rather decreased it except Ce which increase the capacity from 0.531 mmol/g-A to 0.541 mmol/g-A.

The one interesting thing is that Ag was the best loaded metal improving the breakthrough capacity for both the sulfur compounds (DBT and 4,6-DMDBT) among the tested metals on activated carbon while it was the worst one on the capacity for both the nitrogen compounds. Therefore, the adsorption of sulfur compounds has very different mechanism on Ag/activated carbon with nitrogen compounds. It has been reported that metal ions such as Cu^+, Ag^+, etc. can form π-complexes with olefins and aromatics and, recently, Cu^+ and Ag^+-exchanged Y-zeolites were used for the separation of thiophene from benzene and olefin from diene by π-complexation. In our study, Ag was reduced under N_2 flow at 400°C and it might be Ag^+ on activated carbon, which greatly improved the adsorption of DBT. It may be that the different adsorption mechanism from that in the literatures works on this Ag adsorbent because DBT generally prefers to adsorb through direct S-Metal interaction while 4,6-DMDBT does through π-complexation.

On the overall adsorption of sulfur and nitrogen compounds, Ce loaded activated carbon was the best adsorbent among other metals (Cu, Ni, Fe and Ag) loaded adsorbents and activated carbon. The adsorbent improved mainly the adsorption capacity for nitrogen compounds and also DBT.

3.1.3 Conclusions

3.1.3.1 Unsupported Mo sulfide catalysts

The adsorption of DBT and 4,6-DMDBT provided adsorption properties of the sulfur compounds on the unsupported Mo sulfide catalyst because the compounds were also used as reactants for HDS reaction. The sulfur compounds had different adsorption properties on each unsupported sulfide catalysts although total adsorption amount of the sulfur compounds was similar. The unsupported Mo sulfide had higher capacity for 4,6-DMDBT than for DBT while the unsupported NiMo sulfide did higher for DBT than for 4,6-DMDBT. The unsupported CoMo sulfide had almost same adsorption capacity with similar breakthrough and saturation performance. This means the methyl groups in 4,6-DMDBT are affected differently by these sulfide catalysts. The adsorption experiments also provide the number of active sites on the sulfide catalysts which is more reasonable data than other chemisorption method to measure the number of active sites. Turnover frequency was calculated on the basis of the results with HDS results. The promotion of Ni and Co provided significant HDS activity on each active site because the conversion of DBT and 4,6-DMDBT increased but the adsorption amount of the compounds was almost similar on the unsupported sulfide catalysts. The promoted unsupported sulfide catalysts had much higher HDS activity than commercial promoted catalysts as reported previously. Specifically, they had higher activity for HYD reaction pathway because they had high adsorption capacity for 4,6-DMDBT as well as DBT as observed in this study.

3.1.3.2 Modification of activated carbon for adsorptive denitrogenation and desulfurization

Adsorptive desulfurization and denitrogenation of a model fuel containing aromatic, sulfur and nitrogen compounds on activated carbon-based adsorbents provided that the adsorption properties (selectivity and capacity) of loaded metals for each compounds. The most loaded metals improved the adsorption capacity for DBT and quinoline while they did not on that of 4,6-DMDBT and indole. Specifically, Ag improved most the adsorption capacity DBT, but did not perform well for nitrogen compounds. Ce improved the adsorption capacity for both quinoline and DBT in this study. Therefore, activated carbon or other adsorbents might be modified with these metals examined in this study to increase adsorption capacity and selectivity on fuels which containing different type of sulfur and nitrogen compounds.

Table 3-1. Adsorption capacities, HDS activities and turn over frequency (TOF) of three unsupported catalysts for DBT and 4,6-DMDBT on the basis of GC-FID analysis.

	DBT	4,6-DMDBT	Total
MoS_2			
Breakthrough (mmol/g)	0.014	0.019	0.033
Saturation (mmol/g)	0.033	0.068	0.101
Net[a] (mmol/g)	0.032	0.068	0.100
HDS Activities (10^{-5}/s.g)	166	298	
TOF[b] (s^{-1})	53	44	
NiMoS			
Breakthrough (mmol/g)	0.018	0.018	0.037
Saturation (mmol/g)	0.061	0.049	0.110
Net[a] (mmol/g)	0.061	0.048	0.109
HDS Activities (10^{-5}/s.g)	1290	921	
TOF[b] (s^{-1})	213	190	
CoMoS			
Breakthrough (mmol/g)	0.020	0.020	0.040
Saturation (mmol/g)	0.064	0.056	0.120
Net[a] (mmol/g)	0.064	0.056	0.120
HDS Activities (10^{-5}/s.g)	1316	1289	
TOF[b] (s^{-1})	207	229	

[a] Net adsorption capacity when the adsorption was ended.

[b] TOF on the basis of adsorption capacities.

Table 3-2. Breakthrough capacities (mmol/g-A) for aromatic, sulfur and nitrogen compounds on activated carbon-based adsorbents

	Nap	1-MN	Quinoline	Indole	DBT	DMDBT
Cu	0.069	0.090	0.452	0.482	0.188	0.213
Ce	0.071	0.071	0.466	0.541	0.215	0.241
Ni	0.068	0.068	0.455	0.476	0.179	0.223
Fe	0.069	0.070	0.466	0.463	0.172	0.213
Ag	0.055	0.056	0.324	0.490	0.224	0.248
AC	0.054	0.054	0.343	0.531	0.173	0.244

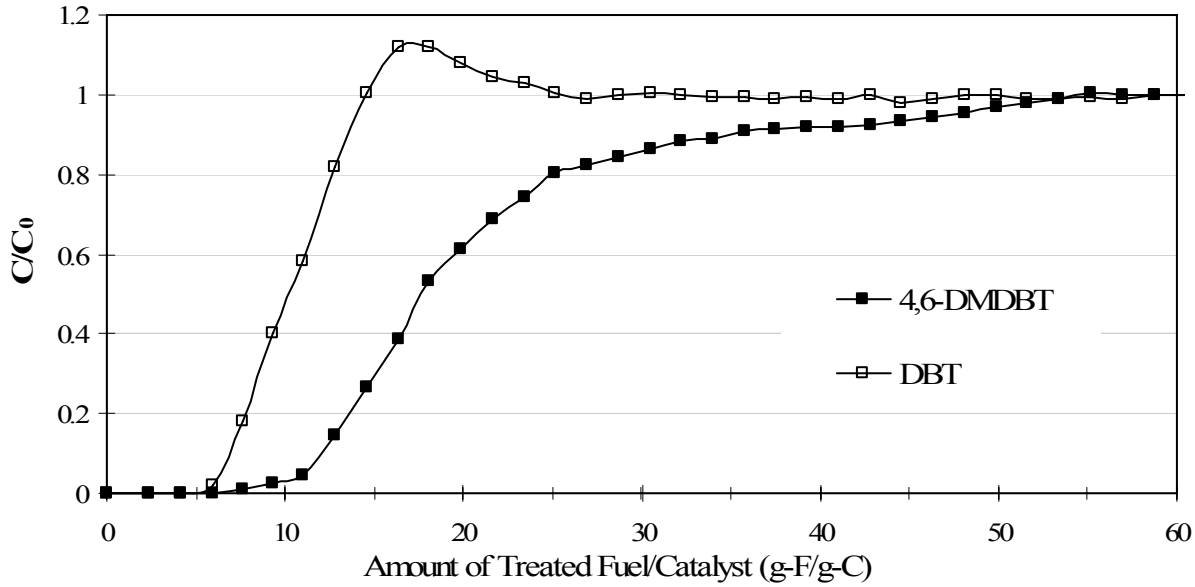

Figure 3-1. Breakthrough curves for the liquid-phase adsorption of 4,6-DMDBT and DBT at ambient temperature and pressure over the unsupported Mo sulfide catalyst.

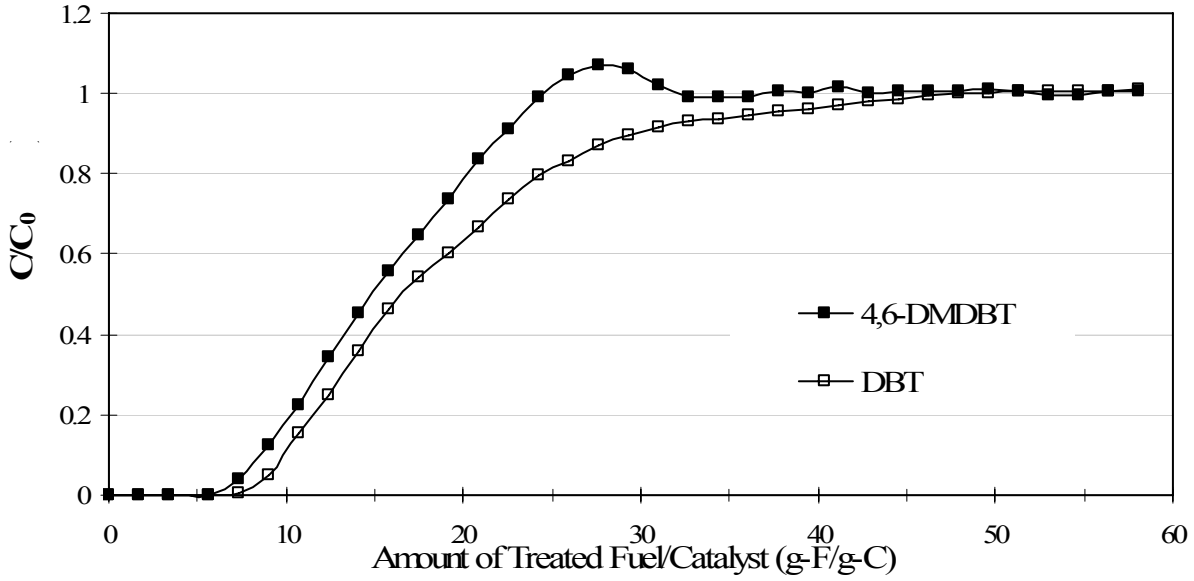

Figure 3-2. Breakthrough curves for the liquid-phase adsorption of 4,6-DMDBT and DBT at ambient temperature and pressure over the unsupported NiMo sulfide catalyst.

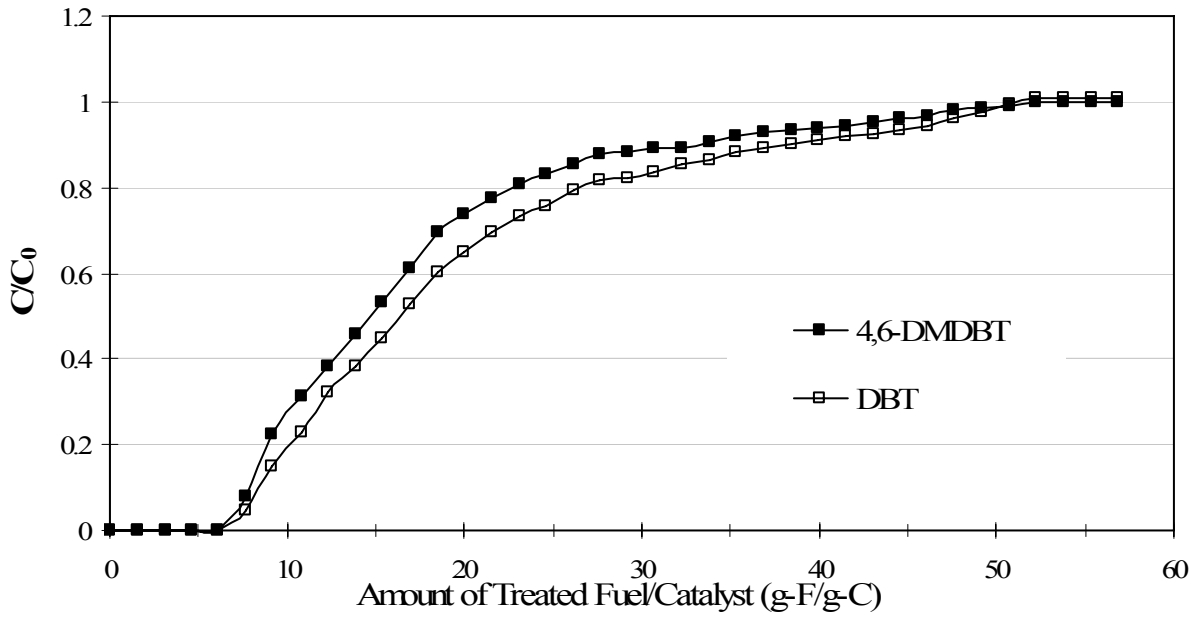

Figure 3-3. Breakthrough curves for the liquid-phase adsorption of 4,6-DMDBT and DBT at ambient temperature and pressure over the unsupported CoMo sulfide catalyst.

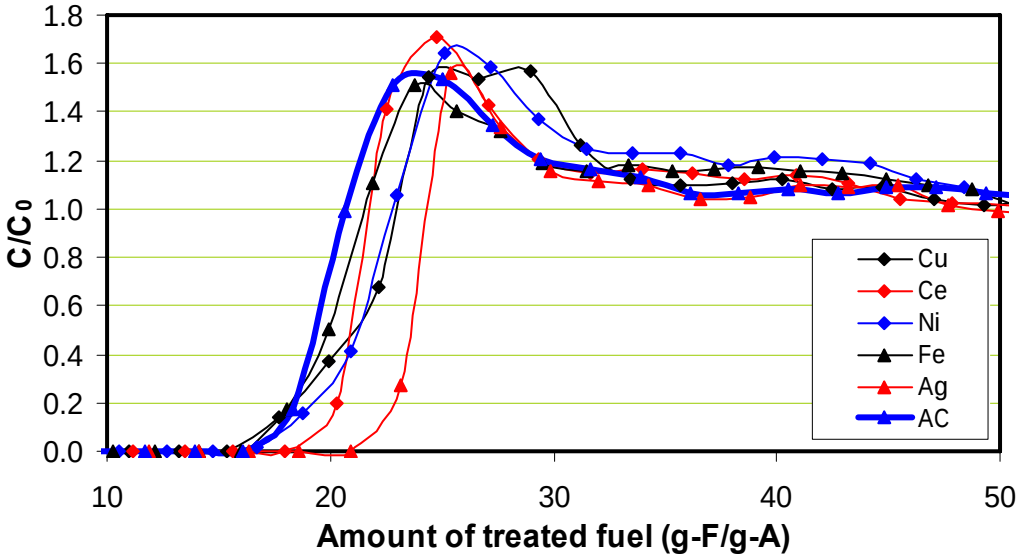

(a)

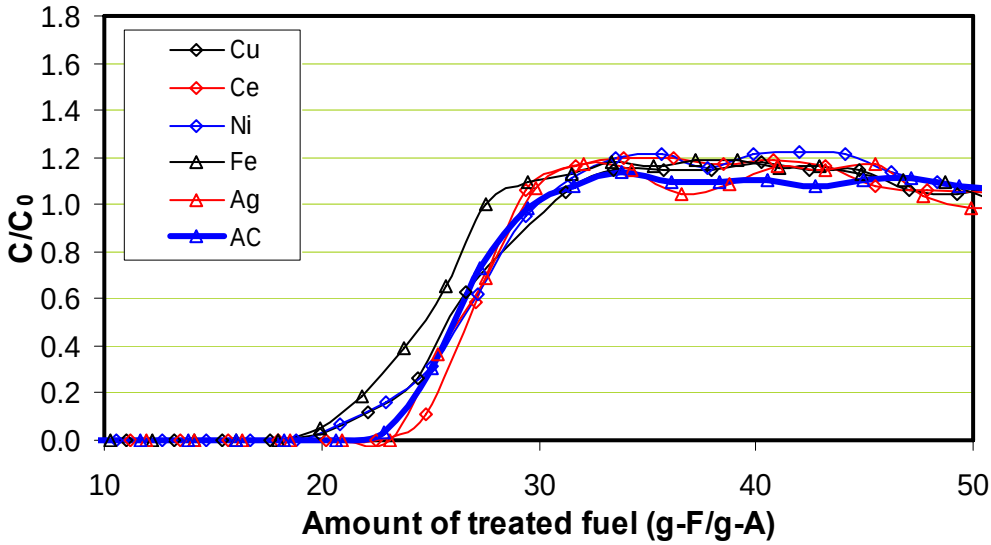

(b)

Figure 3-4. (a) DBT and (b) 4,6-DMDBT breakthrough curves on activated carbon modified with metals.

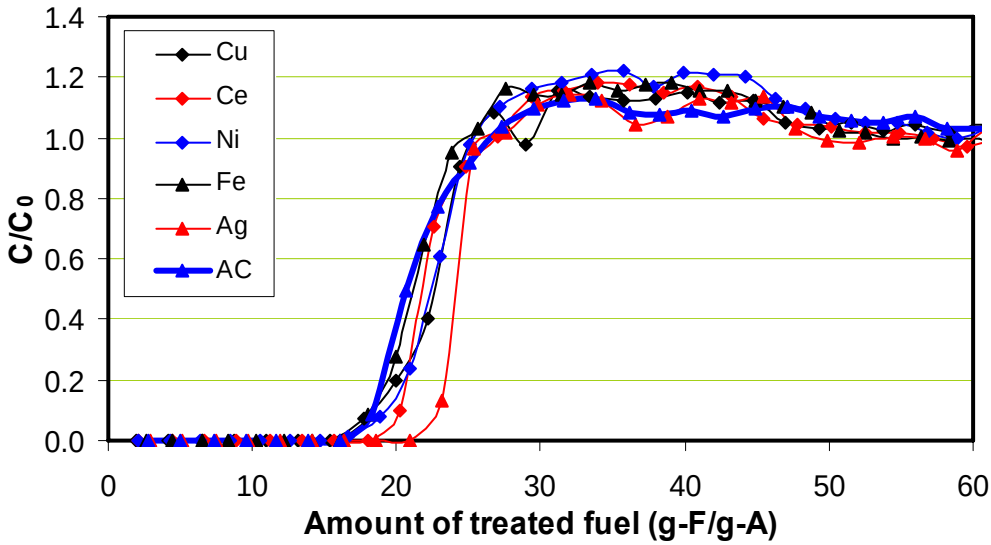

Figure 3-5. Sulfur breakthrough curves on activated carbon modified with metals.

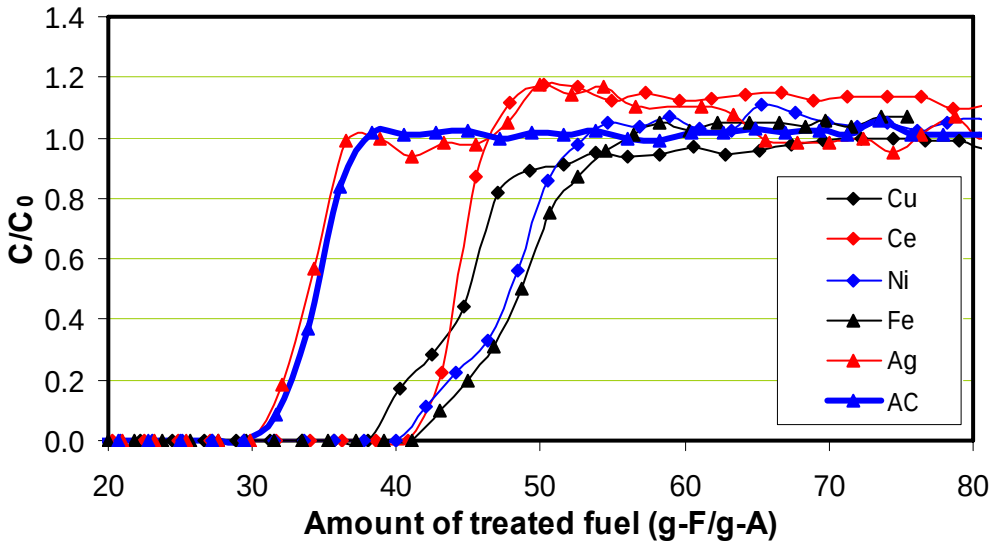

(a)

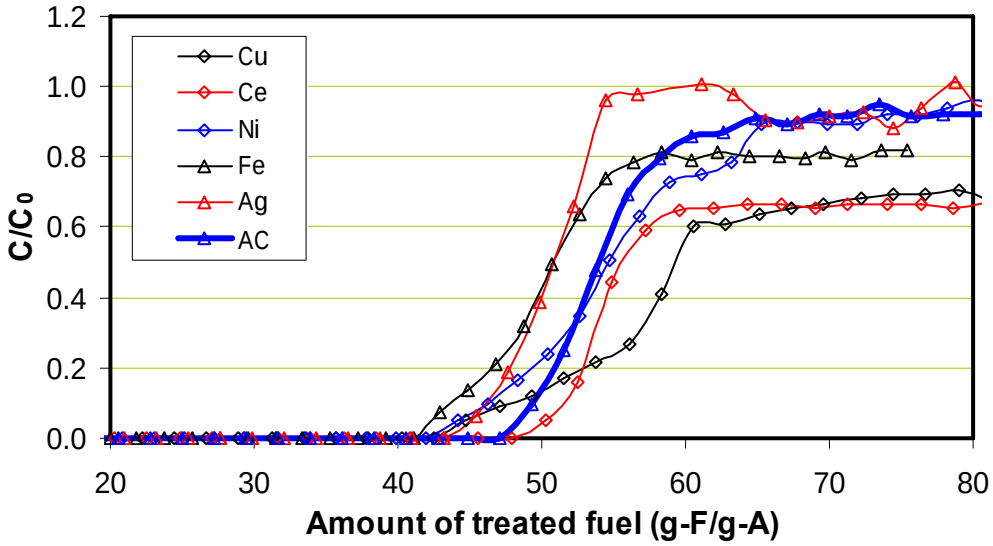

(b)

Figure 3-6. (a) Quinoline and (b) indole breakthrough curves on activated carbon modified with metals.

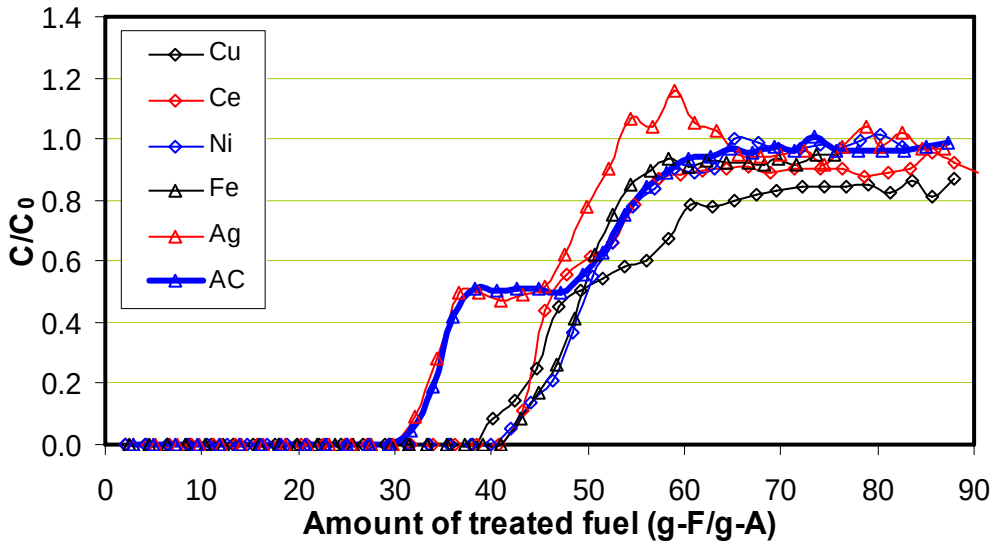

Figure 3-7. Nitrogen breakthrough curves on activated carbon modified with metals.

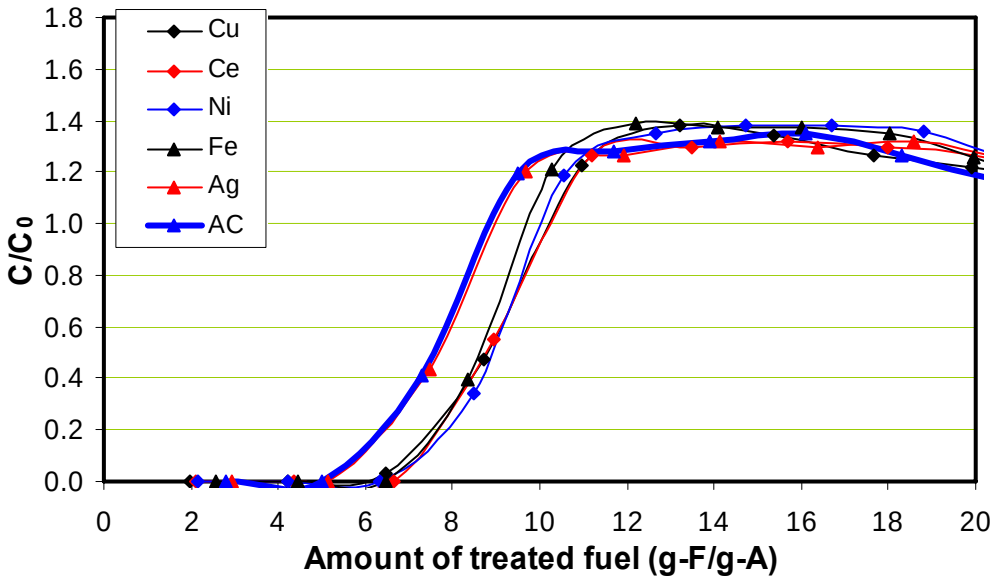

Figure 3-8. Aromatic compounds (Naph and 1-MNaph) breakthrough curves on activated carbon modified with metals.

Subtask 3.2 Saturation of Two-Ring Aromatics

As a part of the DOE refinery integration project, this sub-task aims at saturating aromatics for high-quality diesel and distillate fuels. High aromatics content in distillate fuels is undesirable since it lowers the fuel quality and contributes to the formation of environmentally harmful emissions. In general, lower aromatics content leads to higher thermal stability of fuels, better combustion characteristics and less soot formation. The conventional dearomatization is aromatics saturation (hydrogenation) on sulfided $CoMo/Al_2O_3$ or $NiMo/Al_2O_3$ catalysts. However, these catalysts are active at higher temperatures where equilibrium limitations may prevent complete hydrogenation. Otherwise, Noble-metal catalysts are active at lower temperatures, where equilibrium limitations can be overcome, but sulfur-tolerance on catalysts is a major obstacle to their commercial application.

To meet the fuel performance and compositional specifications for diesel fuel, it is necessary for both RCO and LCO to be hydrogenated. This work focuses on the development of noble-metal catalysts with increasingly sulfur-tolerance for the low-temperature hydrotreating and dearomatization (LTHDA) of distillate fuels for the production of ultra-clean and low-aromatic diesel fuels.

Our group previously proposed the shape selective noble metal catalysts using zeolite support to prepare bimodal pore distributions of noble metal particles [**3-14**]. In this reporting period, we tried to develop the hybrid catalyst to verify the effectiveness of shape selectivity. Two kinds of zeolite which have different pore size were used, zeolite Y (7.4Å) and zeolite A (4.1Å). It is expected that the sulfur molecules adsorbed on noble metal particles of zeolite Y can be eliminated by hydrogen spillover from zeolite A

supported catalyst, meanwhile, the noble metal particles inside the zeolite A pores may be still accessible to hydrogen molecules. It is reported that pore opening of zeolite A can be modified to 3Å by potassium ion exchange [**3-15**], which is smaller than the size of hydrogen sulfide. In this pore system, the incorporated noble metal cluster can be protected from sulfur poisoning. In order to examine the proposed shape selective noble metal catalyst, we employed two techniques which are the ion exchange of zeolite A and silica coating of catalysts to eliminate catalytic activity on the catalyst outer surface through excluding hydrogen sulfide on Pd catalyst. Therefore, we can only observe the performance of metal particle inside the zeolite pore. Hybrid catalyst was prepared with the catalysts prepared from above technique and compared the hydrogenation activity and resistance to sulfur poisoning with other unmodified catalyst.

3.2.1 Experimental

3.2.1.1 Catalyst preparation

Zeolite A was obtained from Zeolyst International (formerly PQ Corporation). As Zeolite A was the sodium form (NaA), it was pretreated for ion exchange to generate the proton form (HA) and potassium form (KA). At first, 30 g of zeolite NaA was dispersed in 1 M ammonium chloride solution 330 ml. The zeolite and supernatant solution were then agitated by continuous shaking at room temperature for 6 h to reach equilibrium and then separated by vacuum filtration. The zeolite was rinsed with de-ionized water to remove excess ammonium solution. This procedure was repeated 3 times in order to produce thoroughly ammonium form zeolite. The ammonium ion exchanged zeolite was dried in an oven at 80^{o}C and calcined at 450 °C in air flow (~60 mL/min) for 4 h with a

heating rate of approximately 1.5 °C/min. Finally, H^+ form zeolite A was obtained from NH_4^+ form zeolite.

Zeolite KA was also prepared by ion exchange of zeolite HA. Likewise, 20g of zeolite was dispersed in 1 M potassium chloride solution 330 ml then agitated by continuous shaking at room temperature for 6 h to come to equilibrium and then separated by vacuum filtration. This procedure was repeated 3 times in order to produce thoroughly potassium form zeolite. The potassium ion exchanged zeolite was dried in an oven at 80^oC and calcined in air flow (~60 mL/min) for 4 h at 450 °C at a heating rate of 1.5 °C/min.

For comparison with other zeolites supported Pd catalysts, silica alumina support was prepared and calcined in air flow (~60 ml/min) for 4 h at 450 °C, with a heating rate of 1.5 °C/min, before catalyst preparation.

All catalysts were prepared by the incipient wetness impregnation (IWI) technique. The metal precursor with desired metal loading was dissolved in a total volume of water (and HCl) equal to the pore volume for the support. The metal precursors used in this study were $PdCl_2$ (Sigma Aldrich). In order to dissolve $PdCl_2$ in water, it is necessary to add HCl to form soluble $PdCl_4^{2-}$ species. For the zeolite A supported Pd catalysts, a sufficient amount of HCl was used to prepare the metal precursor solution.

All catalysts in this work contain 2wt% of metal loading. The metal precursor solution was then added dropwise to the support. Whenever a few drops were added, the mixture was stirred thoroughly and the procedure was repeated until all of the metal solution was loaded on the support. After impregnation was complete, catalysts were

dried at 80 °C for over 2 h. After drying, the catalysts were calcined in air flow (~60 ml/min) at 450°C for 4 h at a heating rate of approximately 1.5 °C/min. The calcined catalysts were then pelletized, crushed and sieved to a particle size of 18-35 U.S.A. standard testing sieve mesh (0.5 – 1.0 mm). Pd/HA and Pd/KA catalysts were modified with tetraethylorthosilicate (TEOS) to form a silica wall on the catalyst surface. The modification technique applied was the chemical vapor deposition (CVD) of TEOS in the flow type reactor system as shown in Figure 3-9 [**3- 17**]. The procedure of CVD technique is as follow: 0.55g of catalyst particles were loaded into the reactor and activated at 450^{o}C under 20 ml/min of N_2 flow for an hour. The temperature is brought down to 200°C and subsequently TEOS is fed at the rate of 3 ml/h (0.05 ml/min) for an hour using a liquid syringe pump. Then the carrier gas was switched to air (20 ml/min), the temperature was increased slowly (15°C/min) to 450°C and held at that temperature for 2 h. The reactor was cooled down to room temperature and the surface modified catalyst was collected from the reactor for reaction and characterization.

The silica coated Pd/KA was mixed with HY zeolite catalyst in order to investigate the catalytic activity of HY zeolite itself. It was prepared by mixing with silica coated Pd/KA granule and HY zeolite granule (CBV 720, Proton form, 0.5 – 1.0 mm of particle size) at the weight ratio of 1:3.

To verify the concept of bimodal shape selective catalyst, two kinds of silica coated Pd on zeolite A (silica coated Pd/HA, silica coated Pd/KA) were mixed with Pd/HY zeolite catalysts. These were prepared by mixing with silica coated Pd/KA or Pd/HA catalyst granule and Pd/HY catalyst granule (0.5 – 1.0 mm of particle size) at the

weight ratio of 1:2. Table 3-3 shows catalysts prepared for hydrogenation reaction in this study.

3.2.1.2 Catalyst Evaluation in Hydrogenation Experiments

Two feedstocks were used in this work: a sulfur free one and one containing 100 ppm S. The composition of sulfur free feedstock was 20 wt% tetralin (Aldrich, 99%), 75 wt% hexadecane (Aldrich, 99+%), and 5 wt% nonane (Aldrich, 99+%). The feedstock with 100 ppm S was prepared by adding 100 ppm quantities of sulfur as benzothiophene (BT) (Aldrich, 99%) to the sulfur free one.

The reaction was done in a down flow reactor system. For each experiment, 0.5 g of catalyst particles (18-35 mesh) were mixed with 3.0 g of α-Al_2O_3 particles (18-35 mesh) as a diluent. The mixture catalyst was loaded in a flow reactor of which the catalytic bed volume was around 10 cm^3 (hollow cylinder type with bed length: 3.7 cm, outer diameter: 0.99 cm and inner diameter: 0.32 cm). Prior to each experiment, catalysts were reduced *in situ* under a hydrogen flow of 100 ml/min and 100 psi of H_2 pressure. The temperature was increased from room temperature to 225 °C at a rate of 2 °C/min and then maintained for 2 h until the introduction of liquid feed. After the reduction step was complete, the pressure was increased to 600 psi and the hydrogen flow was reduced to 80 ml/min. Sulfur free feed was then introduced at a rate of 0.08 ml/min into the catalyst bed. This corresponds to a gas-to-liquid ratio (G/L) of approximately 1000 and a weight hourly space velocity (WHSV) of approximately 8 h^{-1} and liquid hourly space velocity (LHSV) of approximately 0.5 h^{-1}. After introducing liquid feedstock by HPLC pump, the system was allowed to be stabilized for 1.5 h. Therefore, 90 min after the

introduction of feedstock was designated as time-on-stream (TOS) equal to zero. Liquid samples were then collected at 30 min intervals until the TOS is 3 h. After TOS is 3 h, the sulfur free feed was changed to 100 ppm S feed and continued until the experiment finished.

3.2.1.3 Characterization

In order to examine the characteristics of catalysts prepared, Micromeritics AutoChem 2910 was used for temperature programmed reduction (TPR), temperature programmed desorption (TPD), and pulse chemisorption. TPR is used to reveal the temperature at which the reduction of Pt occurs and hydrogen-TPD analysis can determine the type and strength of active metal sites available on the surface of a catalyst from measurement of the amount of gas desorbed at various temperatures. Metal dispersion data were also obtained by using a Micromeritics Autochem 2910. For hydrogen chemisorption, the sample was dosed with 25% hydrogen in argon and the doses were repeated 15 times. The volume of hydrogen adsorbed was used to calculate the percent metal dispersion, assuming a metal: hydrogen ratio of 2:1 (metal atom: hydrogen atom = 1:1).

3.2.2 Results and discussion

3.2.2.1 TPR, TPD and Pulse Chemisorption Study

TPR profiles for zeolite A supported palladium catalysts are shown in Figure 3-10. The TPR peak profiles have two groups: the positive sharp peaks at 70°C, which was due to H_2 evolution from hydride decomposition and the negative broad peaks caused by

H_2 consumption, corresponding to reduction of Pd^{2+} to Pd^{o}. The positive hydrogen production peak is observed in Pd/KA, which means Pd metal formed β-Pd hydride. The peak shifts from high temperature to low temperature in the order of Pd/NaA > Pd/KA > Pd/HA. Pd/NaA had the highest reduction temperature at 184 °C. Pd/HA had the lowest reduction temperature at 74°C and it was much easier to be reduced than others. Pd/KA had the second highest reduction temperature and the potassium ions in KA zeolite support may affect on the increase of the reduction temperature to 148°C.

During the preparation of the zeolite supported Pd catalysts, Pd^{2+} ions are favorably coordinated on the framework of zeolite during the calcination, so that there is a strong interaction between metal and support. In other words, the reducibility of the supported metal is closely related to the interaction between metal and ions on zeolite support. The stronger interaction leads the more difficult reduction of the metal. In Na and K ion exchanged zeolite A, the interaction between Pd and support is stronger than the proton exchanged one, which makes the Pd^{2+} ions more difficult to be reduced. The previous report can be referred to support this result, where TPR profile of three types of proton exchanged zeolite were compared and all types had the low reduction temperature between 70-100^{o}C. (Figure 3-11)

Figure 3-12 shows the TPD profile of hydrogen over zeolite A supported Pd catalysts, where the peaks correspond to desorption of H from the surface of Pd metal particles. Comparing to other supported Pd catalysts, Pd/NaA had the TPD peak at the highest temperature (109°C) at lower temperature region and this implies that hydrogen adsorbed on the Pd metal surface more strongly and was more difficult to desorb, while

the other catalysts show the TPD preaks at 85°C, which means weaker bonding between adsorbed hydrogen and Pd metal on the other supports.

Table 3-4 shows the results of hydrogen pulse chemisorption for zeolite A supported palladium catalysts. All catalysts have low metal dispersion as compared with Pd/Silica alumina. In the case of Pd/silica-alumina, even though the silica/alumina ratio (SAR) is almost 11 times higher than that in zeolite A (SAR=1). This means it has low Brønsted acid site concentration and the dispersion of Pd/silica alumina is higher than other zeolite A because it doesn't have small pore and the hydrogen is adsorbed on the catalyst surface easily. However, the dispersion of all zeolite A supported Pd catalysts were very low and active particle diameters of them were over 5 nm.

Pd/NaA zeolite shows a different trend. The reason can be explained by the Brønsted acid site concentration. In Na form, as Na anchored on the sites, the Brønsted acid site concentration is lower than that of other forms, which made the Pd cluster grow bigger than others. In the case of Pd/KA, even though it is ion exchanged 3 times, KA might not be fully ion exchanged and enough Brønsted acid sites remain to anchor Pd cluster. To get the exact result of the ion exchange effect, it needs to be further studied with other characterization techniques.

3.2.2.2. Catalyst Evaluation in Hydrogenation Reaction

3.2.2.2.1 Effect of support type

The result for conversion of tetralin and the trans-/cis-decalin ratio over 2 wt% Pd on various support catalysts (Pd on mordenite, zeolite A, zeolite Y and silica-alumina) were compared. Silica-alumina supported catalyst exhibited good tetralin conversion until

6 h of TOS, but then deactivated drastically and showed around 22% of tetralin conversion at 8.5 h of TOS. As sulfur deactivation proceeds, the selectivity toward trans-decalin decreased and trans-/cis-decalin ratio was converged at around 1.8 over all catalysts. The best catalyst with highest activity is Pd/HY even though SAR was less than Pd/HM. Since Pd/silica-alumina has low SiO_2/Al_2O_3 ratio (11), it showed less sulfur tolerance than mordenite (SiO_2/Al_2O_3:37.5) and zeolite Y (SiO_2/Al_2O_3:20), but better than zeolite A (SiO_2/Al_2O_3:1)

3.2.2.2.2. Effect of cation type

The effect of cation was examined with three types of catalysts; Pd on proton, sodium and potassium form zeolites A as shown in Figure 3-14. Potassium form catalyst showed initially more sulfur resistance than other cation form catalysts, but decreased drastically after 6 h of TOS which was 1 h later than the other catalysts. These results didn't fully support the hypothesis that potassium ion exchanged zeolite A makes pore opening contract and prevents palladium in pore from sulfur poisoning perfectly. However, the results showed potassium ion contributed sulfur resistance than other ion. The trans-/cis-decalin ratio of zeolite A supported catalyst were approximately 2-3 all over reaction time, which suggested that zeolite A supported Pd catalysts produce low trans-decalin compared with other zeolite supported catalysts.

3.2.2.2.3 Effect of Silica coating

Two Pd catalysts, Pd/HA and Pd/KA, were coated by the Chemical Vapor Deposition (CVD) technique of tetraethylorthosilicate (TEOS) to examine the effect of

internal pore on catalytic characteristics and performance. It was hypothesized that since the molecule size of TEOS was too large to enter the small pore of the zeolite, silica wall would be formed not inside of zeolite pore but on outer surface of the granule, allowing catalysts to perform inside pore opening but on outer surface reaction of zeolite.

As shown in Figure 3-15, silica coated Pd/HA showed around 10% of tetralin conversion but as it was exposed to sulfur feed, the catalytic activity was decreased more. It was thought the silica was coated well on the surface of zeolite A since the amount of TEOS introduced by CVD was enough. However, the result of coated Pd/HA suggested that external surface of catalyst might not be well coated and remain metal active site. Silica coated Pd/KA showed low tetralin conversion (around 1%) and it can be considered that it lost hydrogenation catalytic activity on outer surface by silica coating. HY zeolite blank test was confirmed that it also didn't have any distinctive catalytic activity for itself (but it showed 1.5% tetralin conversion).

3.2.2.2.4 Effect of hybrid catalysts

First of all, Pd/KA and its hybrid catalysts were compared based on its higher performance as shown in Figure 3-14. Figure 3-16 shows the reaction conversion and selectivity of decalin over silica coated Pd/KA, silica coated Pd/KA-HY hybrid catalyst (catalyst granules mixing). The coated Pd/KA-HY hybrid catalyst prepared by physical granule mixing didn't show the catalytic activity at all. It means that there is no interaction between Pd/KA and HY zeolite and HY zeolite didn't participate in hydrogenation reaction at all even though hydrogen spillover was occurred at Pd/KA catalysts.

Figure 3-17 shows the comparison of terralin conversion and decalin selectivity over Pd/HA, Pd/HY, silica coated Pd/HA and silica coated Pd/HA mixed with Pd/HY hybrid catalyst. The hybrid catalyst had the better performance than any other catalyst in this study. We already showed that the silica coated Pd/HA catalyst itself didn't show any good catalytic activity for hydrogenation. However, the hybrid catalyst shows the higher conversion than Pd/HY catalyst. It means the silica coated Pd/HA catalyst plays a role of hydrogen spillover. According to our hypothesis, hydrogen molecules enter the pore of silica coated zeolite catalysts and are dissociated on metal particles. Spillover hydrogen in the pore of Pd/HA migrates to the surrounding Pd/HY zeolite and recover the poisoned metal site. Likewise, silica coated Pd/KA mixed with Pd/HY hybrid catalyst also showed the higher tetralin conversion than Pd/HY catalyst (Figure 3-18).

Three hybrid catalysts, Pd/HA mixed with Pd/HY, silica coated Pd/HA mixed with Pd/HY and silica coated Pd/KA mixed with Pd/HY, are compared with Pd/HY catalysts at Figure 3-19. Conversion of all hybrid catalysts was higher than Pd/HY and silica coated Pd/KA catalysts maintain its activity until 14 h. It was reported that zeolite A had a pore opening of 4Å which can be modified to 3Å by ion exchange with potassium [**3-15**]. The result of tetralin conversion over Pd/KA didn't satisfy our expectation well, but CVD also can control the pore opening of zeolite [**3- 16**]. Even though the characterization was not performed for the size of pore opening of zeolite A, it can be explained that the potassium ion exchange and silica coating successfully shrank the pore opening and potassium exchanged zeolite A prevented hydrogen sulfide and organosulfur molecule from entering the pore and poisoning metal particles. However,

none of these catalysts showed any significant change of trans-/cis-decalin ratio at all. The trans-/cis-decalin ratio of all catalysts including Pd/HY were converged to around 2.

3.2.3 Conclusions

In this reporting period, we tried to develop the shape selective catalyst for aromatic hydrogenation. Two kinds of zeolites with different pore size were used, zeolite Y (7.4Å) and zeolite A (4.1Å), which were expected that the contact of sulfur molecules with noble metal particles in zeolite Y can be eliminated by hydrogen spillover from zeolite A supported catalyst and that meanwhile, the noble metal particles inside the zeolite A pores may be still accessible to hydrogen molecules. We adopted two techniques, the ion exchange of zeolite A and silica coating of catalysts, to exclude hydrogen sulfide and eliminate catalytic activity on the catalyst outer surface. Silica coating and ion exchange successfully shrunk the pore opening and prevented hydrogen sulfide and organosulfur molecule from entering the pore and poisoning metal particles. These coated catalysts itself didn't participate in the hydrogenation reaction, but helped the Pd on Y zeolite catalysts maintain the high hydrogenation conversion by supplying spillover hydrogen. Based on reaction and characterization experiments, the results demonstrated that these hybrid catalysts are applicable to testing the catalyst design concept of shape selectivity and hydrogen spillover.

Table 3-3. Catalysts Prepared for this Work

Catalyst	Metal Loading (wt%)	Precursor Metal	Support (SiO_2/Al_2O_3)	Notes
Pd/HA	2.0	$PdCl_2$	A Zeolite (1.0)	
Pd/NaA	2.0	$PdCl_2$	A Zeolite (1.0)	
Pd/KA	2.0	$PdCl_2$	A Zeolite (1.0)	
Pd/HY	2.0	$PdCl_2$	Y Zeolite (20)	
Pd/HM	2.0	$PdCl_2$	Mordenite (37.5)	
Pd/SiO_2-Al_2O_3	2.0	$PdCl_2$	SiO_2-Al_2O_3(11)	
Silica coated Pd/HA	2.0	$PdCl_2$	A Zeolite (1.0)	TEOS CVD
Silica coated Pd/KA	2.0	$PdCl_2$	A Zeolite (1.0)	TEOS CVD
Silica coated Pd/KA mixed with HY zeolite	2.0	$PdCl_2$	A Zeolite (1.0)	Silica coated Pd/KA:HY =1:3
Pd/HA mixed with Pd/HY	2.0	$PdCl_2$	A and Y zeolite	Pd/HA:HY=1:2
Silica coated Pd/HA Mixed with Pd/HY	2.0	$PdCl_2$	A and Y zeolite	Silica coated Pd/HA:HY =1:2
Silica coated Pd/KA mixed with Pd/HY	2.0	$PdCl_2$	A and Y zeolite	Silica coated Pd/KA:HY =1:3

Table 3-4. Pulse Chemisorption over Pd supported on different zeolite support

	Cumulative Volume (ml/g STP)	Metal Dispersion (%)	Metallic Surface Area (m^2/g sample)	Metallic Surface Area (m^2/g metal)	Active Particle Φ (nm)
Pd-NaA	0.169	4.0	0.36	17.8	27.99
Pd-HA	0.556	13.2	1.18	58.8	8.47
Pd-KA	0.635	15.1	1.34	67.1	7.44
Pd-SiO_2-Al_2O_3	1.315	31.2	2.78	139.0	3.592

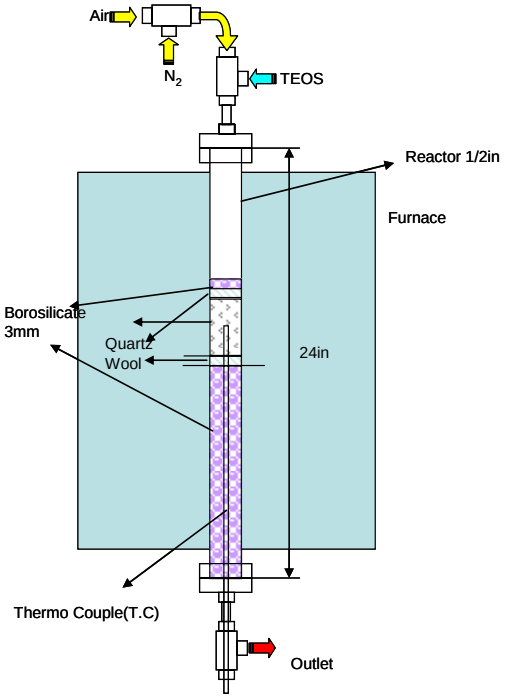

Figure 3-9. Chemical Vapor Deposition (CVD) of tetraethylorthosilicate (TEOS) on Catalyst.

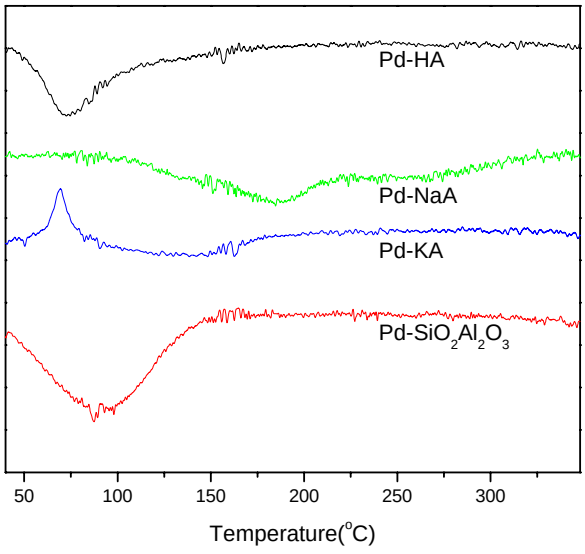

Figure 3-10. TPR profile of four different zeolite supported Pd catalysts.

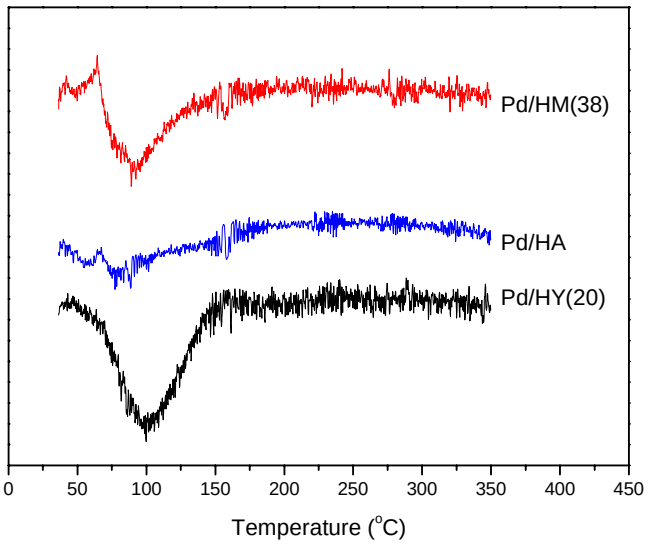

Figure 3-11. TPR profile of three types of proton exchanged zeolite supported Pd catalysts.

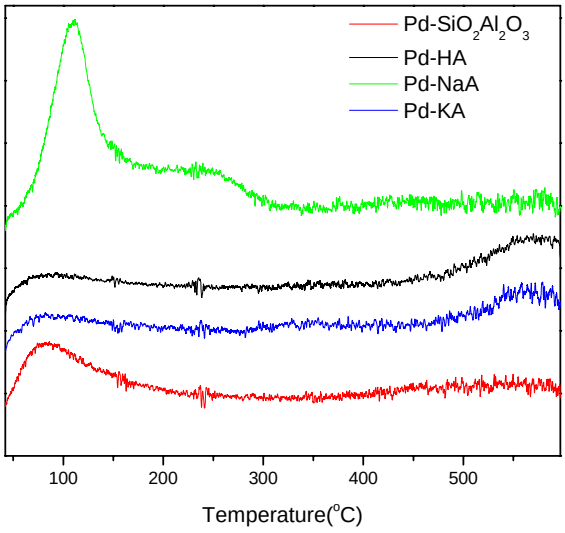

Figure 3-12. TPD profile of four different zeolite supported Pd catalysts.

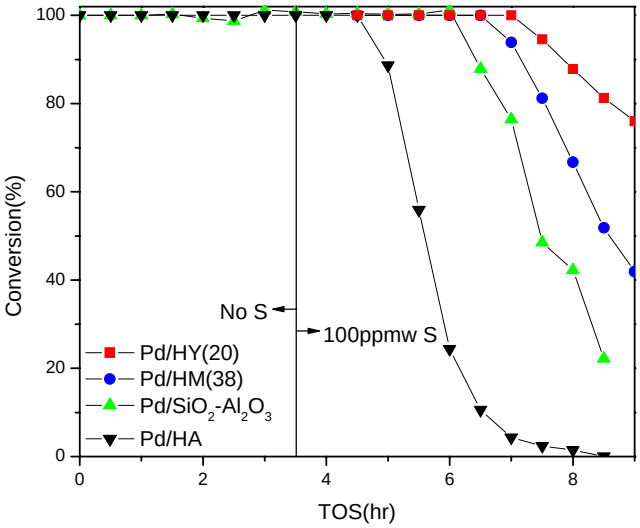

(a)

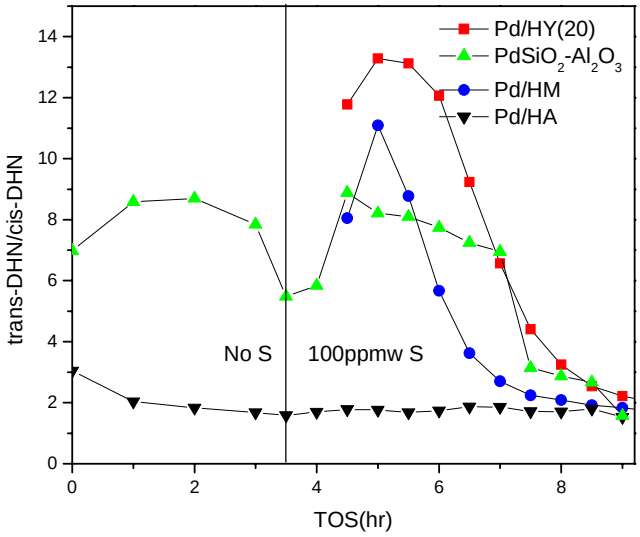

(b)

Figure 3-13. (a) Conversion vs. TOS for the hydrogenation of tetralin and (b) trans-/cis-DHN ratios for the hydrogenation of tetralin over Pd on various support types.

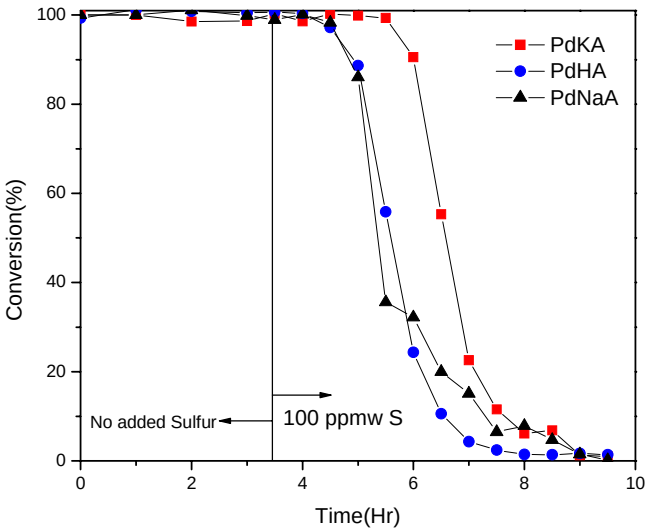

(a)

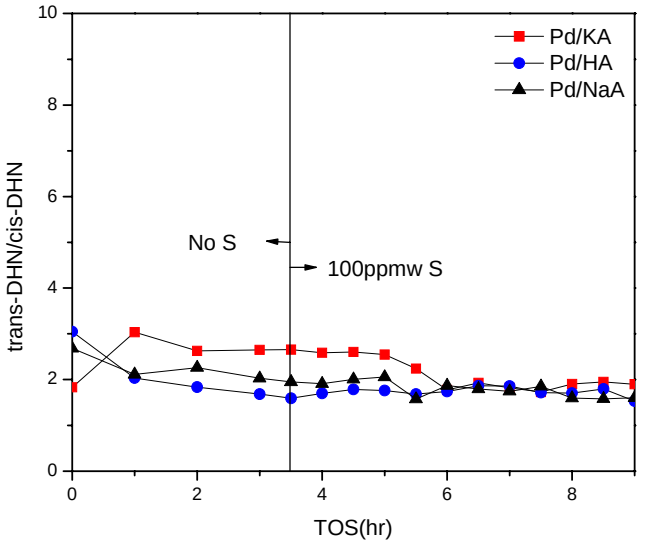

(b)

Figure 3-14. (a) Conversion vs. TOS for the hydrogenation of tetralin and (b) trans-/cis-DHN ratios for the hydrogenation of tetralin over Pd on various cation type zeolite A supports.

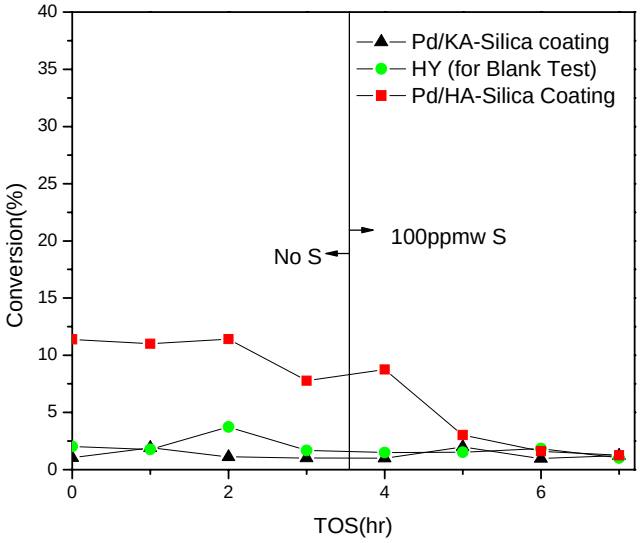

(a)

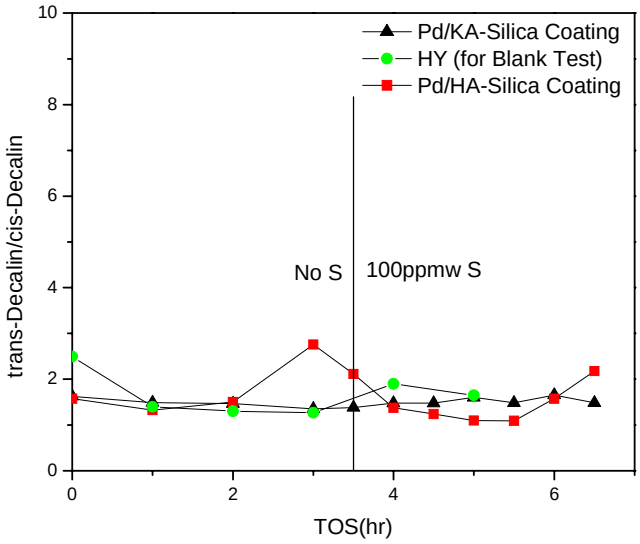

(b)

Figure 3-15. Conversion vs. TOS for the hydrogenation of tetralin and **(b)** trans-/cis-DHN ratios for the hydrogenation of tetralin over silica coated Pd on zeolite A catalysts

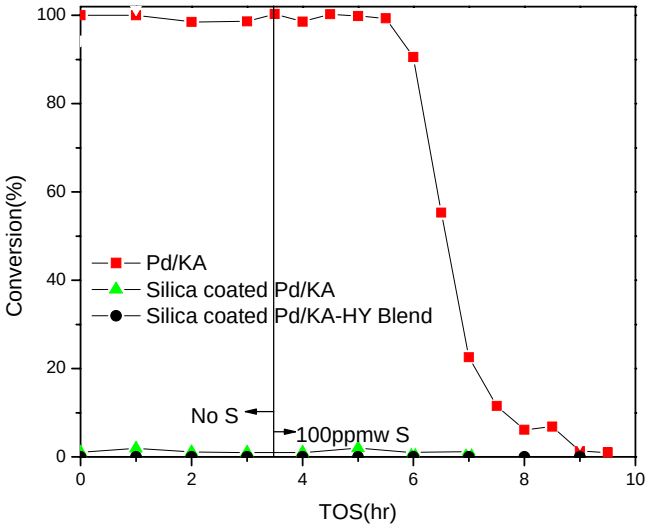

(a)

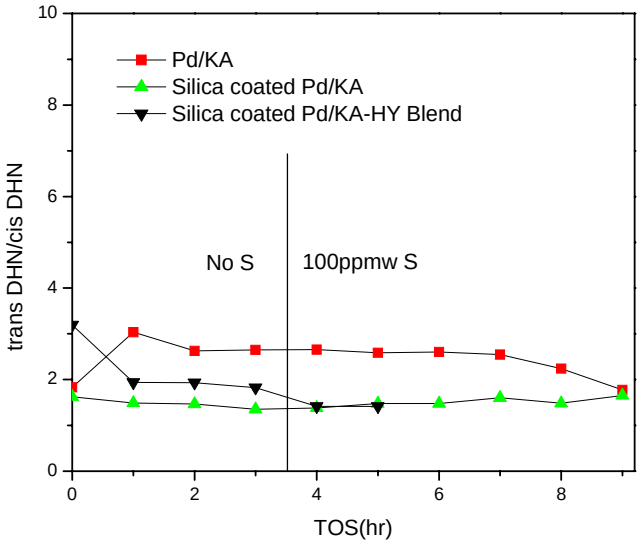

(b)

Figure 3-16. Conversion vs. TOS for the hydrogenation of tetralin and **(b)** trans-/cis-DHN ratios for the hydrogenation of tetralin over silica coated Pd/KA catalyst and its mixture with HY zeolite

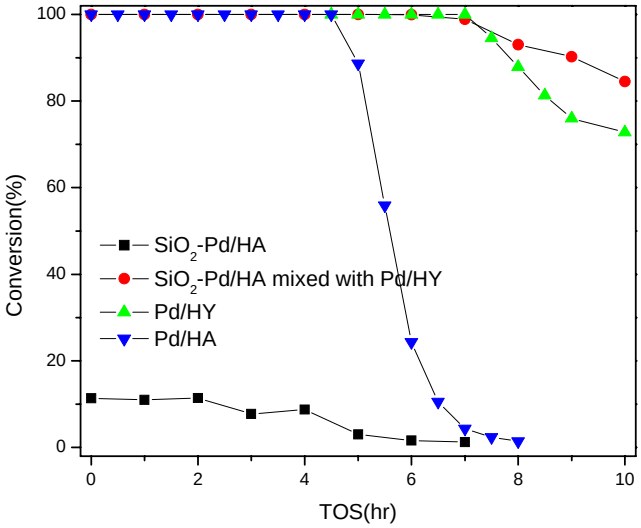

(a)

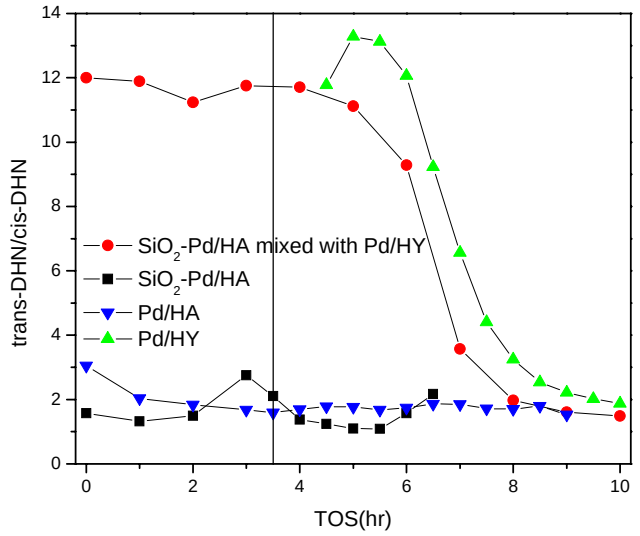

(b)

Figure 3-17. (a) Conversion vs. TOS for the hydrogenation of tetralin and (b) trans-/cis-DHN ratios for the hydrogenation of tetralin over coated Pd/HA catalyst and its hybrid catalyst.

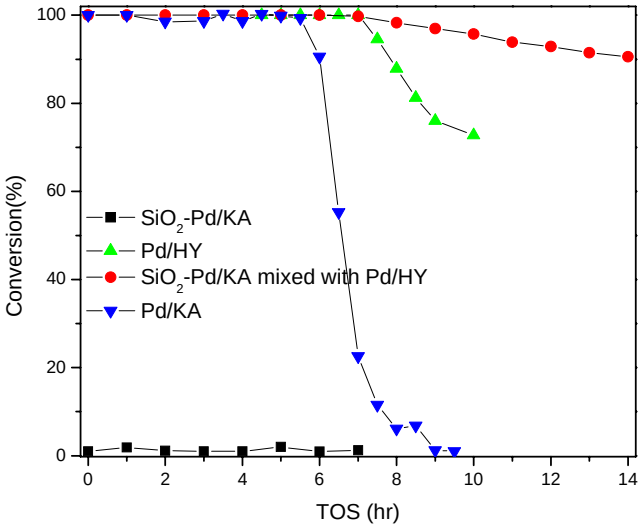

(a)

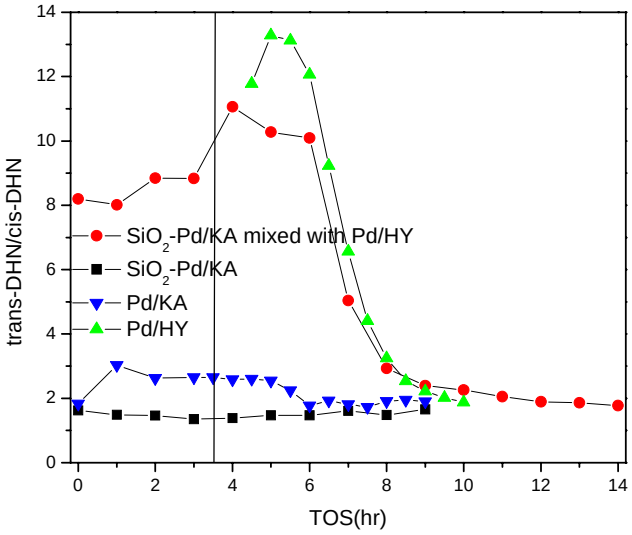

(b)

Figure 3-18. Conversion vs. TOS for the hydrogenation of tetralin and **(b)** trans-/cis-DHN ratios for the hydrogenation of tetralin over coated Pd/HA catalyst and its hybrid catalyst.

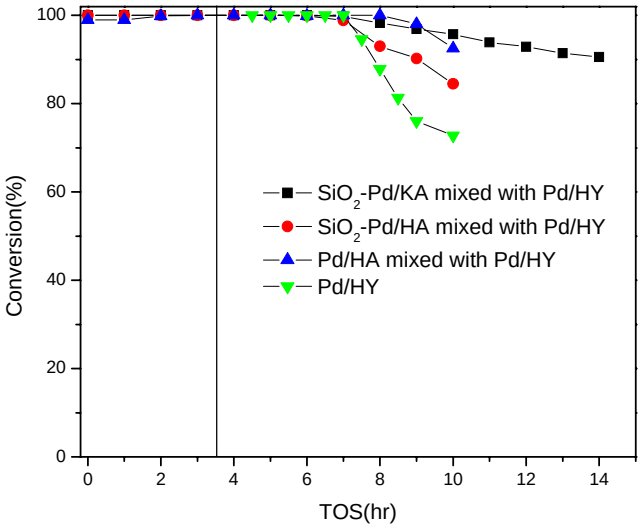

(a)

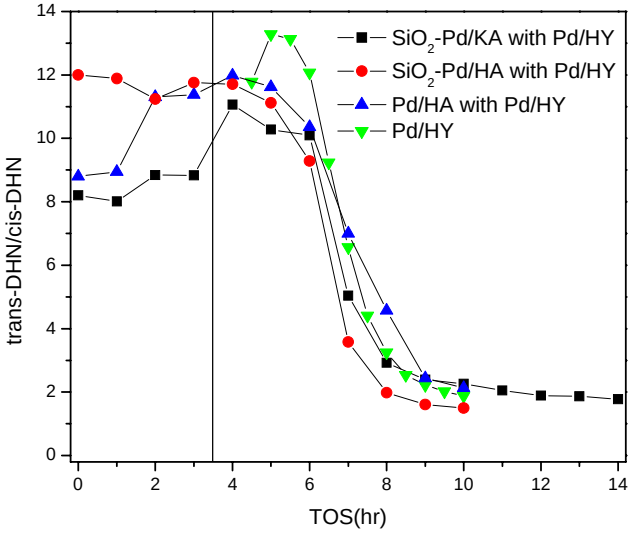

(b)

Figure 3-19. (a) Conversion vs. TOS for the hydrogenation of tetralin and **(b)** trans-/cis-DHN ratios for the hydrogenation of tetralin over various hybrid catalysts.

Subtask 3.3 Introduction to Value-Added Chemicals from Naphthalene

The application of the shape selective catalysis concept to various industrial aromatic alkylation processes has been well documented in literature [**3-38**]. In the recent past, the drive for alternate sources of fuel led us to look into the possibilities of liquid fuels from coal and the realization of the concept of a "coalfinery" [**3-39**]. Since naphthalene constitutes a major portion of these fuels and their derivatives, the use of naphthalene as a feed stock for the manufacture of 2,6-dimethyl naphthalene using environmentally benign catalysts was being explored to compete with the existing technologies. The shape-selective alkylation of naphthalene is carried out to develop 2,6-dialkylnaphthalene which is one of the monomers for highly value-added chemicals for making advanced polymer materials such as liquid crystalline polymers (LCPs) [**3-40**]. LCPs have outstanding mechanical properties at high temperature, excellent chemical resistance and good weatherability. However, the key challenge lies in the selection of materials for shape-selective catalysis for the formation of 2,6-dialkylnaphthalene (2, 6-DMN). In the previous reports, different molecular sieves were tested as catalysts for the alkylation reaction and it was observed that medium pore zeolites modified with metals like Fe, Mg and Zn. Of these metal modified zeolites tested, Fe modified ZSM 5 catalysts seemed promising. As reported in previous reports, these catalyst samples were modified by trying to exchange the aluminum ions with the iron ions. These catalysts were then characterized for acidity studies using NH_3 TPD. The spent catalyst samples were analyzed for the percentage of carbon during the reaction by temperature programmed oxidation. This time further characterization was carried out on the parent zeolite and Fe ZSM 5 samples.

3.3.1 Modification of ZSM 5 using Iron

Iron-modified ZSM-5 catalysts were prepared by modifying the HZSM-5 with iron (III) fluoride ($FeF_3.3H_2O$) and ammonium hydrogen fluoride (NH_4HF_2) at a temperature of 92+/-5°C. The ZSM 5 was first converted to the HZSM 5 form from the ammoniated form by calcining in a muffle furnace at a temperature of 550°C for 6 h. The temperature ramp was 1.52°C/min. The ZSM-5 (supplied by Zeolyst International) with SiO_2/Al_2O_3 ratio of 50 (CBV5524G) was used. Four samples were prepared by this method and used for catalytic testing of the methylation of 2-methylnaphthalene (2-MN). The catalysts were characterized by surface area measurements, micro calorimetric studies and X – Ray Diffraction studies.

3.3.1.1 Catalyst preparation

In this modification procedure, about 15 g of HZSM 5 (50) was mixed in 150 g of deionized water and was placed in a stirrer for an hour in an oil bath at 92+/-$^{\circ}$C. A slurry of $FeF_3.3H_2O$ and NH_4HF_3 was made in 100 g of deionised water. This salt slurry was added to the ZSM 5 – water slurry mixture drop by drop in one hour. The solution was then stirred at total reflux for 24 hr at 92+/-$^{\circ}$C. The resultant solution was then washed, filtered by a vacuum filter and then dried in an oven at 110°C for 12 h. This mixture was powdered and then calcined in a muffle furnace for 6 h at a temperature of 450°C for 6 h at a temperature ramp of 1.52°C/min. The calcined catalysts were then pelletized, crushed and sieved to a particle size of 18-35 U.S.A. Standard Testing Sieve Mesh (0.5 – 1.0 mm).

3.3.1.2 Catalyst Testing and Characterization

3.3.1.2.1 Catalyst Testing

Catalytic testing was carried out in a down-flow fixed bed reactor system. In a typical run, ~ 0.3 gram catalyst (10-18 mesh) loaded in reactor tube (Pyrex, I.D.: 1/2inch) was placed in the furnace center. The catalyst was activated at 450°C for 1 h under the inert N_2 gas flow (20 ml/min). Then the temperature was cooled down to the reaction temperature. Reactant dissolved in mesitylene solvent (2-MN:methanol:mesitylene=1:5:5 mol ratio) was fed into reactor through a HPLC pump at the flow rate of 1.98 ml/min together with 20 ml/min carrier N_2 gas flow. The reaction product was collected at 1 h interval. Both the reactants and products were analyzed by HP 5890 gas chromatography (GC) with a β-Dex 120 capillary column (60 m, 0.25 mm I.D. column with 0.25 μm coating film thickness). Approximately 0.05 g of the spent catalyst was used in determining the extent of the carbon deposition on the sample during the reaction.

3.3.1.2.2 Surface Area Measurements

The surface area and pore size distribution analyses were carried out on a static high vacuum volumetric unit Micromeritrics ASAP 2010. The sample was pretreated by passing Nitrogen at 350°C under vacuum for 12 h. Table 3-5 shows the surface area and pore size distribution for Iron modified ZSM 5 containing ascending order of iron concentrations and compared with the parent HZSM 5. The total surface area was measured by the BET surface area method and the pore size was determined from the Horvath-Kawazoe method. All the other samples VGD 02–VGD 07 are iron modified

zeolite samples having increasing weight percent of iron loaded. By observing the data in the table below, we can observe, there is an overall decrease in the micro pore area as the iron loading increases. There is an increase in the external surface area during modification. This might be attributed to some of the zeolite structure collapsing during the modification process. There is a minor variation in the pore diameter. Only one sample VGD 03 shows an increase in the pore diameter. It may be suggested that during modification, the pore size increases initially reaches a maximum and then gradually decreases almost settling down close to the original pore size of the parent zeolite. Coincidentally, as mentioned in the previous reports, the sample VGD 03 was the best in the activity measurements. So it may be inferred that the increased activity was due to the expansion of the pore mouth in this sample. The micro pore area showed a decreasing trend with the increase in the iron loading.

3.3.1.2.3 Acidity Measurements (Microcalorimetric Studies of Fe Modified ZSM 5)

Microcalorimetric studies of adsorption of ammonia have been performed to determine the total acidity and the acid strength distribution using a Tian–Calvet type heat flux microcalorimeter (model C – 80, Setaram, France) that is connected to a volumetric adsorption unit for sample treatment and a probe molecule delivery unit. The samples were preheated at 450°C under vacuum for 4 h prior to micro calorimetric measurements. Ammonia was adsorbed onto the sample in sequential doses. The heats evolved from these sequential doses onto the sample were measured at 175°C. The heat of adsorption generated from each dose was calculated from the resulting thermo grams and the amount of ammonia absorbed from the pressure change. Sequential doses of NH_3

give the differential heats of NH_3 adsorption as a function of coverage (i.e differential heat curves). This technique provides the information about the number and the strength of the acid sites on the samples. Table 3-6 lists out the acidity distribution of the acid sites in the parent zeolite and the iron modified zeolites.

Microcalorimetric adsorption of ammonia and the resulting enthalpy of adsorption as a function of the volume of ammonia adsorbed over ZSM-5 samples are given in Figure 3-20. It can be seen that ammonia interacted with these sites in a heterogeneous manner. In this case, the heat of adsorption varied in the wide range between 140 to 40 kJ/mol. As the dealumination increased or the wt% of iron in the modification increased, the amount of ammonia adsorbed on the surface of these samples decreased. The heat of adsorption decreased with coverage in well defined steps, in all of the samples. This systematic decrease of the differential heats observed in the present case is due to the consequence of the interaction of ammonia with a variety of the surface sites that exhibit different strengths [**3-42**]. The curves become steeper with the increase in the iron concentration in the samples. This indicates that there is dealumination in these samples very evident by the decrease in the acid strength. A decrease in the total number of acid sites cans also be observed.

Figure 3-21 gives the differential curves of acid strength of the samples. In this plot, the distribution of acid strengths namely dn/dq vs Q were plotted for the five samples investigated. As the iron content of the samples increased, the intensity of the peaks decreased showing a remarkable decrease in the number of acid sites [**3-42**].

3. 3.1.3 Summary

- BET surface area studies done on the parent zeolite and the iron modified zeolites indicate that the external surface area increases with an increase in the concentration of iron in the catalyst. This may be due to a structure modification in the parent zeolite during modification

- The acidity decreases due to the increase in iron loading on the catalyst. This may be due to the destruction of external surface acid sites during modification.

Table 3-5. Surface area and pore size distribution of iron modified ZSM 5 samples

Sample Name	Total Surface Area (m^2/g)	Micropore Area (m^2/g)	External Surface Area (m^2/g)	Micropore Volume (cm^3/g)	BJH pore Diameter (mesopore) (A°)	HKmethod pore diameter (A°)
VGD – 01	443	315	128	0.127	62.4069	5.0013
VGD – 02	453.	279	174	0.120	56.86	4.73
VGD – 03	412	155	257	0.068	67.12	5.18
VGD – 04	418	163	255	0.071	59.35	4.9
VGD – 05	400	144	256	0.064	62.94	4.9
VGD – 06	408	183	225	0.078	63.70	4.84
VGD – 07	411	164	246	0.072	65.47	4.9

Table 3-6. Acidity distribution of the acid sites in the parent zeolite and the iron modified zeolites

S.No.	Catalyst Samples	Total Acidity (mmol/g)	*Acid Strength Distribution**				Initial Heats (kJ/mol)
			VS	S	M	W	
1.	H-ZSM-5	0.823	0.015	0.335	0.140	0.313	120.62
2.	Fe-ZSM-5 -01	0.759	0.200	0.125	0.115	0.319	141.65
3.	Fe-ZSM-5-2	0.518	0.105	0.160	0.065	0.188	134.31
4.	Fe-ZSM-5-3	0.396	0.065	0.105	0.085	0.141	137.04
5.	Fe-ZSM-5-4	0.603	0.065	0.205	0.175	0.158	140.08

* VS (Very Strong) Acid sites = > 120 mmol/g of catalyst
S (Strong) Acid sites = > 100 < 120 mmol/g of catalyst
M (Medium) Acid sites = > 80 < 100 mmol/g of catalyst
W (Weak) Acid sites = < 80 mmol/g of catalyst

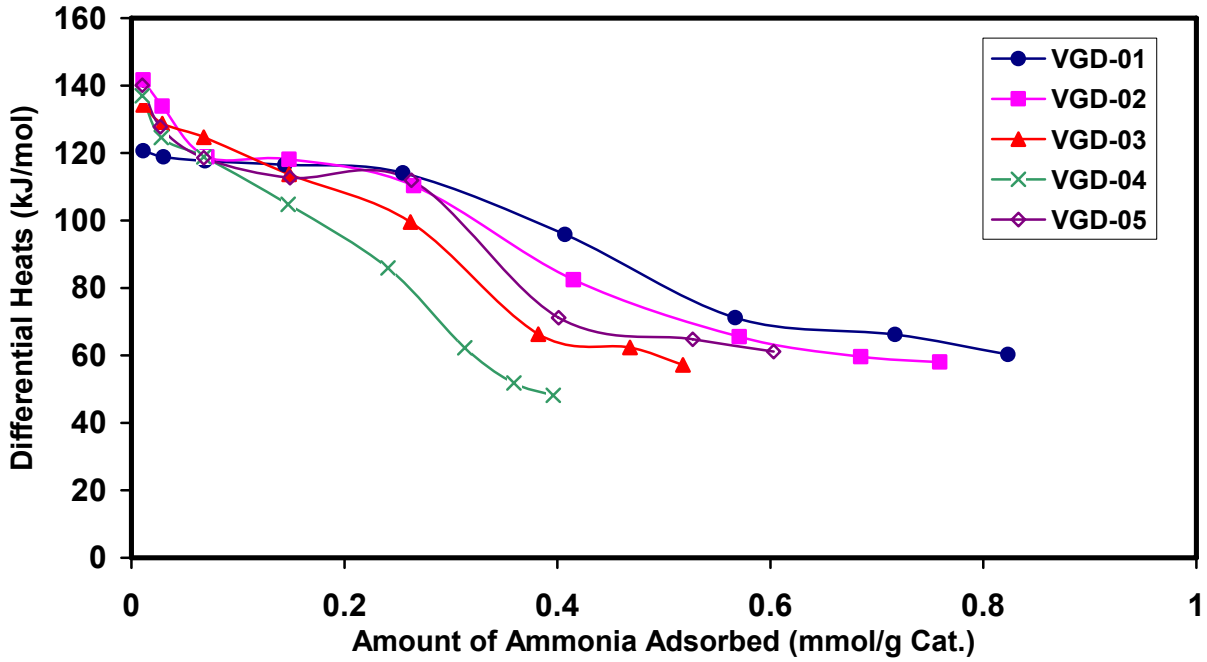

Figure 3-20. Differential heat curves of Fe-ZSM-5 samples.

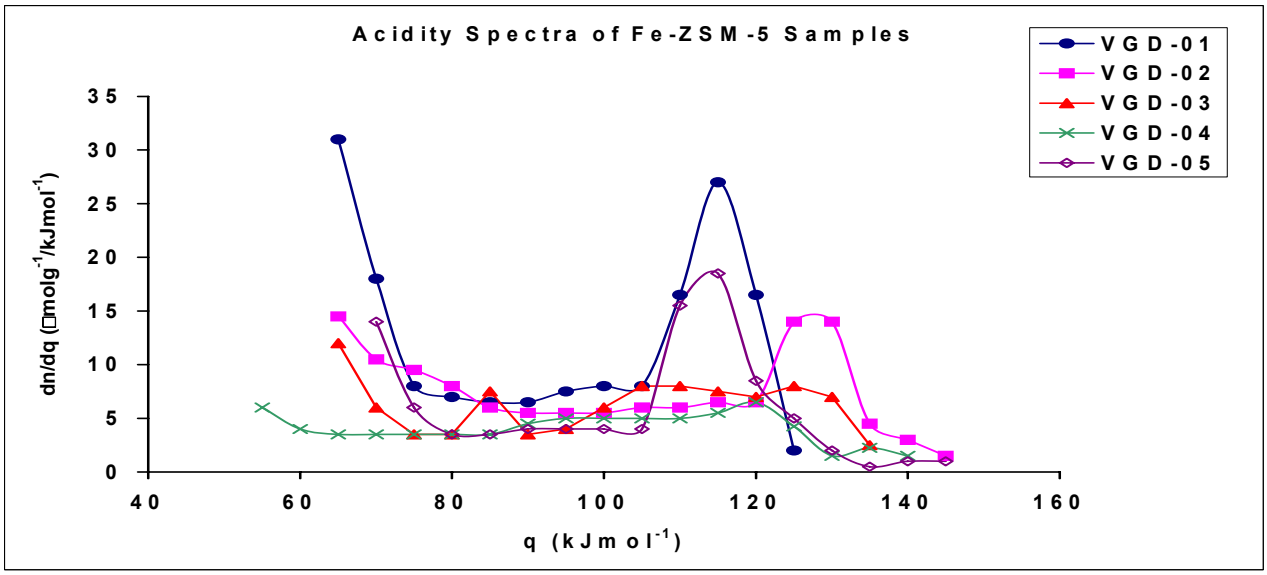

Figure 3-21. Acidity spectra of Fe-ZSM-5 samples

Task 4. Evaluation of Coal-Based Fuel Products

The objective of the Task 4 activities is to evaluate the effect of introducing coal into an existing petroleum refinery on the fuel oil product. To accomplish this, the combustion performance and trace element emissions of two fuel oils produced from either refined chemical oil (RCO) or a blend of RCO and light cycle oil (LCO) were measured in Penn State's watertube research boiler. The fuel oils were produced by different methods. The first fuel oil (sample X610) was derived by hydrotreating followed by fractionation of a 1:1 blend of RCO and LCO. The second fuel oil (sample X1333) was derived from the bottoms fractionated out of the RCO. The combustion performance and trace element emissions for the fuel oils produced by further refining of either the RCO or LCO-RCO blend were then compared with that from a commercial/petroleum-based No. 6 fuel oil. The testing was performed to determine if differences in the combustion behavior or emissions of the two fuel oils would result from variations in the API gravity, viscosity, or changes in composition including trace elements present in either fuel oil.

Subtask 4.1. Fuel Oil Analysis

Analysis of trace metals in liquid hydrocarbons is very difficult and can not be done in the same manner as solid hydrocarbons. Solid hydrocarbons samples are generally heated forming an ash which is subsequently heated with lithium borate to form a glass phase which stabilizes the elements. The glass phase is then digested in an acid solution which is then aspirated into a flame. The volatilization of the material via a flame or plasma ionizes the element. The emission spectrum of an element's ionization

energy is then measured which reflects the concentration of the species in the sample. This technique is not suited to analyze volatile trace elements such as mercury or arsenic as they are lost to the atmosphere. In this case, solid hydrocarbon can be digested directly (whole fuel) and not ashed. The solution can then be analyzed by different spectroscopic techniques. The fuel analysis in **Table 4-1** was conducted using EPA 3052 (Microwave Assisted Acid Digestion of Siliceous and Organically Based Matrices) **[4-1]** in which the liquid hydrocarbons are digested and the solution is then analyzed using inductively coupled plasma spectroscopy (ICP). Mercury must be analyzed by cold-vapor atomic adsorption spectroscopy. The analysis presented is not complete as many of the elements were reported as below detection limits of the ICP. In addition, mercury analysis has not been completed.

Table 4-1. Fuel Analysis

	#6 Fuel Oil	Co-Processed Fuel Oil X610	RCO Bottoms X1333
Element	**ppm**		
Al	17.9	<2.85	<2.60
As	*	**	1.52
Ba	1.15	**	***
Be	*	**	***
Cd	*	**	***
Co	0.913	**	***
Cr	0.396	0.451	1.46
Cu	*	**	0.265
Hg	na	na	na
Mn	*	**	***
Mo	0.303	**	***
Ni	50.0	0.405	0.629
Pb	*	**	***
Sb	0.442	**	***
Se	*	**	***
Sr	*	**	***
V	182	0.307	0.362
Zn	0.869	0.479	1.67

*Less than 0.287 ppm
** Less than 0.285 ppm
*** Less than 0.260, na Not available

Subtask 4.2 Fuel Atomization

In the subtask, the fuel oil is to undergo atomization tests at the conditions (*i.e.*, temperature and atomization pressures) it will be tested in the watertube boiler. However, due to the difficulty and cost of preparing large quantities of fuel oil, it is likely that atomization tests will not be performed in order to have sufficient quantities for the combustion and emissions testing.

Subtask 4.3. Watertube Boiler Combustion Tests

The activity conducted during this reporting period are under Subtask 4.3.3 Watertube Boiler Combustion Tests, Emission Testing of Co-Processed Fuel Oil. The chemical and physical analysis of the X610 and X1333 and No. 6 fuel oils, description of the research boiler and testing conditions, combustion performance and efficiencies were reported in the April –October 2006 Semi-annual Report, Subtasks 4.1 and 4.3. **[4-2]**

Emissions and Thermal Efficiencies:

The most noticeable difference between the emissions produced from burning the RCO/LCO-derived fuel oils and the baseline No. 6 fuel oils is the large reduction in both the sulfur dioxide (SO_2) and oxides of nitrogen (NO_x). The reduction in the sulfur dioxide levels observed burning the RCO/LCO-derived fuel oils is attributed to the lower sulfur content of these fuel oils compared to the baseline No. 6 fuel oil. As reported in the April-October 2006, Semiannual Report (**Table 4-1)**, the weight percent of sulfur in the No. 6, co-processed, and RCO bottoms fuel oils is 1.8, 0.06 and 0.54 wt.%, respectively. **[4-2]**

Although numerous researchers have shown fuel NO_x to be an important mechanism in NO_x formation from fuel oil with a strong correlation between the percent nitrogen in the fuel oil versus NO_x formation, there appears to be no such correlation in the various fuel oils tested. This may suggest that the differences can be attributed to a more dominant mechanism of thermal NO_x formation within the oil flames.

The thermal efficiency of the watertube boiler was determined for each test in accordance with the input-output method as described in the ASME Power Test Codes for Steam Generating Units – Section 4.1 **[4-3]**. The efficiency for this method is expressed by the following equation:

$$\text{Boiler Efficiency (\%)} = \frac{\text{Output}}{\text{Input}} = \frac{\text{Heat adsorbed by working fluids}}{\text{Heat in fuel + heat credits}} \text{ x } 100$$

The efficiency for the six tests performed burning the baseline No. 6 fuel oil varied between 70.3 and 73.3%, while the efficiency determined when burning the co-processed fuel oil on 05/24/05 and 08/02/06 was 71.6% and 70.4%, respectively (**Table 4-4**, April-October 2006, Semiannual Report **[4-2]**). The efficiency determined for the RCO bottoms testing was lower because of the reduced firing rate (1.13 MM Btu/h). Since the efficiency for the co-processed fuel oils lie within the spread of efficiencies determined for the baseline fuel oil, there appears to be no differences in boiler performance between the fuel oils. The detailed thermal efficiency calculations are provided in the April – October 2006 Semiannual Report, Appendix A. **[4-2]**

4.3.3 Emission Testing of Co-Processed Fuel Oil

Trace metal emissions sampling was performed during combustion testing of the baseline No. 6 fuel oil (duplicate sample trains conducted on 08/07/06), sample X610 (conducted on 08/02/06), and the X1333 sample (conducted on 08/14/06) using the PSU Method **[4-4, 4-5]**, which is a combination of the procedures outlined in the EPA Method 29 (Determination of Metals Emissions from Stationary Sources to measure trace elements in the gas and particulate phases of the flue gases generated during coal combustion) and Ontario Hydro Mercury Speciation Methods (**Figure 4-1**). **[4-4 – 4-6]** The reagent in each impinger is shown in "red" type and the elements measured in each impinger is also shown. The recovery and analytical protocol for each impinger is shown in **Figure 4-2**. It was not possible to conduct two sequential sample trains during testing of the co-processed fuels as there was not enough of either fuel to burn in order to sample the total volume of flue gas as prescribed by the EPA Method 29. **[4-4 – 4-6]** Detailed emissions are given in the Appendix of the April-October, 2006, Semiannual Report. **[4-2]**

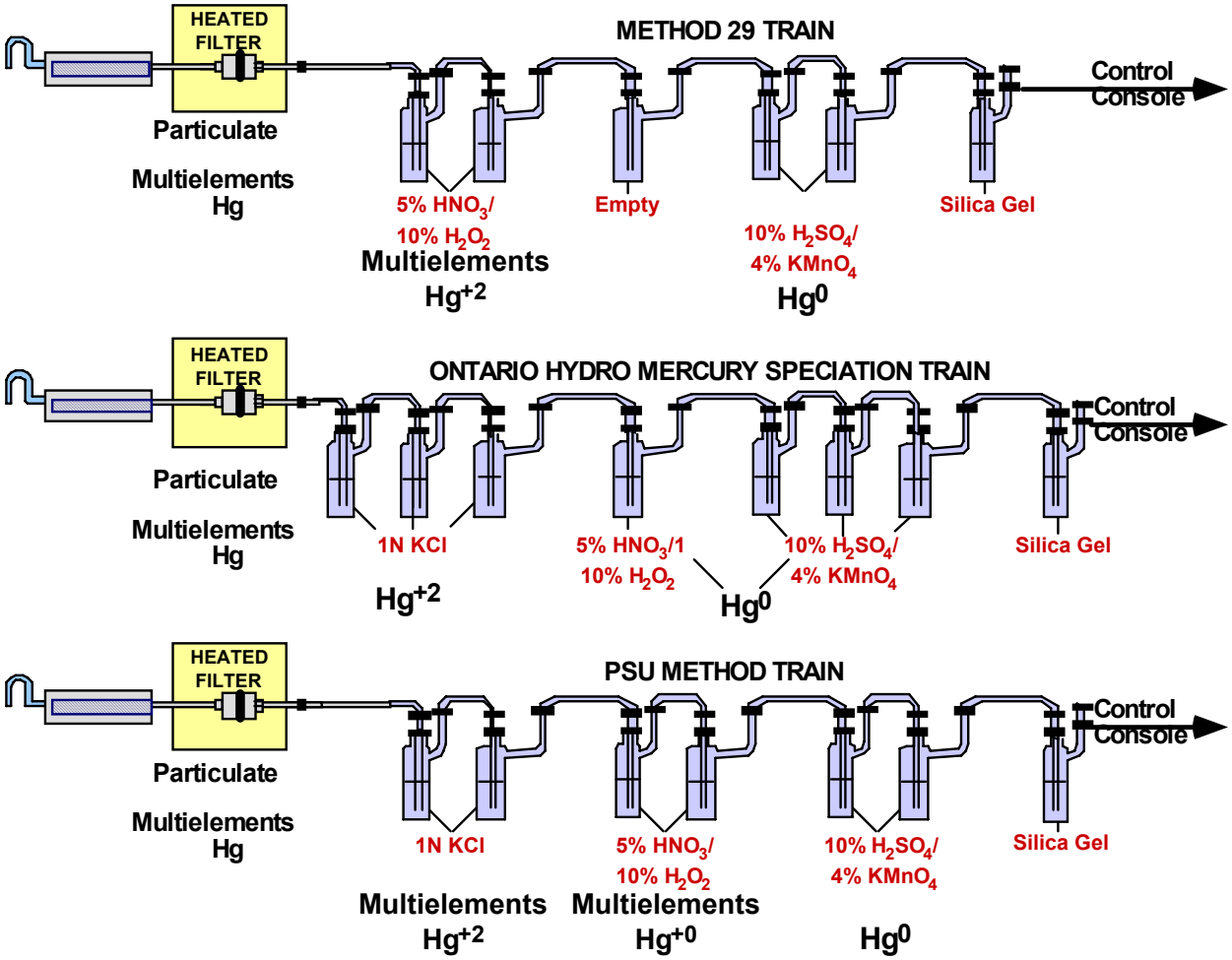

Figure 4-1. Sample train for elemental analysis of emissions

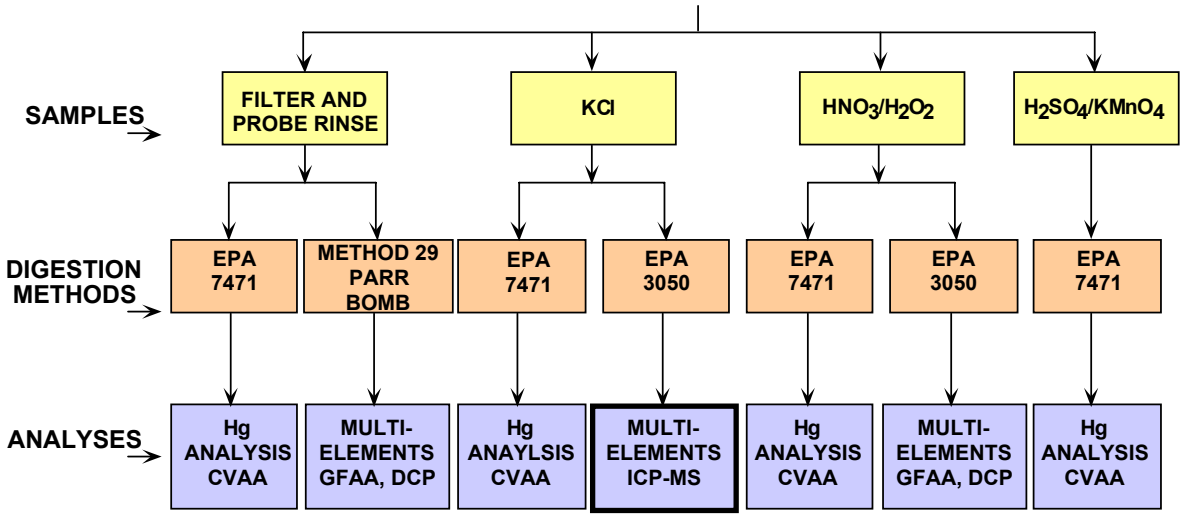

Figure 4-2. Sample preparation and analytical protocol for impingers in sample train.

The elements analyzed for and the emissions measured for the fuels fired during the previous reporting period are given in **Table 4-2**. All elements measured except for Hg are referred to as "Multielements" in **Figure 4-1**. Elements of major environmental concern are As, Cd, Hg, Mo, Pb, and Se and are indicated in "red" type. Elements of moderate concern are Cr, Cu, Ni, V, and Zn and are indicated in "green" type. Elements of minor concern are Ba, Co, Mn Sb and Sr and are indicted in "blue" type. A series of graphs showing the relative amounts of emissions of trace metals is given in **Figures 4-3 – 4-13**. The graphs are grouped in order of greatest to least environmental concern.

Table 4-2. Elemental emissions measured at research boiler outlet for test fuels.

Date	8/7/2006	8/7/2006	8/2/2006	8/14/2006
Fuel	#6 Fuel Oil	#6 Fuel Oil	Co-Processed Fuel Oil X610	RCO Bottoms X1333
	Emissions (lbs per trillion Btu)			
Al	467.1	788.3	1,678.7	2,541.4
As	6.2	21.2	14.4	14.7
Ba	66.5	65.9	24.5	69.4
Be	0.1	0.1	0.2	1.2
Cd	0.1	0.1	0.2	0.3
Co	25.2	23.5	2.4	9.8
Cr	1.9	2.1	6.5	65.6
Cu	3.4	4.8	11.1	31.4
Hg	0.3	0.3	0.2	0.3
Mn	14,585.4	13,201.5	3,423.7	9,676.9
Mo	4.9	4.4	5.7	6.7
Ni	1,228.3	1,065.0	60.2	164.9
Pb	9.7	7.4	8.9	16.7
Sb	1.8	1.8	1.6	3.3
Se	0.9	0.7	0.6	4.5
Sr	7.6	6.7	14.3	22.8
V	3,811.1	3,732.0	110.1	209.5
Zn	161.6	171.7	172.7	789.2

Elements of Greatest Environmental Concern (**Figures 4-3 – 4-7**)

The reason for analyzing for trace metals in the emissions from the co-processed fuels is to determine if coal-derived liquids introduce elements, normally associated with coal, of environmental concern into a liquid hydocarbon fuel that are not commonly found in petroleum-derived fuels.

Co-processed fuel X1333 had the highest level of emissions for four (Pb, Cd, Mo, and Se) of the six elements of greatest environmental concern. Interestingly the No 6 fuel oil had the highest levels of As and Hg emissions which represent the top two elements of greatest environmental health concern due to their neurological effects on humans (**Figures 4-3 and 4-4**) The X610 and X1333 fuels had 38 and 15% less in Hg emissions. It should be noted that the level of As measured in the duplicate sample trains run during the fuel oil test had the least agreement than any other element. The No. 6 fuel oil averaged 13.7 lbs per trillion Btu which is very close to the 14.4 and 14.6 $lb/10^{12}$ Btu for the X610 and X1333, respectively. Therefore it is difficult to tell if there is significant difference in As emission between the fuels due to questionable reproducibility of the No. 6 fuel oil test.

The selenium emission level for X1333 was significantly greater (4.5 lbs/1012 Btu) than that for the X610 fuel (0.56 lbs/1012 Btu) and the No. 6 fuel oil ((0.70-0.89 lbs/1012 Btu) Figure 5).

Mercury speciation was also determined by the PSU Method sample train. **[4-4 – 4-6]** Oxidized mercury (Hg^{+2}), elemental mercury (Hg^{0}) and mercury in the particulate was determined. The data is given in **Table 4-3** and **Figures 4-6 and 4-7**. If the amount of a particular mercury species is present below detection limits then it is treated as a

"non-detect" and no values are reported. The oxidized form of Hg is soluble in water and is the most reactive in the atmosphere forming methyl mercury as it reacts with surface and atmospheric water. This reactivity also makes oxidized mercury easier to recover (via control technologies) from the flue gas prior to being emitted into the atmosphere. Current control technologies are focused on oxidizing the elemental Hg so that it may be removed as well.

The mercury in the No. 6 fuel oil emissions is present mostly as Hg^{+2} (> 70%) followed by Hg^{0} (approximately 20%) with the remainder (5%) as mercury associated with particulate. Note that there is good agreement between the mercury analyses of the duplicate fuel oil trains. The mercury in the flue gas stream had very different modes of occurrence for the co-processed fuels. The X610 fuel has most of the mercury as particulate (65%) and the rest as Hg^{0} (35%) and essentially no Hg^{+2}. The X1333 fuel had significant Hg^{+2} (60%) and 40% particulate Hg.

A high percentage of mercury in the particulate during coal combustion is generally associated with low burnout efficiencies resulting in a char with high carbon content. This results in the gas phase mercury reacting with the carbonaceous portion of the char. However, these fuels have low ash content and it is difficult to speculate what the reasons are for the mercury speciation seen in the different flue gases.

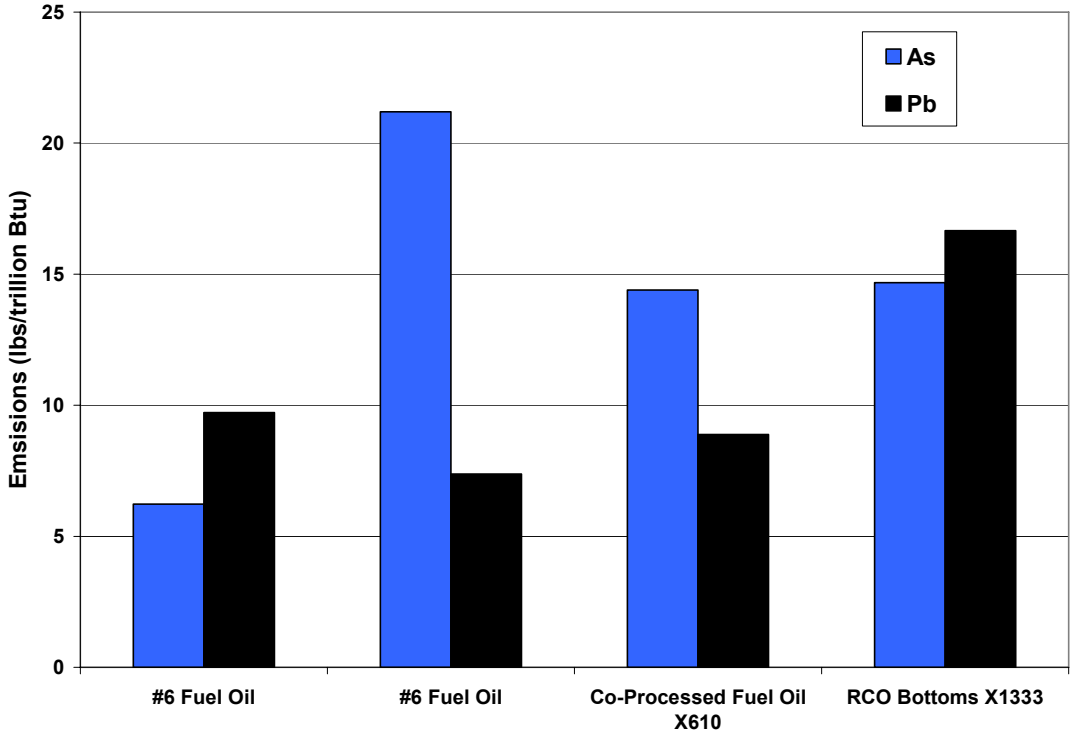

Figure 4-3. Arsenic and lead emissions for test fuels.

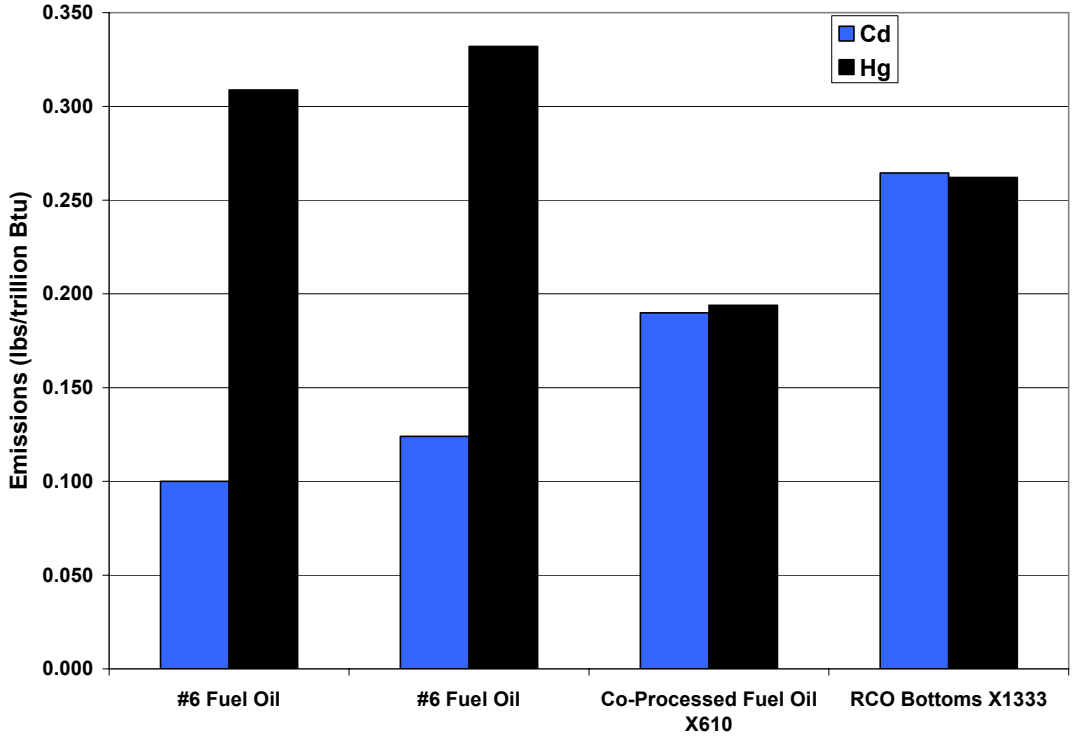

Figure 4-4. Cadmium and mercury emissions for test fuels.

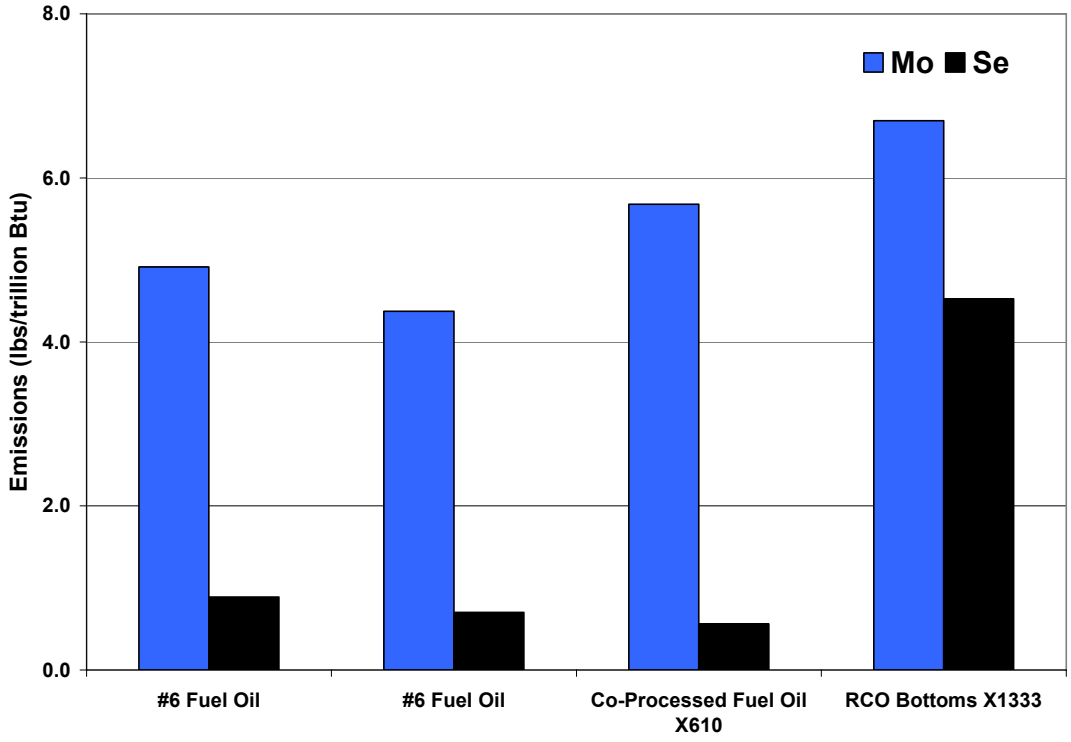

Figure 4-5. Molybdenum and selenium emissions for test fuels.

Table 4-3. Distribution of mercury species in emissions from fuels.

Species	Hg^{+2}		Hg^{0}		Hg Particulate	
	Weight %	lbs/10^{12} Btu	Weight %	lbs/10^{12} Btu	Weight %	lbs/10^{12} Btu
No. 6 Fuel Oil	72.6	0.224	22.2	0.069	5.13	0.016
No. 6 Fuel Oil	74.1	0.246	20.4	0.067	5.49	0.018
X610			35.3	0.069	64.7	0.125
X1333	59.7	0.156			40.3	0.106

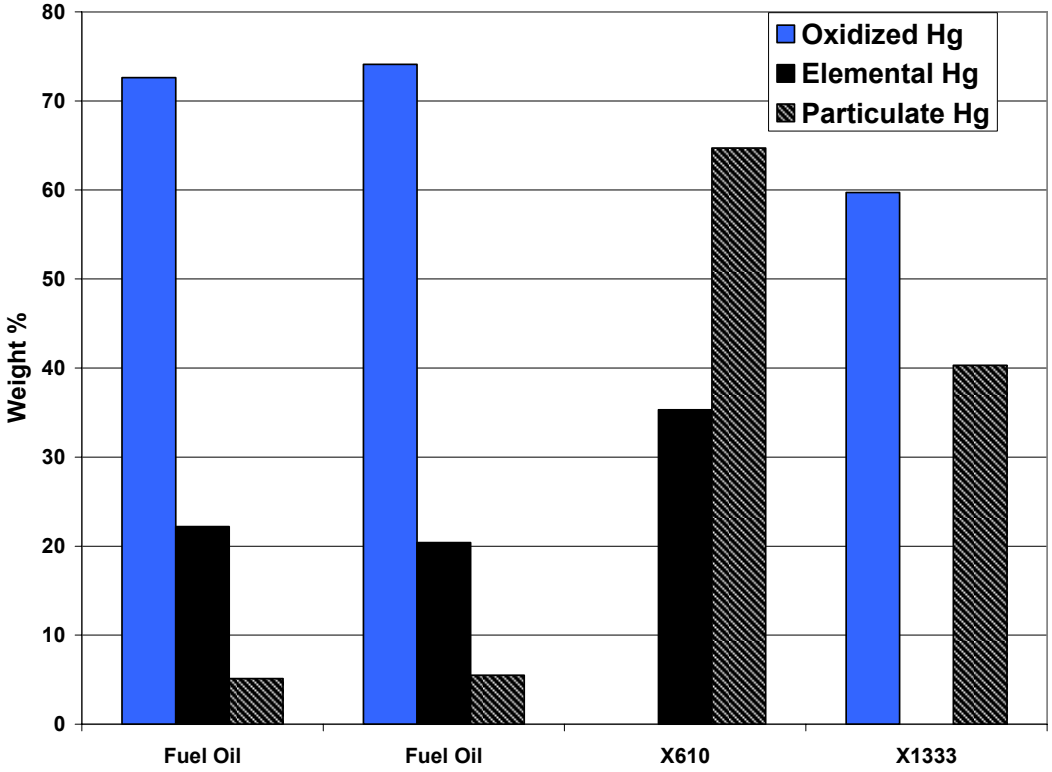

Figure 4-6. Weight percent of total mercury, by species, measured in emission for each fuel.

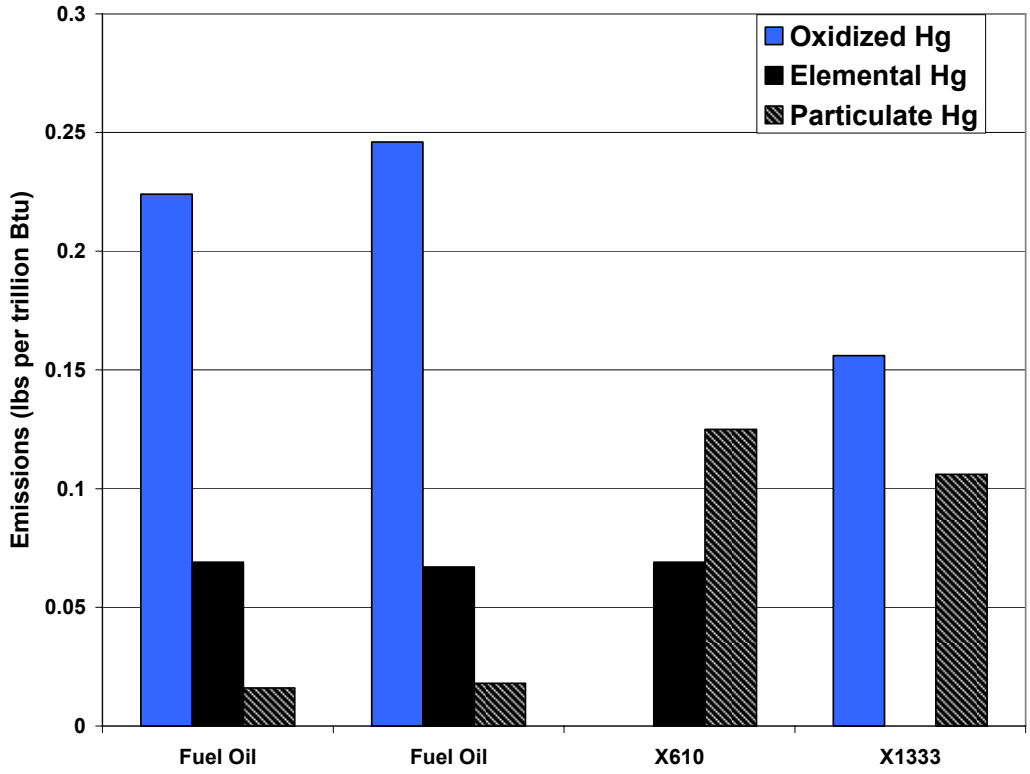

Figure 4-7. Mercury emissions, by species, measured for each fuel.

Elements of Moderate Environmental Concern (**Figures 4-8 – 4-10**)

Again the X1333 fuel had the highest concentration in three (Cr, Cu and Z) of the five elements of moderate environmental concern. The No 6 fuel oil had the highest emission levels of Ni and V.

Chromium emissions for the X1333 fuel were approximately 10 times higher than measured for the X610 fuel. Copper emission in the X1333 fuel was 3 times higher than in the X610 and 9 times higher than in the fuel oil (**Figure 4-8**). Zinc emission for the X1333 was approximately 5 times higher than the X610 and fuel oil (**Figure 4-9**). The X610 and fuel oil Zn emissions were essentially the same.

Nickel emissions were a factor of 7 to 19 times greater in the fuel oil than for the X1333 and X610 fuels, respectively (**Figure 4-9**). Vanadium emissions were a factor of

18 to 34 times greater in the fuel oil than for the X1333 and X610 fuels (**Figure 4-10**). This is consistent with the higher levels of Ni and V associated with petroleum-derived fuels as compared to coal. The addition of the coal-derived liquid in the X610 and X1333 acts as a diluent reducing the amounts of these elements. Since the percent of coal-derived liquids in the X610 and X1333 is not known it is difficult to confirm the dilution effect.

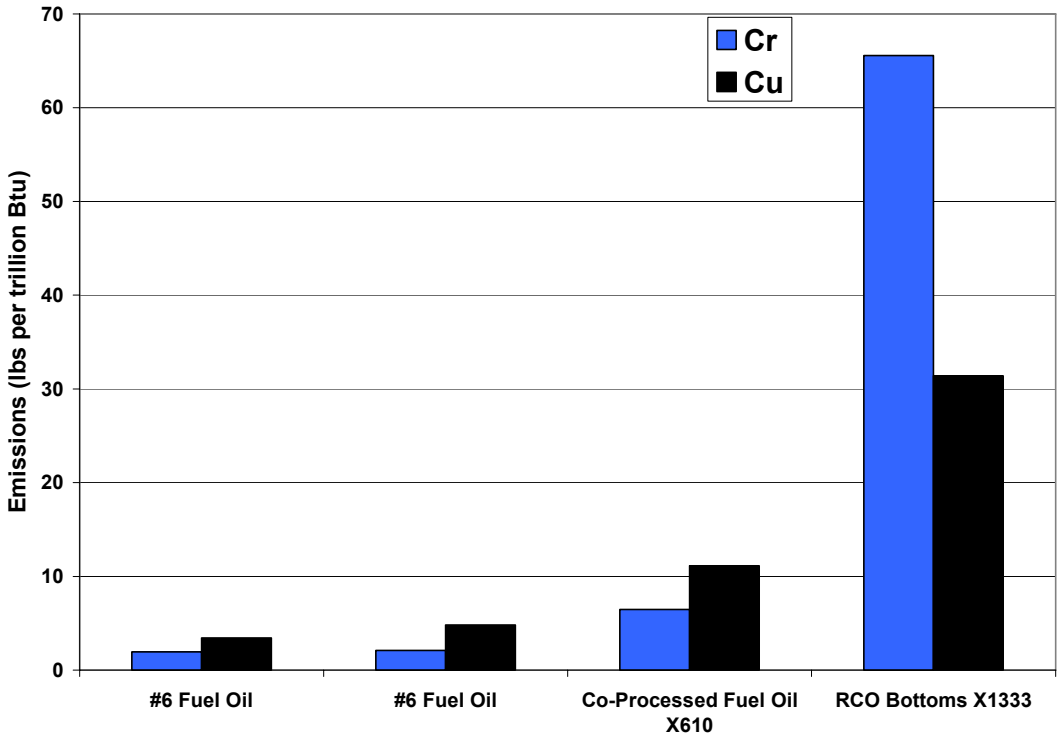

Figure 4-8. Chromium and copper emissions for test fuels.

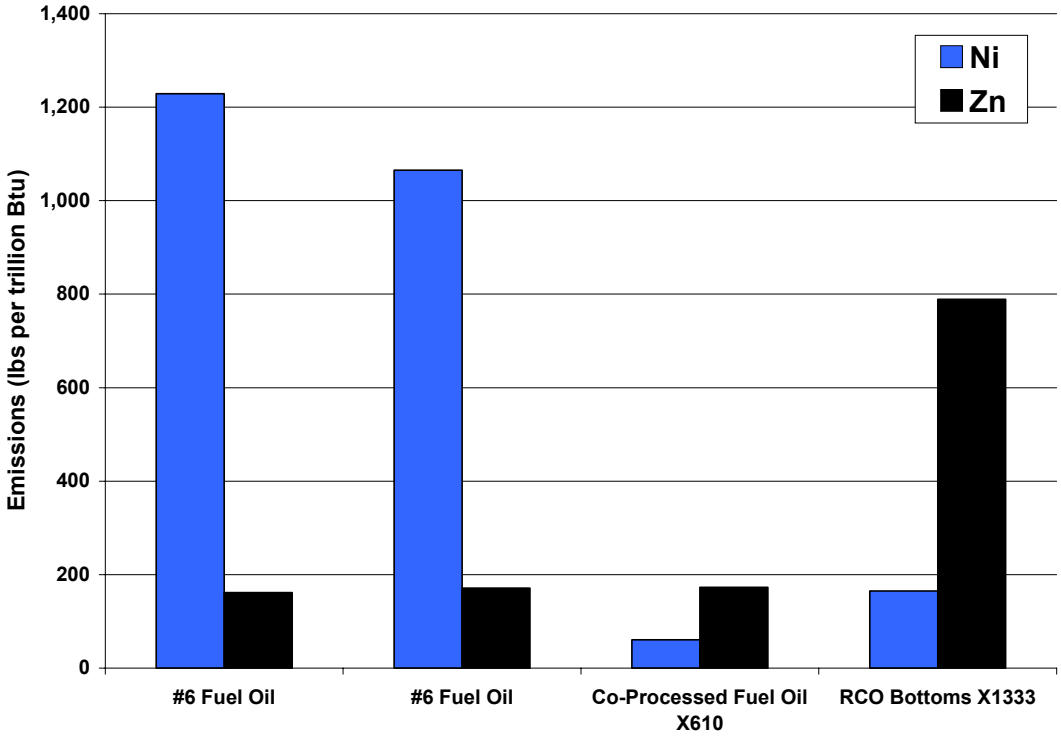

Figure 4-9. Nickel and zinc emissions for test fuels.

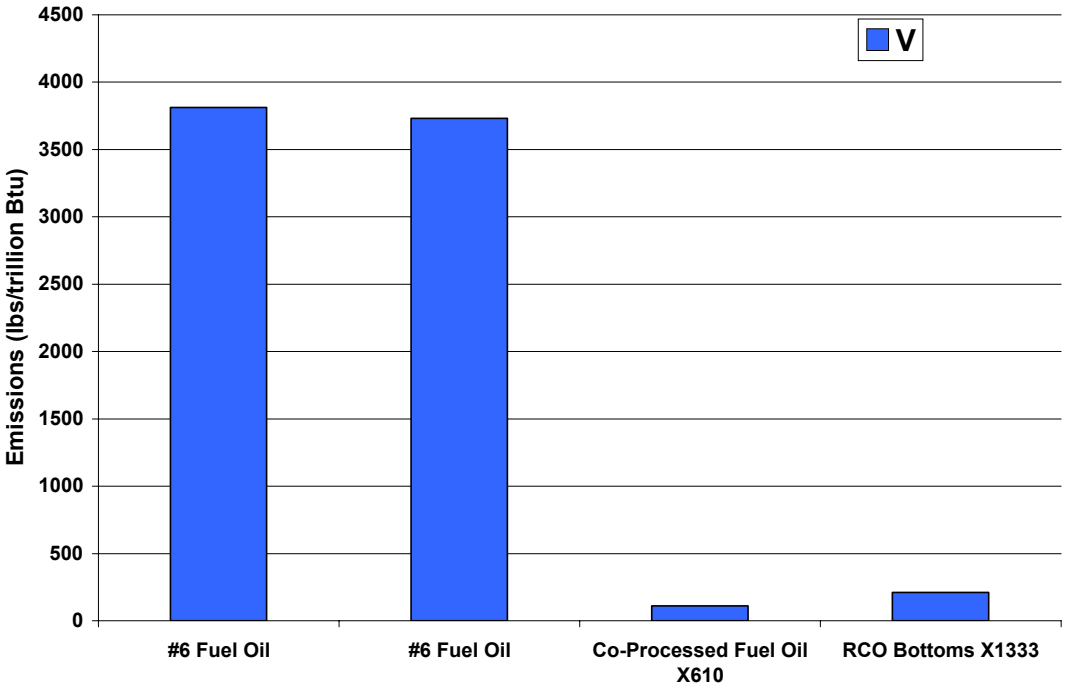

Figure 4-10. Vanadium emissions for test fuels.

Elements of Minor Concern (**Figures 4-11 – 4-13**)

Again fuel X1333 had the highest emission levels of Sr (**Figure 4-11**) and Sb (**Figure 4-13**). The X611 fuel had the lowest emission levels of Co and Ba (**Figure 4-11**) and Mn (**Figure 4-12**). Antimony levels were essentially the same for the fuel oil and the X611 fuel (**Figure 4-13**). Barium emissions for the fuel oil and the X1333 fuel were similar.

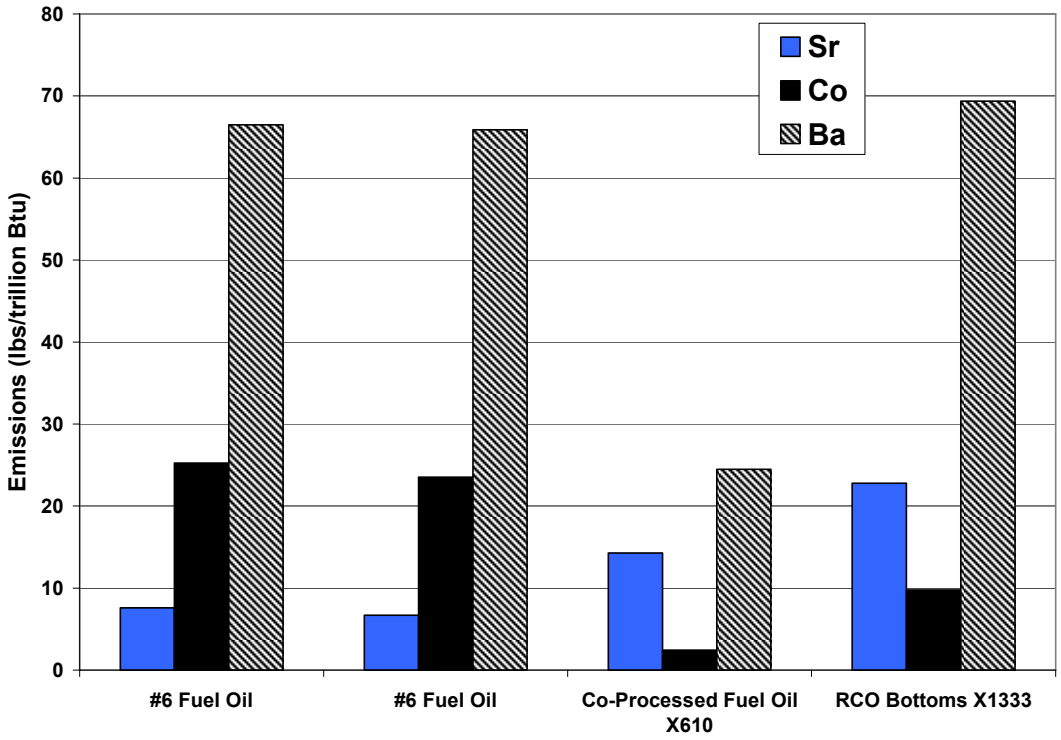

Figure 4-11. Strontium, cobalt and barium emissions for test fuels.

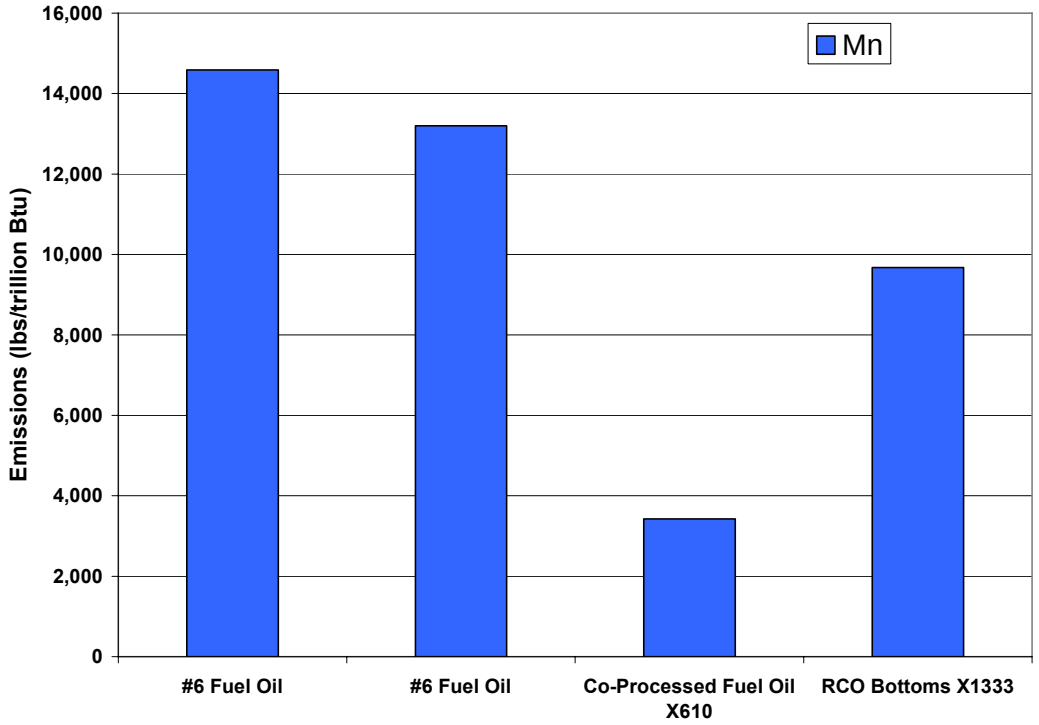

Figure 4-12. Manganese emissions for test fuels.

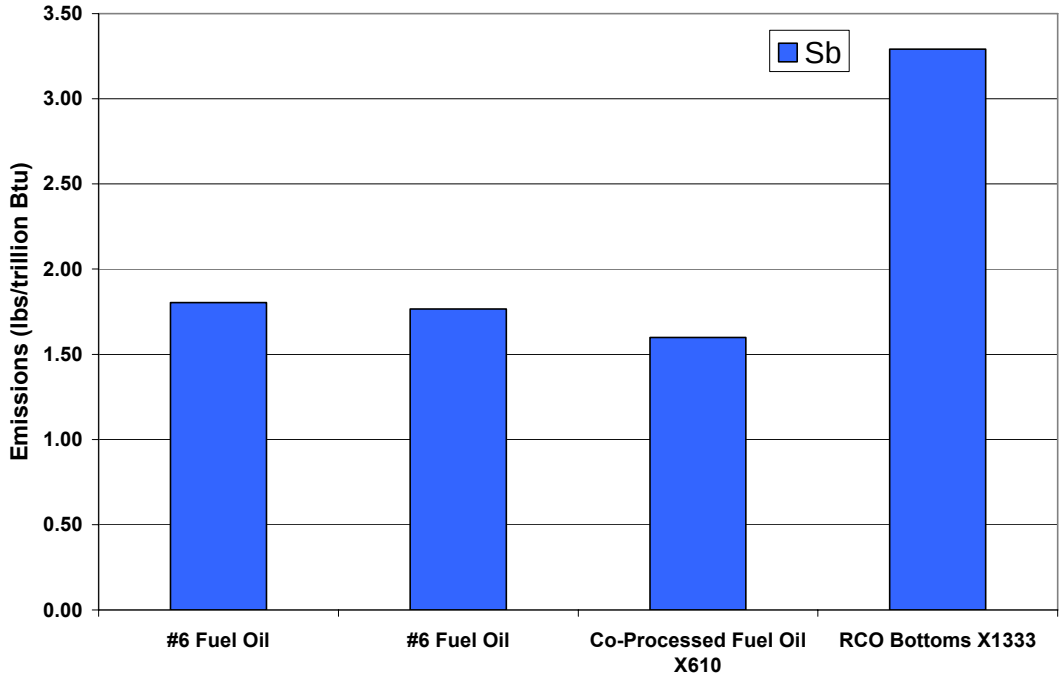

Figure 4-13. Antimony emissions for test fuels.

Overall the X611 fuel had lower emissions of those elements that are of major or moderate environmental concern than the X1333 fuel. The X1333 fuel had the highest emission levels of more elements than any of the other fuels. Fuel oil had the highest levels of emissions for Ni, V, Hg, Co, and Mn. The average As levels in the fuel oil were essentially the same as the two co-processed fuels.

No comment can be made as to why the two co-processed fuels differ so much in their emission character as no information was provided regarding the feedstocks and processes used to produce the X611 and X1333 fuels.

Task 5. Pitch and Coke Material (G. Mitchell, C. Clifford, M. Escallon, Y. Suriyapraphadilok, Ron Wasco)

Progress made over the past six months was diminished because of the loss of a certain amount of funding for the project. However, the new clean coal sample for laboratory-scale co-coking was completed, after some difficulties, and two of the twelve co-coking runs have been completed. As discussed in the 2006 Annual Report **[5-1]**, our efforts have been directed at generating sufficient coke and pitch products that may be suitable for anode-grade quality used by the aluminum industry. Also, additional laboratory-scale work has been completed on the characterization of carbon products derived from deeply hydrotreated decant oils. Areas of investigation, including tar from coal extracts and manufacture and testing of carbon artifacts has been suspended until funding issues are resolved. The following is a summary of the research that has been completed during this performance period.

Subtask 5.1 Sample Procurement and Preparation

5.1.1 Experimental

As reported in the 2006 Annual Report **[5-1]**, a new coal from A.T. Massey's Marfork Cleaning Plant in Raleigh County, WV was procured for the preparation of an ultra-clean sample for co-coking. Two sample types were collected that included a run-of-mine sample (DECS-36) and about 760 kg of a Jameson cell effluent (JCE) for the preparation of clean coal. As a reminder, the Marfork cleaning plant generates a metallurgical coking coal product and on the day of sampling (7-20-06) was processing a mixed feed from five different mines that included four different coal seams. The exact concentration of each seam was unknown, but included the Eagle seam from the River

Fork mine, the #2 Gas seam (locally called the Upper Powellton) from the White Queen Mine, the Powellton from the River Fork Mine, and the Lower Cedar Grove seam from the Marsh Fork and Slip Ridge Mines. Because of the uncertainty regarding the origin of the coal the sample will be discussed as the "**Marfork Product**". The run-of-mine sample was stage crushed, homogenized and packaged for inclusion in to the Penn State Coal Sample Bank as DECS-36. An aliquot was sent to Standard Laboratories for complete analysis, some of this data is given in **Table 5-1**.

Processing of the larger Jameson cell sample was begun August 21, 2006 using the Derrick Model K Vibrating Screen Machine our combination vibrating/wet sieving apparatus. As with the Pittsburgh seam frother effluent, the Marfork Jameson cell sample was processed through two nested 58"l x 17.5"w screens with opening of 150 µm and 45µm that were adjusted to 15º from horizontal and vibrated at 3600 cycles per minute. A high-pressure spray of water was maintained across the entire width of the screens and the >150 µm and 150 µm x 45 µm products were collected. The higher ash <45 µm material was not collected. Many problems were encountered during initial operation mostly involving screen blinding which slowed the process. A high pressure washer was used on the screens at regular intervals to improve production, but eventually this lead to the screens being damaged. Screens were replaced in October and more care was taken in cleaning the screens so that the complete Jameson cell sample was processed and dried by the end of November. About 108 kg of 100 x 325 mesh (149 x 44 µm) coal fines (18.2% of the original sample) was collected.

A series of float/sink tests were conducted on representative aliquots of the raw 100 x 325 mesh product to determine what specific gravity liquid would provide the

lowest ash yield and highest yield to meet our requirements, i.e., target was <1.0% ash and 16 kg of clean coal product. It was determined that a starting specific gravity solution of tetrachloroethlyene and toluene in the range of 1.265 – 1.270 g/mL gave the best quality. Several 100g grab samples were introduced into 1800 mL of each mixture, stirred and were left to settle overnight. The float product was skimmed from the top of the solutions and air-dried. Yield from the 1.265 g/mL float sample was about 18% with a 0.9% ash yield (dry basis), whereas the 1.270 g/mL float gave a 39% yield at 1.0% ash. The 108 kg of sized material was floated at 1.268 g/mL during December and 35.6 kg of dry product was recovered, which represents 4.9% recovery of material from the original Jameson cell effluent sample. The final product was homogenized, split into 1.3 kg aliquots and stored under argon gas in foil multilaminate bags to protect them from deterioration.

5.1.2 Results and Discussion

Subsamples were taken from one of the storage bags at random for evaluation. Owing to the amount of time that had passed between original sample collection and because of the many stages of processing and intermediate drying, there was concern that the properties of the clean coal effluent may have deteriorated. Analytical information provided in **Table 5-1**, compares the Marfork products with those of the Pittsburgh seam sample, which showed that the thermoplastic properties were largely intact and that the cleaning process had concentrated the vitrinite portion of the coal. However, we were surprised to find a relatively higher (1.2%) ash yield than anticipated. Because of this,

co-coking tests and the remaining analyses were delayed and a new series of float/sink tests were initiated.

Hundred-gram aliquots were prepared from the same bag from which analytical testing was conducted, and three tests were performed. The first attempted to determine if a lower specific gravity solution (1.260 and 1.265 g/mL) would affect an improvement in the ash yield. Using the same procedure as described above, these tests provided a float yield of 2-3%, which was insufficient for our co-coking work. A second test was performed in which the volume of media was increased and was stirred with high shear for one hour. After standing overnight the float product was skimmed and dried, but the yields from the 1.260 g/mL and 1.265 g/mL were found to be in the 2-3% range. In an attempt to increase yield, additional samples of the 1.268 g/mL float product were placed in mixtures of 1.272 g/mL and 1.277 g/ml again under high shear and allowed to equilibrate overnight. Product yields were higher in each case (18% and 21%), but the ash yield was considerably worse (1.28% and 1.26%, respectively).

Table 5-1 – Comparison of Coal Properties of Run-of-Mine and Clean Coal Samples for the Pittsburgh Seam FCE (EI-186) and Marfork JCE (EI-187)

Analytical Procedure	Pittsburgh Seam DECS-34	Pittsburgh FCE 1.280 Float EI-186	Marfork Product DECS-36	Marfork JCE 1.268 Float EI-187
Proximate Analysis: (dry)				
Fixed Carbon, %	54.3	63.4	58.3	nd
Volatile Matter, %	38.4	35.6	34.5	nd
Ash, %	7.4	1.0	7.2	1.2
Ultimate Analysis: (dry)				
Carbon, %	78.2	84.6	80.8	nd
Hydrogen, %	5.2	5.3	5.1	nd
Nitrogen, %	1.6	1.6	1.5	nd
Sulfur, %	1.6	1.1	1.0	nd
Oxygen, % (diff.)	6.0	6.4	4.4	nd
Gieseler Plastometer:				
Softening Temperature, °C	381	385	384	375
Fluid Temperature Range, °C	91	93	108	121
Maximum Fluidity (ddpm)	16,418	29,527	30,000	29,516
Temperature at Maximum, °C	435	436	448	439
Ash Mineral Composition:				
Silicon Dioxide, %	48.47	41.8	57.38	nd
Aluminum Oxide, %	23.15	27.3	25.60	nd
Ferric Oxide, %	14.84	13.6	11.36	nd
Titanium Oxide, %	1.00	nd	1.44	nd
Phosphorus Pentoxide, %	0.53	0.61	0.23	nd
Calcium Oxide, %	2.49	5.65	1.21	nd
Magnesium Oxide, %	0.76	0.74	0.93	nd
Sodium Oxide, %	0.69	0.72	0.72	nd
Potassium Oxide, %	1.87	1.64	1.87	nd
Sulfur Trioxide, %	1.95	nd	0.47	nd
Organic Petrography: (volume %)				
Total Vitrinite	82.8	96.2	73.8	91.4
Total Liptinite	4.0	1.5	5.3	3.9
Total Inertinite	13.2	2.3	20.9	4.7

The fact that ash yield information appeared to be inconsistent from the various aliquots of 1.268 g/mL product, four additional ash determinations were conducted on the analysis sample and gave dry basis ash values of 0.80%, 0.89%, 0.92% and 1.02%.

Analyses were performed using a LECO MAC 400 using the thermogravimetric determinator according to ASTM D 5142-04, which should give 0.09% repeatability for this sample set. Because our analyses were clearly outside of this repeatability limit, a test was performed to determine whether the LECO MAC 400 was functioning properly. Eighteen 1 g samples of LECO Proximate Plus Coal Standard #502-442 were analyzed to find that ash yield from all test samples fell within the repeatability limits of the ASTM standard. Immediately following this test, six additional ash determinations were performed using the analysis sample and again resulted in a broad range of values (i.e., 0.99%, 1.01%, 1.02%, 1.46%, 1.21% and 1.17%).

As the variability in dry ash data from the analysis sample appeared not to be a function of the equipment, but rather an unknown factor (inhomogeneity) in the 1.268 g/mL float product,

a decision was made to accept the product as originally produced for co-coking. However, during the course of these experiments a rather broad range of ash yields was recorded, ranging from 0.80% to 1.28%, which suggested that mineral matter in the Marfork JCE product may not be evenly distributed. Inspection of the product under an optical microscope revealed little mineral matter, some small lenses and infillings of clay minerals and micron size particles of pyrite, but none separated from the organic matrix. Consequently, we will monitor the ash yield of individual charges to the delayed coker.

In addition to the values shown in **Table 5-1**, particle size distribution and vitrinite reflectance analyses were determined for the Marfork JCE 1.268 product (EI-187). Particle size was measured using a Malvern 2600C Droplet and Particle Sizer using ethanol as a dispersant and carrier. The test showed that particles range in size

from 293 to 16 μm where 80% of the particles were between 50 and 148μm and 10% were above or below this range. A comparison of the vitrinite reflectance distributions of the run-of-mine and EI-187 clean coal product (**Figure 5-1**) shows that about 15% of the higher reflectance vitrinite particles were eliminated from the whole coal product (DECS-36) either in the cleaning plant or as a result of our processing scheme. The Pittsburgh seam FCE product (EI-186) showed no change in vitrinite distribution as a result of processing because it was derived from a single seam. Segregation of components from different seams may have occurred during processing in the Marfork product.

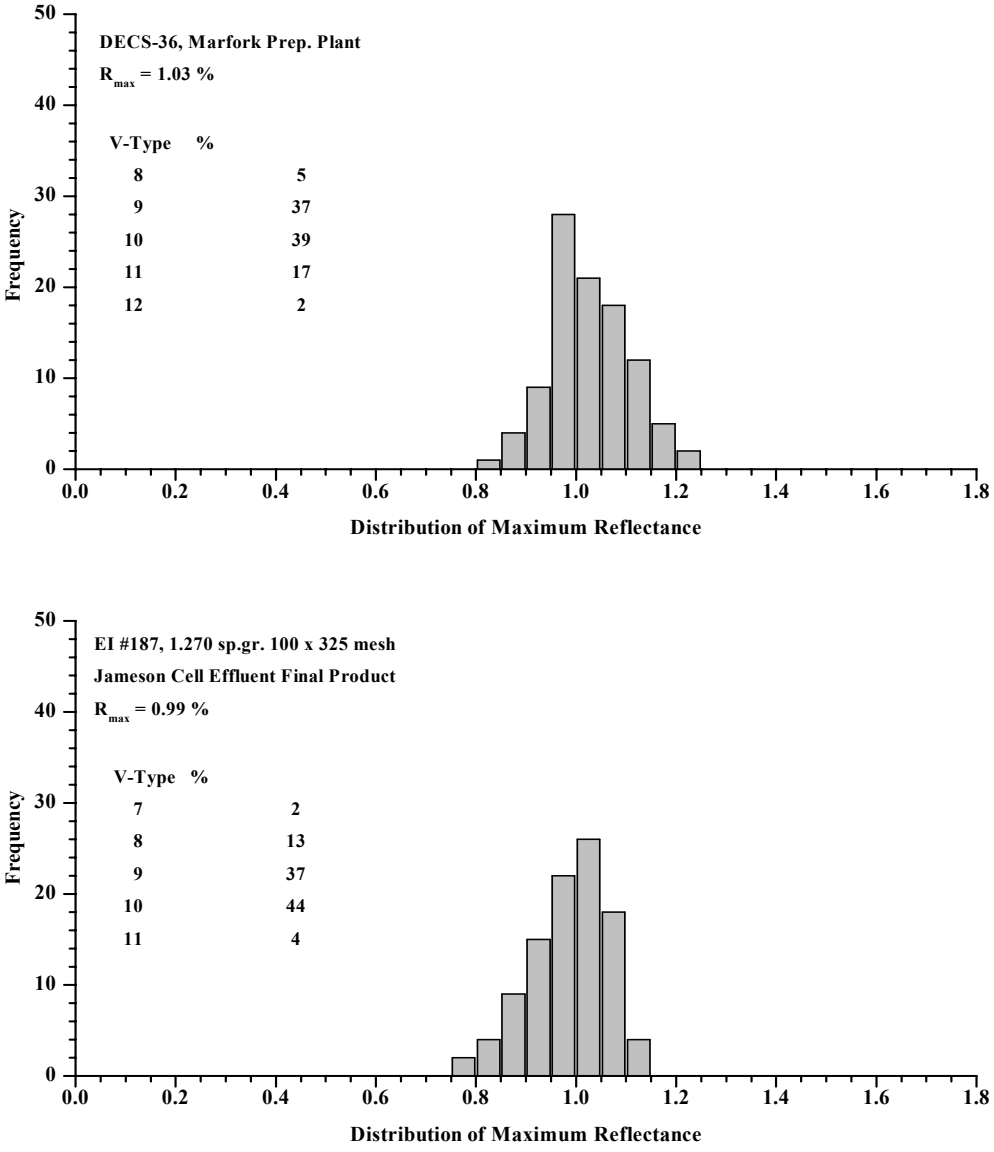

Figure 5-1 Comparison of Vitrinite Reflectance Distributions of the Marfork Run-of-Mine Product (DECS-36) with Clean Coal Jameson Cell Effluent (EI-187)

5.1.3 Conclusions

Progress of the Marfork Jameson Cell Effluent sample into a relatively clean coal product for co-coking has been completed. Although our analyses show that the ash yield of this product is higher than was wanted, the thermoplastic properties and organic

composition were acceptable. Shortly our Marfork JCE clean coal product will be sent for major and trace element analyses to determine if the iron and silica levels are sufficiently low for the coke to be considered as anode-grade coke. However, because of the inhomogeneous distribution of mineral matter (leading to ash yield variations) in the coal product, analysis of the coke composite sample after all coking runs are completed will provide the only reliable values.

Subtask 5.2 Deeply Hydrotreated Decant Oil: Characterization of Petroleum Cokes Generated from Tubing Bomb by X-Ray Diffraction and CTE

Introduction

In the last Annual Report **[5-1]** we reported on the laboratory-scale evaluation of co-cokes produced from a decant oil and a series of hydrotreated products with 20% coal under a variety of reaction conditions. It was found that the best conditions for co-coking of hydrotreated decant oil in tubing reactors was under atmospheric conditions at 18 h. When co-coking with hydrotreated decant oil in the lab scale coker, it was found that increasing level of hydrotreatment improved the quality of the liquids produced. Hydrotreatment reduced levels of heteroatoms and increased coke quality under atmospheric conditions; however, when using autogeneous conditions, the original decant oil produced the best quality products.

The former work focused on the correlation of the chemical composition of the feedstock with the coke quality which was largely defined by the distribution of optical textures. This current investigation seeks to extend our analytical range and understanding of coke quality by using other techniques such as X-ray diffraction and the coefficient of thermal expansion (CTE) by using a Thermal Mechanical Analyzer (TMA)

as a means of establishing end-use from laboratory scale testing. Although prediction of end-use may be the ultimate goal, correlation of these measured properties with results from optical microscopy will be the immediate challenge.

5.2.1 Experimental

X-ray Diffraction

Cokes (THF-insoluble fraction) generated under different conditions of pressure and derived from different decant oils (an original decant oil and its three different hydrotreated derivatives) were analyzed by X-ray diffractions. The samples were first ground to a fine powder with a mortar and pestle and then sprinkled over the surface of quartz zero background sample holder. X-ray diffraction data were acquired using a Philips MPD X-ray Diffractometer. The scan conditions were 5-60 degrees 2-Thetha, continuous scan, employing a step size of 0.02 2-theta, with a 2.5 second step time, and power setting 45kV and 40mA. To correct for instrument broadening, an external standard (silicon) was measured before each sample and then, the broadening determined from the standard was subtracted from that of the sample. Results from each coke sample were compared with a needle coke provided by GrafTech (Conoco needle coke).

The parameters, full width half maximum (FWHM), d-spacing (d_{002}), diffraction angle and Lc were calculated using Jade 7.5 software from the broadening of the Gaussian profiles for the 002 peak using the Scherrer equation and a shape factor of 0.85. An example of calculations applied to determine the Lc, which is the mean average thickness of crystallites in a sample expressed in angstroms (Å), is described in conjunction with **Figure 5-2**. The average low and high background (at positions A and B, respectively) was determined on the diffraction scan by connecting them with a

straight line. A line (CD) drawn through the apex of the peak at point G [(hkl=002 at 3.35 Å)] was constructed parallel to line AB. The full width half maximum (FWHM) of the peak was determined by measuring the vertical distance between lines CD and AB. The line EF was constructed such that it intersects the peak at half of its maximum value. The points at which EF intersects the peak are $2\theta_1$ and $2\theta_2$, respectively.

$$\Delta po = 2 (\sin \Theta_1 - \sin \Theta_2)/\lambda$$

where:
Δpo = FWHM
λ= the wavelength of the target material of the X-ray, expressed in Å,
Θ_1 = the angle at the half peak intensity ($2\theta_1/2$) width on the low side, and
Θ_2 = the angle at the half peak intensity ($2\theta_2/2$) width on the high side

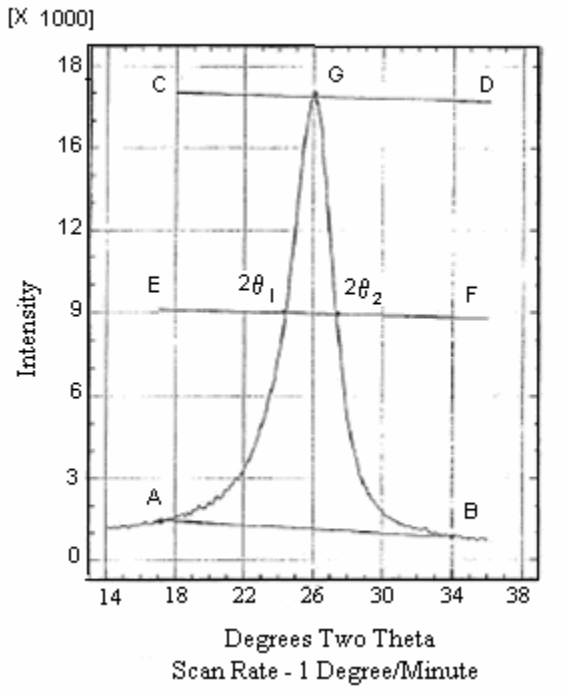

Figure 5-2: Typical Diffraction Scan of Petroleum Coke [5-2]

The above calculation was derived from the Scherrer equation:

$$\mathbf{Lc = (K\lambda)/ (\beta \cos \Theta)}$$

where:

K = an arbitrary constant that is equivalent to 0.89 for Lc

λ = wavelength of the source radiation measured in Å

β = line breadth of the pure diffraction peak measured in radians, and

Θ = angular location of the peak maximum ($2\theta/2$) measured in degrees

The mean crystallite height is determined by:

$$\mathbf{Lc = 0.85/\Delta \mathit{po}}$$

Coefficient of Thermal Expansion (CTE)

Generally, the coefficient of thermal expansion (CTE) is conducted using bulk samples of coke over 1000g. To perform CTE measurements on smaller samples like those generated from laboratory scale conditions a different instrument and procedure had to be devised. A thermal mechanical analyzer model TMA –2940 was used in this investigation that employed a temperature range from room temperature to 100°C at a

heating rate of 5°C/min. These conditions were chosen according to the conditions followed in the CTE measurements carried out by GrafTech. Although TMA has not been used to determine CTE values in coke samples, it has been widely used to determine other materials such as nanotubes **[5-3]**. In this procedure, the coke powder, previously ground using mortar and pestle, is poured into a die of 12.7 mm in diameter. To determine the amount of sample needed, the following calculation was made:

$Volume\ of\ the\ die = \pi r^2 h$; r = (12.7/2) = 6.35mm; h = 2mm, which is the desired thickness of the pellet because of height limitation in the TMA instrument. This information provides a pellet volume of V=253mm^3.

To determine the mass required, coke density was determined by measuring the density of some green cokes and was found to be in the range 1.42-1.60g/mL. The lowest density value was chosen for the purpose of calculations δ=1.42 g/cm^3= 1.42mg/mm^3

$$mass = V * \delta = 253mm^3 * 1.42 \frac{mg}{mm^3} = 359.7mg = 0.3597g$$

Therefore, standard pellets were made by adding about 0.36 g of green coke to the die.

5.2.2 Results and Discussion

X-Ray Diffraction (XRD)

In an attempt to corroborate the results found by optical microscope, some parameters were calculated by using XRD. Alvarez et al. **[5-4]** suggested that the (002) peak is associated with the ordering of the mesogen molecules constituting the mesophase. According to these authors, the decrease in the FWHM values (which implies the increase in the stack height Lc) gives an indication of an increase in the

number of molecules being ordered during the initial growth of the mesophase. They found that as the extent of carbonization increased (i.e., increasing anisotropic carbon), the d_{002} and Lc also increased.

Oya et al. **[5-5]** also tried to correlate data found from optical microscope with XRD. They found that as the concentration of isotropic carbon decreased (in other words, increasing anisotropic carbon) and as the concentration of flow domain and domains increased, the half width decreased while the diffraction angle increased.

Therefore, FWHM, d_{002}, diffraction angle and Lc have been calculated from diffraction patterns of the cokes being studied to answer three questions:

- How these parameters vary when the concentration of anisotropic carbon was about constant (close to 100%) and revealing the level of variation that may be attributed to the size of the isochromatic units alone?
- How these XRD parameters vary when the amount of anisotropic carbon is low and variable? and,
- According to the XRD parameters, can the best coke and hence, the best decant oil, be determined?

XRD parameters are shown in **Table 5-2** for cokes where the concentration of anisotropic carbon was fairly constant (varying from 95.2 to 98.8). Because the best values for optical microscope were obtained under atmospheric pressure, these were the coke selected for comparison with XRD parameters. The sample set can be divided into

Table 5-2: The relationship between optical textures and X-ray diffraction parameters when constant anisotropic carbon content. Coke obtained under open system at 18h reaction time.

		X-ray diffraction parameters			*Optical texture*				
SAMPLE ID	**fa (decant oil)**	**FWHM (°)**	**diff angle**	**Lc (Å)**	***I***	***m***	***d***	***D***	***OTI***
DO107	0.71	3.376	26.029	24	3.0	5.3	57.0	34.7	23.8
DO135	0.67	3.361	25.998	24	1.2	5.2	68.2	25.4	19.1
DO134	0.64	3.236	26.083	25	1.4	1.8	48.6	48.2	29.6
DO138	0.62	2.950	26.038	28	4.8	2.2	50.3	42.7	25.3
needle coke‡	unknown	3.180	26.016	26	0.0	0.8	57.9	40.5	---

‡ this sample is a commercial needle coke; this coke was not obtained under the conditions stated for the other cokes. I=isotropic carbon; m=mosaic; d=small domain; D=flow domains + domains.

two groups based on the aromaticity of the original decant oil, i.e., group one (fa=0.71 and fa=0.67) and group two (fa=0.64 and fa=0.62). The first group displayed higher values of FWHM, hence, lower Lc values, when compared to cokes derived from the least aromatic (fa=0.64 and fa=0.62). Observing the optical textures, because *I* and *m* were nearly constant, variation in XRD parameters may be attributable to the size of isochromatic units alone. The larger the size of isochromatic units, the lower the value of FWHM, the higher Lc and the larger the diffraction angle. Also, values derived from the lower aromaticity group compare better with the values obtained from the commercial needle coke. Based on this comparison, the best cokes appear to be those derived from the most hydrotreated or least aromatic decant oils that is DO138 according to XRD and DO134 according to optical microscope.

The XRD diffraction patterns for cokes made from the DO107 and DO138 decant oils are compared in **Figure 5-3**. Both cokes were obtained under the same conditions of temperature, pressure and reaction time; 465°C, open system and 18h, respectively.

These cokes have comparable isotropic carbon content, but different size of isochromatic units or size of coalesced mesophase, which is reflected in the OTI value; it is observed that the coke derived from the most hydrotreated decant oil (fa=0.62), which have higher concentration of domains and OTI show a sharper peak when compared to the original decant oil (fa=0.71) which have a lower concentration of domains and OTI.

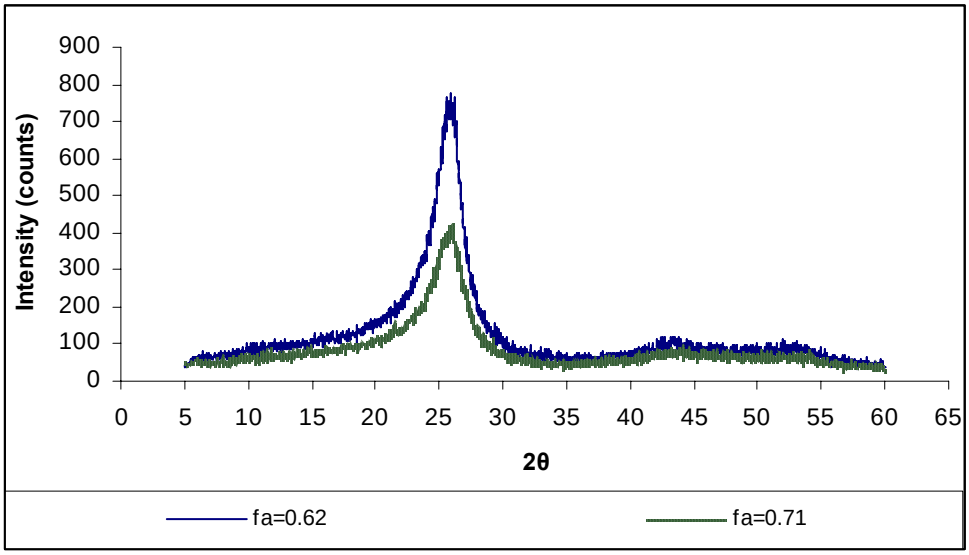

Figure 5-3: XRD comparison between the coke derived from the original feedstock (fa=0.71) and the coke derived from its most hydrotreated version (fa=0.62). Same reaction conditions, open system, 18h reaction time

Variation in XRD parameters with changing concentration of anisotropic carbon (or changing isotropic carbon) can be observed from cokes made from different reaction times as shown in **Table 5-3.** It can be observed that as the isotropic carbon decreased, the FWHM and diffraction angle decreased, while the Lc and d_{002} increased.

Table 5-3: Relationship between optical textures and X-ray diffraction parameters when varying anisotropic carbon content. Coke obtained under open system varying the reaction time.

			X-ray diffraction parameters				Optical texture			
Sample id	**fa (decant oil)**	**Reaction time (h)**	**FWHM (°)**	**Diff. angle**	**Lc (Å)**	**d_{002}**	***I***	***m***	***d***	***D***
DO107	**0.71**	6	3.701	26.063	22	3.4161	22.0	13.4	41.0	23.6
		12	3.613	26.077	23	3.4144	4.6	13.9	54.8	26.7
		18	3.376	26.029	24	3.4205	3.0	5.3	57.0	34.7
DO134	**0.64**	6	3.358	26.137	24	3.4067	10.3	18.9	51.2	19.6
		12	3.265	26.129	25	3.4077	6.1	3.7	55.5	35.1
		18	3.236	26.083	25	3.4136	1.4	1.8	48.6	48.2
DO138	**0.67**	6	3.692	26.127	22	3.4080	35.7	46.2	14.8	6.8
		12	3.600	26.119	23	3.4089	9.1	8.6	56.2	26.5
		18	2.950	26.038	28	3.4194	4.8	2.2	50.3	42.7
needle coke[‡]	**unknown**	---	3.180	26.016	26	3.4222	0.0	0.8	57.9	40.5

Figure 5-4 compares the XRD diffraction patterns of cokes derived from the most hydrotreated decant oil carbonized at 6h and 18h where the isotropic carbon content varies from 1 to 10%. A higher intensity was observed when the isotropic content was low, at 18h reaction time.

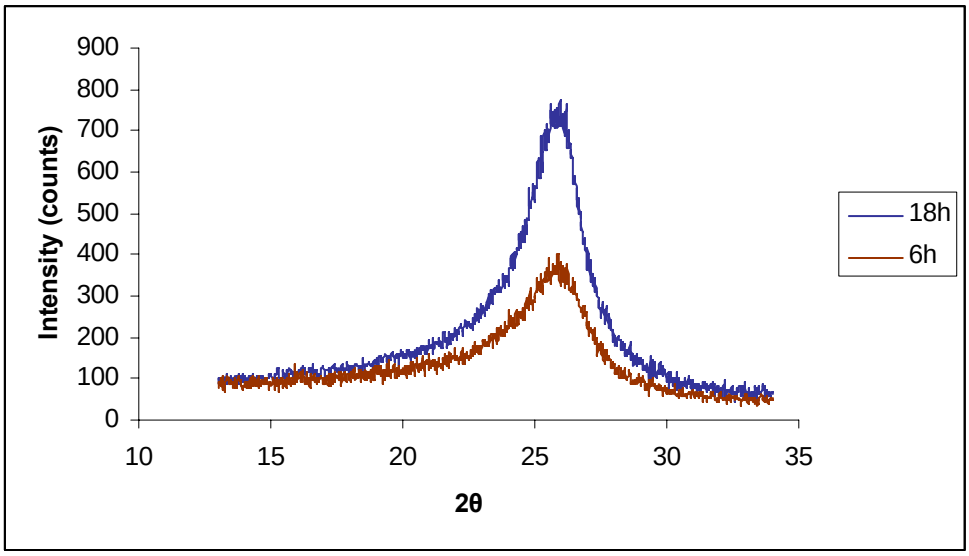

Figure 5-4: XRD comparison of the cokes derived from the most hydrotreated decant oil (fa=0.62) carbonized under different reaction time. Same conditions of temperature and pressure

According to the XRD, the best coke appeared to be derived from the most hydrotreated decant oil. Therefore, coke made from the most hydrotreated decant oil (fa=0.62) was compared with the commercial needle coke provided by GrafTech. **Figure 5-5** shows that there was no significant difference between these two cokes; hence, it is expected that the coke derived from the most hydrotreated feedstock under 18h and open system is of better quality.

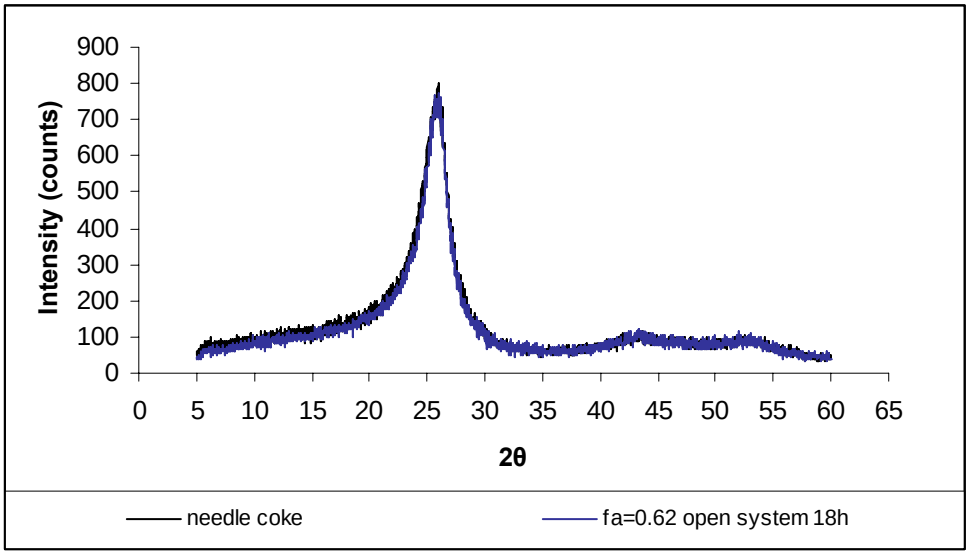

Figure 5-5: XRD comparison between needle coke and coke derived from the most hydrotreated decant oil (fa=0.62)

Two general trends have been observed with the cokes obtained under atmospheric pressure when analyzed using the X-ray diffraction and optical microscope:

- The intensity in the XRD increased as the size of isochromatic units grew larger.
- The intensity in the XRD increased as a function of carbonization reaction time (lower content of isotropic carbon).
- The FWHM decreased and Lc increased as the size of isochromatic units grew larger.
- The FWHM decreased and Lc increased as the reaction time was increased (lower content of isotropic carbon)

Table 5-4 shows the main optical textures and the X-ray diffraction parameters of the cokes generated at 18h under autogenous pressure. Comparing the parameters obtained under these two pressures (**Tables 5-2** and **5-4)**, the main difference appears to

be the concentration of isotropic carbon texture and domain. Isotropic carbon texture was higher for the cokes formed under autogenous pressure whereas domain content was higher for the cokes formed under atmospheric pressure. The difference in domain content was accentuated as the aromaticity of the decant oil decreased.

Table 5-4: Optical textures and X-ray diffraction parameters of the cokes generated at 18h under autogenous pressure

SAMPLE ID	fa (decant oil)	FWHM (°)	diff angle	d_{002}	Lc (Å)	*I*	*D*	*OTI*
DO107	0.71	3.281	26.183	3.4008	25	14.4	33.4	23.8
DO135	0.67	3.362	26.001	3.4242	24	29.1	17.3	19.1
DO134	0.64	3.342	26.170	3.4024	25	28.0	20.6	29.6
DO138	0.62	3.122	26.191	3.3998	26	27.5	19.8	25.3

Figure 5.6 shows the intensity comparison between the cokes generated under the same conditions of reaction time, but different pressure. One might expect that the X-ray peak intensities of the cokes formed under autogenous pressure to be lower when compared with their counterparts formed under atmospheric pressure, because they possess greater amounts of isotropic carbon and lower domain content. However, coke derived from the most aromatic feedstocks (fa=0.71 and 0.67) exhibited intensities that were comparable (autogenous/atmospheric) and the FWHM was smaller or comparable. Although the intensity and Lc were similar, cokes from these feedstocks showed a shift in diffraction angle to higher 2θ and hence a lower d_{002}.

The apparent contradiction between XRD and optical microscope may be explained by the existence of or possible contribution of mesophase below the detection limits of the optical microscope. That is to say the isotropic texture determined in the cokes generated under the closed system at 18h and the isotropic texture determined in the cokes generated under open system at 6h are different. The first might correspond to

submicron mesophase while the second might correspond to pre-mesogen units which have not grown enough to form mesophase, because of a short carbonization time. This hypothesis is supported by the work of Santamaria-Ramirez et al. **[5-6]**, who found that high pressure (10 atm) favored the coalescence of mesophase, however, the spheres did not grow beyond a certain size, suggesting that the coalescence rate exceeded the spheres growth rate. On the other hand, the cokes derived from decant oils with lower fractional aromaticity (fa) followed the expected patterns of intensity and FWHM, being more accentuated for the coke derived from the least aromatic decant oil (fa = 0.62). Consequently, the isotropic carbon might contain mostly pre-mesogen units which have not grown enough to form mesophase.

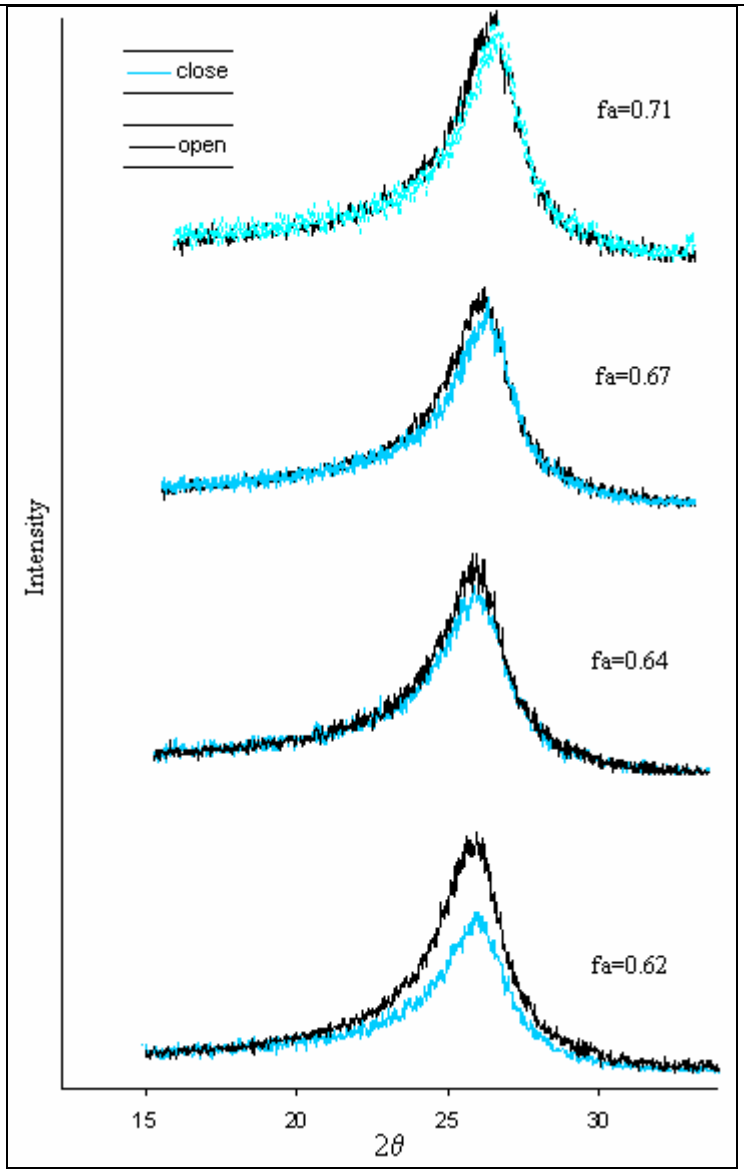

Figure 5-6: Intensities comparison at 002 peak for the cokes derived from the different feedstocks, carbonized under 18h, but different pressures (atmospheric and autogenous)

Thermal Mechanical Analysis (TMA)

In this part of the investigation TMA is used to determine a value for the coefficient of thermal expansion (CTE), with the full recognition that the CTE value derived cannot be compared with CTE values reported by the carbon industry **[5-7]**. In the industrial technique, CTE values are derived from artifacts where coke and pitch are mixed, cooled and extruded, then the mixture is baked, pitch impregnated, and graphitized. The extrusion allows the coke grains to be oriented and the CTE is measured along the axial plane of oriented grains. Therefore, in order to distinguish the CTE from industry and the CTE obtained from the TMA, the last will be identified as "*cte*". The temperature range of the CTE reported is in between room temperature and 100°C.

The *cte* value calculated from TMA is carried out on green cokes which have not been extruded and therefore the grains are oriented randomly. The *cte* was calculated for the range at which the slope is constant, or from 60-100°C in accordance with the ASTM standard **[5-8]**:

L_0= original length of specimen at temperature T_0
L_1=length of specimen at temperature L_1
L_2=length of specimen at temperature L_2
ΔL= change in length of specimen between any two temperatures T_1
$(\Delta L/L_0)$= expansion
T_0=temperature at which length is L_0, °C
T_1, T_2= two temperatures at which measurements are made, °C

Table 5-5 shows an example of the calculation for a commercial green needle coke.

Table 5-5: Calculation example to determine the expansion $\Delta L/L_0$

Instrument	2940 TMA					
Sample	needle coke 3				Gas	Air 100mL/min
Size	2.6925	mm	2692.5 µm			
				ΔL	ΔL	ΔL/L0
T_0	27.70000	L_0 (µm)	2692.50000			
T_1	60.08700	L_1(µm)	2698.54321	L_1-L_0	6.04321	0.002244
T_2	60.58214	L_2(µm)	2698.77212	L_2-L_0	6.27212	0.002329

Figure 5-7 shows the determination of the coefficient of thermal expansion which is calculated graphically from a tangential segment of the $\Delta L/L_0$ curve. Using the complete curve the coefficient is determined from a segment that provides a constant slope in the range 60-100°C. In this example, the slope corresponds to a *cte* value of 2.69E-04/°C with an experimental error of ±0.25E-3. The needle coke was run by triplicate in order to obtain the experimental error.

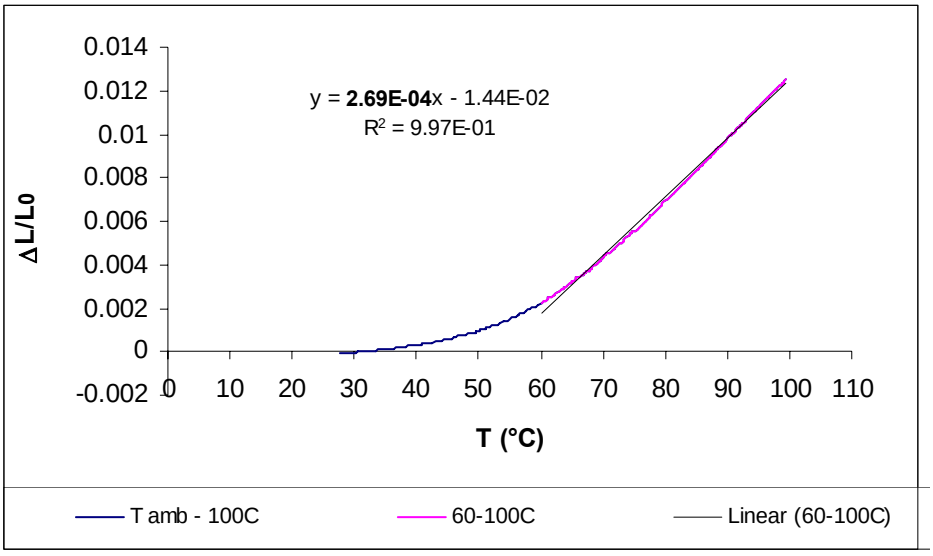

Figure 5-7: Calculation of the coefficient of thermal expansion (*cte*)

Because *cte* values derived from TMA of non-extruded green cokes have never been attempted before, its significance as an analytical procedure needs to be determined. Generally, industrial cokes of good quality possess a lower CTE. However, *cte* derived from TMA of green coke appeared to show the opposite trend as seen in **Table 5-6**. Since the coke particles are not oriented by extrusion, *cte* might correspond to an average smaller value.

Table 5-6 compares the determined *cte* value of needle coke with those obtained from hydrogenated decant oil after 18h under atmospheric pressure. The highest *cte* value was determined for the needle coke and showed a general decrease with increasing level of hydrogenation for the laboratory cokes, without regard to the amount of isotropic carbon present or degree of OTI.

Table 5-7 shows the *cte* of cokes generated under autogenous pressure for 18h. These cokes have significantly more isotropic carbon, but still have fairly high *cte* values; higher perhaps than should be measured considering that their expansion should be nearly isotropic. This finding might suggest that the degree of anisotropy was comparable between the cokes generated under autogenous and atmospheric pressure and may lend support to the presence of submicron mesophase in the isotropic carbon generated under autogenous pressure.

Table 5-6: Optical textures and *cte* of the cokes generated at 18h under atmospheric pressure

SAMPLE ID	fa (decant oil)	*cte E-04*	*I*	*m*	*d*	*D*	*OTI*
needle coke‡	unknown	2.86	0.0	0.8	57.9	40.5	---
DO107	0.71	1.93	3.0	5.3	57.0	34.7	23.8
DO135	0.67	1.79	1.2	5.2	68.2	25.4	19.1
DO134	0.64	1.69	1.4	1.8	48.6	48.2	29.6
DO138	0.62	1.44	4.8	2.2	50.3	42.7	25.3

Table 5-7: Optical textures and *cte* of the cokes generated at 18h under autogenous pressure

SAMPLE ID	fa (decant oil)	*cte 10E-04*	*I*	*D*	*OTI*
DO107	0.71	1.78	14.4	33.4	23.8
DO135	0.67	1.02	29.1	17.3	19.1
DO134	0.64	1.59	28.0	20.6	29.6
DO138	0.62	1.34	27.5	19.8	25.3

Cokes made from 6h of reaction time under atmospheric pressure generated significant isotropic carbon and, as shown in **Table 5-8,** exhibited the lowest *cte* values. Even those cokes having a lower amount of isotropic carbon have lower *cte* values, which may be indicative of the degree of coalescence and chemical condensation of the mesophase that did form after 6h of reaction.

As measured by TMA, *cte* values of green coke tended to decrease with increasing isotropic carbon content, although there was a good deal of scatter. However, the cokes generated under the best conditions (18h under atmospheric pressure) tended to form a tight group. By increasing the pressure (autogenous runs) *cte* values for most of the cokes were comparable with those produced under atmospheric pressure even though the isotropic carbon content was high. This may suggest that a submicron mesophase

could be uniformly distributed within the isotropic fraction as was suggested by X-ray evaluation. When reaction time was reduced significantly, *cte* was lowest, and may suggest that mesogen molecules have yet to develop in the isotropic phase. In comparing the different decant oils of all groups, those having the highest aromaticity generated the highest *cte* values, except DO135 of the autogenous run.

Table 5-8: Optical textures and *cte* of the cokes generated at 18h and 6h under atmospheric pressure

SAMPLE ID	fa (decant oil)	*CTE 10E-04 (18h)*	*CTE 10E-04 (6h)*	*I (18h)*	*m (18)*	*I (6)*	*m (6)*
DO107	0.71	1.93	1.28	3.0	5.3	22.0	13.4
DO135	0.67	1.79	1.11	1.2	1.8	10.3	18.9
DO134	0.64	1.69	0.87	1.4	5.2	19.3	16.8
DO138	0.62	1.44	0.86	4.8	2.2	35.7	42.6

5.2.3 Conclusions

1. Based on optical microscope and XRD, the best cokes appear to be those generated from the most hydrotreated decant oils (fa=0.64 and 0.62).
2. TMA of green cokes showed values of *cte* were lower for our laboratory scale cokes than for a commercial green needle coke. Also, that there was an overall decrease in *cte* values with increasing isotropic carbon content and *cte* values were higher for the feedstocks having greater aromaticity depending upon reaction conditions.
3. Information given by TMA shows that the *cte* of cokes generated from the most hydrotreated versions were inferior to cokes derived from the original (0.71) and mildly hydrotreated decant oils (fa=0.67 and 0.64).

Subtask 5.3 Co-Coking of Coal and Heavy Petroleum Stream:

5.3.1 Co-coking Runs Using the Marfork JCE 1.268 Coal Product (EI-187)

Introduction

A new series of consecutive delayed coker runs were begun during this report period using the same decant oil (EI-107) used for our earlier run using the cleaned Pittsburgh seam frother cell effluent and the newly cleaned Marfork Jameson cell effluent discussed previously in this report. The objective of this work is to generate sufficient material for coke and liquids evaluation which will require 12 consecutive runs to generate. Runs of 20 wt.% coal and 80 wt.% decant oil were begun in the Penn State laboratory-scale delayed coker on March 20, 2007 (run #84) and will proceed for the next eleven weeks. The following describes the progress that has been made during this report period.

5.3.1.1 Experimental

Materials

A commercial petroleum-based decant oil (EI-107) obtained from United Refining Corporation of the type used for making premium needle coke was used in this study. Ash and sulfur yields of the original decant oil (EI-107) were found to be 0.22% and 2.99%, respectively.

The coal used in this study (EI-187) was a deeply cleaned blend of coals obtained from the fines circuit of the Marfork Cleaning Plant and is of high volatile A bituminous rank. Proximate and ultimate analyses, fluidity and organic petrography results for these feedstocks are shown in **Table 5-9**.

Table 5-9 Proximate and Ultimate Analysis of the Feeds Used in this Study

	Coal	Decant Oil
Proximate analysis [a]	EI-187	EI-107
Ash (%)	1.2	0.22
Volatile matter (%)	-	-
Fixed carbon (%)	-	-
Ultimate analysis [a]		
Carbon (%)	-	89.59
Hydrogen (%)	-	7.32
Nitrogen (%)	-	0.22
Sulfur (%)	-	2.99
Oxygen (by diff.) (%)	-	
Fluidity Data [b]		
Fluid Temperature Range (°C)	121	na
Maximum Fluidity (ddpm)	29,516	na
Softening Temperature (°C)	375	na
Organic Petrography, vol%		
Total Vitrinite (vol. %)	91.4	na
Total Liptinite (vol. %)	3.9	na
Total Inertinite (vol. %)	4.7	na

[a] values reported on a dry basis [b] Determined using a Gieseler plastometer

Apparatus

The pilot-scale delayed coker at The Energy Institute is used to provide reliable continuous delayed coking for 6 hours to provide acceptable quantities of liquid and coke products for evaluation. The unit is capable of operating under most delayed coking process conditions. The system pressure, temperature and flow rates are monitored by a number of computer-controlled devices, and data from these devices is recorded throughout the run. The slurry feed rate in these experiments was continuous and constant and was measured gravimetrically with time. Some of our earlier results from this PSLC were published recently **[5-9]** and previous work has shown good reproducibility in terms of product distribution of delayed coker and vacuum fractionation distillates **[5-10].**

As shown in **Figure 5-8**, the apparatus consisted of a stirred and heated feed tank that was maintained at 77 ºC during the current experimental program. This was connected to a 0.635 cm (1/4 in.) o.d. line that carried feedstocks from the feed pump. Feed materials were pumped to the superpreheater (part 4 in **Figure 5-8**) through a 0.953 cm (3/8 in.) o.d. line that was heated to 120 ºC using heating tape. The preheater (part 5 in **Figure 5-8**) consists of a 2.5 cm o.d. x 51 cm stainless steel tube fitted directly to the bottom of the reactor. The temperature gradient through this 51 cm preheater was on the order of 200 °C, with an outlet temperature of 420-460 °C. The pilot-scale laboratory coker (PSLC) consisted of a 7.5 cm i.d. x 102.5 cm cylindrical reactor unit (coker drum) having an internal volume of approximately 4.5 L. Vaporous materials (liquid and gaseous products) are vented at the top of the reactor drum and collected for evaluation and analysis.

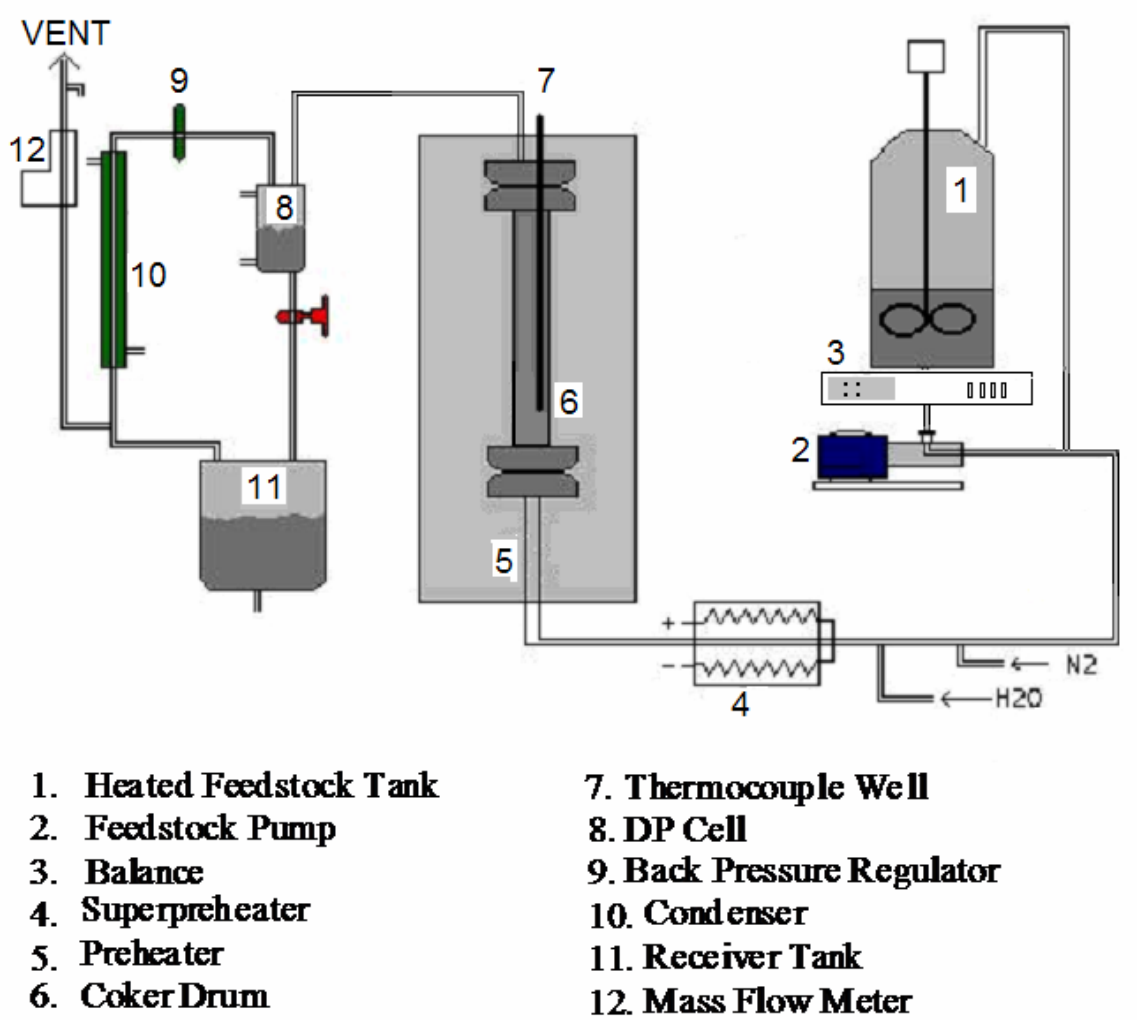

Figure 5-8 A schematic of pilot-scale delayed coker (5-9)

Reaction Procedures

Table 5-10 provides the desired run conditions for the Marfork co-coke experiments by reporting the average conditions employed during the preparation of the Pittsburgh seam co-coke. The Table also shows the conditions achieved during processing of the first two Marfork runs (#84 and #85). In general, in the co-coking experiments, a slurry of coal and decant oil was fed into the coker where the volatile components of the coal and oil were vaporized and subsequently condensed. The vented reactor system allowed for flash vaporization of the volatiles and subsequent

carbonization of the heavy petroleum fraction and coal. In the delayed coking process, feedstock is pumped (16.7 g/min) into the coker drum where reactions between the coke and the liquid lead to the formation of light desirable liquids and carbonaceous solid.

Table 5-10 - Run Conditions used for Pittsburgh Seam FCE (EI-186) Compared with Marfork Clean Coal Product (EI-187)

Conditions	Coker Runs #50 - #61 Pittsburgh FCE EI-186			Marfork Runs EI-187	
	Average	Range	Condition Desired	#84	#85
Feed Stock, hrs	5.86	5.6 – 6.0	6.0	6.0	6.0
Steam Stripping	0	0	0	0	0
Hold at 500°C, hrs	24	-	24	24	24
Feed Rate, g/min	16.76	16.7 – 16.8	16.8	16.7	16.7
Preheater inlet, °C	120.9	119 – 124	120	118	115
Preheater Outlet, °C	438.7	432 – 443	440	432	426
Coke Drum Inlet, °C	499.2	483 – 512	500	504	509
Coke Drum Low/Mid, °C	496.3	487 – 505	500	486	502
Coke Drum Top, °C	478.8	468 – 499	475	475	473
Material Fed, g	5750	5206 – 6054	6000	5938	5898
Products:					
% Coke	27.42	-	-	26.29	27.20
% Liquid Products	62.82	-	-	70.24	70.14
% Gas (diff.)	9.76	-	-	3.47	2.66

The feed was initially charged to a feedstock vessel that was heated to 77 ºC and continuously mixed throughout the co-coking experiment to achieve and maintain homogeneity. The vessel was placed on a balance for monitoring the feeding rate. The feed was incrementally heated along the feed line to the preheater. Feed was heated in the lines prior to the preheater to about ~120 °C and, then, to about ~440 °C in the preheater before being introduced in to the vertical coker drum. Thermocouples attached at different positions along the coke drum were used to measure and to control the temperature during the experiment. Light hydrocarbons vapor exited from the top of coker drum and pass through a series of condensers. Gases were passed through a flow regulator and were vented.

In the experiments reported here, the liquid products from the reaction were passed through a series of condensers and valves that facilitated their isolation. At the conclusion of the experiment, the mass of the liquid condensate and the carbonaceous solid removed from the coke drum and weighed; gas was determined by difference.

5.3.1.2 Results and Discussion

As shown in **Table 5-10**, operating conditions for the first two Marfork runs fall within the range of those of the earlier Pittsburgh FCE runs. Also, product yield is included in the Table which shows that considerable more liquid products were produced from the Marfork co-coking than the Pittsburgh apparently at the expense of gas generation which is lower. The Marfork product is slightly higher in rank and lower in volatile matter than the Pittsburgh coal, and therefore one might expect a lower yield of liquids. Consequently, it the chemical nature of these liquids will be of great interest, particularly those in the jet fuel range. This work will be started when the consecutive runs are completed and when the funding issues for this project are resolved.

Because of the apparent inhomogeneous distribution of mineral matter in the Marfork JCE 1.268 g/mL float product, ash yield was determined on coal remaining after each co-coking run. **Table 5-11** provides the raw data on each of the runs completed so far and shows that most of the

Table 5-11 Ash Yield Determinations on Marfork JCE Product (EI-187) for Each Co-coker Run

Run #	#84	#85	#86
Date	3-20-07	3-27-07	4-4-07
Replicate % Ash, dry basis	0.71, 0.61, 1.01, 0.95	0.60, 1.02	1.06, 0.79, 1.03, 1.04
Average %Ash Yield	**0.82**	**0.81**	**0.98**
Standard Deviation	0.19	0.30	0.13

determinations were below our 1.0% ash threshold, even though there was a great deal of variation. It can only be hoped that these values are representative of the coal that was fed to the delayed coker.

Subtask 5.3.2 Production of Coal Tar from Coal Extraction

The investigation of coal tar from coal extraction techniques has been moved to another project until funding issues with the project are resolved.

Subtask 5.4 Analysis of Co-Coke

There was only minor activity in the area of analyzing co-coke during this reporting period, because our efforts were directed at acquiring and preparing a new coal for additional co-coking experiments. However, one co-coking run using the Pittsburgh FCE clean coal product (EI-186) was performed in order to determine the product yield, coke quality and operating efficiency using a 30 wt.% blend with the EI-107 decant oil. Only one other test had been performed using this higher concentration of coal, but the coal used turned out to be a blend of different rank coals, was fairly high in ash yield and had high organic inerts. Because of operating difficulties the run was terminated early and a 30% concentration of coal was avoided in subsequent work. The obvious

advantage of using a greater amount of coal would be to increase coal liquids boiling in the jet fuel range. Preliminary results and their implications are discussed.

5.4.1 Experimental

Table 5-12 shows the base properties of two coals that were tested at 30 Wt.% concentration in the Penn State delayed coker. As seen the Canterberry Lower Kittanning seam coal was relatively higher in rank and ash yield and had been an early candidate for deep cleaning and consecutive co-coking runs. However, during the course of evaluation it was found that the coal product was a blend of two coals of distinctly different rank, i.e., high volatile A and medium volatile bituminous. Even though the thermoplastic properties of the test sample was within our experimental range, potential variable contributions of medium volatile coal fed to the cleaning plant and the potential that medium volatile coal could be concentrated by our cleaning technique, resulted in this product being rejected as a potential for co-coke. During the course of evaluating the Canterberry product, several co-coking runs were conducted that included using 30 wt.% coal. Because the coal was rejected from our experimental plan for the reasons outlined above, no further work was performed on the delayed coke liquid or solid products. During this reporting period, increasing the weight percentage of coal to 30% was revisited using the Pittsburgh FCE clean coal product.

Table 5-12 – Comparison of Properties of the Pittsburgh Seam FCE (EI-186) and Canterberry Lower Kittanning Coals Used in Co-coking Runs Using 30 Wt. % Coal

Analytical Procedure	Pittsburgh FCE 1.280 Float EI-186	Canterberry Lower Kittanning*
Proximate Analysis: (dry)		
Fixed Carbon, %	63.4	68.5
Volatile Matter, %	35.6	31.5
Ash, %	1.0	10.0
Ultimate Analysis: (dry)		
Carbon, %	84.6	87.2
Hydrogen, %	5.3	6.0
Nitrogen, %	1.6	1.5
Sulfur, %	1.1	1.9
Oxygen, % (diff.)	6.4	3.3
Gieseler Plastometer:		
Softening Temperature, °C	385	381
Fluid Temperature Range, °C	93	110
Maximum Fluidity (ddpm)	29,527	27,469
Temperature at Maximum, °C	436	449
Organic Petrography: (volume %)		
Total Vitrinite	96.2	81.7
Total Liptinite	1.5	2.4
Total Inertinite	2.3	15.9

* Vitrinite reflectance analysis revealed this coal sample to be composed of two distinct coals; 73% hvAb and 27% mvb.

5.4.2 Results and Discussion

Run conditions and product yield comparing the Canterberry and Pittsburgh seam products are giving in **Table 5-13**. As shown, operating conditions for three of the runs were similar, but the feed rate used for run #83 was much higher, owing to gearing problems with the newly repaired feed pump. Also, the standard soak time for coke held in the reactor at 500°C had been increased from 6h to 24h. Nevertheless, for both coals the overall liquids yields were lower and coke yields higher when 30 wt.% coal was used compared with 20 wt% concentration.

Table 5-13 – Run Conditions used for Pittsburgh Seam FCE (EI-186) and Canterberry Lower Kittanning Coals at 30 wt.% Co-coking

Conditions	Canterberry Lower Kittanning		Pittsburgh FCE EI-186	
Run #	**35**	**36**	**50-61**	**83**
Wt. % Coal	**20**	**30**	**20**	**30**
Feed Stock, hrs	5.5	5.5	5.86	3.75
Steam Stripping	0	0	0	0
Hold at 500°C, hrs	6	6	24	24
Feed Rate, g/min	16.7	16.7	16.76	26.6
Preheater inlet, °C	108	109	120.9	116
Preheater Outlet, °C	443	436	438.7	425
Coke Drum Inlet, °C	470	468	499.2	466
Coke Drum Low/Mid, °C	471	468	496.3	491
Coke Drum Top, °C	470	474	478.8	474
Material Fed, g	4931	4676	5750	5558
Products:				
% Coke	30.2	37.5	27.42	33.6
% Liquid Products	60.4	51.8	62.82	58.4
% Gas (diff.)	9.4	10.7	9.76	8.0

Liquid products obtained for these runs have yet to be evaluated, but some of the coke materials have been evaluated by optical microscopy and these results are provided in **Tables 5-14** and **5-15**. What prompted this evaluation was the observation that the new 30% Pittsburgh FCE run generated shot coke. As seen in the photograph below (**Figure 5-9**), the cross-sectional area of the coke artifact about 14 cm above the coker inlet shows the aggregate of rounded (1-3mm diameter) particles filling the interior and surrounded by a competent rim of coke that formed against the reactor wall. As has been discussed in previous work, a higher feed rate tended to generate a minor amount of rounded particles similar to shot coke, this was the first observation of significant production. Although difficult to know exactly, it appears that a

Figure 5-9: Cross-sectional View of Coke Artifact from Run #83 Using 30 wt.% Pittsburgh FCE Clean Coal Product Showing the Development of Shot Coke

combination of higher feed rate and coal concentration may be at fault. This led us to investigate the nature of the coke produced from 30% run using the Canterberry coal. That coke artifact, generated at the lower feed rate also exhibited shot coke in a manner similar to the Pittsburgh run (#83).

Comparison of the distribution of carbon textures in these cokes are given in **Tables 5-14 and 5-15** to show that at least for the Pittsburgh seam coal, the amount of mosaic carbon has increased significantly apparently at the expense of the small domain texture. Furthermore, a marked increase was observed in the amount of carbon textures that were derived from coal. For both coals textures derived from vitrinite were larger (or were enhanced) than would have been produced out of the presence of decant oil. In comparison, the amount of coal-derived material observed in the Canterberry coke far

exceeds that found in the Pittsburgh specimen, which might suggest a lower inter-reactivity of coal and decant oil.

Table 5-14 – Petrographic Analysis of Carbon Textures in Composite of Twelve Coker Runs of Pittsburgh FCE (Green and Calcined) at 20% Compared with 30% Runs of Pittsburgh (#83) and Canterberry (#36) by Size and Origin, Vol. %

Sample Id. & Run #	Vitrinite-derived		Inert-derived	Isotropic Vitrinite	Min. Matter	Isotropic Pet.-derived	Mosaic, <10µm	Small Domain, 10-60µm	Domain >60µm	Flow Domain, >60µm L, <10µm W
	En-hanced	Non-enhanced								
Green	10.7	1.4	0.8	0.0	0.3	0.3	29.4	52.4	3.5	1.2
Calcined	10.4	2.8	1.0	0.0	0.0	0.2	37.4	43.9	2.0	2.3
#83, 30%	37.0	2.9	1.2	0.0	0.2	0.2	42.2	16.1	0.0	0.2
#36, 20%	nd	nd	nd	nd	nd	nd	nd	nd	nd	nd
#36, 30%	53.1	8.2	12.3	0.0	0.7	0.0	21.2	4.5	0.0	0.0

Table 5-15 – Proportion of Textures Derived from Coal and Decant Oil Compared with the Normalized Concentration of Decant Oil Textures in 20% Composite and 30%, Vol. %

Sample Id. & Run #	% Coal-derived	% Petroleum-derived	Isotropic Petroleum-derived	Mosaic, <10µm	Small Domain, 10-60µm	Domain >60µm	Flow Domain, >60µm L, <10µm W
Green	13.2	86.8	0.3	33.9	60.4	4.0	1.4
Calcined	14.2	85.8	0.2	43.6	51.2	2.3	2.7
#83, 30%	41.3	58.7	0.3	71.9	27.5	0.0	0.3
#36, 20%	nd	nd	nd	nd	nd	nd	nd
#36, 30%	74.3	25.7	0.0	82.5	17.5	0.0	0.0

5.4.3 Conclusions

From this investigation it appears that the co-coking of several coals at 30 wt. % concentration decreased the overall liquids yield and increased the amount of coke produced. Although the operating conditions were different (higher feed rate) which might have contributed to the formation of shot coke, the quality of the coke was much diminished as well. Shot coke is a low value carbon that is generally sold or used as a combustion product. This series of tests will be repeated for the Pittsburgh seam when

the Marfork clean coal product can be included in the study under similar coker operating conditions.

Subtask 5.5 Analysis of Co-Coking Binder Pitch

As discussed in the Semi-Annual Report 2006 **[5-1]** the liquid product from the co-coking Run #50 was further distilled to yield a pitch material, namely CCP-2. It was reported that the mass distribution of CCP-2 was too light to be used as a binder for aluminum anode production. Two methods of heat treatment were used to produce more condensed aromatic-fused-ring compounds: heat soaking and oxidation. It was aimed to prepare new co-coking pitch samples to get a mass distribution closer to that of a standard coal tar pitch (SCTP) and petroleum pitch (PP).

5.5.1 Experimental

Materials

The material for generating co-coking pitch was obtained by using a laboratory-scale vacuum distillation apparatus. The distillates from co-coking were placed in a round-bottom flask, which was connected to a riser and condenser assembly. The temperature of the boiling liquid was measured by a thermocouple. A cold trap immersed in liquid nitrogen was used to collect any light product not condensed in the collection flask. After the pressure was reduced to 5 mmHg using a rotary-vane vacuum pump, the heating mantle was switched on. The temperature was increased and the distillates were collected until the desired cut point temperature reached. A 360°C cut point was chosen to obtain a final product of 360°C-FBP (Final Boling Point) remaining in the round-bottom flask. From GC/MS analysis (the spectra not shown in this report),

this fraction did not contain any aliphatic compound and should be a good starting material to obtain good binder pitch samples.

There are two main methods of producing heavy compounds from petroleum fractions: heat soaking and oxidation (or polymerization with oxygen) **[5-11]**. These methods combining with distillation and solvent extraction have been widely used to produce petroleum pitch **[5-11]**. The 360°C-FBP fraction of co-coking liquid Run #50 was heat soaked and oxidized using the conditions described in **Table 5-16**. Thirty grams of the sample were placed in a 120 mL reactor. UHP N_2 and O_2 were used to purge and pressurize the sample in the heat soaking and oxidation experiments, respectively. A pressure gauge was attached to each reactor to monitor the pressure before, during and after the reactions. The reactor was immersed in a fluidized, temperature controlled sand bath. After the reaction, the reactor was quenched in water. Noted that the term "heat-treated" has been used generally to describe both the heat-soaked and the oxidized experiments.

Table 5-16: Heat treatment conditions of co-coking liquid distillate Run#50.

Sample #	Type of Gas	Heat Soaking Conditions		
		Temp. (°C)	Time (min)	P_{ini} (psig)
HT111, HT112	UHP N_2	460	75	0
HT113, HT114	UHP N_2	460	45	0
OX107-OX110	O_2	250	2	300

The heat-soaked (a mixture of HT111-HT114) and oxidized (a mixture of OX107-OX110) composites were mixed and distilled to remove light compounds using aforementioned vacuum distillation unit. The final cut point for pitch was ~350°C-FBP. Both heat-treated pitches were then mixed with SCTP-2 at 30% by weight. The mixing

was done at 100°C for 15 hours under nitrogen atmosphere. Final blends of the heat-soaked and oxidized pitch are referred to as "heat-soaked co-coking pitch" (HTCCP) and "oxidized co-coking pitch" (OXCCP), respectively.

Characterization of Pitch

Pitches are complex mixtures of polycyclic aromatic hydrocarbons and some heterocyclic compounds. Generally, compounds are in pitch range from about 150 to ~2500 amu **[5-12]**. Each characterization technique has its own limitations of measurement. Hence, combining different techniques will provide better and useful information on the pitch composition. The following sections summarize the techniques used in this study.

General Characterization of Pitch

In general, pitch samples were characterized by their softening point, solvent extractability, viscosity at different temperatures, proximate and ultimate analyses as summarized in **Table 5-17**.

Table 5-17: General characterization of pitch.

Properties	**Method or Instrument**
Softening Point	ASTM D3104
γ-resin (HI-TI)	Soxhlet extraction
β-resin (TI-PI)	Soxhlet extraction
QI	ASTM D2318
Mesophase	ASTM D4616
Ash	Proximate analysis
Viscosity	ASTM D5018
CHN content	Ultimate analysis
Sulfur	Sulfur analyzer

Note: HI = hexane insoluble's; TI = toluene insoluble's, PI = pyridine insoluble's, QI = quinoline insoluble's

Soxhlet Extraction

Soxhlet extraction was done using both cellulose and ceramic thimbles. Thimbles were dried in an oven for at least 1 hour and subsequently cooled in a desiccator. A 2-gram ground pitch sample of 60-100 mesh size was weighed, placed in a weighed dried thimble and then put into a Soxhlet unit. About 250 mL of solvent was used to extract the pitch. The series of solvents used in the extraction were hexane, toluene and pyridine, respectively. For each solvent, the extraction was continued until the color of the solvent ran clear from the sample chamber. This process normally took about 1-3 days per solvent depending on the sample. After the first solvent was removed from the Soxhlet extraction apparatus, the second one was put in and the extraction continued while the insoluble material remained in the thimble.

The solvent was then separated from the extracted material using a vacuum rotary evaporator. The extracted material from each solvent was subsequently dried in a vacuum oven at ~60-80°C and weighed. This process was repeated for the next solvent, i.e. toluene and pyridine, respectively. These extractable materials were called HI-TI for the fraction of hexane insoluble and toluene soluble and TI-PI for the fraction of toluene insoluble and pyridine soluble. The final insoluble material, i.e. from the pyridine extraction, remained in the thimble was washed with acetone and air-dried for 1 hour and then placed into a vacuum oven at ~60-80°C overnight to remove all remaining solvent. The thimble with dried pyridine insoluble material was then placed in a desiccator before weighing.

Chemistry, Structure and Molecular Masses Distribution of Pitches

The characterization techniques of the pitch samples include Laser Desorption Mass Spectrometry (LDMS), Gas-Chromatography/Mass Spectrometry (GC/MS), High Performance Liquid Chromatography (HPLC), and ^{13}C Nuclear Magnetic Resonance (^{13}C NMR). A summary of techniques used for characterization of different fractions of the pitch samples along with the molecular mass range limitations are shown in **Table 5-18**.

Table 5-18: Summary of techniques used for characterization of different fractions of the pitch samples and the molecular mass ranges of each technique.

Technique	Fraction	Molecular mass ranges
Solid-state ^{13}C NMR	Whole pitch	No limit
GC/MS	HS	< 350 amu
HPLC	HI-TI	< 600 amu
LDMS	Whole pitch	> 200 amu

Laser Desorption Mass Spectrometry (LDMS)

Since compounds in pitch are complex and distributed up to 2500 amu **[5-13]**, the characterization of pitch by many techniques is limited. Laser desorption mass spectrometry provides a considerable extension of mass ranges to very high values. It was reported that compounds in pitch could be detected as high as 100,000-200,000 amu when the matrix assistance was used **[5-13]**. In this study, pitch samples were sent for analysis at the Huck Institute, Department of Chemistry, PSU.

A Waters Micromass Matrix Assisted Laser Desorption Ionization Time of Flight (MALDI-TOF) mass spectrometer was used to determine the average molecular weight of the pitch samples. The MALDI-LR is equipped with linear and reflectron detectors. The linear detector has a mass range of 3000 m/z to 200,000 m/z, while the reflectron

detector works best in a mass range of 10 m/z to 3000 m/z. MALDI experiments were carried out by pulsing a Nitrogen UV laser (337nm wavelength) onto the sample. The UV laser light was absorbed and vaporizes small amounts of protonated, non-fragmented ions, which are carried then into the gas phase. The ions were accelerated by a high voltage and travel into a field-free region. Ions with a low m/z travel faster than ions with a high m/z. The time required for ions to travel the length of the field-free region was measured by the time-of flight (TOF) detector. A TDC (time to digital converter) calculates the velocity and ultimately the m/z of the ion.

The MALDI-LR was operated in a positive reflectron mode in a mass range of 10 m/z to 3,000 m/z. A 20 mg whole pitch was dissolved in 1 mL toluene and sonicated for 30 minutes. A 1.0μL of each sample was spotted in a separate well on a 96 stainless steel well plate and air dried before insertion in the mass spectrometer ion source. No matrix was used in the experiments. The sample itself absorbed laser energy sufficiently for the ionization of molecules. Each spectrum represents a sum of 20 individual spectra. The background of the summed spectrum was subtracted and the spectrum itself was smoothed, which leaves monoisotopic ions. Monoisotopic ions are composed only of the lightest isotopes of various elements (C, H, N, O and S).

Gas-Chromatography/Mass Spectrometry (GC/MS)

GC is the method for determining pitch constituents with molecular masses less than 350 amu **[5-14]**. The smallest molecules present in the HS fraction of pitch can be individually identified. Analyses were performed on a Shimadzu QP5000 with 70 eV electron ionization. The GC was equipped with an XTi-5 fused silica capillary column (30m x 0.25mm. x 0.25μm). A 20 mg pitch sample was dissolved in 1 mL

dichloromethane (DCM) and sonicated for 5 minutes in a vial with a septum. A 0.5µL solution was automatically injected into a GC using a splitless mode. The temperature of the GC/MS transfer line was set at 290°C. The GC interface and injector temperatures were both held at 290°C. The temperature program applied to the GC oven was: isothermal at 40°C for 4 min; temperature programmed at 10°C/min to 180°C; at 4°C/min to 320°C; isothermal at 320°C for 15 min. The mass spectrometer was operated in full scan mode (m/z 40–450 and 1 scan/s).

High Performance Liquid Chromatography (HPLC)

HPLC is suited for the detection and quantitative determination of higher-molecular weight compounds up to 600 amu **[5-14]**. The HI-TI fractions were analyzed by HPLC using a Waters system incorporated with the Pinnacle II™ PAH column from Restek USA. The Pinnacle II™ PAH stationary phase is packed with a specialized polymer with pore size 110 Å and has an average particle size of 5µm. The mobile phase was Acetonitrile (ACN), water and Dichloromethane (DCM). A gradient flow was used and the solvent program is shown in

Table 5-19. An HPLC equipment (Waters Model 600E) incorporating a Waters 996 Photodiode array detector, operating between 190 and 800 nm, was used to obtain UV spectra. To obtain most of the polycyclic aromatic compounds peaks in pitch, a UV detector operating at 254 nm was generally used.

Table 5-19: Gradient flow of solvents used in the HPLC analyses.

Time	Flow	%ACN	%DCM	%Water	Curve

0	0.5	60	0	40	6
180	0.5	100	0	0	5
200	1	100	0	0	1
300	1	0	100	0	6
330	1	0	100	0	1

Note: ACN = acetonitrile; DCM = dichloromethane;
*Curve "1" = linearly increase concentration; Curve "6" = same concentration from the beginning time and sharply ramp up at the final time.

The HI-TI fraction of pitch was dried by purging with UHP N_2 at room temperature. A 20 mg dried sample was dissolved in 1 mL dichloromethane (DCM) and sonicate for 5 minutes in a vial. A 5μL solution was injected into the HPLC for analysis.

Solid State ^{13}C Nuclear Magnetic Resonance (Solid State ^{13}C NMR)

It has been accepted that single-pulse excitation (SPE) or simple Bloch decay by the solid-state ^{13}C NMR can be used to obtain reliable aromaticity values and the degree of condensation **[5-15, 5-16]**. In this study both cross-polarization magic-angle-spinning (CP/MAS) and SPE techniques were employed. Dipolar dephasing (DD) experiments were performed in both CP/MAS and SPE techniques to obtain the degree of condensation as explained by Love et al. **[5-16]**.

Cross-polarization (CP) and simple Bloch decay or single-pulse excitation (SPE) measurements were carried out at 75.47 MHz on a Bruker 300 MHz spectrometer with magic-angle-spinning (MAS) at 12 kHz at the Energy Institute, PSU. A Bruker wide-bored variable temperature magic angle probe was used in this study. The magnetic field was adjusted weekly with adamantane to obtain a lower frequency resonance at 29.5 ppm.

CP/MAS

A 90° ^{13}C pulse width of 4 μs with ~83 kHz ^{1}H decouple was used. A recycle delay of 5 seconds was generally used for all samples.

SPE

A high power decoupling (hpdec) was used in the SPE experiment. A 90° ^{13}C pulse width of 4 μs with ~40 kHz ^{1}H decoupling was used. Recycle delays of 400 to 960 seconds were used depending on the spin-lattice relaxation time of each sample.

Dipolar Dephasing

Dipolar dephasing (DD) experiments were performed in both CP/MAS and SPE using dephasing times of 1-600 μs to determine the fraction of non-protonated carbon and further calculation of bridgehead aromatic carbons (C_{BR}).

5.5.2 Results and Discussion

General characterization of pitch

General properties of SCTP-2, PP-1, HTCCP and OXCCP are compared as listed in **Table 5-20**. The HS fractions of HTCCP and OXCCP were 16% and 20% by weight, respectively. This shows that too many light compounds have been removed from the samples during the vacuum distillation. Although these light compounds cause the pitch to have lower softening point, they are important and could help the pitch wet the surface of the coke particles during the carbon anode forming. The majority of the compounds in HTCCP and OXCCP were in the range of HI-TI fractions which were 70% and 66% by weight, respectively. These percentages were too high for pitch as compared to SCTP-2 and PP-1. The TI-PI fractions of HTCCP and OXCCP were 7% and 10% by weight, respectively, and are comparable to those of SCTP-2 (i.e. 8% by weight). The PI

fractions of HYCCP and OXCCP were 8% and 7% by weight, respectively. Since these HTCCP and OXCCP contain 30% by weight of SCTP-2, the PI fractions may be derived mainly from the SCTP-2.

Another important property of the pitch was the percentage of fixed carbon which contributes to the property of the baked carbon anodes. The higher the fixed carbon, the lower the mass lost during the baking process of carbon anodes. From **Table 5-20**, the percentages of fixed carbon of HTCCP and OXCCP were 38% and 33% by weight, respectively. These values were considerably lower than those of SCTP-2 and PP-1 which are 59% and 47% by weight, respectively.

Table 5-20: General properties of SCTP-2, PP-1, HTCCP and OXCCP.

Property	**SCTP-2**	**PP-1**	**Run#50 (360°-FBP)**	**HTCCP**	**OXCCP**
Elemental Analysis†					
C	93.83±0.20	93.48±0.21	N.A.	N.A.	N.A.
H	3.87±0.16	5.55±0.44	N.A.	N.A.	N.A.
N	1.03±0.05	0.20±0.07	N.A.	N.A.	N.A.
S	0.56±0.01	1.21±0.08	N.A.	N.A.	N.A.
O (by calculation)	0.71	-0.45	N.A.	N.A.	N.A.
Atomic H/C	0.50	0.71	N.A.	N.A.	N.A.
Other Properties					
Softening Point (°C) †	112.2±0.8	113.1±1.5	N.A.	72.5±0.3	78.1±0.1
HS (wt%)†	24.67±0.35	47.77±0.63	N.A.	15.52±3.49	19.41±0.23
HI-TI (wt%)†	43.08±2.61	42.77±3.27	N.A.	70.34±1.25	65.77±0.76
TI-PI (wt%)†	8.31±0.20	3.72±1.63	N.A.	6.67±1.47	10.32±1.53
PI (wt%)†	30.64±0.19	N.D.	N.A.	7.59±1.27	6.90±0.31
QI (wt%)	15‡	0.1‡	N.A.	N.A.	N.A.
Moisture (wt%, dry) †	0.08±0.06	0.00±0.00		0.06±0.06	0.06±0.06
Volatile Matter (wt%, dry) †	40.56±0.22	53.46±0.12	99.75±0.24	62.42±0.36	67.13±0.43
Fixed Carbon (wt%)†	59.12±0.34	46.51±0.06	0.25	37.58	32.81
Ash Content (wt%)†	0.25±0.06	0.04±0.06	0.00±0.00	0.00±0.06	0.06±0.06

N.D. = Not Determined; N.A. = Not Available; † Data obtained from The Energy Institute; ‡ Data provided by Koppers Co., Ltd

Chemistry, Structure and Molecular Masses Distribution of Pitches

Mass Distribution by LDMS

Figure 5-10 shows the LDMS spectra of the HTCCP and OXCCP as compared to those of SCTP-2 and PP-1. Consider the materials ranging from 175-350 daltons as a monomer group (see **Figure 5-10(c)**). After heat soaked and oxidized the 360°C-FBP fraction, di-, tri-mers and so on were formed (see **Figure 5-10(d)** and **Figure 5-10(e)**). OXCCP contained more heavy mass material than HTCCP; however, they both were lighter than SCTP-2 and PP-1. Although both HTCCP and OXCCP were mixed with SCTP-2 at 30% by weight, there was still a gap of masses ranging from 350-450 daltons that needed to be filled.

Since many heat soaking and oxidation conditions have been tested as discussed in the previous report **[5-1]**, masses ranging from 350-450 daltons were still vacant. This task will be left for the future work to find other technique to produce this mass range.

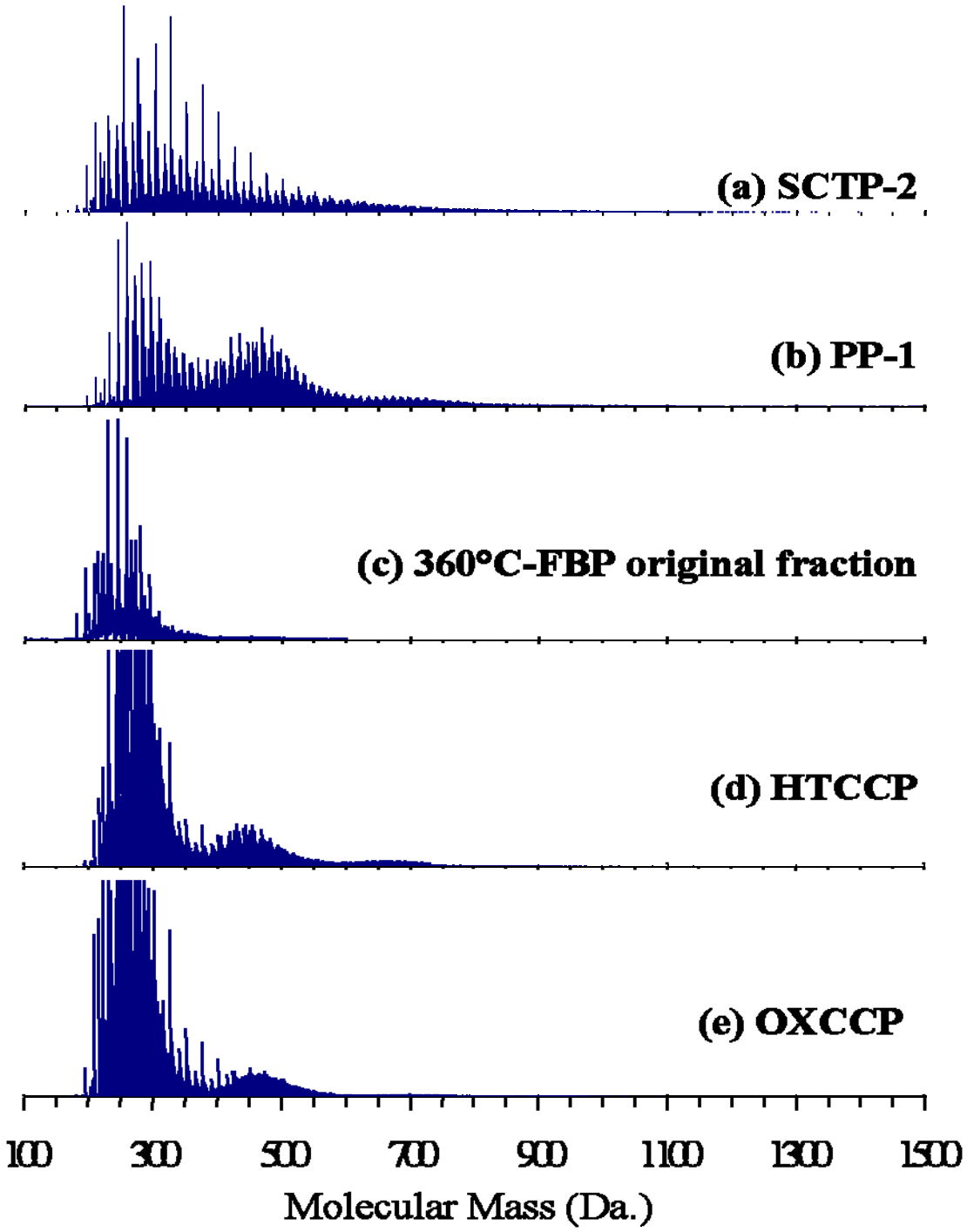

Figure 5-10 LDMS spectra of (a) SCTP-2; (b) PP-1; (c) 360°C-FBP original fraction; (d) 360°C-FBP after heat soaked at 475°C, 1 hr; and (e) 360°C-FBP after oxidized at 250°C, 4 hr.

Chemical Analysis of HS Fraction by GC/MS

From **Figure 5-11**, the HS fractions of all pitch samples consist of 3-6 fused-ring polycyclic aromatic compounds (PACs). The highest molecular masses that could be analyzed from these HS fractions were in the range of 270-280 daltons. Although the mass spectrometer of the instrument can analyze compounds up to 450 daltons, it was the limitation of the volatility and size of the compounds to pass into the GC column. **Figure 5-11** shows that HTCCP and OXCCP were very complex and the level of complexity was comparable to that of PP-1. The qualitative analysis of PP-1, HTCCP and OXCCP showed that these pitch samples contained a tremendous amount of alkyl-substitutes PACs, while the spectrum of SCTP-2 was less complex and contain less alkyl-substituted PACs.

Chemical Analysis of HI-TI and TS Fraction by HPLC

HPLC was used to analyze the HI-TI and TS fractions of the decant oil, co-coking liquid and pitch samples. **Figure 5-12** shows chromatograms of DO107, Run#50 (360°C-FBP), and the HI-TI fractions of HTCCP and OXCCP. Run#50 (360°C-FBP) contained less concentration of light compounds than DO107 as shown at the retention times of 0-50 min and the rest of the chromatograms of both samples look very similar from this HPLC analysis. They contain no peak after the retention of ~190 minutes. From these results, it can be said that compounds in condensed liquid obtained from the co-coking of coal and decant oil, i.e. DO107, were mainly derived from the decant oil.

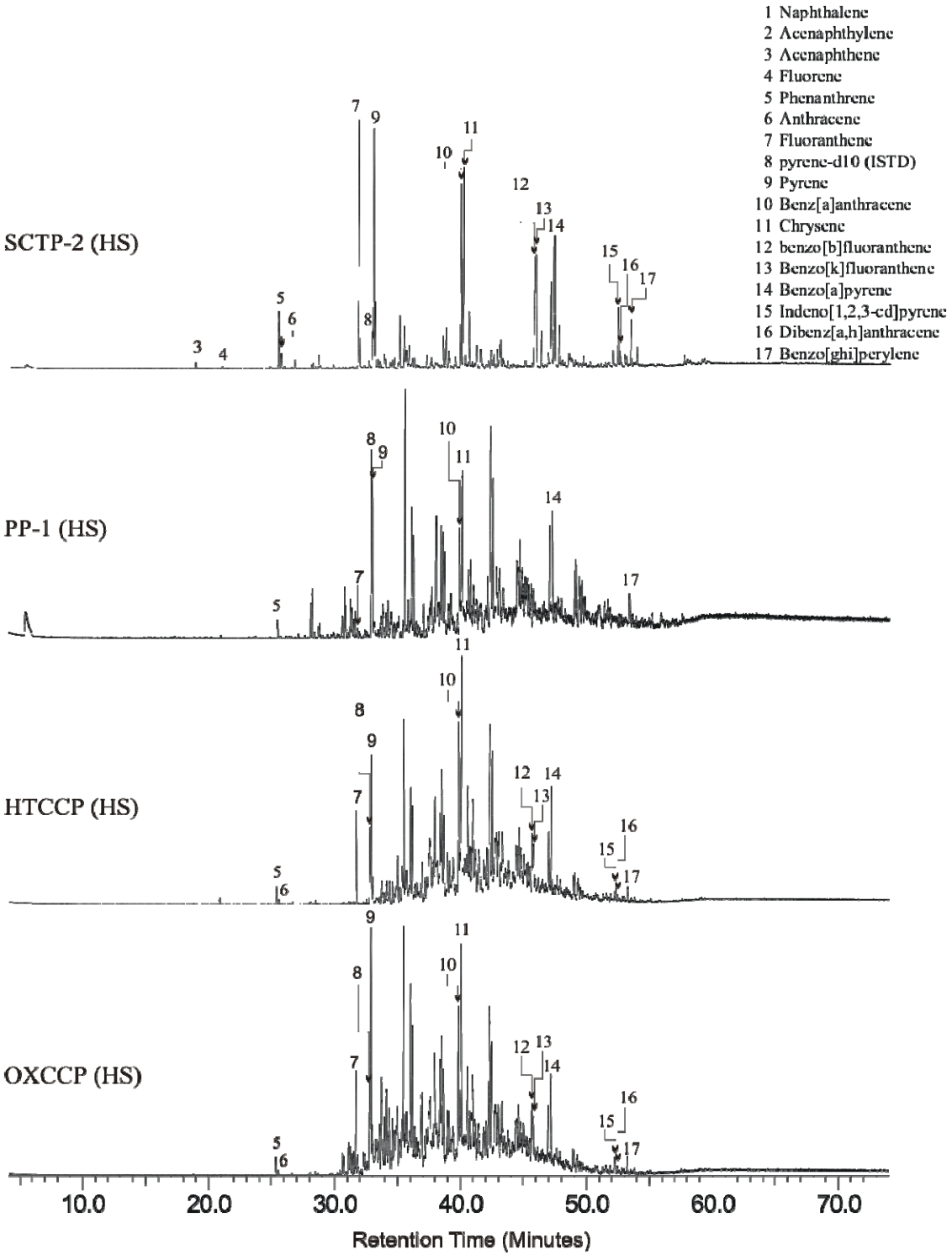

Figure 5-11: GC/MS Chromatogram of HS fractions of SCTP2, PP-1, HTCCP and OXCCP.

HTCCP and OXCCP contain many more heavy compounds than their original material, i.e Run#50 (360°C-FBP). The shift of the baseline after the retention time of 200 minutes from the HTCCP and OXCCP indicates that there were a number of heavy compounds in the samples.

Figure 5-13 shows a comparison of HPLC Chromatograms of HI-TI fractions of SCTP2, HTCCP and OXCCP and TS fraction of PP-1. The baselines of the PP-1, HTCCP and OXCCP at the retention times of 0-200 min were considerably shifted compared with that of SCTP-2. This revealed that PP-1, HTCCP and OXCCP were more complex than SCTP-2 as shown earlier in the GC/MS chromatograms (**Figure 5-11**). The HPLC chromatograms showed very important information of high molecular masses PACs contain in the pitch samples. Since there is only a UV detector attached to the HPLC unit, the only way to identify the compounds was to inject the known standard samples. Although only 17 known standard samples were used in this study as shown in **Figure 5-13**, the HPLC chromatograms were still useful in term of comparison between samples.

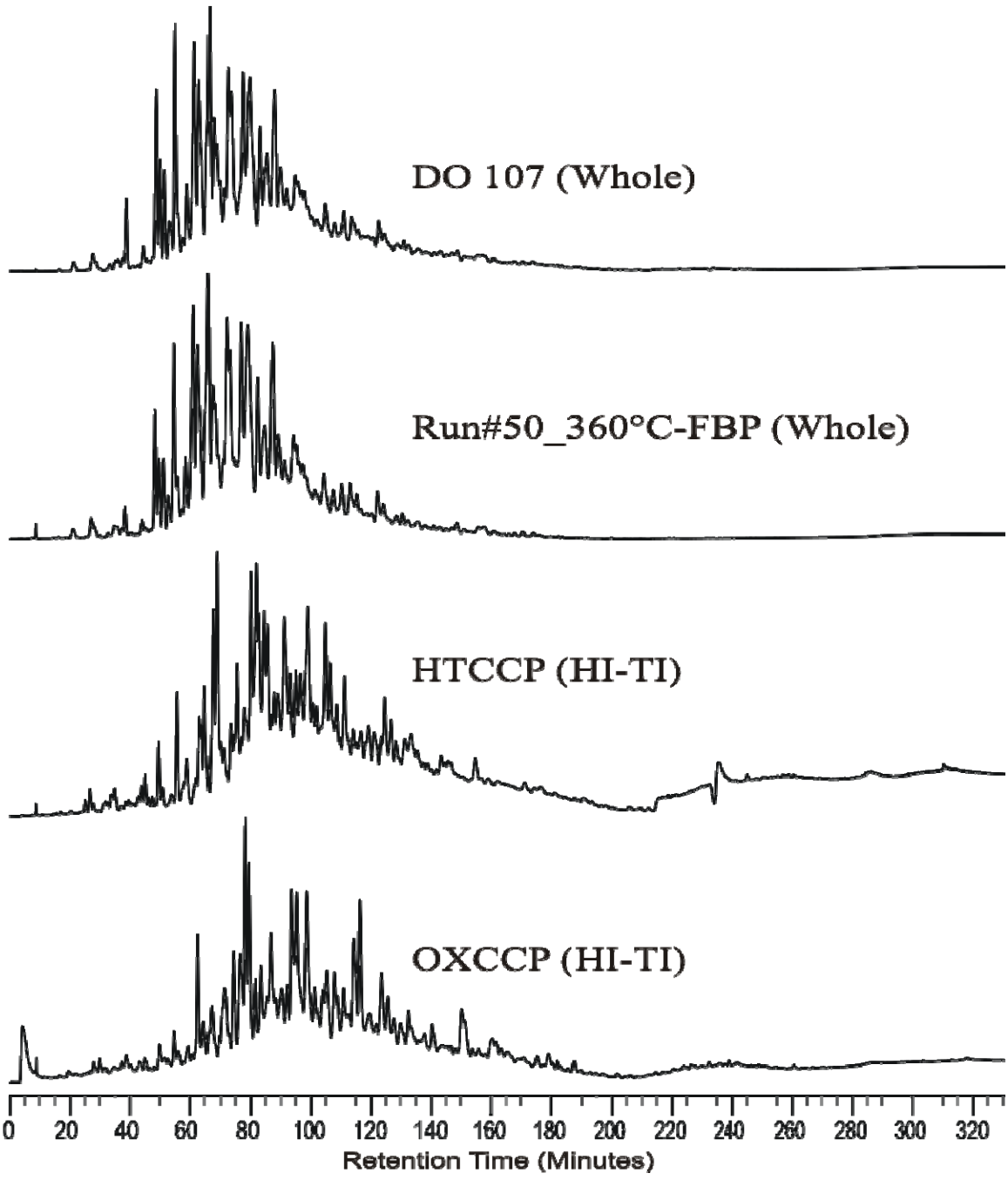

Figure 5-12: HPLC Chromatograms of DO 107, Run#50 (360°C-FBP), and HI-TI fraction of HTCCP and OXCCP.

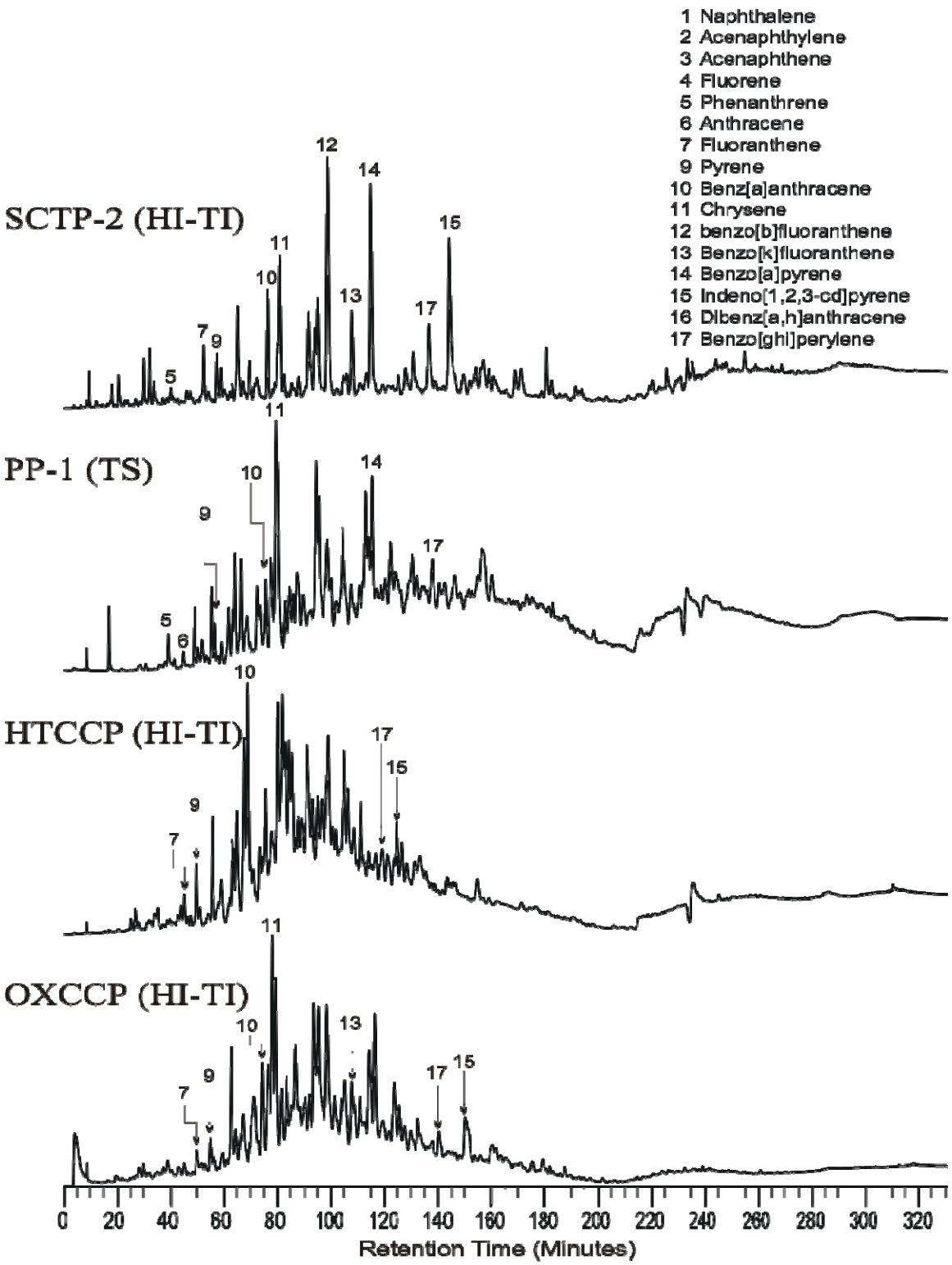

Figure 5-13: HPLC Chromatograms of HI-TI fractions of SCTP2, HTCCP and OXCCP and TS fraction of PP-1.

Structure Determination of Whole Pitch by Solid State ^{13}C NMR

From the previous sections, the different extracted fractions of pitch were analyzed by GC/MS and HPLC techniques. None of those techniques can be used to analyze the pitch as a whole sample. In this section, solid state ^{13}C NMR was utilized to analyze the whole pitch sample as a bulk property. Solid-state ^{13}C NMR can be used to obtain reliable aromatic content and the degree of condensation. CP/MAS was done in all SCTP-2, PP-1, HTCCP and OXCCP samples; however, only SCTP-2 and PP-1 were analyzed by SPE by the end of this report period.

Figure 5-14 shows ^{13}C NMR CP/MAS spectra of (a) SCTP-2, (b) PP-1, (c) HTCCP, and (d) OXCCP. Spectra of HTCCP and OXCCP were similar to that of PP-1. **Table 5-21** shows a comparison of the weight percentages of aromatic and aliphatic carbons of SCTP-2, PP-1, HTCCP and OXCCP obtained from the ^{13}C NMR CP/MAS experiments. The aromaticity of HTCCP and OXCCP was comparable with that of PP-1, as well confirms that these blended pitch fraction (HTCCP and OXCCP) were mainly derived from petroleum products from their original material, i.e. decant oil (DO107).

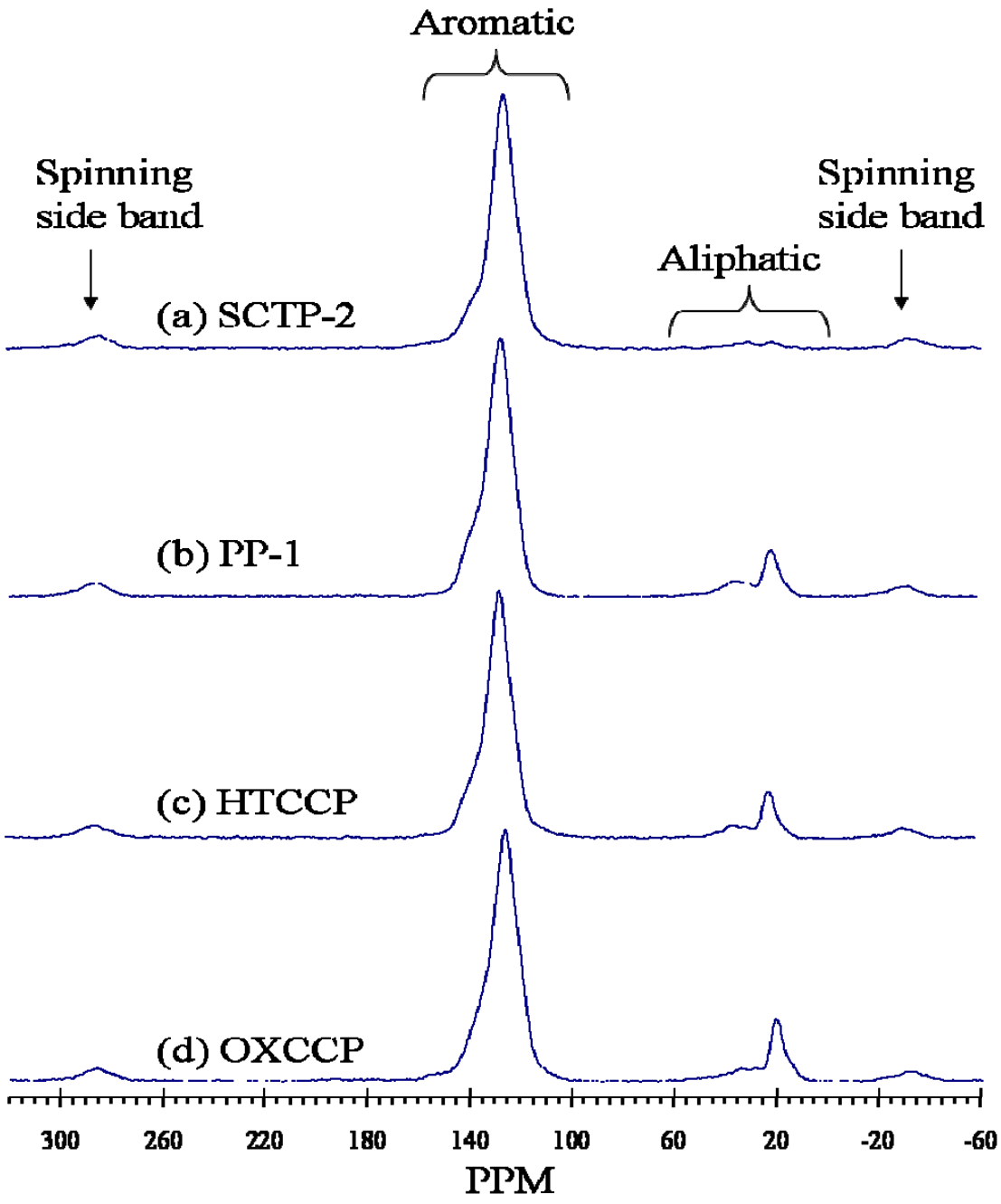

Figure 5-14: ^{13}C NMR CP/MAS spectra of (a) SCTP-2; (b) PP-1; (c) HTCCP; and (d) OXCCP.

Table 5-21: Weight percents of aromatic and aliphatic carbons of SCTP-2, PP-1, HTCCP and OXCCP from ^{13}C NMR CP/MAS and SPE experiments.

	CP/MAS		SPE	
	% Aromatic C	% Aliphatic C	% Aromatic C	% Aliphatic C
SCTP-2	97.17%	2.83%	97.83%	2.17%
PP-1	87.15%	12.85%	91.180%	8.82%
HTCCP	88.50%	11.50%	N.A.	N.A.
OXCCP	86.15%	13.85%	N.A.	N.A.

5.5.3 Conclusions and Future Work

Heat soaking and oxidation were performed on the Run#50 360°C-FBP fraction. Oligomers were formed as a result of heat treatment. Resulting pitches from this work are called heat-soaked co-coking pitch (HTCCP) and oxidized co-coking pitch (OXCCP). The LDMS analyses show that both HTCCP and OXCCP contain lighter PACs than those of SCTP-2 and PP-1 and masses range of 350-450 daltons are missing. This task is left for the future work to find another technique to produce these masses range and to obtain a better property of the pitch suitable for the carbon anode production. One potential technique was solvent extraction using alkanes. Since smaller alkanes, i.e. pentane, has a potential to remove more materials which are valuable to the pitch property, heptane might be a better solvent to remove a smaller fraction of the light compounds. Heat treatment, solvent extraction and distillation could be combined in order to produce a good pitch.

Chemical analyses were performed on the extracted fractions of pitches using GC/MS and HPLC, and on the whole pitch using ^{13}C NMR. These results show that HTCCP and OXCCP contain a lot of heaver masses than their original material due to the heat treatment. All results from GC/MS, HPLC, and ^{13}C NMR confirm that HTCCP and

OXCCP were mainly derived from petroleum fraction of the original material, i.e. decant oil (DO107).

The next phase of this investigation will be to study the interaction of pitch and petroleum coke; an important aspect of carbon anode production for the aluminum industry.

Subtask 5.6 Manufacture and Testing of Carbon Artifacts

Work on this subtask was suspended pending resolution of funding issues and until the Marfork co-coking tests have been completed.

References Cited

1-1 Schobert, H. H., Advanced Thermally Stable Coal-Based Jet Fuels, *Annual Progress Report,* AFOSR Grant F49620-99-1-0290, 2001-2002

1-2 Schobert, H. H., Advanced Thermally Stable Coal-Based Jet Fuels, *Annual Progress Report,* AFOSR Grant F49620-99-1-0290, 2000-2001

1-3 Schobert, H. H., Advanced Thermally Stable Coal-Based Jet Fuels, *Annual Progress Report,* AFOSR Grant F49620-99-1-0290, 1999-2000

1-4 Coleman, M. M., Fearnley, S. P., Kumar, S. and Sobkowiak, M., Fuel Stabilization, AFRL-PR-WP-TR-2000-2007, Final Report for 07/01/1995 – 12/31/1998, September 1999.

1-5 Song, C., Lai, W.-C., Schobert, H.H. Hydrogen-Transferring Pyrolysis of Long-Chain Alkanes and Thermal Stability Improvement of Jet Fuels by Hydrogen Donors. *Ind. Eng. Chem. Res.,* **1994**, 33 (3), 548-557

1-6 Lai, W.-C and Song, C., *Prepr. Pap.- Amer. Chem. Soc. Div. Fuel Chem.* **1996a** 41:524

1-7 Lai, W.-C and Song, C., *Fuel Processing Technology,* **1996b** 48:1

1-8 Selvaraj, L., Sobkowiak, M., Song, C., Stallman, J., Coleman, M. M. A Model System for the Study of Additives Designed to Enhance the Stability of Jet Fuels at Temperatures Above 400°C. *Energy & Fuels,* **1994**, 8 (4), 839-845.

1-9 Yoon, E.M., Selvaraj, L., Song, C., Stallman, J., Coleman, M. M., High Temperature Stabilizers for Jet Fuels and Similar Hydrocarbon Mixtures. 1. Comparative Studies of Hydrogen Donors. *Energy & Fuels,* **1996a**, 10 (3), 806-811.

1-10 Yoon, E.M., Selvaraj, L., Eser, S. and Coleman, M. M., High Temperature Stabilizers for Jet Fuels and Similar Hydrocarbon Mixtures. 2. Kinetic studies, *Energy & Fuels,* **1996a**, 10 (3), 812-815.

1-11 Andrésen, J.M., Strohm, J.J., Boyer, M.L., Song, C, Schobert, H.H. and Butnark, S., *Am. Chem. Soc. Div. Petrol. Chem. Prepr.,* **2001a**, 46(1), 208-209.

1-12 Andrésen, J.M., Strohm, J.J., Sun, L., Song, C. *Energy & Fuels,* **2001b**, 15(3), 714-723.

1-13 Badger, M. W., Fickinger, A. E.,Martin, S. C.,Mitchell, G. D. and Schobert, H. H., *Proc. 8th Austrlian Coal Science Conference,* **1998**, 245.

1-14 Badger, M. W., Fickinger, A. E., Mitchell, G. D., Adams, A. N. and Schobert, H. H., *Proc. 205th International Technical Conference on Coal Utilization and Fuel Systems (in press).*

1-15 Butnark, S., Badger, M.W. and Schobert, H.H., *Amer. Chem. Soc., Div. Fuel Chem. Prepr.,* **1999**, 44 (3), 662-665.

1-16 Butnark, S., Badger, M. W. and Schobert, H. H., *Prepr. Pap.- Amer. Chem. Soc. Div. Petrol. Chem.,* **2000** 45:493.

1-17 Fickinger, A. E., **2000**, M. S. Thesis, The Pennsylvania State University, University Park, PA.

1-18 Fickinger, A. E., Badger, M. W., Mitchell, G. D. and Schobert, H. H., , *Prepr. Pap.- Amer. Chem. Soc. Div. Fuel Chem*, **1999**, 44:106.

1-19 Fickinger, A. E., Badger, M. W., Mitchell, G. D. and Schobert, H. H., , *Prepr. Pap.- Amer. Chem. Soc. Div. Fuel Chem,* **2000**, 45:299.

1-20 Song, C., and Schobert, H. H., , *Prepr. Pap.- Amer. Chem. Soc. Div. Fuel Chem.,* **2000**, 45:819.

1-21 Butnark, S., Badger, M. W. and Schobert, H. H., Determining the Desired Chemical Composition for Thermally Stable Jet Fuel, *Amer. Chem. Soc., Div. Fuel Chem. Prepr.,* **2001**, 46 (2), 492-494.

1-22 Butnark, S., Badger, M. W. and Schobert, H. H. and Wilson, G. R., Selection of Prototype Thermally Stable Jet Fuels 3. Jet Fuel Boiling Range and its Affect on Pyrolytic Stability, *Prepr. Pap.- Amer. Chem. Soc. Div. Petrol. Chem.,* **2002**, 47(3), 201.

1-23 Schobert, H. H., Badger, M. W. and Santoro, R. J., Progress Toward Coal-Based JP-900, *Prepr. Pap.- Amer. Chem. Soc. Div. Petrol. Chem.,* **2002**, 47:192.

1-24 Wilson, G. R., Project Report on AFOSR-Subcontract for Advanced Thermally Stable Coal-Based Jet Fuels for the Pennsylvania State University, PARC Technical Services Inc., Pittsburgh, PA. August **2002**.

1-25 Rudnick, L. R., et al. "Refinery Integration of By-Products from Coal-Derived Jet Fuels", Year Annual Progress Report, Grant No. DE-FC26-03NT41828, November 17, **2005**.

2-1 Yang, Y., J. P. Szybist, and A. L. Boehman, "Low Temperature Oxidation of Methylcyclohexane in an SI Engine," *Prepr. Pap.-Am. Chem. Soc., Div. Fuel Chem.* **2006,** *51(1),* 329-330.

2-2 Yang, Y., J.V. Zello, and A. L. Boehman, "Oxidation of Methylcyclohexane in a Motored CFR Engine," to appear in *Prepr. Pap.-Am. Chem. Soc., Div. Fuel Chem.* **2007,** *52(2).*

2-3 Szybist, J., A.L. Boehman, D. C. Haworth, and H. Koga. "Premixed Ignition Behavior of Alternative Diesel Fuel-Relevant Compounds in a Motored Engine Experiment," Submitted to *Combustion and Flame*, **2007**, *149*, 112–128.

2-4 Burgess-Clifford, C.E., Boehman, A., Song, C., Miller, B., Mitchell, G., "Refinery Integration of By-Products from Coal-derived Jet Fuels," Semi-Annual Progress Report for Grant DE-FC26-03NT41828, November 30, 2006.

3-1 Song, C. and Ma, X. *Appl. Catal. B:Env.*, 2003, 41, 207.

3-2 Lee, S.-W.; Ryu, J. W. and Min, W. *Catal. Surv. Asia* 2003, 7, 271.

3-3 Sano, Y.; Choi, K.-H.; Korai, Y. and Mochida, I. *Appl. Catal*. B 2004, 49, 219.

3-4 Oyama, S. T.; Wang, X.; Lee, Y.-K.; Bando, K. and Requejo, F. G., *J. Catal.* 2002, 210, 207.

3-5 Stinner, C.; Prins, R. and Weber, Th., *J. Catal*. 2001, 202, 187.

3-6 Oyama, S. T., *J. Catal*. 2003, 216, 343.

3-7 Sie, S. T., *Fuel Proc. Tech*. 1999, 61, 149.

3-8 Sano, Y.; Choi, K.-H.; Korai, Y. and Mochida, I. *Energy & Fuels* 2004, 18, 644.

3-9 J.H. Kim, X. Ma, C. Song, Y. Lee and S. T. Oyama, *Energy & Fuel*, 2005, 19, 353-364.

3-10 Topsoe, H., Clausen, B. S., Topsoe, N. Y., Pedersen, E., Niemann, W., Müller, A., Bögge, H., and Lengeler, B., *J. Chem. Soc. Faraday Trans,* 1987, 83, 2157.

3-11. J.H. Kim, X. Ma, A. Zhou and C. Song, *Catalysis Today*, 2006, 111, 74-83.

3-12 B. Delmon, *Surf. Rev. Lett*, 1995, 2, 1, 25-41.

3-13 Song, C. *Am. Chem. Soc. Div. Petrol. Chem. Prepr*., 1998, 43, 573.

3-14 Song, C. *CHEMTECH*, 1999, March, 26.

3-15 D.W. Breck, zeolite molecular sieve, structure, chemistry, and use, Wiley, New York, 1974.

3- 16 M.Niwa, K. Yamazaki and Y.Murakami, Ind. Eng. Chem. Res. 30 (1991) 38.

3- 17. K.M. Reddy, L, Sun, C.S. Song, ABSTR PAP AM CHEM S 215: 049-PETR Part 2 APR 2 1998.

3-18 Johnson,C.D and Worrall, F. *Microporous and Mesoporous Materials* 2004, 73, 191.

3-19 S.T. Wilson, B.M. Lok, C.A. Messina, E.R. Cannan and E.M. Flanigen, J. Am. Chem. Soc. 104 (1982) 1146.

3-20 M.E. Davis, Nature 417 (2002) 813.

3-21 3. S.T. Wilson, B.M. Lok, E.M. Flanigen, US Pat. 4 310 440, (1982).

3-22 J.M. Bennett, Jr. Richardson, J.W. Pluth, J.V. Smith, Zeolite, 7, (1987) 160.

3-23 D.B. Akolekar, J. Mol. Catl. A: Chem., 104 (1995) 95.

3-24 S.H. Jhung, J-S. Chang, D.S. Kim, S-E. Park, Micropor. Mesopor. Mater. 71 (2004) 135.

3-25 M.H. Kim, H.X. Li, M.E. Davis, Micropor. Mater. 1 (1993) 191.

3-26 M. Matsukata, M. Ogura, T. Osaki, P.R.H.P. Rao, M. Nomura, E. Kikuchi., Topics in Catal. 9 (1999) 77.

3-27 Bandyophadhyay, R.K. Ahedi, Y. Kubota, M. Ogawa, Y. Goto, Y. Fukushima, and Y. Sugi, J. Mater. Chem. 11 (2001) 1869.

3-28 R. Bandyopadhyay, Y. Kubota, N. Sugimoto, Y. Fukushima, and Y. Sugi, Micropor. Mesopor. Mater. 32 (1999) 81.

3-29 T. Tatsumi and N. Jappar, J. Phys. Chem. B, 102 (1998) 7126.

3-30 A. Bhaumik and T. Tatsumi, Micropor. Mesopor. Mater. 34 (2000) 1.

3-31 R. Bandyopadhyay, M. Bandyopadhyay, Y. Kubota, Y. Sugi, J. Porous Mater. 9 (2002) 83.

3-32 S.K. Saha, Y.Kubota, Y. Sugi, Chem. Lett. 32(11) (2003) 1026.

3-33 S.K. Saha, S.B. Waghmode, Y.Kubota, Y. Sugi, Mater. Lett. 58 (2004) 2918.

3-34 S.B. Waghmode, S.K. Saha, Y.Kubota, Y. Sugi, J. Catl. 228 (2004) 192.

3-35 S.K. Saha, S.B. Waghmode, H. Maekawa, K. Kumora, Y.Kubota, Y. Sugi, Y.Oumi and T. Sano, Micropor. Mesopor. Mater. 81 (2005) 289.

3-36 T. Tatsumi, Q. Xia, N. Jappar, Chem. Lett. (1997) 677.

3-37 P.R.H.P. Rao, M. Matsukata, Chem. Commun. (1996) 1441.

3-38. Chen N.Y.; Garwood, W.E.; Dwyer, F.G. *Shape selective catalysis in Industrial Applications.*2nd edition, Marcel and Dekker, New York,1996.

3-39. Song C.; Schobert H.H. *Fuel Process Technol*., 1993, 34,157.

3-40. Song C. *CatTech*, 2002, 6 (2), 64.

3-41. Aurox A. *Topics in Catalysis*, 1997, 4, 71.

3-42. Viswanadham N. et.al *Energy and Fuels*, 2006, 20, 1806.

4-1 US Environmental Protection Agency, Methods 3050, 3051, 3052, 6010, 7470, 7471, Test Methods for Evaluating Solid Waste: Physcial/Chemical Methods. SW-846, 3rd Edition, NTIS, September, 1988.

4-2 Burgess-Clifford, C.E., Boehman, A., Song, C., Miller, B., Mitchell, G., "Refinery Integration of By-Products from Coal-derived Jet Fuels," Semi-Annual Progress Report for Grant DE-FC26-03NT41828, October, 2006.

4-3 Steam Generating Units Power Test Codes, ASME PTC 4.1, The American Society of Mechanical Engineers, 1965 (with 1968 and 1969 addenda, reaffirmed in 1973).

4-4 Falcone Miller, S., Wincek, R.T., Miller, B.G. and Scaroni, A.W., Evaluation of a Hybrid Sampling Train for Measuring Trace Elements and Identifying Mercury Species in Combustion Flue Gas, presented at the 24th International Technical Conference on Coal Utilization and Fuel Systems, Clearwater, FL, March 8-11, 1999.

4-5 Falcone Miller, S., Wincek, R.T., Miller, B.G. and Scaroni, A.W., Development of a PSU Methodology for Measuring Trace Elements and Identifying Mercury Species in Combustion Flue Gas, presented at EPRI-DOE-EPA Combined Utility Air Pollution Control Symposium: The MEGA Symposium, Atlanta, GA, August 16-20, 1999.

4-6 U.S. Environmental Protection Agency, Standard Test Method for Elemental, Oxidized, and Particle-bound and Total Mercury in Flue Gas Generated from Coal-Fire Stationary Sources (Ontario-Hydro Method), May 12, 1999.

5-1 Burgess-Clifford, C.E., Boehman, A., Song, C., Miller, B., Mitchell, G., "Refinery Integration of By-Products from Coal-derived Jet Fuels," Semi-Annual Progress Report for Grant DE-FC26-03NT41828, October, 2006.

5-2 ASTM D5187-91. 1997, Standard Test Method for determination of Crystallite size (Lc) of Calcined Petroleum Coke by X-ray Diffraction.

5-3 Gonnet, P. 2004, MS Thesis, The Florida State University.

5-4 Alvarez, A. G.; Martinez-Escandell, M.; Molina-Sabio, M.; Rodriguez-Reinoso, F. 1999, *Carbon*, *37*,Pyrolysis of petroleum residues: analysis of semicokes by X-ray diffraction. 1627.

5-5 Oya, A.; Qian, Z.; Marsh, H., 1983, *Fuel*, *62*,Structural study of cokes using optical microscopy and X-ray diffraction. 274-278.

5-6 Santamaria-Ramirez, R.; Romero-Palazon, E.; Gomez-de-Salazar, C.; Rodriguez-Reinoso, F.; Martinez-Saez, S.; Martinez-Escandell, M.; Marsh, H., 1999, *Carbon*, *37*,Influence of pressure variations on the formation and development of mesophase in a petroleum residue. 445-455.

5-7 Chang, J., 2005, Personal communication, State College, PA.

5-8 ATSM/E228-06, 2006, In *ASTM International*.

5-9 Gül, Ö.; Rudnick, L.R.; Schobert, H.H. "Delayed Coking of Decant Oil and Coal in a Laboratory-Scale Coking Unit" Energy & Fuels, 2006, 4, 1647-1655.

5-10 Gül, Ö., Clifford,C.E.B., Rudnick, L.R. and Schobert, H.H. "Process repeatability of co-coking of coal and decant oil in a pilot-scale delayed coker" , , .

5-11 Newman, J.W., and Newman, K.L. (1997). A History of Pitch Technologies. In Introduction to Carbon Technologies, H. Marsh, Heintz, E. A., and Rodriguez-Reinoso, F., ed. (Secretariado de Publicaciones), pp. 269-328.

5-12 Boenigk, W., Haenel, M.W., and Zander, M. (1990). Structural features and mesophase formation of coal-tar pitch fractions obtained by preparative size exclusion chromatography. Fuel *69*, 1226-1232.

5-13 Lazaro, M.J., Herod, A.A., Cocksedge, M., Domin, M., and Kandiyoti, R. (1997). Molecular mass determinations in coal-derived liquids by MALDI mass spectrometry and size-exclusion chromatography. Fuel *76*, 1225-1233.

5-14 Zander, M. (1997). Pitch Characterization for Industrial Applications. In Introduction to Carbon Technologies, H. Marsh, Heintz, E. A., and Rodriguez-Reinoso, F., ed. (Secretariado de Publicaciones), pp. 425-459.

5-15 Franz, J.A., Garcia, R., Linehan, J.C., Love, G.D., and Snape, C.E. (1992). Single-pulse excitation carbon-13 NMR measurements on the Argonne premium coal samples. Energy & Fuels *6*, 598-602.

5-16 Love, G.D., Law, R.V., and Snape, C.E. (1993). Determination of nonprotonated aromatic carbon concentrations in coals by single pulse excitation carbon-13 NMR. Energy & Fuels *7*, 639-644.

List of Acronyms and Abbreviations

1THQ	1,2,3,4-tetrahydroquinoline
5THQ	5,6,7,8-tetrahydroquinoline
AEL	international zeolite code of AlPO4-11 material
AFOSR	Air Force Office of Scientific Research
ADN	Adsorptive Denitrogenation
ADS	Adsorptive Desulfurization
AlPO	aluminophosphate
ATTM	Ammonium Tetrathiomolybdate
API	American Petroleum Institute
BCH	bicyclohexane
BP	biphenyl
BT	benzothiophene
CFR	Cooperative Fuels Research
CHB	cyclohexylbenzene
DBT	dibenzothiophene
DDC	Detroit Diesel Corporation
DDS	direct desulfurization
DGC	dry-gel conversion
DHN	decahydronaphthalene
DHQ	decahydroquinoline
DMBP	dimethyl biphenyl
DMDBT	dimethyldibenzothiophene
DMDCH	dimethyl dicyclohexyl
DMN	dimethyl naphthalene
DPA	dipropylamine
EN	ethyl naphthalene
EPA	Environmental Protection Agency
FBP	final boiling point
FCC	fluid catalytic cracking
FID	flame ionizaton detector
FTIR	Fourier Transform Infrared
GCMS	gas chromatography-mass spectrometry
HDMDBT	hydrodimethyl dibenzothiophene
HDS	hydrodesulfurization
HDT	hydrotreated
HM	H-mordenite
HPLC	high performance liquid chromatography
HTS	hydrothermal synthesis
HY	H Y-type zeolite
HYD	hydrogenation pathway
HZSM	H-synthetic zeolite material
IBP	initial boiling point
IC	internal combustion
IQT	ignition quality test

JP-900	jet fuel prototype stable to 900 F
LCO	light cycle oil
LDMS	laser desorption mass spectrometry
LHSV	liquid hourly space velocity
LTHDA	low temperature hydrotreating and dearomatization
MAPO	metal substituted aluminophosphate
MCHT	methyl cyclohexyl toluene
MCM	mesopourous catalytic material
MDBT	methyldibenzothiophene
MN	methyl naphthalene
NTP	normal temperature and pressure
PARC	Pennsylvania Applied Research Corporation
PB	propyl benzene
PCH	propyl cyclohexane
PCHE	propyl cyclohexene
PFPD	pulsed flame photometric detector
PP	petroleum pitch
PSU	Penn State University
RCO	refined chemical oil
SARS	selective adsorption for removing sulfur
SAC	steam-assisted conversion
SAPO	silicon substituted aluminophosphate
SDA	structure-directing agent
SEM	scanning electron microscopy
SI	spark ignited
SpGr	specific gravity
SwRI	Southwest Research Institute
TEM	transmission electron microscopy
TEOS	tetraethyl orthosilicate
THDBT	tetrahydrodibenzothiophene
THDMDBT	tetrahydrodimethyldibenzothiophene
TLP	total liquid product
TMBT	trimethylbenzothiophene
TOS	time on stream
TPD	temperature programmed desorption
TPO	temperature programmed oxidation
TPR	temperature programmed reduction
VPT	vapor-phase transport
WHSV	weight hourly space velocity
XPS	x-ray photoelectron spectroscopy

Appendix 1-A

Data for distillation cuts and simulated distillation of cuts for RCO from Intertek PARC

Sample Name: **X1333 CUT1 OP-560F**
Acquired On: 20060628160136-0500
Recovered 100.00

BP Distribution

IBP	353.53
1%	402.51
2%	484.43
3%	499.12
4%	506.81
5%	508.06
6%	508.68
7%	508.47
8%	508.25
9%	509.12
10%	508.99
11%	508.86
12%	508.74
13%	509.65
14%	509.55
15%	509.45
16%	509.36
17%	509.26
18%	510.17
19%	510.05
20%	509.94
21%	509.82
22%	510.71
23%	510.42
24%	510.89
25%	514.15
26%	517.73
27%	518.15
28%	518.82
29%	518.62
30%	518.41
31%	519.27
32%	519.13
33%	518.98
34%	519.86
35%	519.73
36%	519.60
37%	519.47
38%	520.33
39%	520.12
40%	519.91
41%	522.90
42%	530.39
43%	536.83
44%	537.08
45%	537.79
46%	537.55
47%	538.39
48%	538.26
49%	538.12
50%	537.99
51%	538.90
52%	538.82
53%	538.74
54%	538.65
55%	538.57
56%	538.48
57%	539.42
58%	539.36
59%	539.30
60%	539.24
61%	539.17
62%	539.11
63%	539.05
64%	538.99
65%	539.93
66%	539.87
67%	539.82
68%	539.76
69%	539.70
70%	539.64
71%	539.58
72%	539.53
73%	540.47
74%	540.36
75%	540.25
76%	540.15
77%	540.04
78%	540.80
79%	541.86
80%	542.66
81%	543.92
82%	544.41
83%	544.99
84%	544.52
85%	545.86
86%	546.10
87%	547.10
88%	549.40
89%	549.70
90%	550.88
91%	552.72
92%	553.01
93%	554.38
94%	555.58
95%	563.04
96%	569.63
97%	574.75
98%	583.28
99%	592.48
FBP	607.91

Cut Points Listing

D86 Correlations

D1160 Correlations

Sample Name:	X1332 CUT1C 433-560F	X1332 CUT2 560-570F	X1332 CUT3 570-580F	X1332 CUT3 570-580F
Acquired On:	20060614095834-0500	20060614102642-0500	20060614110213-0500	20060614110213-0500
Recovered	100.00	100.00	100.00	100.00

BP Distribution

IBP	407.28	407.46	450.15	449.44
1%	407.61	487.32	497.22	497.26
2%	408.17	506.19	507.43	507.44
3%	408.88	507.96	508.61	508.61
4%	408.70	508.47	508.21	508.21
5%	408.53	509.16	508.98	508.98
6%	409.36	508.94	508.73	508.74
7%	409.23	508.72	509.54	509.54
8%	409.10	509.57	509.34	509.34
9%	408.97	509.41	510.12	510.13
10%	409.81	509.25	509.83	509.83
11%	409.65	510.10	510.24	510.26
12%	409.49	509.92	514.64	514.75
13%	410.19	509.74	518.16	518.18
14%	410.43	510.40	518.67	518.68
15%	424.45	512.14	519.34	519.35
16%	441.20	515.96	519.11	519.11
17%	447.41	518.05	518.87	518.88
18%	447.97	518.62	519.67	519.68
19%	448.62	519.32	519.45	519.46
20%	449.24	519.11	520.16	520.18
21%	449.63	518.90	520.66	520.71
22%	453.31	519.75	529.15	528.55
23%	453.56	519.59	537.45	536.53
24%	454.59	519.42	537.79	537.81
25%	472.27	520.25	538.43	538.45
26%	474.75	520.06	538.23	538.24
27%	475.12	520.84	538.02	538.03
28%	476.42	521.20	538.87	538.88
29%	482.17	529.13	538.74	538.74
30%	485.03	536.80	538.60	538.61
31%	485.82	537.83	538.47	538.48
32%	489.72	538.44	539.38	539.38
33%	490.71	538.22	539.28	539.29
34%	491.73	538.00	539.18	539.19
35%	496.26	538.85	539.09	539.09
36%	500.14	538.71	538.99	539.00
37%	507.98	538.56	539.90	539.91
38%	508.40	539.44	539.82	539.83
39%	509.10	539.34	539.73	539.74
40%	508.88	539.24	539.64	539.65
41%	509.69	539.15	539.56	539.56
42%	509.57	539.05	540.47	539.48
43%	509.44	539.96	540.33	540.34
44%	509.31	539.88	540.18	540.19
45%	510.20	539.80	540.03	540.04
46%	510.12	539.72	540.59	540.65
47%	510.03	539.64	542.94	542.09
48%	509.94	539.56	543.84	543.92
49%	509.85	539.48	544.13	544.20
50%	509.76	540.39	545.47	544.54
51%	510.69	540.30	546.43	545.55
52%	510.62	540.20	547.18	547.38
53%	510.54	540.11	549.09	549.22
54%	510.47	540.01	550.11	550.23
55%	510.39	540.81	552.73	552.89
56%	510.31	540.53	553.80	553.89
57%	510.24	542.21	553.97	554.09
58%	511.16	543.06	559.72	558.24
59%	511.06	544.33	565.84	563.90
60%	510.96	544.75	569.98	570.20
61%	510.86	545.08	572.17	571.51
62%	510.76	546.11	575.38	574.80
63%	511.55	547.91	581.43	580.90
64%	511.24	550.00	582.65	582.79
65%	515.06	550.14	583.64	583.79
66%	518.08	552.85	587.17	586.16
67%	518.54	553.86	589.48	589.56
68%	519.23	554.11	590.01	590.06
69%	518.99	557.35	589.72	589.76
70%	519.81	564.08	590.49	590.51
71%	519.64	570.18	590.31	590.33
72%	519.48	572.18	591.10	591.12
73%	520.33	576.00	590.98	591.00
74%	520.19	581.89	590.85	590.87
75%	520.05	583.24	590.73	590.75
76%	519.90	584.95	591.57	591.59
77%	520.69	589.58	591.48	591.49
78%	520.47	590.04	591.38	591.40
79%	521.81	589.73	591.29	591.31
80%	528.96	590.48	591.19	591.21
81%	537.22	590.29	592.06	592.08
82%	537.50	591.08	591.96	591.98
83%	538.19	590.94	591.87	591.89
84%	538.92	590.80	591.77	591.79
85%	538.72	590.67	591.68	591.70
86%	538.51	591.50	592.52	592.55
87%	539.31	591.38	592.35	592.39
88%	539.10	591.25	592.19	592.22
89%	539.84	592.09	592.87	592.95
90%	540.47	591.91	593.44	593.51
91%	542.68	591.72	593.07	593.15
92%	544.87	592.38	593.72	593.78
93%	547.40	592.82	594.32	594.41
94%	551.35	593.25	594.63	594.87
95%	556.72	593.72	598.34	598.67
96%	574.64	595.44	606.07	603.78
97%	588.92	600.96	619.80	616.52
98%	590.59	617.77	625.56	624.65
99%	591.86	634.59	657.52	649.06
FBP	596.47	657.89	677.71	667.21

Cut Points Listing

D86 Correlations

D1160 Correlations

150 Gallon Still Distillation

Distillation # X-1333 | **Gross:** 640030 (gms) | **Tare:** (gms) | **Net Volume, Ml:** 608820 | **Gal:** 160.8 | **Date:** 6/14/2006
Project # 114014 | **Net Weight,Gm:** 640030 | **Reflux Ratio:** 20:10
Charge: PR-1660 | **Takeoff Rate:** 3-5 GAL/HR | **Max. Still Temp-°F:** 640
Charged by: AP | **Obs.Temp:** | **Grav:** 3.1 | **Gravity:** 3.1 | **SpGr:** 1.051 | **Cuts:** 560f

Time	CUT		D P (in.H20)	Weight (gms) Cut Gross	Cut Tare	Cut Net	Total	%	Cum	%Cum	Volume Ml	%	% Cum	Gravity Observed Temp	API	Calc. API	SpGr	Vapor @760 mmHg	Ovhd #13	Still Btms #4	Top #7	Column Btms #9	Mid #11	Abv Rflx #14	Goose #16	Coolant IN 19	OUT 18	Reflux Timers(secs) OFF	ON	Heater Amperage #1 btm	#2 mid	#3 top	Pot %	Press mm Hg	Oper
	1A			168240		168240	168240	26.3	168240	26.3	#DIV/0!	#####	#DIV/0!						429	471	451	436	432	428	427	45	50	20	10	22	20	22	50	ATMS	GS
	1B			183164		183164	183164	28.6	351404	54.9	#DIV/0!	#####	#DIV/0!						481	578	558	514	503	475	472	181	224	10	5	24	22	24	56	ATMS	HR
	1C			115214		115214	115214	18.0	466618	72.9	#DIV/0!	#####	#DIV/0!						560	637	621	595	577	556	554	224	225	10	5	26	24	26	58	ATMS	GS
	BTMS			159486		159486	159486	24.9	626104	97.8	#DIV/0!	#####	#DIV/0!																						

150 Gallon Still Distillation

Distillation # X-1332 | **Gross:** 640937 (gms) | **Tare:** (gms) | **Net Volume, Ml:** 608324 | **Gal:** 160.7 | **Date:**
Project # 114014 | **Net Weight,Gm:** 640937 | **Reflux Ratio:** 20;10
Charge: PR-1660 | **Takeoff Rate:** 3,5 | **Max. Still Temp-°F:** 640
Charged by: GS | **Obs.Temp:** | **Grav:** 2.8 | **Gravity:** 2.8 | **SpGr:** 1.054 | **Cuts:** 560 570 580

Time	CUT		D P (in.H20)	Weight (gms) Cut Gross	Cut Tare	Cut Net	Total	%	Cum	%Cum	Volume Ml	%	% Cum	Gravity Observed Temp	API	Calc. API	SpGr	Vapor @760 mmHg	Ovhd #13	Still Btms #4	Top #7	Column Btms #9	Mid #11	Abv Rflx #14	Goose #16	Coolant IN 19	OUT 18	Reflux Timers(secs) OFF	ON	Heater Amperage #1 btm	#2 mid	#3 top	Pot %	Press mm Hg	Oper
	1			180306		180306	180306	28.1	180306	28.1	#DIV/0!	#####	#DIV/0!						428	428	474	452	430	428	427	420	49	52	20	10	24	22	24	54	ATMOS	EH
	1			181077		181077	181077	28.3	361383	56.4	#DIV/0!	#####	#DIV/0!						433	433	550	522	476	457	435	433	45	49	20	10	24	22	24	54	ATMOS	HR
	1			82555		82555	82555	12.9	443938	69.3	#DIV/0!	#####	#DIV/0!						560	420	559	542	510	421	415	409	47	56	20	5	30	28	30	60	100	HR
	2			8177		8177	8177	1.3	452115	70.5	#DIV/0!	#####	#DIV/0!						570	429	566	549	534	432	428	421	49	55	20	5	30	28	30	60	100	HR
	3			10140		10140	10140	1.6	462255	72.1	#DIV/0!	#####	#DIV/0!						580	438	570	552	538	438	434	427	47	55	20	5	30	28	30	60	100	HR
	BTMS			142793		142793	142793	22.3	605048	94.4	#DIV/0!	#####	#DIV/0!																						

150 Gallon Still Distillation

Distillation # X-1318 | **Gross:** 648467 (gms) | **Tare:** (gms) | **Net Volume, Ml:** 614554 | **Gal:** 162.4 | **Date:** 4/25/2006
Project # 114014 | **Net Weight,Gm:** 648467 | **Reflux Ratio:** 20:10
Charge: PR-1660 | **Takeoff Rate:** 3-5 gal/hr | **Max. Still Temp-°F:** 640
Charged by: AP | **Obs.Temp:** | **Grav:** 2.6 | **Gravity:** 2.6 | **SpGr:** 1.055 | **Cuts:** 560,570,580F

Time	CUT		D P (in.H20)	Weight (gms) Cut Gross	Cut Tare	Cut Net	Total	%	Cum	%Cum	Volume Ml	%	% Cum	Gravity Observed Temp	API	Calc. API	SpGr	Vapor @760 mmHg	Ovhd #13	Still Btms #4	Top #7	Column Btms #9	Mid #11	Abv Rflx #14	Goose #16	Coolant IN 19	OUT 18	Reflux Timers(secs) OFF	ON	Heater Amperage #1 btm	#2 mid	#3 top	Pot %	Press mm Hg	Oper
	1	A		183118		183118	183118	28.2	183118	28.2	#DIV/0!	#####	#DIV/0!						418	418	472	453	425	422	420	418	52	55	20	10	24	22	24	52	760	GS
	1	B		208429		208429	208429	32.1	391547	60.4	#DIV/0!	#####	#DIV/0!						465	356	436	409	412	393	367	367	66	89	20	10	28	26	28	58	150	hr
	1	C		70308		70308	70308	10.8	461855	71.2	#DIV/0!	#####	#DIV/0!						560	430	506	486	479	461	432	430	48	58	10	10	30	28	31	60	120	hr
	2			3780		3780	3780	0.6	465635	71.8	#DIV/0!	#####	#DIV/0!						570	439	510	492	486	475	445	443	48	59	10	10	30	28	31	60	120	hr
	3			5130		5130	5130	0.8	470765	72.6	#DIV/0!	#####	#DIV/0!						580	449	513	497	491	481	459	455	48	60	10	10	30	28	31	60	120	GS
	BTMS			150368		150368	150368	23.2	621133	95.8	#DIV/0!	#####	#DIV/0!																						
									621133																										
	LOSS			27334		27334	27334	4.2	648467	100.0	#DIV/0!	#####	#DIV/0!																						

Appendix 1-B

Data for simulated distillation of cuts for LCO from Intertek PARC (material supplied by United Refining).

Sample Name: **PF-1639 LT CYCLE OIL**
Acquired On: 20060601161544-0500
Recovered 100.00

BP Distribution

IBP	233.03
1%	282.08
2%	333.54
3%	360.73
4%	389.05
5%	404.75
6%	413.18
7%	433.87
8%	445.31
9%	446.06
10%	447.29
11%	450.59
12%	452.04
13%	468.63
14%	478.77
15%	480.86
16%	482.77
17%	484.02
18%	485.07
19%	487.59
20%	487.89
21%	488.37
22%	489.82
23%	490.73
24%	493.94
25%	497.60
26%	503.14
27%	509.69
28%	513.00
29%	515.25
30%	516.20
31%	517.38
32%	519.91
33%	521.54
34%	522.41
35%	524.07
36%	526.93
37%	528.76
38%	531.28
39%	532.63
40%	535.77
41%	538.17
42%	540.28
43%	541.57
44%	543.10
45%	545.85
46%	548.25
47%	550.89
48%	553.28
49%	556.82
50%	561.27
51%	565.80
52%	567.97
53%	570.13
54%	571.43
55%	573.54
56%	575.71
57%	577.45
58%	580.53
59%	582.79
60%	586.60
61%	588.46
62%	590.77
63%	596.34
64%	599.24
65%	601.04
66%	604.07
67%	607.34
68%	609.51
69%	613.04
70%	616.46
71%	617.85
72%	618.97
73%	619.90
74%	623.17
75%	624.76
76%	626.06
77%	630.50
78%	634.65
79%	637.52
80%	640.01
81%	643.80
82%	646.46
83%	647.75
84%	649.39
85%	652.12
86%	652.93
87%	654.44
88%	657.05
89%	661.08
90%	664.88
91%	669.75
92%	672.49
93%	677.28
94%	680.03
95%	683.91
96%	690.74
97%	697.42
98%	708.18
99%	724.63
FBP	739.26

Cut Points Listing

D86 Correlations

D1160 Correlations

Sample Name: **PR-1850 LT CYCLE OIL**
Acquired On: 20060530120206-0500
Recovered 100.00

BP Distribution

IBP	284.21
1%	325.67
2%	371.73
3%	399.16
4%	414.19
5%	436.18
6%	445.32
7%	447.58
8%	448.14
9%	448.80
10%	448.47
11%	449.07
12%	450.11
13%	452.56
14%	453.91
15%	454.38
16%	454.53
17%	463.44
18%	470.06
19%	475.20
20%	479.16
21%	481.52
22%	481.84
23%	483.16
24%	483.81
25%	485.01
26%	485.57
27%	486.22
28%	485.89
29%	486.55
30%	487.08
31%	488.63
32%	489.67
33%	490.25
34%	489.93
35%	490.67
36%	490.42
37%	491.18
38%	490.92
39%	491.61
40%	492.23
41%	492.45
42%	495.66
43%	496.87
44%	497.11
45%	500.50
46%	501.18
47%	506.09
48%	508.83
49%	511.63
50%	513.46
51%	515.47
52%	516.55
53%	516.93
54%	518.26
55%	519.24
56%	520.75
57%	522.15
58%	523.17
59%	524.41
60%	524.67
61%	524.94
62%	526.49
63%	529.25
64%	530.40
65%	530.59
66%	532.74
67%	534.27
68%	535.38
69%	537.04
70%	539.24
71%	541.46
72%	542.37
73%	543.20
74%	544.20
75%	545.16
76%	546.77
77%	549.44
78%	550.95
79%	552.16
80%	553.50
81%	555.98
82%	558.61
83%	562.17
84%	565.05
85%	568.51
86%	570.58
87%	572.00
88%	574.23
89%	575.64
90%	576.75
91%	579.45
92%	582.40
93%	585.66
94%	589.30
95%	594.13
96%	599.79
97%	606.20
98%	615.51
99%	628.91
FBP	645.01

Cut Points Listing

D86 Correlations

D1160 Correlations